Investigation and Control of Filler-Matrix Interactions Applied to Dental Composites

A Thesis Submitted to the

Faculty of

the University of Colorado at Boulder

by

Parag K. Shah

B.Tech. & M.Tech., Indian Institute of Technology, Bombay, 2003

in Partial Fulfillment of the

Requirements for the Degree of

Doctor of Philosophy

Department of Chemical & Biological Engineering

November 2012

This thesis entitled:

Investigation and Control of Filler-Matrix Interactions

Applied to Dental Composites

Written by Parag Shah

Has been approved for the

Department of Chemical & Biological Engineering

_____

Dr. Jeffrey W. Stansbury

_____

Dr. Chrisopher N. Bowman

Date _____

The final copy of this thesis has been examined by the signatories, and we find that both the content and the form meet acceptable presentation standards of scholarly work in the above mentioned discipline.

ABSTRACT

Shah, Parag K. (Ph.D., Chemical & Biological Engineering)

Investigation and Control of Filler-Matrix Interactions Applied to Dental Composites

Thesis directed by Professor Jeffrey W. Stansbury, Ph.D.

The demand and use of polymer-based dental restorative materials continues to rise as advances in materials research continue to improve their performance. In spite of the many advances, there remain some shortcomings in their behavior. Polymerization shrinkage and the associated shrinkage stress continue to be detrimental to the long term performance of these materials. A majority of the current research is focused on developing low shrinkage resin systems to alleviate the problem of high volumetric shrinkage. There is relatively less focus on developing novel fillers and surface modification techniques to improve material properties. This thesis focuses on studying the effect of fillers on composite properties, mainly shrinkage stress development, and the development of a novel technique to modify the surface of the fillers to control shrinkage stress and optical properties of the composites.

The effect of monomer conversion and filler content was studied on the development of shrinkage, modulus and shrinkage stress. Fillers and monomer conversion were found to affect all the properties. Shrinkage stress was found to have a complex relationship with both shrinkage and modulus, with shrinkage apparently dominating the modulus at high values of monomer conversion.

A novel surface modification technique was developed, utilizing the concept of polymer brushes, to alleviate shrinkage stress in composites. Oligomers, both commercial and synthesized in the lab, were covalently attached to the surface of fillers and mixed with a model dental resin

to form composite pastes. These pastes, when photopolymerized in a shrinkage stress measuring apparatus, showed that the composites with the experimental surface modified fillers outperformed conventional filler-based composites by achieving a reduced final stress. The final stress was found to depend on various characteristics of the oligomers. In general, the higher the molecular weight of the brush, the lower was the shrinkage stress. Increased in reactive group concentration on the oligomer backbone had the effect of increasing the stress. Flexibility of the oligomers appeared to play a less significant role, with low flexibility oligomers showing a slightly lower stress than flexible oligomers.

Modern dental composites utilize different filler sizes to optimize material properties. To explore this practical scenario, composites were made with two different sizes of filler, with varying ratios of nano-fillers and submicron-sized fillers. Each filler type was treated with either a conventional silane treatment or with the experimental oligomer. It was found that composites with the experimental oligomer had reduced shrinkage stress and also better light transmission properties. The nano-fillers affected both the properties to a more significant effect than the larger fillers.

Stress development in polymerizing composites is a combination of stress increase and stress reduction. Stress reduction occurs by relaxation processes in the composite, even as the composite is polymerizing. There is a potential to increase the magnitude of the stress relaxation leading to a lower final stress. Stress relaxation was measured as a function of monomer conversion and also filler surface treatment, using a standard stress relaxation experiment. The experimental composites exhibited faster stress relaxation as compared to conventional composites, showing potential for utilizing the novel surface treatment in commercial composites.

Dedicated to my wife and parents for their enormous love, support

and encouragement and without whom my existence would have no meaning

Acknowledgements

First and foremost, I would like to thank my advisor, Dr. Jeffrey W. Stansbury, for his enormous and never-ending support for me throughout my graduate life in his lab. He has tolerated me and overlooked all my faults so that I could progress along and do good research. Whenever things were hitting a wall, every problem would automatically be solved once I talked to him. I appreciate his kindness and generosity over all these years, a debt I can never repay in this life time. I would like to thank Dr. Christopher Bowman, who, along with being a committee member, has helped me all along the way, right from the time I entered the department. I thank my other committee members, Dr. Kristi Anseth, Dr. Dan Schwartz, Dr. Virginia Ferguson and Dr. Yifu Ding. They have been very patient with me and helped me along the way whenever needed. I appreciate their feedback and the use of their lab facilities, without which this thesis would not have been possible.

I have met many people on this long journey. All of them have contributed in one way or the other towards this thesis. My mentor in the lab, Junhao Ge, was a friend, philosopher and guide, in his own quiet way. He gave me a sense of support in my early days in the lab and taught me to find my way around. Hui Lu helped me learn the art of making dental composites and I will always appreciate him for helping me take my baby steps. There have been many other people in the lab and in CU like Ryan Hansen, Leah Johnson, Devatha Nair, Aditya Kausik, Navakanth Reddy, Karthik Venkatesh, Prasanna Rao, Sachit Grover, Raveesh Shenoy, Malar Azhagan, Tao Gong, Sheng Ye, Heeyoung Park, Richard Sheridan, Dongkwon Kim, Zachary Lakeman, Rami Foster, Mitesh Shah, Parag Nemade, Sajjad Maruf, Sanjay Mohanty, Krishna Madhavan, Vaibhav Khire, Matthew Barros, Steven Lewis who have helped in many ways and in general have been great friends and great company. This list is by no means complete and I

apologize to any person I may have missed. I want to thank Prof. Kiryong Ha from Keimyung University in South Korea for many insightful discussions on nanoparticle surface analysis and also for doing solid state NMR for me. Prof. John Pellegrino also gave some useful advice for characterizing surfaces. There are many people who helped analyze samples using their expertise – Virginia Anderson for X-ray reflection, Andrew Cavanagh for XPS, James Goetz from University of Southern Mississippi for PALS, Suraj Thiagarajan for DSC and Brandi Jackson for MTS – I appreciate all their help. Dr. Sheldon Newman has been helpful in teaching me about the practical side of the world of dental materials. Jason Killgore from NIST helped in starting work on nanomechanical measurements of my composites.

I have to thank my moral support team – Mohan Dunga, Gunjan Thakur and Titas Sridharan for their moral support through the difficult times in my life here. Without them, I do not think I would have made it in one piece through grad school. I went through a difficult time financially and I would have not made it without the generous help given my Mohan Dunga, my cousin Paresh Kariya, my wife's uncle Nitin Dedhia and my parents. I believe in the power of positive thinking and also positive praying. I know all my friends and family prayed that I would overcome the difficult times that life threw at me and emerge successful. Besides my parents and all my friends and family, my mother-in-law Pushpa, has been praying that my wife and I would survive the rough times and I am sure the Almighty listened to her ardent and constant praying.

I believe in the Force, the positive vibration that goes through all of us and which runs the Universe. Although our destinies are in our hands, there is a higher purpose to everything that we do and that is what drives us in an invisible manner. Maybe there was a higher purpose to taking the long and tortuous path that I had to undertake in finishing my work here. I hope whatever I have done ultimately helps people.

CONTENTS

Chapter Pages

1 INTRODUCTION 1
1.1 History and Overview of Polymeric Dental Restorative Materials 1
1.2 Resin Matrix 3
1.3 Filler Systems 3
1.4 Coupling Agent 8
1.5 Drawbacks and Limitations of Dental Composites 10
1.6 Resin Monomer Development 12
1.7 Role of the Interface on Properties of Dental Composites 16
1.8 References 20

2 OBJECTIVES 28

3 DYNAMIC PROPERTY EVOLUTION IN POLYMERIC DENTAL RESTORATIVES: ROLE OF FILLER LOADING AND MONOMER CONVERSION 33
3.1 Introduction 34
3.2 Materials and Methods 36
3.2.1 Materials 36
3.2.2 Sample Curing 37
3.2.3 Infrared Spectroscopy 37
3.2.4 Shrinkage Stress Measurement 37
3.2.5 Shrinkage Measurement 39
3.2.6 Flexure Modulus Measurement 39
3.2.7 Scanning Electron Microscopy 40
3.2.8 Vicker's Microhardness Test 40
3.3 Results and Discussion 41
3.4 Conclusion 56
3.5 Acknowledgements 56
3.6 References 57

4 SHRINKAGE STRESS REDUCTION IN POLYMER-BASED DENTAL RESTORATIVES BY SURFACE MODIFICATION OF FILLERS 60
4.1 Introduction 61
4.2 Materials and Methods 64
4.2.1 Materials 64
4.2.2 Modification of Epoxy Oligomers 64
4.2.3 Modification of the Filler Surface 66
4.2.4 Composite Preparation 67
4.2.5 Characterization of Fillers 67

4.2.6 Shrinkage Stress Measurements 67
4.2.7 Shrinkage Measurements 68
4.2.8 Flexural Modulus and Strength Measurements 69
4.2.9 Infrared Spectroscopic Characterization 69
4.3 Results and Discussion 70
4.3.1 FTIR Characterization 72
4.3.2 Shrinkage Stress Results 73
4.3.3 SEM Characterization 87
4.4 Conclusion 87
4.5 Acknowledgements 88
4.6 References 89

5 INFLUENCE OF SURFACE MODIFICATION ON SHRINKAGE STRESS IN A MODEL DENTAL COMPOSITE: A MECHANISTIC STUDY 92
5.1 Introduction 93
5.2 Materials and Methods 95
5.2.1 Materials 95
5.2.2 Synthesis of Oligomers 96
5.2.3 GPC Characterization 98
5.2.4 Differential Scanning Calorimetry 98
5.2.5 Modification of the Filler 99
5.2.6 Composite Preparation 100
5.2.7 Thermogravimetric Analysis 101
5.2.8 Shrinkage Stress Measurements 101
5.2.9 Shrinkage Measurements 102
5.2.10 Flexural Modulus and Strength Measurements 102
5.2.11 Infrared Spectroscopic Characterization 103
5.2.12 Dynamic Mechanical Analysis 103
5.2.13 Rheometery 103
5.3 Results and Discussion 104
5.3.1 GPC and DSC Characterization of Oligomers 104
5.3.2 Shrinkage Stress Measurements 106
5.3.3 Crossover Point Measurements 112
5.3.4 Rheology of Composite Pastes 116
5.3.5 Interface Characterization by Staining with RuO_4 124
5.4 Conclusion 130
5.5 Acknowledgements 131
5.6 References 132

6 STRESS RELAXATION BEHAVIOR OF A MODEL DENTAL RESIN FILLED WITH CONVENTIONAL AND EXPERIMENTAL FILLERS 135
6.1 Introduction 136

6.2 Materials and methods 138
6.2.1 Materials 138
6.2.2 Oligomer Synthesis 139
6.2.3 GPC Characterization 140
6.2.4 Modification of the OX50 filler 141
6.2.5 Composite Preparation 141
6.2.6 Stress Relaxation Test 142
6.3 Results and Discussion 143
6.3.1 Stress Relaxation of Unfilled Resin and Composite with 0.7 µm Barium Glass Filler 143
6.3.2 Effect of Surface Modification on Stress Relaxation 149
6.3.3 Stress Relaxation Modeling 153
6.4 Conclusion 160
6.5 Acknowledgements 161
6.6 References 162

7 INFLUENCE OF NANOFILLER AND MICROFILLER FRACTIONS ON SHRINKAGE STRESS AND LIGHT TRANSMISSION IN DENTAL COMPOSITES 164
7.1 Introduction 165
7.2 Materials and Methods 168
7.2.1 Materials 168
7.2.2 Synthesis of Oligomer 169
7.2.3 GPC Characterization 170
7.2.4 Modification of the Filler 171
7.2.5 Composite Preparation 171
7.2.6 Shrinkage Stress Measurements 172
7.2.7 Flexural Modulus Measurements 173
7.2.8 Infrared Spectroscopic Characterization 173
7.2.9 Light Transmission 174
7.2.10 Refractive Index Measurements 174
7.3 Results and Discussion 174
7.3.1 Shrinkage Stress Study 175
7.3.2 Modulus Measurements 181
7.3.3 Light Transmission 182
7.4 Conclusion 191
7.5 Acknowledgements 192
7.6 References 193

8 BIBILIOGRAPHY 201

LIST OF TABLES

Table Pages

1.1. Types of fillers and filler sizes used in dental composites.....15

4.1. Weight loss contribution on the filler and fraction of the surface silanol sites covered by the modified epoxy oligomer series. 72

4.2. Storage modulus and Tg of composites 85

5.1. Terminology that is used for the synthesized oligomers.....99

5.2. GPC and DSC characterization of oligomers.....105

5.3. Shrinkage stress, Shrinkage, Flexural Modulus, Glass Transition and Storage Modulus for the entire range of samples. 109

6.1. Summary of results for unfilled resin and filled composite (0.7 µm filler at ca. 60 wt%) 147

6.2. Listing and terminology for OX50 filler-based samples used in the stress relaxation study. 150

6.3. Summary of stress relaxation results for composites based on OX50 filler particles with different surface treatments. Loading level of OX50 is 30 wt %. 153

6.4. Results of fitting stress relaxation data to a two time constant Maxwell model.....156

7.1. Filler combinations used in the mixed filler composites 172

7.2. Shrinkage stress values for composite systems with a mixture of OX50 and 0.7 µm fillers. Standard deviation values are in parentheses. 178

LIST OF FIGURES

Figure Page

1.1. Structure of some common dimethacrylate monomers used in dental composites....4

1.2. Evolution of filler sizes in dental composites (from reference [21]). 7

1.3. Nanomers and nanoclusters (from [8]). 7

1.4. Structure of 3-methacryloxypropyltrimethoxysilane 9

1.5. Simplified reaction of organotrialkoxysilanes with silica surfaces [28]. 9

3.1. Variation of volumetric shrinkage as a function of conversion and filler loading – lines connecting data points are provided for visual assistance. 42

3.2. Flexural modulus development profiles as a function of conversion for different filler loading levels. Lines connecting the data points are provided for visual assistance. 44

3.3. Real-time polymerization shrinkage stress versus conversion. Irradiation condition – 250 mW/cm^2 for 60 s. 45

3.4. Plot of shrinkage stress as a function of conversion and filler loading. Lines connecting the data points are provided for visual assistance. 47

3.5. Plot of shrinkage, modulus and stress as a function of methacrylate conversion. Curves with only lines represent the unfilled resin and lines with points represent the 70 wt% composite. (Color legend: - Blue =Modulus; Black = Shrinkage; Red = Stress). 47

3.6. Plot of shrinkage stress versus fractional conversion. Each line represents the same irradiation condition but different filler contents – Condition 1 – 35 mW/cm^2 for 5 s; Condition 2 – 35 mW/cm^2 for 10 s; Condition 3 – 35 mW/cm^2 for 20 s; Condition 4 – 700 mW/cm^2 for 5 s; Condition 5 – 700 mW/cm^2 for 10 s; Condition 6 – 700 mW/cm^2 for 60 s. Lines connecting the data points are provided for visual assistance. 50

3.7. Scanning electron micrographs of polished surfaces of samples: (a) 0 wt%; (b) 20 wt%; (c) 40 wt%; (d) 60 wt%; (e) 70 wt%. All images are taken at 2000x magnification. The scale bar is 10 µm. 53

3.8. Contribution to methacrylate peak areas as a function of filler loading level from: (1) Composite (♦), (2) Resin (▲) and (3) Interface (■). 54

3.9. Vicker's hardness number (HV) as a function of filler loading. 54

4.1. Structure of epoxy oligomer series used to modify the OX50 surface (n varies from 2 to 20) 65

4.2. Final structure of the epoxy oligomers 66

4.3. TGA curves for the OX50 particles with different surface modifications 71

4.4. DRIFTS spectra of OX50 particles at various stages of surface modification - (a) Unmodified OX50, (b) OX50 with MAPTS, (c) OX50_6100-10%, and (d) OX50_6100-100%. 73

4.5. Shrinkage stress measurements of experimental composites with 10 % hydroxyl group modification of oligomers, compared with the γ-MPS control. Irradiation conditions – Visible light at 350 mW/cm^2 for 40s 74

4.6. Shrinkage stress measurements of experimental composites with 100 % hydroxyl group modification of oligomers compared with the γ-MPS control. Irradiation conditions – Visible light at 350 mW/cm^2 for 40s. 74

4.7. Comparison of double bond conversion of experimental composites with γ-MPS-based control. Irradiation conditions – Visible light at 350 mW/cm^2 for 40s. 76

4.8. Comparison of shrinkage of experimental composites with γ-MPS-based control. Irradiation conditions – Visible light at 350 mW/cm^2 for 40s. 76

4.9. Flexural (a) strength and (b) modulus of experimental composites compared with γ-MPS-based control 79

4.10. Real-time shrinkage stress with respect to conversion. 82

4.11. Viscosity of composite pastes 84

4.12. Storage modulus of experimental composites compared with γ-MPS control. 86

4.13. Loss tangent of experimental composites compared with γ-MPS control. 86

4.14. SEM fracture surface images of (a) OX50-γ-MPS based composite, (b) OX50_4000-100% based composite 87

5.1. Monomers used in the synthesis of flexible and rigid oligomers 97

5.2. General scheme for attaching isocyanatoethyl methacrylate (IEM) to an oligomer. A generic structure representing the final oligomer is presented. R’ and R” represent the different functionalities that can replace the existing –OH functionality. 3 cases are presented -1) R’, R” = OH - 0 % methacrylate on oligomer; 2) R’ = OH and R” = urethane functionality with methacrylate at free end – 50 % methacrylate on oligomer; 3) R’,R”

= urethane functionality with methacrylate at free end – 100 % methacrylate on oligomer. 98

5.3. Scheme for attaching oligomer to silica particle. 100

5.4. Comparison of shrinkage stress of the rigid high molecular weight series with the γ-MPS control. Visible light irradiation at t = 30s, for 40 s.....106

5.5. Shrinkage stress values for the rigid oligomer series at varied reactive group concentration. Visible light irradiation at t = 30s, for 40 s. Shrinkage stress values were taken at the end of the run at t = 16 min. 107

5.6. Final shrinkage stress values for the flexible brush series at varied reactive group concentration. Visible light irradiation at t = 30s, for 40 s. Shrinkage stress values were taken at the end of the run at t = 16 min. 108

5.7. Variation of shrinkage stress with respect to conversion of the rigid high molecular weight series with the γ-MPS control. Visible light irradiation at t = 30 s, for 40 s. Shrinkage stress values were taken at the end of the run at t = 16 min. 110

5.8. Variation of shrinkage stress of the rigid and low high molecular weight systems that have 0 % methacrylate groups. Visible light irradiation at t = 30s, for 40 s. Shrinkage stress values were taken at the end of the run at t = 16 min. 111

5.9. Typical plot of crossover of storage modulus (G') over loss modulus (G)" during cure during real time cure in a photorheometer.....113

5.10. Effective gel point of photocured composite samples based on rigid ologomers. Irradiation intensity = 1 mW/cm^2 for the duration of the experiment.....114

5.11. Effective gel point of photocured composite samples based on flexible oligomers. Irradiation intensity = 1 mW/cm^2 for the duration of the experiment.....115

5.12. Complex viscosity as a function of frequency for composites based on particles treated with flexible oligomers. (The terms short, medium and long refer to high, medium and low molecular weight oligomers, respectively). 117

5.13. Complex viscosity as a function of frequency for composites based on particles treated with rigid oligomers . (The terms short, medium and long refer to high, medium and low molecular weight oligomers, respectively). 119

5.14. Storage and loss moduli of composites based on particles treated with flexible oligomers with no methacrylate coverage compared with the γ-

MPS control system. (The terms short, medium and long refer to high, medium and low molecular weight oligomers, respectively). 121

5.15. Storage and loss moduli of composites based on particles treated with flexible oligomers with 100 % methacrylate coverage compared with the γ-MPS control system. (The terms short, medium and long refer to high, medium and low molecular weight oligomers, respectively) 122

5.16. Store and loss moduli of composites based on particles treated with rigid oligomers with no methacrylate coverage compared with the γ-MPS control system. (The terms short, medium and long refer to high, medium and low molecular weight oligomers, respectively) 122

5.17. Store and loss moduli of composites based on particles treated with rigid oligomers with 100 % methacrylate coverage compared with the γ-MPS control system. (The terms short, medium and long refer to high, medium and low molecular weight oligomers, respectively) 123

5.18. TEM images of OX50 particles treated with RH0 oligomer (rigid, high molecular weight, 0% methacrylate functionality. (a) Particles sprinkled on TEM grid (b) Section of composite with particles embedded in the resin.....126

5.19. TEM images of OX50 particles treated with γ-MPS (a) Particles sprinkled on TEM grid (b) Section of composite with particles embedded in the resin.....126

5.20. TEM images of untreated OX50 (a) Particles sprinkled on TEM grid (b) Section of composite with particles embedded in the resin. 127

5.21. TEM images of particles treated with RH100 oligomer (rigid, high molecular weight, 100% methacrylate functionality. (a) Particles sprinkled on TEM grid (b) Section of composite with particles embedded in the resin. 127

6.1. Structures of monomers used for the oligomer synthesis 140

6.2. Structures of oligomers used to treat fillers 140

6.3. Comparison of normalized stress relaxation curves for (a) Unfilled BisGMA/TEGDMA resin at approximately 60 % conversion and (b) BisGMA/TEGDMA resin filled with 0.7 μm barium glass particles at 60 wt%. Stress values have been normalized by the peak stress for the respective measurement. 146

6.4. Comparison of fractional residual stress for (♦) Unfilled resin at 60% conversion and (■) resin filled with 0.7 μm particles at 60 wt%. All stress

values have been normalized with respect to the peak stress for the respective measurement. 146

6.5. Comparison of stress relaxation rates for (♦) unfilled resin and (■) resin filled with 0.7 micron filler at 60 wt %, as a function of conversion. All stress values have been normalized with respect to the peak stress for the respective measurement. 149

6.6. Comparison of stress relaxation of 30 wt% OX50 in BisGMA/TEGDMA with three different surface modifications – 1) (●) – γ-MPS; 2) (■) – High Mw rigid brush – 100% methacrylate; 3) (▲) High Mw rigid brush – 0% methacrylate. 152

6.7. Maxwell element, representing series array of springs and dashpots. 154

6.8. Generalized Maxwell model, consisting of Maxwell elements connected in parallel. 155

6.9. First time constant, τ_1, plotted a function of conversion for composite samples based on OX50 filler - – 1) (●) γ-MPS; 2) (■) High M_w rigid oligomer – 0% methacrylate; 3) (▲) High M_w rigid oligomer – 100% methacrylate. 156

6.10. Second time constant, τ_2, plotted a function of conversion for composite samples based on OX50 filler – 1) (●) γ-MPS; 2) (■) High M_w rigid brush – 0% methacrylate; 3) (▲) High M_w rigid brush – 100% methacrylate. 157

7.1. Structures of monomers used for synthesis of the oligomer 170

7.2. Structure of final oligomer. 170

7.3. Comparison of shrinkage stress between 0.7 µm fillers treated with γ-MPS control and experimental oligomer at various loading levels of the filler 176

7.4. Comparison of shrinkage stress between OX50 fillers treated with γ-MPS control and oligomer 177

7.5. Comparison of shrinkage stress for composites with varying ratios of OX50/0.7 µm barium glass fillers. The total mass fraction of fillers is 50 wt%. 178

7.6. Flexural modulus of composites with different ratios of OX50 to 0.7 µm glass filler. 182

7.7. Comparison of optical translucency of composites made with fillers treated with 1) γ-MPS and 2) Experimental oligomer. The proportion of OX50 is increasing from left to right. 183

7.8. Comparison of light transmission through samples with different filler ratios and surface treatments. The light source was an infrared beam from the FT-IR with a wavelength of 760 nm. 185

7.9. SEM images of polished surfaces of composites with 10/40 ratio of OX50/0.7 μm fillers surface treated with (a) γ-MPS and (b) Experimental oligomer. 185

7.10. Refractive indices of cured samples with varying OX50 particle loading and filler surface treatment. 188

7.11. Refractive indices of cured samples with varying 0.7 μm particle loading and filler surface treatment. 188

7.12. Refractive index variation in cured composites with different filler ratios and filler surface treatments.....189

CHAPTER 1

INTRODUCTION

1.1 History and Overview of Polymeric Dental Restorative Materials

With well over 100 million polymer-based dental restoratives placed in the teeth of patients in the US annually, these materials have rapidly overtaken traditional amalgam restoratives as the demand for more esthetic and environmentally friendly material alternatives has grown [1]. The formulations and performance of these materials have improved over the years. Earlier esthetic materials used in dentistry included silicate cements, that had the ability to release fluoride, but these materials were subject to solubilisation and eroding in the oral environment [2], [3]. Acrylic resins then replaced the silicates during the 1950s due to their tooth-like appearance, insolubility in the oral cavity, easy workability and low cost. These materials however were subject to high shrinkage, which caused them to pull away from the tooth walls and cause severe microleakage. Internal stresses would be high due to excessive thermal expansion and contraction during intake of hot and cold food. To overcome this issue, quartz powder was added to these resins in order to reduce the shrinkage and thermal expansion, signaling the beginnings of composites as dental restoratives. These quartz particles, however, were not bonded to the resin, and the same issues of thermal expansion and contraction would cause defects around the particles as the resin contracted away from the particle surface.

A major step towards solving this issue came in the form of the development of 2,2-bis[4(2-hydroxy-3-methacryloxy-propyloxy)-phenyl] propane, now more popularly known as BisGMA, by Dr. Raphael L. Bowen [4]. This dimethacrylate monomer, which was designed to provide high strength crosslinked polymer networks, continues in widespread use as the major

component of dental materials to this day. Bowen's invention came as a compromise between the epoxy and methacrylate resins that were being used at that time, but had problems with adhering to the teeth, especially after long exposures to the wet oral environment [5]. BisGMA is non-volatile and has relatively low polymerization shrinkage due to its high molecular weight and low double bond concentration. It can be used as a binder for reinforcing fillers and it polymerizes rapidly in oral conditions when mixed with a suitable initiator system. Introduction of the BisGMA monomer provides a high modulus material but at the same time, the rigidity of its bisphenol A core structure [6] and the high viscosity due to intermolecular hydrogen bonding restricts the reaction progress due to vitrification at moderate levels of conversion [7]. The high resin viscosity and high filler loading in dental composites can also lead to poor handling of the composite paste and difficulty in placing it properly in the restoration site.

Modern dental composites have overcome many of the limitations of BisGMA and further improved upon the mechanical properties. These materials are a complex mixture of a variety of components, the major ones being the following: 1) an organic resin matrix, usually based on dimethacrylate monomers, that forms a continuous phase and binds the filler particles; 2) reinforcing filler –particles that are dispersed in the matrix; and 3) a coupling agent that promotes adhesion between the filler and resin matrix phases. In addition to these, the other important components are an activator-initiator system that is required to convert the composite from its soft, fluid paste state to a hard, long-lasting restoration; pigments that help to match the composite to tooth structure; UV absorbers and other additives to improve color stability and inhibitors to increase the shelf life of the composites [2], [8].

1.2 Resin Matrix

The high viscosity of BisGMA (about 1000 cp at 23 ^{o}C) [9] makes it particularly difficult to handle and manipulate. To overcome this problem, comonomers like triethylene glycol dimethacrylate (TEGDMA) are added as reactive diluents to reduce the final resin viscosity to make it manageable for clinical manipulation while also providing for higher conversion [6]. Analogues of BisGMA such as urethane dimethacrylate (UDMA), ethoxylated bisphenol A dimethacrylate (BisEMA), are also commonly used in place of or along with BisGMA. The lower viscosity of these monomers with respect to BisGMA can lead to improved monomer conversion. This has been observed in the case of mixtures of TEGDMA with BisGMA and UDMA, where incremental amounts of UDMA led to higher conversion and crosslinking than a mixture of TEGDMA with the same molar fraction of BisGMA [10]. BisEMA has the identical rigid aromatic core structure as BisGMA, except that it lacks the pendant hydroxyl groups and hence no hydrogen bond donating capability, which dramatically lowers its viscosity compared with BisGMA. The structure of these common monomers is shown in Figure 1.1.

1.3 Filler Systems

Inorganic fillers are used in polymeric dental restoratives to provide reinforcement and strength. Fillers are chosen based on their effect on all of the following desirable properties: (i) reinforcement of the resin matrix to impart increased hardness [11], [12], strength [13], fracture toughness [14], [15], moduli [11], [16], [17] and wear resistance, (ii) reduction in polymerization shrinkage [18–20], (iii) reduction in the coefficients of both thermal expansion and conductivity, (iv) radioopacity and diagnostic sensitivity via the introduction of strontium, barium, zirconium and ytterbium glass fillers as well as several other heavy metal compounds that absorb x-rays, (v) reduction in water sorption, softening and staining [2], [8]. Quartz and silica are also used as

non-radioopaque fillers. These fillers display a wide range of densities and refractive indices, which when combined with specific resins, offer a means to achieve appropriate esthetic character in the composite that can mimic the translucency of dental enamel.

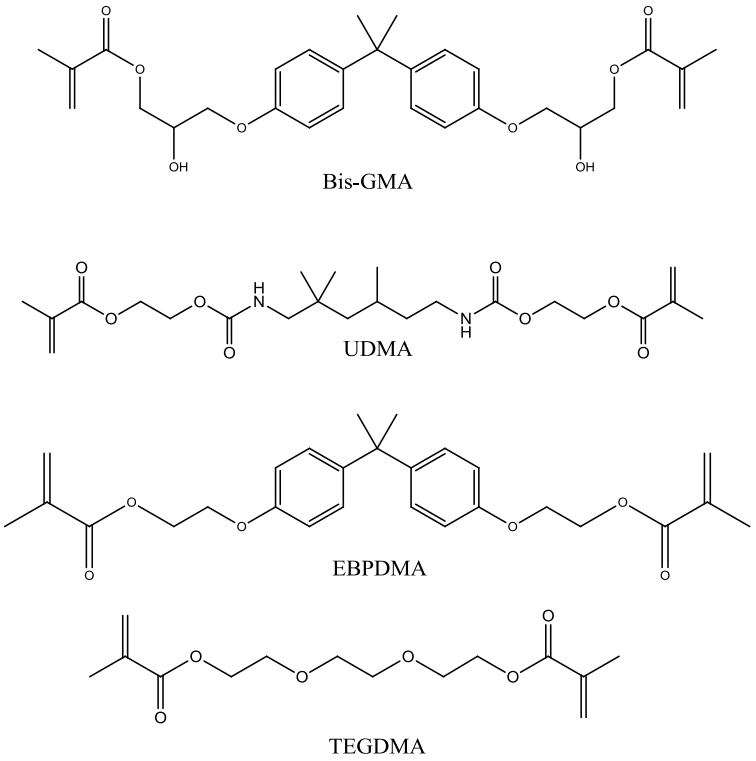

Figure 1.1. Structure of some common dimethacrylate monomers used in dental composites.

Besides the many different types of fillers that are used in current dental composites, the particle morphology varies considerably as well. Micron-sized fillers are typically produced by grinding or milling quartz or various glasses to produce particles in the 0.1 – 100 µm range [2]. It should be pointed out that the term “microfillers” is a very broad generalization and is used in the dental industry for any fillers that are in the aforementioned size range, even if they may technically be less than a micron in size. In some cases, nano-sized fillers (2 – 20 nm) are produced by sol/gel methods as organically modified ceramics (Ormocer) or based on polyhedral oligomeric silsesquioxane (POSS) chemistry in some cases [21], [22]. However, dental

composites make much more common use of nanofillers that are obtained by a pyrogenic process wherein a silicon compound (for example, $SiCl_4$), is subjected to a continuous flame hydrolysis in a hydrogen and oxygen atmosphere to form sintered multi-particle chains/clusters of SiO_2 [23]. These colloidal size (typically 40 nm) inorganic silica particles are widely used in conjunction with other micofillers to enhance filler loading levels, to modify composite paste handling properties, to improve wear characteristics, and to provide glossy composite surfaces.

Based on the wide variety of sizes of fillers and the combinations that are used, commercial dental composites have been classified according to the following schemes (Figure 1.2):

1) Traditional resin composites or "macrofills" – These were among the first conventional dental composites and had sizes of fillers far exceeding 1 µm and were typically in the range of 40-50 µm. Although extremely strong, these composites had very low wear resistance and poor aesthetic properties.

2) Microfills – These composites were introduced to overcome the problems due to the macrofills. These materials had particles in the size range of 0.01 to 0.05 µm. These were true nanocomposites but in typical dental materials misnaming fashion, they were called microfills. The filler loading in these composites was low, due to the higher surface area of the nanofillers and the attractive interactions that caused the viscosity to increase rapidly, limiting the addition of more fillers. The presence of nanofillers gave the composites good polishing ability, but their strength was low, especially in areas where high masticatory forces were present.

3) Hybrid resin composites – A compromise between macrofills and microfills was hybrid resin composites, which, as the name suggests, were a hybrid between the two existing

composites. These had a mix of micro- and nano- particles and provided good mechanical properties and intermediate aesthetics.

4) Small particle hybrid composites – Further refinements and grinding down of particles reduced the overall sizes of fillers being used to produce small particle hybrids that had a mixture of the 0.04 µm particles and ground particles with average sizes slight more than 1 µm. These were labeled as “midfills” and further gave rise to “minifills” where the larger particles were further reduced to sizes below 1 µm. The wide distribution of sizes and irregular shapes that are used in these composites helps in packing as much filler as possible, which is a major goal of manufacturers. The highly packed microhybrid composites have as much as 60-70 volume % filler. These hybrid composites have good wear resistance and mechanical properties but they can lose their surface polish with time and become dull.

More recently, nanotechnology has come to the aid of filler development [24] and has aided in driving down particle sizes to the 1-100 nm range, to give what are called “nanofill” composites. These were created by making “nanoclusters” (Figure 1.3), made by tethering together nanoparticles that have a controlled size distribution, ranging from 5 to 75 nm. If only single nanoparticles are used, the rheological properties make it difficult to have a high filler loading. Creating nanoclusters solves this problem and also allows for higher filler loading giving better strength, while retaining the benefits of using nanoparticles, such as better wear properties and better polishing. In addition to these benefits, nanoparticles being much smaller than the wavelength of light will scatter less light compared to micrometer sized particles and result in composites that are more translucent. This allows further processing in terms of matching a wide variety of shades and optical densities of the composite material to that of natural teeth.

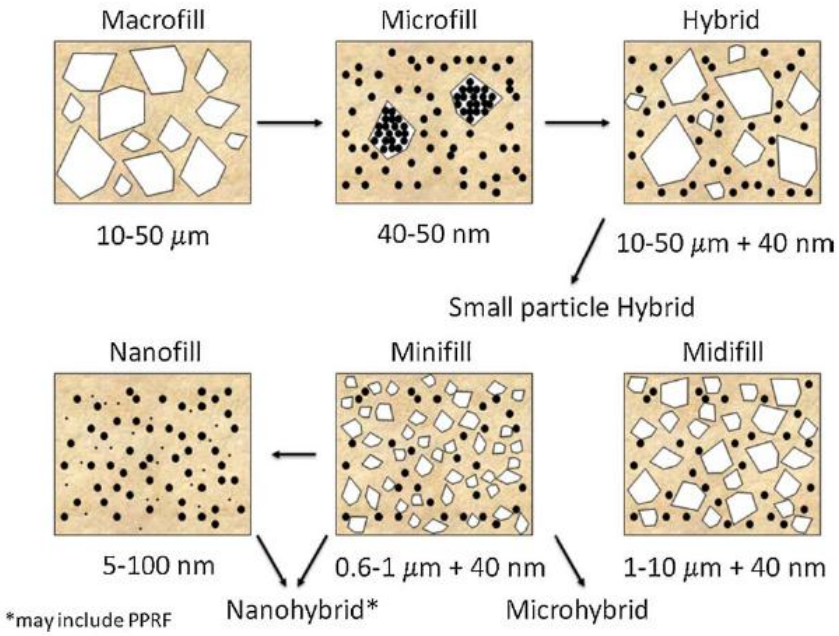

Figure 1.2. Evolution of filler sizes in dental composites (from reference [21]).

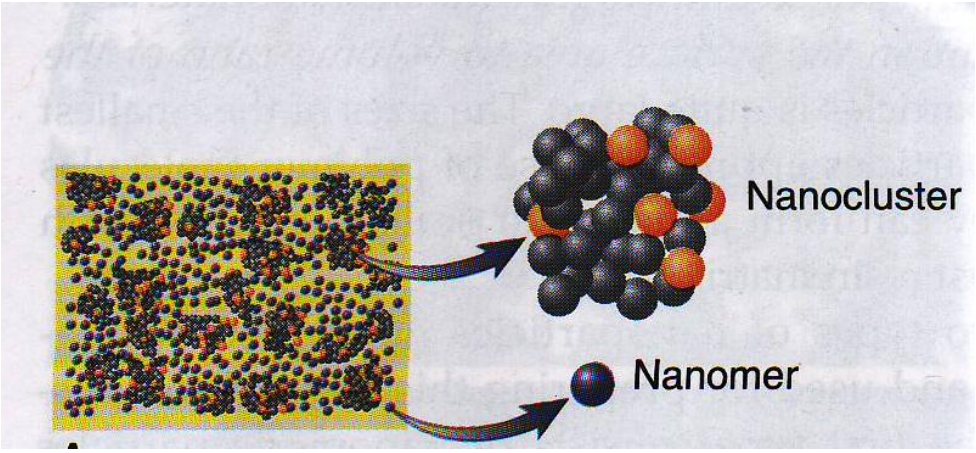

Figure 1.3. Nanomers and nanoclusters (from [8]).

1.4 Coupling Agent

In order for the composite to maintain its mechanical integrity, it is essential to have a good bond between the filler particles and the resin matrix phase. Failure to do so can result in a weak interface between the fillers and the polymeric phase, resulting in weakening of the overall composite properties [25], [26]. Silane coupling agents, as the name indicates, act as adhesion promoters between the organic resin matrix and the inorganic filler, by coupling the two phases covalently, resulting in a strong bond between them [27]. Attaching the fillers to the resin helps prevent filler particles from getting dislodged from the matrix during wear. It is also critical in maintaining acceptable levels of fracture toughness for the composite materials. Most importantly, the covalent linkage also serves as a bridge to transfer stresses from the polymer matrix to the high modulus fillers, which effectively increases the strength and modulus of the composite compared with the neat resin.

The most common silane used in the dental industry is 3-methacryloxypropyltrimethoxysilane, more commonly known as γ-MPS (Figure 1.4). The silane end of γ-MPS attaches to the silica filler through the scheme shown in Figure 1.5 and the methacrylate end co-polymerizes with the methacrylate-based dental resin. The methoxy groups in γ-MPS undergo hydrolysis in a base or acid catalyzed reaction and generate hydroxyl groups. These then undergo condensation with the surface silanols and get covalently attached to the filler surface. Bimodal and trimodal silanes can undergo condensation with neighboring silanes on the filler surface to form a three-dimensional network [28].

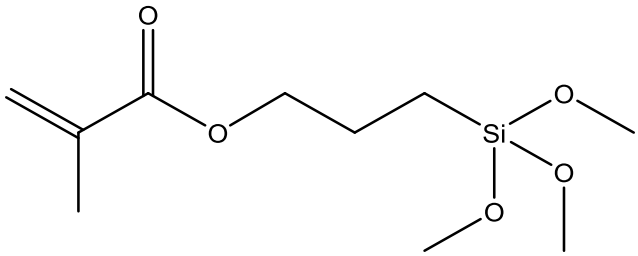

Figure 1.4. Structure of 3-methacryloxypropyltrimethoxysilane

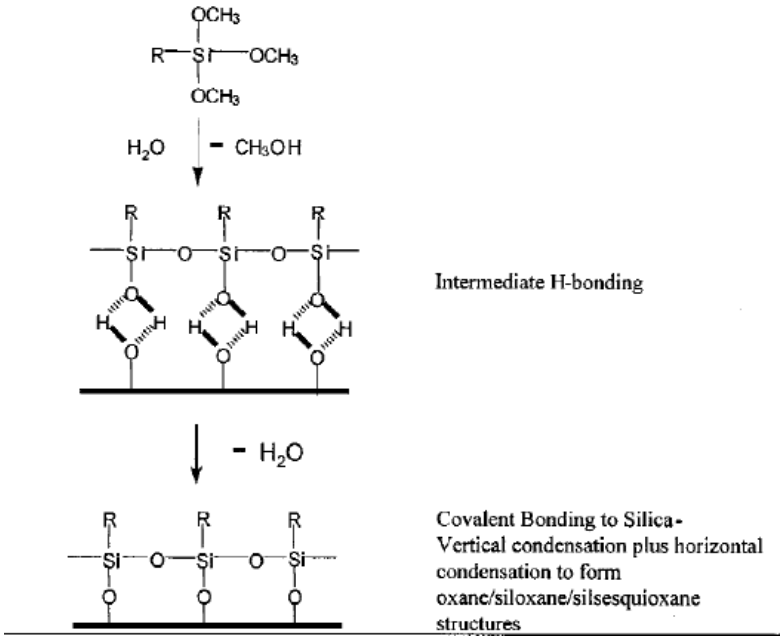

Figure 1.5. Simplified reaction of organotrialkoxysilanes with silica surfaces [28].

1.5 Drawbacks and Limitations of Dental Composites

Despite the steady improvements in properties of dental composites due to new materials innovations, several challenges still remain in achieving the "ideal" composite. The most significant drawback is due to the volumetric shrinkage that occurs as monomer is converted to polymer with the critical challenge being the subsequent polymerization shrinkage stress that develops as a consequence of the shrinkage. As polymerization occurs, the van der Waals distance between adjacent monomers reduces from about 3-4 Å [29] to the covalent bond distance of about 1.5 Å [9], [20], [30], increasing the density of the system. There is a reduction in the free volume due to the reduced mobility of the polymer chains and this contributes to the densification as well. The shrinkage is a function of double bond conversion of the monomer system, depending on the molar concentration of the double bonds, the degree of conversion and the shrinkage factor, which is the volumetric shrinkage per mole, for that particular system. The average molar shrinkage for methacrylates has been found to be in the range of 22.5 cm^3/mol [31]. The volumetric shrinkage for a typical mixture of BisGMA and TEGDMA in the 70:30 weight ratio is about 5 % to 7 % (Chapter 3), depending on the final conversion achieved. Commercial dental composites can have shrinkage from anywhere between 1 % for highly filled composites and about 5.5 % for flowable composites that have a low filler loading [30].

In a clinical situation, the composite is placed in between the walls of a cavity and has to adhere to the cavity. A liquid paste is placed in the dental cavity and then polymerized. During cure, the monomers go from the uncured state, pass the gel point, and reach the glassy state upon vitrification, where the samples glass transition temperature exceeds the curing temperature. The restriction of the developing shrinkage by the walls of the cavity leads to the build-up of stresses within the composite. In the pre-gel phase of the polymerizing monomer, it is possible to

compensate the shrinkage by flow of the monomer as its motion is not restricted. Once the gel-point is achieved, there is formation of a continuous infinite network. The bulk, thermodynamically driven contraction of this network is restricted by the cavity boundaries, which experience only a small degree of compliance as the polymer network formation continues, and this restriction of free shrinkage leads to the development of stress. In dimethacrylate systems, the gel-point is reached very quickly and at a very early stage upon polymerization. A bulk dimethacrylate monomer or comonomer mixture would be theoretically expected to exhibit a onset of macrogelation at less than 1 % methacrylate conversion. In practice, the gel point may occur around 1-5 % conversion due to non-idealities such as cyclization, reactivity differences of free vs. pendant groups and chain transfer. Hence stress starts building up at a very early stage in conversion of a dental composite. As the conversion proceeds and there is development of a cross-linked network, the modulus of the material, which is directly related to crosslink density, also begins to rise. Stress being a function of shrinkage and modulus, also starts increasing. As the composite is covalently attached to the cavity walls, the developing stress is transferred to the tooth. If the force of contraction with which the composite contracts exceeds the bond strength between the tooth and the composite, it can lead to adhesive failure at the boundary of the restoration. This can cause microcracks to develop in the interface between the tooth and the restoration, leading to micro-leakage and recurrent caries. It has been found that secondary caries is the single largest reason for the failure of restorations [1], [21], [32–34]. Besides damaging the tooth-restoration interface, the transfer of stress to the tooth can result in damage to the tooth structure, by causing deformation of the cusp and cracking in the enamel [35–38].

A separate issue with regards to the dental monomers is their incomplete conversion [29]. The limiting conversion in dimethacrylate is reached upon vitrification of the system, when the development of a highly cross-linked network dramatically limits the mobility of the remaining free monomer as well as the pendant reactive groups [39]. It has been observed that the final conversion of BisGMA-based resin lies between 55 % and 75 % [29]. The conversion drops even further upon addition of fillers [40] . Unreacted monomer can leach out into the body, leading to changing polymer properties and potential cytotoxicity or other biocompatibility issues. Unreacted monomer acts as a plasticizer, leading to less than optimum mechanical properties of the composite. TEGDMA is relatively hydrophilic and being more mobile, it can be leached out of a composite into the oral environment more rapidly than BisGMA[29], [41]. Leached monomer is typically replaced by water, which serves as an even better plasticizer.

All these drawbacks call for better materials and many innovations have been introduced to address them. Here the focus is on the developments in composite technology that deal with the problem of shrinkage stress, with shrinkage reduction being one of the ways to approach the issue. There are two ways to address the problem of shrinkage stress – 1) Materials innovations and 2) Clinical procedures.

1.6 Resin Monomer Development

Since shrinkage during polymerization leads to the development of stress, it is logical to focus on reducing shrinkage to be able to limit the development of shrinkage stress. Many approaches have been tried to develop new monomers that have lower shrinkage than the existing resins but with the constraint that there be no appreciable reduction in mechanical properties. Methacrylate-based monomers show good mechanical properties and can be cured

rapidly. Acrylates are more reactive but generally have reduced mechanical properties and since they are also more cyctotoxic compared with methacrylates, they are rarely used in dental materials. Hence a lot of research has focused on keeping the methacrylate functionality intact and modifying the structure of the connecting groups that ultimately form the crosslinking units. Bulky methacrylates have been made in order to lower the double bond concentration and reduce shrinkage [42], [43]. Multi-methacrylate monomers have also been made in order to take advantage of the methacrylate functionality, but these structures tend to lead to higher stress at a lower monomer conversion [44], [45]. A very promising development has been the development of silorane (siloxane + oxirane) monomers [46], [47]. These polymerize via a ring-opening mechanism using cationic polymerization and have a very low molar shrinkage coefficient. Hybrid thiol-ene-methacrylate polymerizations have been used with great success in reducing shrinkage stress while maintaining good mechanical strength [48]. A novel way to reduce shrinkage stress is via the use of covalent adaptable networks [49]. Addition-fragmentation chain transfer of allyl sulfide groups in radical mediated polymerizations of thiol-yne monomers has been found to alleviate shrinkage stress while maintaining good mechanical strength [50]. A recent study found that even low shrinking composites can develop high stress equivalent to those produced by conventional composites [51]. The conclusion was that since stress in a confined setting is dependent not just on shrinkage but also on other factors like conversion, modulus, shape and boundary conditions. So equating low shrinkage to low stress would be an error, unless all the other factors are also taken into account. This leads us to the importance of fillers in dental composites. Fillers help in reinforcing the polymer to produce a stronger material and also reduce volumetric shrinkage by reducing the amount of resin per unit volume of the composite. The type of fillers and quantity added affect the final properties of the composite.

Klapdohr *et al*. [52] have listed the kinds of fillers that are used in modern dental composites and this is reproduced in Table 1-1.

From Table 1-1, it is evident that there is a wide distribution in sizes and properties of the particles that are used in dental composites. The loading level of each of the components will also affect the overall properties of the composite. The loading level of the fillers is also a major factor in deciding how they are used. For example, there are flowable composites that have a low volume percent of fillers (42 – 62 %) [8], that have a lower modulus and can only be used for anterior applications, since these have a high wear rate. Microfilled composites have an even lower loading level – about 32 – 50 volume % - and are used where very high polish and the best esthetics are required. These have very high shrinkage and cannot be used in stress bearing areas. Multipurpose and packable composites, on the other hand, have a very high filler loading – between 60 to 70 volume % - and can be used where high forces have to be sustained. These materials contain a mixture of nanofillers and microfillers of a variety of sizes as a strategy to maximize the filler content.

Given the wide range of filler loading levels and the potential variations in the degree of conversion achieved, it is evident that the final properties of the dental composites will also be quite distinct. This poses a challenge in terms of predicting the final properties of the composites attained upon polymerization. Each component of the composite has a different property like modulus, thermal expansion coefficient and shrinkage so the bulk mechanics of the entire composite would be dictated by the micromechanics of the components and the final properties cannot be predicted by simple additive rules. Volumetric shrinkage of dental composites has been found to more or less linear with respect to filler loading levels [30], [53–55]. There is an inverse correlation between the volume fraction of the filler and the shrinkage level of the cured

Table 1.1. Types of fillers and filler sizes used in dental composites

Filler Composition	Particle size
Highly dispersed SiO_2	10-40 nm
Radiopaque, finely ground Ba or Sr silicate glasses	0.7 µm, 1.0 µm, 1.5 µm or larger
Radiopaque, finely ground Ba/Sr fluorosilicate glasses	1.0 µm, 1.5 µm or larger
Ground quartz glass	1.0 – 1.5 µm
YbF3, YF3	0.10 – 3.0 µm
Si/Zr mixed oxide	250 – 500 nm
Ti, Zr and Al oxide as opacifier	250 – 500 nm
Splinter polymerisate main based on SiO_2	10-100 µm

composite. One drawback of most of the studies, especially those done with commercial composites, is that the shrinkage is rarely reported as a function of monomer conversion, and if it is reported, the final conversion values vary depending on the curing conditions used and the associated vitrification limits imposed by each material, providing an inconsistent basis for comparisons. The modulus of the composite is also a function of the modulus of the fillers and the filler loading level [11]. The results are further complicated by the presence of nanofillers. The nano-sized fillers, due to their extremely large surface area to volume ratio, affect the properties of the composite in a manner different than that encountered with micrometer sized fillers [56], [57] and thus also needs to be considered. Studies have been done evaluating the effect of filler loading on modulus [18], [19], [58–60] and in general have found that the modulus of the composites increases with filler loading. There is an exponential relation between the modulus and both filler loading and degree of conversion. In this case too, monomer conversion is rarely reported when evaluating cured composite moduli as a function of filler

loading. Shrinkage stress is a function of both the shrinkage and the modulus. Studies have looked at the effect of modulus on shrinkage stress [18], [58] and also the effect of shrinkage on stress [30] as well as monomer conversion on stress [61]. But there is no study that combines the effect of all the factors, namely, shrinkage, modulus, filler loadng and monomer conversion, on shrinkage stress. This type of fundamental study has been conducted as an initial stage of this thesis in order to bring all these factors together and provide a comprehensive look at stress development. A central theme to this thesis is evaluation of properties with concurrent measurements of monomer conversion so that there is a rational basis of comparison of these critical material properties.

1.7 Role of the Interface on Properties of Dental Composites

The interface between fillers and the polymer in a dental composite is essential to the mechanical integrity of the composite. The interface refers to the sharp boundary between the dispersed fillers and the continuous matrix phase [28]. This is the smallest part of the composite, in terms of size [62], but it forms an important link for stress transfer between the two phases [63–66], is essential for determining fracture toughness [67–69] and it can affect the hydrolytic stability of the material by use of hydrophobic groups [70], [71]. The importance of the interface is enhanced in nanocomposites due to the large surface area of the nanofillers, allowing for more interactions as compared to composites with micrometer-sized fillers.

In dental composites, the surface of fillers is generally treated with an organosilane coupling agent, 3-methylpropyltrimethoxysilane (γ-MPS) (Figure 1.4). This is the most common silane used in the dental materials industry. As described previously, the silane functional groups hydrolyze and condense with the surface silanols on the fillers while the methacrylate at the

opposite end reacts covalently during the polymerization of the methacrylate-based dental monomers. The effect of the surface silane amount on the mechanical properties of composites has been studied extensively. A non-optimal concentration of silane can lead to deterioration of mechanical properties like flexural strength and modulus and tensile strength [63], [72], [73]. Mixed silanes can be used to overcome this problem and express the beneficial properties of each individual silane with positive results [70]. Silane treatment of fillers has been found to be essential for better wear resistance in composites [74–76]. Stress development is also affected by the functionalization of filler. It has been observed that composites made with fillers that are silanized with non-functional silanes, that is silanes that do not chemically interact with the monomer system, and untreated fillers, show lower stress than composites made with fillers that are treated with a silane that can copolymerize with the monomer system [77], [78].

The utility of the interface as something more than just a link between the two phases that provides integrity to the material has not been explored fully in the field of dental composites. Research focused on modification of the interface to optimize material properties and performance remains limited. This is evident from the fact that the silane of choice for fillers in dental composites remains γ-MPS and has been so for many years. Even now, the composites literature reports ways to optimize the amount of γ-MPS for better overall performance [79], [80] but there has been very little done in terms of entirely changing the surface treatment and exploring novel new ways of modifying the filler surface [70], [81–84]. Apart from the near universal use of γ-MPS in commercial methacrylate-based dental composites, the new family of commercial "silorane"-based composites, which is predicated on use of cationically activated oxirane ring-opening resin chemistry, uses fillers treated with 3-glycidoxypropyltrimethoxysilane [85].

So the current state-of-the-art in surface modification of fillers in dental composites leaves significant room for improvements. One way of approaching this problem is via the use of polymer brushes. Polymer brushes refer to an assembly of polymer chains that are end-tethered to a surface or an interface that allows the potential extension away from the substrate [86], [87]. Polymer brushes find many applications including stabilizing colloidal particles from flocculation, tailoring surfaces for biological applications, as surfactants and compatibilizers, among many others [86]. It has been reported that the interface between a solid surface and a cross-linked polymer can be strengthened by the addition of such polymer brushes that can extend into the adjacent polymer layer. With the effects on strength of the material, there also exists the potential to tailor the properties of these brushes to be able to control stress, fracture toughness, reactivity at the interface and optical properties. This thesis introduces and details the application of polymer brushes in the area of dental composites.

To conclude, polymeric dental composite materials provide an exciting avenue for research in the general field of composite materials. Despite rapid progress in innovations in new materials for the composites, there remains considerable room for improvement in material properties and performance. Studies on mechanical property evaluation of composites are usually carried out without reporting the double bond conversion, making it difficult to interpret the results. Systematic studies of conversion-dependent composite properties involving both conventional and polymer brush filler surface treatments are explored in this work. The topic of the interface between the fillers and monomers/polymers represents an under-exploited route to alter bulk composite properties, particularly polymerization shrinkage stress. This approach appears highly relevant considering the importance of the filler-resin interface as the link for

stress transfer between the two constituent phases of composites. All these issues are addressed in this thesis.

1.8 References

[1] S. J. Sadowsky, "An overview of treatment considerations for esthetic restorations: a review of the literature," *The Journal of Prosthetic Dentistry*, vol. 96, no. 6, pp. 433–42, Dec. 2006.

[2] K. J. Anusavice, *Phillips' Science of Dental Materials*, 11th ed. Elsevier, 2003.

[3] R. L. Bowen, "Use of Epoxy Resins in Restorative Materials," *Journal of Dental Research*, vol. 35, pp. 360–369, 1956.

[4] R. Bowen, "Method of preparing a monomer having phenoxy and methacrylate groups linked by hydroxy glyceryl groups," U.S. Patent 3,179,6231965.

[5] R. L. Bowen and W. A. Marjenhoff, "Dental Composites/Glass Ionomers: the Materials," *Advances in Dental Research*, vol. 6, pp. 44–49, 1992.

[6] L. F. J. Schneider, L. M. Cavalcante, and N. Silikas, "Shrinkage Stresses Generated during Resin-Composite Applications: A Review," *Journal of Dental Biomechanics*, vol. 2010, pp. 1–15, 2010.

[7] S. H. Dickens, J. W. Stansbury, K. M. Choi, and C. J. E. Floyd, "Photopolymerization Kinetics of Methacrylate Dental Resins," *Macromolecules*, vol. 36, no. 16, pp. 6043–6053, Aug. 2003.

[8] R. L. Sakaguchi and John M Powers, *Craig's Dental Restorative Mateirals*, 13th ed. Elsevier, 2012.

[9] A. Peutzfeldt, "Resin composites in dentistry: the monomer systems.," *European Journal of Oral Sciences*, vol. 105, no. 2, pp. 97–116, Apr. 1997.

[10] C. J. E. Floyd and S. H. Dickens, "Network structure of Bis-GMA- and UDMA-based resin systems," *Dental Materials*, vol. 22, no. 12, pp. 1143–9, Dec. 2006.

[11] M. Braem, W. Finger, V. Vandoren, P. Lambrechts, and G. Vanherle, "Mechanical properties and filler fraction of dental composites," *Dental Materials*, vol. 5, no. 5, pp. 346–349, Sep. 1989.

[12] M. Braem, V. E. Doren, P. Lambrechts, and G. Vanherle, "Determination of Young's modulus of dental composites: A phenomenological model," *Journal of Materials Science*, vol. 22, no. 6, pp. 2037–2042, Jun. 1987.

[13] E. Feresenbet, D. Raghavan, and G. a. Holmes, "The influence of silane coupling agent composition on the surface characterization of fiber and on fiber-matrix interfacial shear strength," *The Journal of Adhesion*, vol. 79, no. 7, pp. 643–665, Jul. 2003.

[14] E. D. Bonilla, M. Yashar, and A. A. Caputo, “Fracture toughness of nine flowable resin composites.,” *The Journal of Prosthetic Dentistry*, vol. 89, no. 3, pp. 261–7, Mar. 2003.

[15] B. Wetzel, P. Rosso, F. Haupert, and K. Friedrich, “Epoxy nanocomposites – fracture and toughening mechanisms,” *Engineering Fracture Mechanics*, vol. 73, no. 16, pp. 2375–2398, Nov. 2006.

[16] P. Lingois and L. Berglund, “Modeling elastic properties and volume change,” *Journal of Materials Science*, vol. 37, pp. 4573 – 4579, 2002.

[17] G. Queiroz, D. M. Monteiro, M. Antonio, and J. Resende, “Evaluation of Linear Polymerization Shrinkage , Flexural Strength and Modulus of Elasticity of Dental Composites,” *Spectrum*, vol. 13, no. 1, pp. 51–55, 2010.

[18] L. C. C. Boaro, F. Gonçalves, T. C. Guimarães, J. L. Ferracane, A. Versluis, and R. R. Braga, “Polymerization stress, shrinkage and elastic modulus of current low-shrinkage restorative composites.,” *Dental Materials*, vol. 26, no. 12, pp. 1144–50, Dec. 2010.

[19] J. Cavalcanti, G. Queiroz, D. M. Monteiro, M. Antonio, and J. Resende, “Polymerization Shrinkage and Flexural Modulus of Flowable Dental Composites,” *Materials Research*, vol. 13, no. 3, pp. 381–384, 2010.

[20] M. Dewaele, D. Truffier-Boutry, J. Devaux, and G. Leloup, “Volume contraction in photocured dental resins: the shrinkage-conversion relationship revisited.,” *Dental Materials*, vol. 22, no. 4, pp. 359–65, Apr. 2006.

[21] J. L. Ferracane, “Resin composite-state of the art.,” *Dental Materials*, vol. 27, no. 1, pp. 29–38, Jan. 2011.

[22] E. Tegou, V. Bellas, E. Gogolides, P. Argitis, D. Eon, G. Cartry, and C. Cardinaud, “Polyhedral Oligomeric Silsesquioxane (POSS) Based Resists: Material Design Challenges and Lithographic Evaluation at 157 nm,” *Chemistry of Materials*, vol. 16, no. 13, pp. 2567–2577, Jun. 2004.

[23] Degussa, “Technical Bulletin Fine Particles.”

[24] S. Mitra, D. Wu, and B. Holmes, “An application of nanotechnology in advanced dental materials,” *Journal of the American Dental Association*, vol. 134, pp. 1382–1390, 2003.

[25] P. G. P. and E. P. Plueddemann, “Methods for improving the performance of silane coupling agents,” *Journal of Adhesion Science and Technology*, vol. 5, no. 10, pp. 831–842, 1991.

[26] E. P. Plueddemann, “Silane adhesion promoters in coatings,” *Progress in Organic Coatings*, vol. 11, no. 3, pp. 297–308, 1983.

[27] T. Druffel, O. Buazza, M. Lattis, S. Farmer, M. Spencer, N. Mandzy, and E. a. Grulke, "The role of nanoparticles in visible transparent composites," in *Nanotechnology Applications in Coatings*, Z. Gaburro, S. Cabrini, and D. Talapin, Eds. San Diego, CA: , 2008, p. 70300F–70309.

[28] J. M. Antonucci, S. H. Dickens, and B. O. Fowler, "Chemistry of Silanes : Interfaces in Dental Polymers and Composites," *Journal Of Research Of The National Institute Of Standards And Technology*, vol. 110, no. 5, pp. 541–558, 2005.

[29] J. W. Stansbury, M. Trujillo-Lemon, H. Lu, X. Ding, Y. Lin, and J. Ge, "Conversion-dependent shrinkage stress and strain in dental resins and composites.," *Dental materials*, vol. 21, no. 1, pp. 56–67, Jan. 2005.

[30] C. J. Kleverlaan and A. J. Feilzer, "Polymerization shrinkage and contraction stress of dental resin composites," *Dental Materials*, vol. 21, no. 12, pp. 1150–7, Dec. 2005.

[31] J. Ge, M. Trujillo, and J. Stansbury, "Synthesis and photopolymerization of low shrinkage methacrylate monomers containing bulky substituent groups," *Dental Materials*, vol. 21, no. 12, pp. 1163–9, Dec. 2005.

[32] J. L. Ferracane, "Current trends in dental composites.," *Critical Reviews in Oral Biology and Medicine*, vol. 6, no. 4, pp. 302–318, Jan. 1995.

[33] J. L. Ferracane, "Placing Dental Composites—A Stressful Experience," *Operative Dentistry*, vol. 33, no. 3, pp. 247–257, May 2008.

[34] K. D. Jandt and B. W. Sigusch, "Future perspectives of resin-based dental materials," *Dental Materials*, vol. 25, no. 8, pp. 1001–6, Aug. 2009.

[35] L. Giachetti, D. Scaminaci Russo, C. Bambi, and R. Grandini, "A review of polymerization shrinkage stress: current techniques for posterior direct resin restorations.," *The Journal of Contemporary Dental Practice*, vol. 7, no. 4, pp. 79–88, Sep. 2006.

[36] A. Versluis, D. Tantbirojn, M. R. Pintado, R. DeLong, and W. H. Douglas, "Residual shrinkage stress distributions in molars after composite restoration.," *Dental Materials*, vol. 20, no. 6, pp. 554–64, Jul. 2004.

[37] P. Ausiello, A. Apicella, and C. L. Davidson, "Effect of adhesive layer properties on stress distribution in composite restorations - a 3D finite element analysis," *Dental Materials*, vol. 18, pp. 295–303, 2002.

[38] L. F. J. Schneider, L. M. Cavalcante, and N. Silikas, "Shrinkage Stresses Generated during Resin-Composite Applications: A Review.," *Journal of Dental Biomechanics*, vol. 2010, pp. 1–40, Jan. 2010.

[39] J. E. Elliott, L. G. Lovell, and C. N. Bowman, “Primary cyclization in the polymerization of bis-GMA and TEGDMA: a modeling approach to understanding the cure of dental resins,” *Dental Materials*, vol. 17, no. 3, pp. 221–229, 2001.

[40] R. H. Halvorson, R. L. Erickson, and C. L. Davidson, “The effect of filler and silane content on conversion of resin-based composite.,” *Dental Materials*, vol. 19, no. 4, pp. 327–33, Jun. 2003.

[41] E. C. Munksgaard, A. Peutzfeldt, and E. Asmussen, “Elution of TEGDMA and BisGMA from a resin and a resin composite cured with halogen or plasma light,” *European Journal of Oral Sciences*, vol. 108, no. 4, pp. 341–5, Aug. 2000.

[42] J. E. Klee, F. Neidhart, and R. Mu, “Monomers for low shrinking composites , 2 Synthesis of branched methacrylates and their application in dental composites,” *Macromolecular Chemistry and Physics*, vol. 523, no. 3, pp. 517–523, 1999.

[43] K. M. Choi and J. W. Stansbury, “New Families of Photocurable Oligomeric Fluoromonomers for Use in Dental Composites,” *Chemistry of Materials*, vol. 4756, no. 20, pp. 2704–2707, 1996.

[44] C. M. Chung, M. S. Kim, J. G. Kim, and D. O. Jang, “Synthesis and photopolymerization of trifunctional methacrylates and their application as dental monomers,” *Journal of Biomedical Materials Research*, vol. 62, no. 4, pp. 622–7, Dec. 2002.

[45] J. A. Payne, L. F. Francis, and A. V. McCormick, “The effects of processing variables on stress development in ultraviolet-cured coatings,” *Journal of Applied Polymer Science*, vol. 66, no. 7, pp. 1267–1277, Nov. 1997.

[46] R. Guggenberger and W. Weinmann, “Exploring beyond methacrylates,” *American Journal of Dentistry*, vol. 13, pp. 82 – 85, 2000.

[47] W. Weinmann, C. Thalacker, and R. Guggenberger, “Siloranes in dental composites,” *Dental Materials*, vol. 21, no. 1, pp. 68–74, Jan. 2005.

[48] N. B. Cramer, C. L. Couch, K. M. Schreck, J. a Carioscia, J. E. Boulden, J. W. Stansbury, and C. N. Bowman, “Investigation of thiol-ene and thiol-ene-methacrylate based resins as dental restorative materials.,” *Dental Materials*, vol. 26, no. 1, pp. 21–8, Jan. 2010.

[49] C. J. Kloxin, T. F. Scott, and C. N. Bowman, “Stress relaxation via addition-fragmentation chain transfer in a thiol-ene photopolymerization.,” *Macromolecules*, vol. 42, no. 7. pp. 2551–2556, 14-Apr-2009.

[50] H. Y. Park, C. J. Kloxin, T. F. Scott, and N. Christopher, “Stress Relaxation by Addition-Fragmentation Chain Transfer in Highly Crosslinked Thiol-Yne Networks,” *Macromolecular Theory and Simulations*, vol. 43, no. 24, pp. 10188–10190, 2011.

[51] D. Tantbirojn, C. S. Pfeifer, R. R. Braga, and A. Versluis, “Do low-shrink composites reduce polymerization shrinkage effects?,” *Journal of Dental Research*, vol. 90, no. 5, pp. 596–601, May 2011.

[52] S. Klapdohr and N. Moszner, “New Inorganic Components for Dental Filling Composites,” *Monatshefte fur Chemie*, vol. 136, no. 1, pp. 21–45, Dec. 2005.

[53] Y. T. Miki Iga, Fumio Takeshige, Mitsuo Torii, “The Relationship between Polymerization Shrinkage Measured by a Modified Dilatometer and the Inorganic Filler Content of Light-Cured Composites,” *Dental Materials Journal*, vol. 10, no. 1, pp. 38–45, 1991.

[54] K. Baroudi, A. M. Saleh, N. Silikas, and D. C. Watts, “Shrinkage behaviour of flowable resin-composites related to conversion and filler-fraction.,” *Journal of Dentistry*, vol. 35, no. 8, pp. 651–5, Aug. 2007.

[55] S. Garoushi, P. K. Vallittu, D. C. Watts, and L. V. J. Lassila, “Effect of nanofiller fractions and temperature on polymerization shrinkage on glass fiber reinforced filling material,” *Dental Materials*, vol. 4, pp. 606–610, 2007.

[56] Q. Chen, I. Chasiotis, C. Chen, and a Roy, “Nanoscale and effective mechanical behavior and fracture of silica nanocomposites,” *Composites Science and Technology*, vol. 68, no. 15–16, pp. 3137–3144, Dec. 2008.

[57] H. Wagner and R. Vaia, “Nanocomposites: issues at the interface,” *Materials Today*, vol. 7, no. 11, pp. 38–42, Nov. 2004.

[58] B. L. Cadenaro M, Codan B, Navarra CO, Marchesi G, Turco G, Di Lenarda R, “Contraction stress, elastic modulus, and degree of conversion of three flowable composites,” *European journal of Oral Sciences*, vol. 119, pp. 241–245, 2011.

[59] S. Lin-Gibson, L. Sung, A. M. Forster, H. Hu, Y. Cheng, and N. J. Lin, “Effects of filler type and content on mechanical properties of photopolymerizable composites measured across two-dimensional combinatorial arrays.,” *Acta Biomaterialia*, vol. 5, no. 6, pp. 2084–94, Jul. 2009.

[60] K. Masouras, N. Silikas, and D. C. Watts, “Correlation of filler content and elastic properties of resin-composites.,” *Dental Materials*, vol. 24, no. 7, pp. 932–9, Jul. 2008.

[61] H. Lu, J. W. Stansbury, S. H. Dickens, F. C. Eichmiller, and C. N. Bowman, “Probing the origins and control of shrinkage stress in dental resin composites. II. Novel method of simultaneous measurement of polymerization shrinkage stress and conversion.,” *Journal of biomedical materials research. Part B, Applied biomaterials*, vol. 71, no. 1, pp. 206–13, Oct. 2004.

[62] K. S. Wilson and J. M. Antonucci, “Interphase structure-property relationships in thermoset dimethacrylate nanocomposites.,” *Dental materials : official publication of the Academy of Dental Materials*, vol. 22, no. 11, pp. 995–1001, Nov. 2006.

[63] I. D. Sideridou and M. M. Karabela, “Effect of the amount of 3-methacyloxypropyltrimethoxysilane coupling agent on physical properties of dental resin nanocomposites.,” *Dental materials : official publication of the Academy of Dental Materials*, vol. 25, no. 11, pp. 1315–24, Nov. 2009.

[64] S. Debnath, “Silane treatment effects on glass/resin interfacial shear strengths,” *Dental Materials*, vol. 19, no. 5, pp. 441–448, Jul. 2003.

[65] S. Debnath, R. Ranade, S. L. Wunder, J. McCool, K. Boberick, and G. Baran, “Interface effects on mechanical properties of particle-reinforced composites.,” *Dental Materials*, vol. 20, no. 7, pp. 677–86, Sep. 2004.

[66] Q. Liu, J. Ding, D. E. Chambers, S. Debnath, S. L. Wunder, and G. R. Baran, “Filler-coupling agent-matrix interactions in silica/polymethylmethacrylate composites.,” *Journal of Biomedical Materials Research*, vol. 57, no. 3, pp. 384–93, Dec. 2001.

[67] B. Pukanszky, “Interfaces and interphases in multicomponent materials: past, present, future,” *European Polymer Journal*, vol. 41, no. 4, pp. 645–662, Apr. 2005.

[68] W. L. Tham, W. S. Chow, and Z. a. M. Ishak, “Effects of titanate coupling agent on the mechanical, thermal and morphological properties of poly(methyl methacrylate)/hydroxyapatite denture base composites,” *Journal of Composite Materials*, May 2011.

[69] K.-J. Soderholm, “Review of the fracture toughness approach.,” *Dental Materials*, vol. 26, no. 2, pp. e63–77, Feb. 2010.

[70] K. S. Wilson, K. Zhang, and J. M. Antonucci, “Systematic variation of interfacial phase reactivity in dental nanocomposites.,” *Biomaterials*, vol. 26, no. 25, pp. 5095–103, Sep. 2005.

[71] N. Nishiyama, T. Ishizaki, K. Horie, M. Tomari, and M. Someya, “Novel polyfunctional silanes for improved hydrolytic stability at the polymer-silica interface,” *Journal of Biomedical Materials Research*, vol. 25, pp. 213–221, 1991.

[72] H. Ishida and J. L. Koenig, “The Reinforcement Mechanism of Fiber-Glass Reinforced Plastics Under Wet Conditions: A Review,” *Polymer Engineering & Science*, vol. 18, no. 2, 1978.

[73] Z. Demmjen and B. Pukanszky, “Effect of Surface Coverage of Silane Treated CaCO3, on the Tensile Properties of Polypropylene Composites,” *Polymer Chemistry*, vol. 18, no. 6, pp. 741–747, 1997.

[74] M. W. Beatty, M. L. Swartz, B. K. Moore, R. W. Phillips, and T. a Roberts, "Effect of microfiller fraction and silane treatment on resin composite properties.," *Journal of biomedical materials research*, vol. 40, no. 1, pp. 12–23, Apr. 1998.

[75] B. Lim, "Effect of filler fraction and filler surface treatment on wear of microfilled composites," *Dental Materials*, vol. 18, no. 1, pp. 1–11, Jan. 2002.

[76] J. Luo, R. Seghi, and J. Lannutti, "Effect of silane coupling agents on the wear resistance of polymer-nanoporous silica gel dental composites," *Materials Science and Engineering: C*, vol. 5, no. 1, pp. 15–22, Sep. 1997.

[77] J. R. Condon and J. L. Ferracane, "Reduced polymerization stress through non-bonded nanofiller particles.," *Biomaterials*, vol. 23, no. 18, pp. 3807–15, Sep. 2002.

[78] J. R. Condon and J. L. Ferracane, "Reduction of composite contraction stress through non-bonded microfiller particles.," *Dental Materials*, vol. 14, no. 4, pp. 256–60, Jul. 1998.

[79] P. Chaijareenont, H. Takahashi, N. Nishiyama, and M. Arksornnukit, "Effect of different amounts of 3-methacryloxypropyltrimethoxysilane on the flexural properties and wear resistance of alumina reinforced PMMA," *Dental Materials Journal*, vol. 31, no. 4, pp. 623–628, 2012.

[80] I. D. Sideridou and M. M. Karabela, "Effect of the amount of 3-methacyloxypropyltrimethoxysilane coupling agent on physical properties of dental resin nanocomposites.," *Dental Materials*, vol. 25, no. 11, pp. 1315–24, Nov. 2009.

[81] K. S. Wilson, A. J. Allen, N. R. Washburn, and J. M. Antonucci, "Interphase effects in dental nanocomposites investigated by small-angle neutron scattering," *Journal of Biomedical Materials Research Part A*, 2006.

[82] J. P. Matinlinna, L. V. J. Lassila, M. Ozcan, A. Yli-Urpo, and P. K. Vallittu, "An introduction to silanes and their clinical applications in dentistry.," *The International Journal of Prosthodontics*, vol. 17, no. 2, pp. 155–64, 2004.

[83] J. P. Matinlinna, L. V. J. Lassila, and P. K. Vallittu, "Evaluation of five dental silanes on bonding a luting cement onto silica-coated titanium.," *Journal of Dentistry*, vol. 34, no. 9, pp. 721–6, Oct. 2006.

[84] J. P. Matinlinna, M. Ozcan, L. V. J. Lassila, and P. K. Vallittu, "The effect of a 3-methacryloxypropyltrimethoxysilane and vinyltriisopropoxysilane blend and tris(3-trimethoxysilylpropyl)isocyanurate on the shear bond strength of composite resin to titanium metal.," *Dental Materials*, vol. 20, no. 9, pp. 804–13, Nov. 2004.

[85] W. Weinmann, C. Thalacker, and R. Guggenberger, "Siloranes in dental composites," *Dental Materials*, vol. 21, no. 1, pp. 68–74, Jan. 2005.

[86] B. Zhao, “Polymer brushes: surface-immobilized macromolecules,” *Progress in Polymer Science*, vol. 25, no. 5, pp. 677–710, Jun. 2000.

[87] S. Minko, “Responsive Polymer Brushes,” *Polymer Reviews*, vol. 46, no. 4, pp. 397–420, Dec. 2006.

CHAPTER 2

OBJECTIVES

Polymer-based dental restorative materials continue to be plagued with the inherent problem of polymerization shrinkage and the resultant stress due to their placement in a confined setting in a clinical situation. Materials innovations in this field have continued to make significant and constant progress, especially in the last few years. However, the problem of polymerization stress development, which challenges the dentin adhesive bond formation and stability, has not been solved. One of the issues is the complexity of dental restorative formulations in terms of filler sizes and loading levels, monomers, initiator systems and curing protocols. Minor changes in even one of these factors can result in significantly different double bond conversion, which ultimately affects the development of the mechanical properties of the final composite modulus, shrinkage and stress. There is an intricate relationship between these properties and that needs to be explored and understood to be able to devise mechanisms to alleviate stress.

The major focus of research in the field of polymeric dental restoratives has been in two areas – 1) Fillers and 2) Monomers. Fillers are used in a variety of sizes, from micrometers to nanometers, and are also made of different materials, depending on the application. While the majority of current commercial dental composite materials continue to rely on a relatively small set of common dimethacrylate monomers to formulate the resin matrix phase, new monomer development has focused on making low shrinkage materials assuming the lower shrinkage will lead to lower stress. A crucial element of the formulation has, however, been neglected and that is the interface between the fillers and the monomers. Interface integrity in a composite is

extremely essential for the load bearing composite to transfer any developed or applied stresses to the high modulus filler particles. Very little innovation has been done in exploring the potential contribution of the silane coupling agent-based interface towards stress development or reduction.

Given this background on the current state of affairs in the area of dental restoratives, this thesis has focused on exploring the relationship that shrinkage stress has with other material properties. A novel strategy to reduce shrinkage stress has been developed by the modification of the interface between fillers and monomers. The following aims form the more specific aspects of this research:

- Investigate the effects of double bond conversion and filler loading on development of shrinkage stress. Explore the individual contributions made by modulus and shrinkage in the evolution of stress.

- To use the interface between filler particles and the monomer phase as a means of reducing shrinkage stress in composites. Explore the effect of the interface modification on optical properties of composites.

- Investigate stress relaxation as a component of stress evolution in unfilled resin and filled composite as a function of double bond conversion. Study the effect of the interfacial layer on stress relaxation.

Stress development in a polymerizing composite is a complex process that depends on the development of modulus and shrinkage. In commercial dental restoratives, this process is further convoluted by wide variation in filler and monomer compositions and curing conditions, all of which affect monomer conversion. In order to understand this interplay between the different parameters, Chapter 3 examines the development of stress and its dependence on modulus and shrinkage, as a function of filler loading and double bond conversion. A monomer mixture consisting of BisGMA/TEGDMA in the weight ratio 70:30 is used as a representative model resin system. Barium glass with average size 0.7 μm is used as the filler. Double bond conversion and filler loading are independently varied to cover a wide range. This study enables a detailed, systematic evaluation of the relative contributions of modulus and shrinkage as the stress develops as a consequence of increasing double bond conversion. Knowing these contributions can help in understanding the fundamental aspects of polymerization-induced stress and also assist in the design of new materials that exhibit low shrinkage stress based on the rational selection of component materials with the appropriate moduli and shrinkage characteristics.

Chapter 4 provides an evaluation of a novel method of reducing shrinkage stress in composites by the surface treatment of filler particles. Filler surfaces are modified with oligomers of varying molecular weights. Oligomeric species were selected so that they had hydroxyl groups that can be readily converted to methacrylate groups by attaching isocyanatoethylmethacrylate (IEM), which can then polymerize with the methacrylate-based resin. Two levels of functionalization of the hydroxyl groups were selected – in one case, 10 % of the hydroxyl groups on the oligomer were reacted with IEM and in the second case, 100 % of the hydroxyl groups were reacted with the IEM. The different molecular weights of the

oligomers and the methacrylate functionalities were hypothesized to have a significant effect on the shrinkage stress and this was indeed found to be the case.

The results of Chapter 4 are based on commercially available oligomers and the encouraging reduction in shrinkage stress that was achieved motivated additional work with in-house synthesized oligomers. Preparation of the oligomers instead of using commercial materials enables specific properties to be tailored. This strategy was employed in Chapter 5, which is a more in-depth inspection into the mechanism of stress reduction based on the interface modification. Two series of oligomers are made, rigid and flexible, by combining different diacrylate and dithiol monomers in various ratios to attain different molecular weights. The rigid oligomers have an aromatic backbone and have a higher glass transition temperature than the flexible oligomers, which have an aliphatic backbone structure. As in Chapter 4, the monomers used to prepare the oligomers are chosen to have available hydroxyl groups that subsequently can be converted to methacrylate groups via IEM addition, giving controlled levels of functionality to interact covalently with the methacrylate-based resin matrix. The systems obtained by mixing of the modified fillers with the resin system are studied using a variety of techniques to elucidate the effect of the oligomer modification of fillers on shrinkage stress. These include rheology, transmission electron microscopy and positron annihilation lifetime spectroscopy, among others.

Having elucidated a mechanism for reduction of stress in Chapter 5, it is important to delve deeper into the overall stress development in polymer-based composites. Stress evolution is composed of stress development and stress relaxation. Polymers being viscoelastic materials have a tendency to relax stress that is built upon an induced strain. This tendency of the material to relax stress is important in a polymerizing system that is constrained by bonded surfaces, as

this is the scenario for a restoration placed in a dental cavity. Chapter 6 explores the phenomenon of classic stress relaxation in which an instantaneous strain is imposed on various materials. The systems studied are 1) the unfilled BisGMA/TEGDMA resin, 2) the same resin system with 0.7 μm filler at 60 wt % loading, 3) this resin containing a fumed silica filler (Aerosil OX50, average diameter 40 nm) surface treated with γ-MPS, which is a control, and 4) OX50 fillers surface treated with a high molecular weight rigid oligomer that was used in Chapter 5. The stress relaxation behavior for all these systems is examined as a function of double bond conversion. The study is important as it helps to draw out differences in the rate and magnitude of stress relaxation that can be attributed to the filler surface modification as well as providing a better understanding of the overall stress evolution process. This can be instructive in the future design and optimization of surface treatments focused on stress reduction in composites.

After all the fundamental studies of the previous chapters, Chapter 7 looks toward applying the knowledge gained to a more practical scenario. Modern dental composites are formulated with a variety of fillers with dimensions that range from nanometers to micrometers. It is important to test whether the positive effects of the surface treatment on stress development can be applied to a situation in which there are fillers of both size ranges. For this, 0.7 μm glass particles and 40 nm OX50 particles are combined in various proportions in the model resin. The fillers are treated with γ-MPS that acts as the control and the high molecular weight rigid brush from Chapter 5. Along with polymerization stress measurements, the optical properties of these composites are also evaluated, since the esthetic appearance and potential depth of cure are also important considerations for dental composite materials.

Finally, Chapter 8 provides a conclusive summary and recommendations of future research directions and opportunities.

CHAPTER 3

DYNAMIC PROPERTY EVOLUTION IN POLYMERIC DENTAL RESTORATIVES: ROLE OF FILLER LOADING AND MONOMER CONVERSION

Abstract

Shrinkage stress in dental composites varies significantly based on material formulation as well as polymerization shrinkage and modulus, which are clearly contingent on reactive group conversion. There is a lack of fundamental research to bring these parameters together to get a comprehensive understanding of stress development in composite materials. This study examined the effect of shrinkage and modulus on the development of shrinkage stress as a function of conversion and filler loading. In a model photocurable dimethacrylate-based resin with a silane-treated particulate barium glass filler. Degree of conversion was controllably varied over a wide range allowing detailed correlated comparisons of shrinkage, modulus and stress evolution. Filler loading was varied in steps between 0 wt% and 70 wt%. It was found that shrinkage increased nearly linearly with respect to double bond conversion, while for a given value of conversion, it decreased proportionally with increasing filler content. At the highest level of conversion, the unfilled resin (0 wt%) had the highest shrinkage of 6.46 ± 0.07 vol% at a conversion of 69.9 ± 0.1 %, while the 70 wt% filled sample had a shrinkage of 3.88 ± 0.06 vol% at a conversion of 65.0 ± 0.1 %. The highest modulus for the unfilled resin was 2.88 ± 0.44 GPa at a conversion of 75.0 ± 1.0 % while that for the 70 wt% composite was 6.75 ± 0.30 GPa at 69 ± 1.5 % conversion with the modulus values rising disproportionately rapidly for the highest filler loading. The highest stress level for the unfilled resin sample was 3.00 ± 0.12 MPa at 68.9 ± 0.1 % conversion while that for the 70 wt% sample was 2.88 ± 0.07 MPa at 57.8 ± 0.1 % conversion. The effect of filler loading was to hasten the development of modulus and stress as conversion

progressed. It was concluded that the stress was proportional to the modulus and shrinkage when the actual shrinkage of the polymer was considered by taking the volume fraction of filler into account.

3.1 Introduction

Dental composite restoratives comprise a tremendously large segment of the biomaterials market. While these esthetic materials continue to be improved, polymerization shrinkage and the resulting shrinkage stress can be extremely detrimental to the performance of polymer-based dental restoratives [1–5]. The vast majority of these dental restoratives continue to be dimethacrylate-based and the monomers undergo significant shrinkage during polymerization [6], [7]. In a clinical setting, shrinkage is not allowed to occur freely as the polymerizing composite is covalently bonded to the tooth substrate to maintain mechanical integrity and an effective seal between the restoration and tooth. Failure to do so can result in marginal leakage between the tooth and the restoration further leading to problems such as marginal staining, secondary caries and post-operative sensitivity [8]. This constraint placed on shrinkage as the viscous composite paste converts into a glassy, high modulus material is the primary source for the buildup of stress within the composite [5]. The resulting stress is also transferred to the adhesive interface and into the adjacent tooth structure. The magnitude of the stress depends on the shrinkage and modulus of the composite, the interaction between the filler particles and the polymer, the exotherm generated due to the polymerization reaction and the boundary conditions under which the composite is cured. All the parameters responsible for stress development are affected by the formulation of the composite, which at the most basic level is composed of an organic resin matrix, reinforcing filler particles, coupling agent between the resin matrix and filler and an initiator system.

Since their introduction in the 1950s, polymeric dental restoratives have undergone significant changes in their formulation [9], along with a steady improvement in performance characteristics. Until the 1990s most of the research contributing towards the evolution of dental composites was in the area of filler development [10]. Filler sizes and composition changed drastically down from a diameter of 10-50 μm or more in the early dental composites to sub-micron range and even extending down to 5 nm in some of the modern nanocomposites [11]. Along with variations in size and composition of the fillers, the filler loading level has also been varied over a considerable range. The volume fraction of fillers in commercial composites span from about 25 % up to about 70 % [12], [13]. Low filled composites typically show lower moduli and strength but exhibit significant flow and adaptability prior to curing. Materials of this type are used in applications like anterior restorations in the oral cavity where there are lower masticatory forces as well as flowable composite liners that produce a somewhat adaptable interface [13]. Highly filled composites are used in posterior restorations where there is a need for sustaining higher recurring loads and greater wear resistance. As shrinkage is one of the main factors leading to high stresses in polymerizing dental restoratives, research over the last few years has focused on developing low shrinkage resins [1], [7], [14]. The changes in formulations also lead to a range of different limiting double bond conversions of the resin systems that form the matrix phase of the composite, due to progressive increases in light intensity used, light penetration through the material, activation system, kinetics and reaction exotherms.

Given a certain formulation, shrinkage stress would depend on shrinkage and modulus, the C-factor (configuration factor, representation of the constrained or bonded to unbonded surface area), viscoelastic behavior of the material, curing and boundary conditions. In this study the C-factor and boundary conditions were kept constant. The aim of this work is to

study the development of shrinkage, stress and flexure modulus as they change when a restorative goes from an uncured state to a fully cured material, with methacrylate conversion used as a coordinating index. In addition to this, filler loading has been varied to represent different loading levels in current commercial dental restoratives. Several studies have looked at the effect of filler loading on each of shrinkage, modulus and stress in isolation or some combination [15–18]. However, only a few ever report the conversion levels at which the measurements are done. The contention here is that an assessment of conversion is necessary to accompany any property measurement that displays conversion dependence to ensure that comparisons between different materials or even within a given material are legitimate. There is a lack of understanding of the effect of filler loading and monomer conversion on shrinkage, modulus and stress as well as how all these factors relate to the development of physical and mechanical properties of composite materials.

3.2 Materials and Methods

3.2.1 Materials

2,2-bis[4(2-hydroxy-3-methacryloxy-propyloxy)-phenyl] propane (Bis-GMA) and triethylene glycol dimethacrylate (TEGDMA) (donated by Esstech Inc., Essington, PA) were used in a 70:30 weight ratio as a model dental resin. A visible light initiating system consisting of 0.3 wt% camphorquinone (CQ) as initiator and 0.8 wt% ethyl 4-dimethylaminobenzoate (EDAB) (Sigma-Aldrich, Milwaukee, WI) as co-initiator was incorporated. Barium glass (mean particle size 0.7 μm) surface treated with a coating of 5 wt% γ-methacryloxypropyltrimethoxysilane (γ-MPS), was used as the inorganic filler (Esstech, Inc., Essington, PA). The filler was mixed with resin in varying amounts to obtain total final weight

percentages of 0, 20, 40, 60 and 70 which correspond to filler volume fractions of 0, 9.4, 21.6, 38.3 and 49.1 respectively, based on densities of filler (2.71 g/cm^3) and uncured resin (1.12 g/cm^3) [19]. Fillers and resin were blended in a centrifugal mixer (DAC 150 FVZ, Flakteck Inc.) to ensure thorough mixing.

3.2.2 Sample Curing

Visible light irradiation was provided by a halogen dental curing lamp (VIP, Bisco Inc., Schaumburg, IL). Light intensities and irradiation times were varied in order to achieve a wide range of conversions for specimens used in the various testing protocols. A Demetron Model 100 radiometer (Demetron Research, Danbury, CT, USA) was used to measure the output light intensity.

3.2.3 Infrared Spectroscopy

Double bond conversion in the resin and composite specimens was monitored in transmission mode using near-infrared (NIR) (Nexus 670, Nicolet Instruments, Madison, WI) spectroscopy. The area of the peak at 6165 cm^{-1} signifying the $=CH_2$ absorption was used to track the double bond conversion. All NIR measurements were taken at a wavenumber resolution of 4 cm^{-1}. For the static measurements, 64 scans per spectrum were taken for, while 2 scans per spectrum were used for collection of real-time series measurements.

3.2.4 Shrinkage Stress Measurement

Shrinkage stress was measured using a cantilever beam-based tensometer, which was designed and fabricated at the Paffenberger Research Center of the American Dental Association

Health Foundation (ADAHF – PRC, Gaithersburg, MD, USA). This device measures the dynamic tensile forces generated by a polymerizing sample that causes deflection of the calibrated beam. This force is used to calculate the stress generated in the sample. A more detailed description of the experimental technique has been reported in a previous study [1]. Briefly, a composite sample is placed between two cylindrical quartz rods that have been treated with a methacrylate functional silane to promote bonding with the resin in the composite. The lower quartz rod is fixed whereas the upper quartz rod is attached to the cantilever. A dental light is placed at the bottom of the lower quartz rod and light is transmitted through the rod and to the composite causing deflection of the cantilever based on the beam compliance. An LVDT (linear variable differential transformer) continuously tracks the beam deflection and this data is converted to a force measurement, which when divided by the composite cross-sectional area, provides the stress in the composite. The cavity in which the samples were placed was 6 mm in diameter and 1.5 mm in thickness. For the simultaneous measurement of conversion with shrinkage stress, the NIR signal was guided to/from the sample using optical fiber cables (1 mm diameter).

For the stress measurements, the samples were irradiated with the VIP curing light at an incident irradiance of 250 mW/cm^2 for 60, 10 and 5 s and also at 35 mW/cm^2 for 20, 10 and 5 s, to obtain a wide range of conversion and associated stress values. Irradiance was measured at the end of the quartz rod in contact with the sample. The coupled stress/conversion data was collected continuously for 15 min.

3.2.5 Shrinkage Measurement

Shrinkage was measured using a linometer (ACTA Foundation, Netherlands). In this method a liquid monomer or uncured composite paste sample was placed between a fixed upper glass plate and a freely moving aluminum disc, both of which are greased to provide radial freedom of movement for the shrinking sample, which allows the linear post-gel shrinkage to be recalculated in terms of volumetric shrinkage. Disc specimens of 6 mm in diameter and 1.5 mm in thickness were irradiated from the upper surface and the displacement of the aluminum disc was monitored by a LVDT to provide linear shrinkage. Irradiation intensity and times were used to coincide with those used for the stress measurements. Shrinkage was monitored continuously for 10 min. NIR scans of the sample were taken prior to polymerization and immediately after removal from the linometer to avoid any significant post-cure conversion development.

3.2.6 Flexure Modulus Measurement

Flexural modulus was measured in three-point bending (MTS 858 Mini Bionix II). The specimen dimensions were 2x2x10 mm. Samples were irradiated on one side and immediately inverted and irradiated from the opposite side in an effort to get uniform conversion throughout the sample. A range of light intensities, from 25 mW/cm^2 to 575 mW/cm^2, were used. Samples were cured for 30 to 60 s on each side. NIR spectra were obtained directly from the flexural test specimens before and immediately after curing. As soon as the NIR polymer spectrum was collected the sample was submitted to mechanical testing. Again this was done to ensure well correlated conversion and mechanical property results.

3.2.7 Scanning Electron Microscopy

Distribution of fillers in the polymer matrix was observed using a Field Emission Scanning Electron Microscope (JSM-7401F FESEM, JEOL, Japan). For this, samples were thoroughly polished using the following protocol. Each sample was first polished with different silicon carbide abrasive papers in increasing order of their grit numbers (240, 320, 600). After every polishing step, the samples were washed with copious amounts of DI water to remove all traces of material from the surface. The samples were further polished by rubbing them on three different cloth pads that had solutions of alumina powder (mean sizes – 5.0 µm, 0.3 µm and 0.05 µm) in DI water spread on them. The polished specimens were mounted on stubs and sputter coated with gold with an average thickness of 2 nm.

3.2.8 Vicker's Microhardness Test

Disc shaped specimens (2 mm thickness and 10 mm diameter) of each formulation were obtained by photopolymerization with the dental light at 700 mW/cm^2 for three minutes on each flat surface. The Vicker's hardness was measured using a microhardness tester (LM700AT, Leco). The specimens were indented with a diamond tip using a force of 300 gf for 15 s. The length of the indents was measured and the VHN was calculated using the following formula –

$$H = \frac{1854.4F}{d^2} \qquad [3.1]$$

Where, F is the applied force in gf and d is the size of the indent in millimeters.

3.3 Results and Discussion

This work examined the dynamic evolution of material properties including volumetric shrinkage, flexural modulus and stress in photopolymerizing dental composites with respect to methacrylate conversion and filler content as independent parameters. Both the parameters were systematically varied over a wide range to study the changes in the material property values. For each filler loading level, shrinkage, flexural modulus and stress were measured in separate experiments with essentially simultaneous measurement of conversion. The conversion measurements allowed rational comparison of all the interrelated properties and it facilitates understanding of the trends in their conversion-driven development.

The variation in volumetric shrinkage of the resin system as a function of methacrylate conversion for each filler loading level is represented in Figure 3.1. The maximum shrinkage for the unfilled resin was 6.5 ± 0.1 % at 69.9 ± 0.8 % conversion while that for the sample with 70 wt% filler loading was 3.9 ± 0.1 % at 65.0 ± 0.7 % conversion. The extrapolation of the static data in Figure 3.1 to zero shrinkage provides a slightly positive conversion intersect that can be expected from this post-gel shrinkage measurement technique. Shrinkage varied linearly with respect to conversion for low to moderate levels of conversion.as has been observed by several authors [20–22]. Studies have also noted the linear variation of shrinkage with respect to filler loading [15], [21], [23]. What is not noted normally, however, is a deceleration in the shrinkage rate as the limiting conversion is attained for all the samples. This phenomenon has been reported before in coupled dynamic shrinkage/conversion measurements [6] involving glassy, crosslinked networks. In the vitrified state, the bulk network densification and the continued molecular level reaction of free monomer and pendant groups tend to occur on diverging time scales, which results in excess free volume. Based on the broad structural heterogeneity that

characterizes dimethacrylate networks, residual monomer pockets may exist throughout the network that can still undergo polymerization. It is this increase in conversion that is seen to occur without significant change in shrinkage. It is expected that the cured composite sample will continue to densify over time and eventually more closely approximate the equilibrium thermodynamic free volume associated with a given conversion.

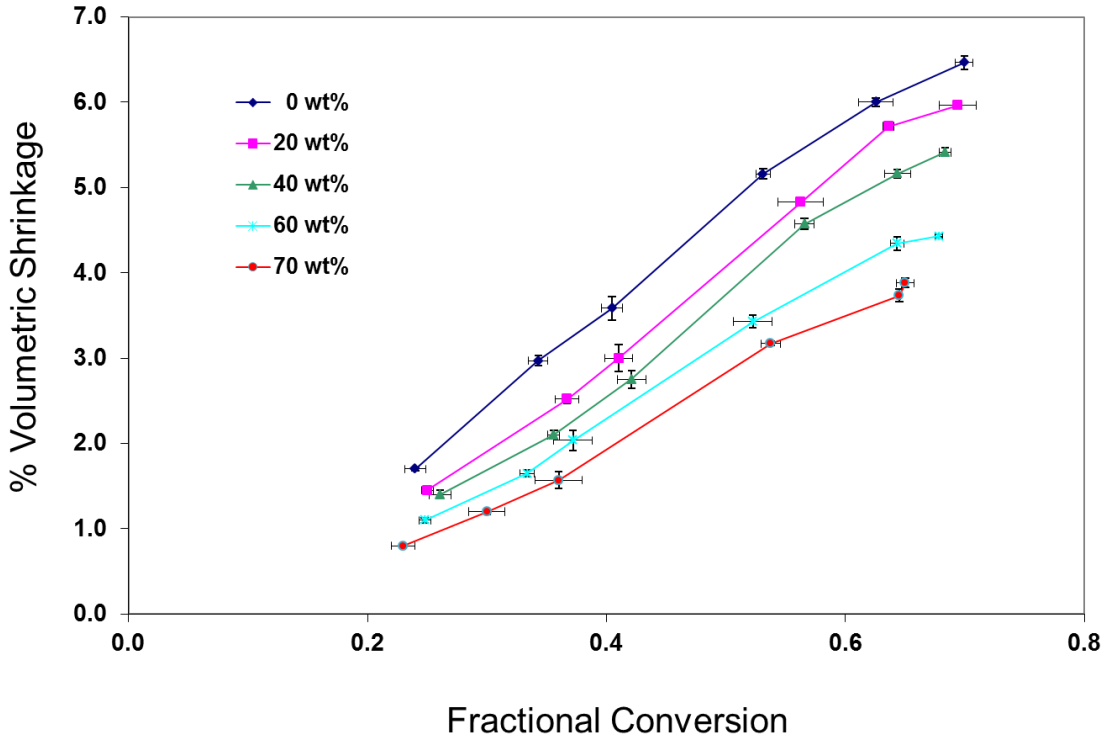

Figure 3.1. Variation of volumetric shrinkage as a function of conversion and filler loading – lines connecting data points are provided for visual assistance.

When variation of flexural modulus as a function of filler loading was considered with respect to conversion (Figure 3.2), there was a precipitous rise in the modulus for each filler loading level after an initial slow change. This rise in modulus can be associated with the onset of the glassy state of the material [24]. The accelerated rise in modulus occurred at progressively lower values of conversion as the filler content increased. This means that for any given level of

conversion, higher filler loading provides a higher modulus value. Studies measuring modulus of fully cured composites with respect to filler loading show an exponential rise in modulus as the amount of filler increases [25]. The positive effect of the filler on modulus is evident in that even though the limiting conversion is reduced as the filler content rises, the modulus values increase significantly. The rationale for the modest reduction in conversion with increasing filler includes a progressive reduction in overall light transmission and a reduced exothermic potential. Scattering and absorption of light by filler particles leads to a progressive reduction in light penetration as the thickness of the composite increases [26–28]. The reaction exotherm potential is also reduced by addition of filler due to the reduction in the overall reactive group concentration. These factors, along with the reduced mobility of the polymer and early vitrification, lead to the gradual lowering of conversion with increased filler loading. For an equivalent, lower level of conversion within the rubbery regime, there are relatively small differences in the modulus among composites containing 0 to 60 wt% filler fraction. The composite with 70 wt% filler fraction shows significantly higher modulus at all conversion levels compared to the other samples. As the filler fraction increases and the matrix shrinks with increasing conversion, there is increased potential for interparticle interactions due to the reduced spacing between the particles. As conversion increases, there is progressive covalent attachment between the filler surface with the densifying matrix and this additional reinforcement of the network also contributes to the late stage modulus development in addition to the corresponding increase in the matrix crosslink density. The most significant modulus effect associated with the filler would be expected where the filler surface affected interphase region becomes a continuous phase, which assuming a relatively small hybrid interphase dimension, would only be expected at very high filler loading levels.

Shrinkage stress and methacrylate conversion were measured simultaneously in real-time under different irradiation conditions. Figure 3.3 shows the variation in stress as conversion progresses at various loading levels, for the highest irradiance conditions (250 mW/cm^2 for 60 s). At the very early stages of polymerization, as conversion increases there is no corresponding rise in the shrinkage stress level. At about 5-6 % conversion, which reasonably approximates the gel point of dimethacrylate systems, stress begins to rise slowly. In order for the tensometer to start

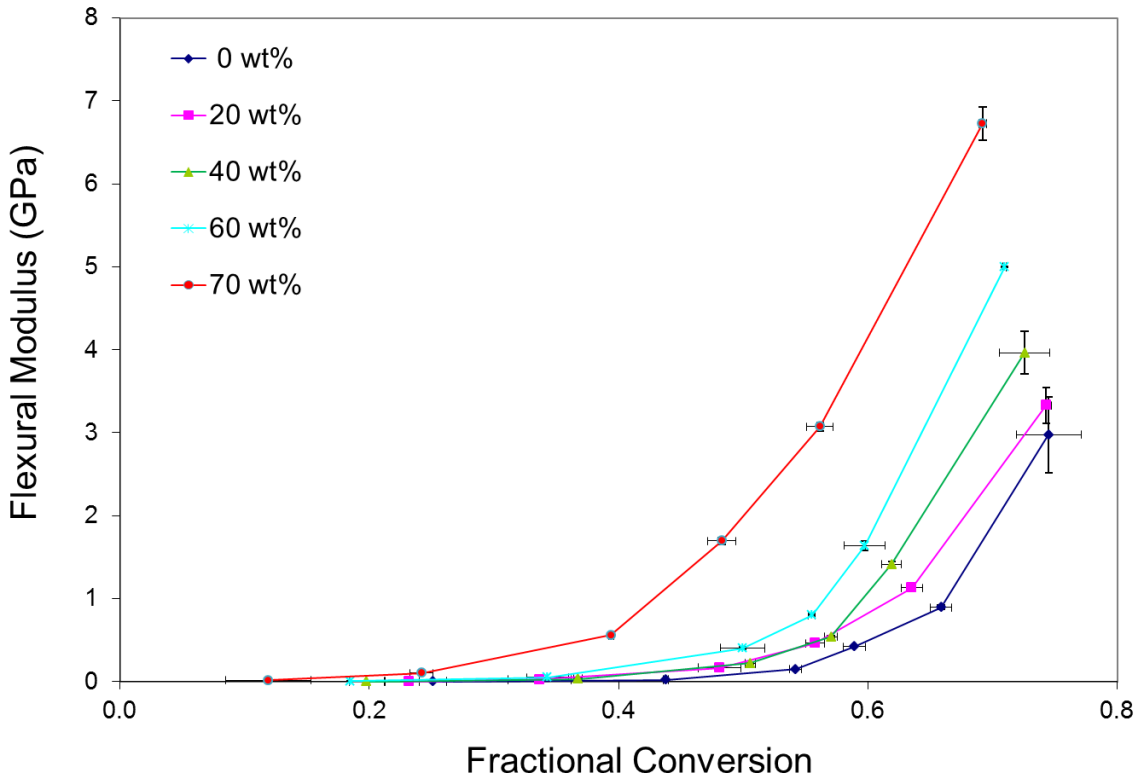

Figure 3.2. Flexural modulus development profiles as a function of conversion for different filler loading levels. Lines connecting the data points are provided for visual assistance.

registering a positive stress value, it is impicit that a continuous load-bearing network form within the sample and thereby covalently attach the upper and lower rods in the tensometer. This can only occur once the gel point has been reached along the z axis. Since gel point is achieved

very early in dimethacrylate network formation and our experience suggests that the reaction between the silane-treated glass rod of the tensometer and the sample is essentially instantaneous, we can say with confidence that the onset of stress development is very close to the gel-point of the sample. Shrinkage that occurs before the gel point does not contribute to stress since this stage of shrinkage is represented as viscous flow [29], [30] that has no elastic memory. After a steady increase in stress initially through the rubbery and leathery regimes, as the limiting conversion is reached in the final vitrification stage of polymerization, stress increases rapidly over a fairly narrow range of conversion. Bulk vitrification occurs when a significant portion of the sample's evolving T_g exceeds the effective curing temperature.

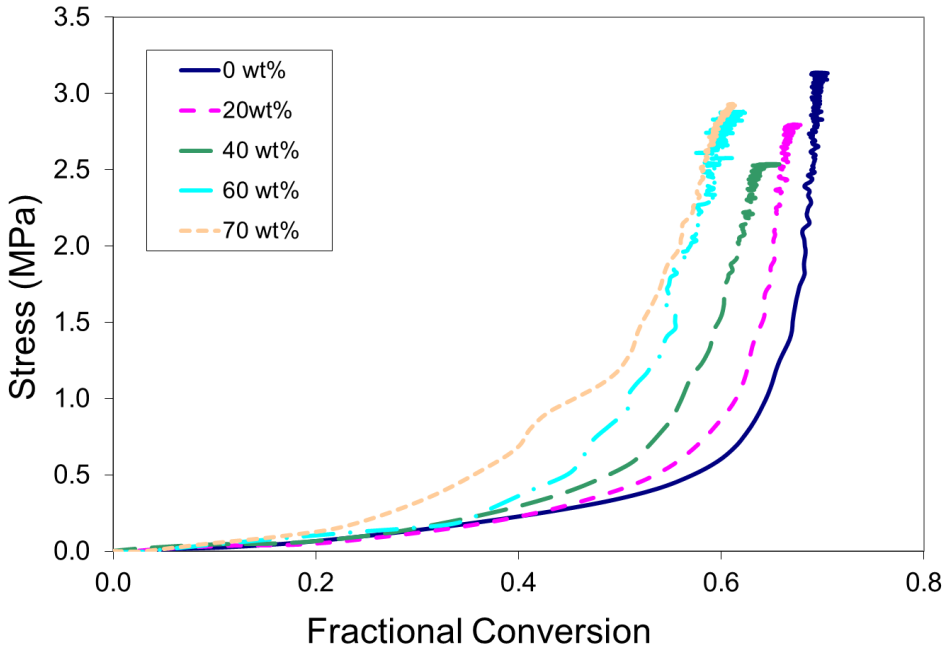

Figure 3.3. Real-time polymerization shrinkage stress versus conversion. Irradiation condition – 250 mW/cm^2 for 60 s.

Addition of increasing amounts of filler increases the available surface area that is in contact with the developing polymer phase. As mentioned earlier, the filler surface places restrictions on the mobility of the polymer in its immediate vicinity [31]. As the volume fraction

of fillers increases, this relatively immobile phase can cause reduced cooperative movement between the polymer chains. In addition to this, the contribution of the highly rigid filler particles to the overall composite modulus and the covalent linkage with the resin phase, all promote the earlier vitrification of the composite.

The dynamic stress data presented in Figure 3.3 represents just one of the irradiation conditions used during the stress measurements. Using the final values of stress and conversion at the end of each such run, Figure 3.4 was generated. It is evident that the progression of data in Figure 3.4 is very similar to the analogous dynamic data in Figure 3.3. This demonstrates that static measurements can be used to represent the dynamic progression of property development, as long as accurately correlated conversion data is included. There are a few subtle differences between the two plots. In considering just the end point of the real-time data, the effect of any exotherm during curing is lost. The exotherm contributes to a delay in vitrification with respect to the conversion and also imparts a thermal contraction effect to the dynamic measurement as the system cools beyond the point of the maximum reaction rate. In the static data, the change in the stress with respect to conversion is somewhat more gradual than in the real-time data.

Figure 3.5 shows the development of shrinkage, modulus and stress as a function of metharylate conversion, for the 0 and 70 wt% samples, which are compared here since they represent the extremes of filler loading for the samples considered in this study. Shrinkage increases linearly for the two samples, albeit at different rates, with respect to conversion due to the different resin phase volume fractions. Modulus and stress progress along an exponential route and follow each other closely. However, while the final stress levels achieved are similar, the final modulus of the unfilled resin remains much lower than that of the highly filled composite. At the limiting conversion for the stress values, in case of the 0 wt% sample, the

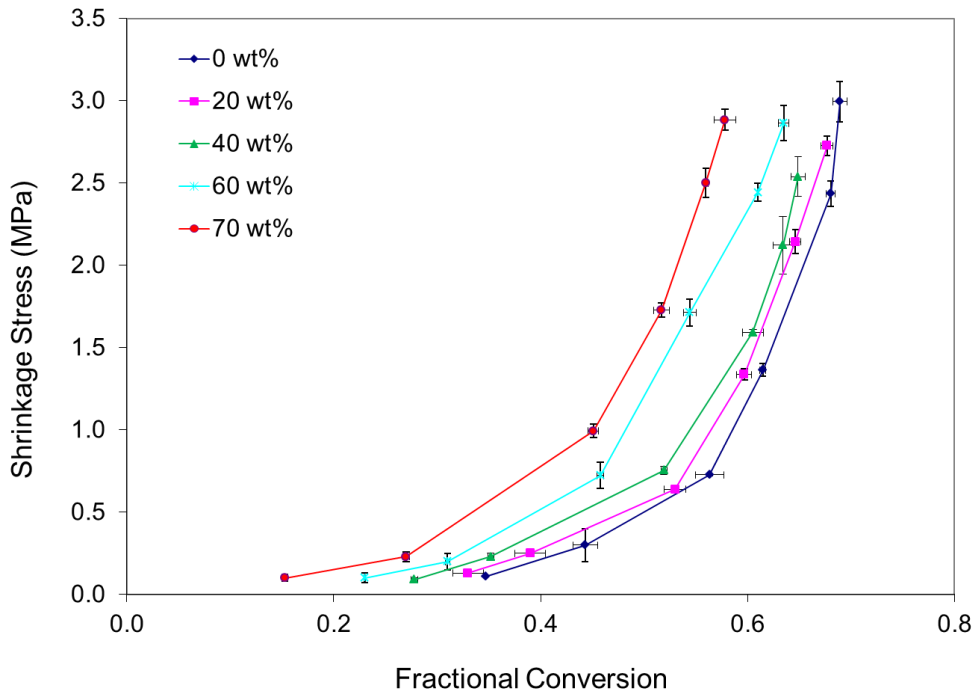

Figure 3.4. Plot of shrinkage stress as a function of conversion and filler loading. Lines connecting the data points are provided for visual assistance.

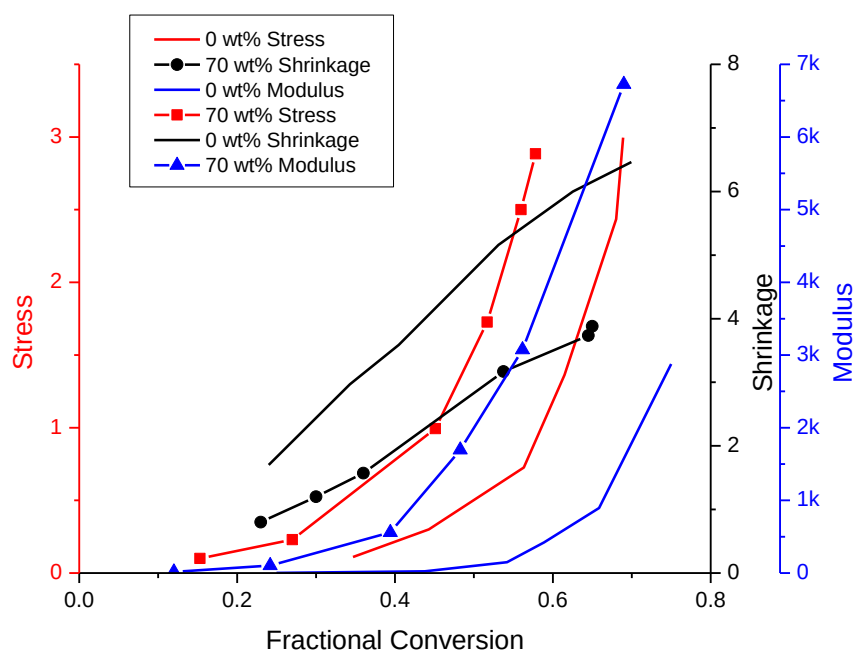

Figure 3.5 Plot of shrinkage, modulus and stress as a function of methacrylate conversion. Curves with only lines represent the unfilled resin and lines with points represent the 70 wt% composite. (Color legend: - Blue =Modulus; Black = Shrinkage; Red = Stress).

modulus is approximately 2.5 GPa and the shrinkage is 6.5 %, while for the 70 wt% filled sample, the modulus is about 3 GPa and the shrinkage is 3%. Multiplying modulus and percentage shrinkage to get the stress value, for the 0 wt% sample, in accordance with Hooke's law, gives a value of 16.3C MPa, where C is a proportionality factor that is assumed to be the same for both the systems. For the 70 wt% sample, this procedure gives us a stress value of 9.0C. Since the final stress values are the same, the discrepancy based on that predicted by Hooke's Law needs to be resolved. It should be noted that the 70 wt % sample has a resin volume of approximately 51 %. With this consideration, the effective strain experienced by the resin phase in the composite sample is double the value of measured strain. Taking this into account, the calculated stress is 18C, which is much closer to the value obtained for the 0 wt% sample. Therefore, the volume fraction of the resin of any material must be taken into account when considering the stress development potential. The small differences in the values can be explained by the fact that the samples are cured in different geometries and hence the exotherm effect is bound to be different in each measurement. Another factor that should be kept in mind is that the magnitude of the measured shrinkage stress values depends on compliance of the measuring system [32]. Higher elastic modulus due to higher filler loading led to high stress in a system with feedback to eliminate compliance [8], and a system with no compliance compensation was found to show that shrinkage stress reduced with filler loading [33]. In our system, we have tried to replicate the effect of a clinically relevant situation in which a shrinking composite causes a slight deflection of the bonded tooth substrate [34].

An alternate way of looking at the stress data is to compare the final stress values when the different samples are subjected to similar irradiation conditions or energy density (Figure 3.6). For the highest irradiance levels (Conditions 5 and 6 in Figure 3.6) the final shrinkage stress

reduces steadily along with conversion as the filler content is increased from 0 to 40 wt%. Above 40 wt% filler loading, the reduction in conversion continues as additional filler is incorporated, but the shrinkage stress increases. This trend is most prominent for the two highest irradiance conditions and less obvious or not present at all in the lower ranges of conversion (Conditions 1 – 4 in Figure 3.6). This has significant implications in a practical situation where a dentist may use a particular curing protocol, regardless of the formulation of the dental composite being used. With the wide variety of filler loading levels and monomer formulations available in current commercial dental restoratives, the same curing protocol used for all of them is certain to result in significant differences in final conversion, shrinkage, modulus and stress. For each particular material, there may exist a region where there is an acceptable target range of conversion that is sufficient for the modulus and other desirable material properties such as fracture toughness to be high and yet have a reasonably lower stress. It is imperative to employ a curing protocol that maximizes the benefits across a wide range of properties without overly sacrificing any one of them.

The effect of energy density on polymerization stress in commercial dental composites has been studied [35] with conversion and stress values found to have a tendency to level off at higher energy densities. Saturation of the conversion is in agreement with our results since the limiting conversion for all loading levels at the higher irradiance conditions is in a fairly narrow range. However, as the limiting conversion is reached, the stress values actually keep on increasing. The disagreement can be explained by the fact that the authors looked at a narrower range of conversion as compared to the range studied in the current research and the stress actually starts building up most rapidly at latter stages of conversion, after vitrification is reached.

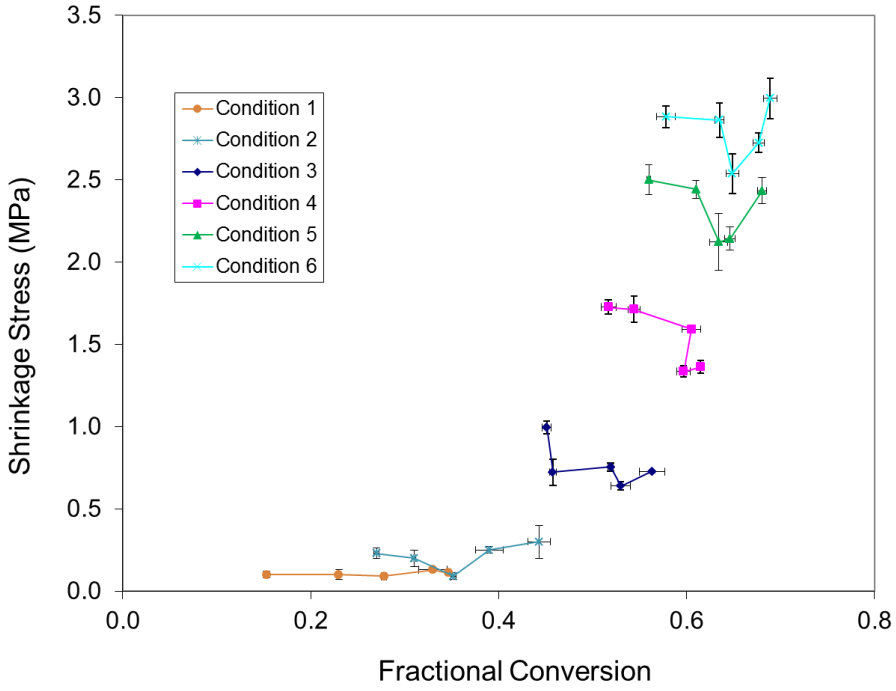

Figure 3.6. Plot of shrinkage stress versus fractional conversion. Each line represents the same irradiation condition but different filler contents – Condition 1 – 35 mW/cm^2 for 5 s; Condition 2 – 35 mW/cm^2 for 10 s; Condition 3 – 35 mW/cm^2 for 20 s; Condition 4 – 700 mW/cm^2 for 5 s; Condition 5 – 700 mW/cm^2 for 10 s; Condition 6 – 700 mW/cm^2 for 60 s. Lines connecting the data points are provided for visual assistance.

Fillers functionalized with a methacrylate silane added to a resin that is based on methacrylates react covalently with the resin upon polymerization. It has been observed that when fillers with non-functional silanes are introduced in a resin matrix, the resulting final stress is lower than composites with fillers that have functional silanes, at the same loading level [36]. This is due to the fact that the reactive surface silanes introduce additional constraints on the polymerizing resin, restricting free shrinkage. This can lead to higher stress concentrations at the surface of the fillers. With an increase in surface area, the magnitude of these stresses increases. Two opposing forces are at work here when the amount of filler is increased. At low to moderate filler loading levels, the fillers tend to reduce the amount of stress as compared to the unfilled resin matrix due to the reduction in total volume of the resin. At higher filler loading levels, the

increased modulus and surface area play a larger role and lead to an increase in shrinkage stress. The extent and type of surface coverage would definitely influence the magnitude of stress development.

Up to about 20 % conversion, there is essentially no difference in modulus as a function of filler loading (Figure 3.2). The stress follows the same trend (Figure 3.4) with the exception that the highest filler loading shows a trend towards higher early stage stress development. As conversion continues to increase, the filler loading level contributes to the dramatic increase in modulus with the corresponding increase in stress. At the lower levels of conversion, the covalent link between the particles and developing polymer is most likely not fully developed. Hence the particles are not able to constrain the resin and the modulus is still not very high resulting in low stress.At these lower levels of conversion, it is the conversion and not the filler particles that determine the modulus, and hence stress, of the composite, while at the higher levels of conversion, it is the modulus and filler loading that dominates to determine the stress levels.

SEM Characterization

Representative SEM images were obtained to examine the dispersion of the filler particles in the polymer matrix and the interparticle distance between them (Figure 3.7). It can be seen that as the filler loading increases, the average distance between the particle surfaces reduces. There are increased chances of particle-particle interactions at close distances and this can contribute to the increased modulus that is observed at all levels of monomer conversion. Also, as the distances between particles approach the nanometer scale, confinement effects due to the narrow spacing can come into play [37]. There is evidence that there is a change in the glass transition temperature of the polymer in the immediate vicinity of particle with respect to the bulk [38].

There can be a gradient in glass transition and consequently, modulus of the polymer layer around the particles. Though this effect possibly extends to a few nanometers, when particles are very close to each other, layers that have properties different from the bulk overlap and this can have a reinforcing effect. This seems to be reflected in the increased modulus of the 70 wt% sample, especially at higher values of conversion where the volumetric shrinkage of the resin phase effectively raises the filler volume fraction.

The abrupt rise of the modulus of the 70 wt% for all values of conversion is noteworthy and reinforces the concept of a threshold where particle-particle interactions become predominant. While modulus represents the bulk properties, the surface properties are also important for dental composites as it is the surface that has to withstand masticatory forces and display appropriate wear resistance. Indentation hardness tests give a relevant measure of the surface strength of materials. Figure 3.8 shows the variation in Vicker's hardness number (HV) with respect to filler loading. It can be seen that after a slow and steady rise in the hardness value, there is a more abrupt rise for the 70 wt% sample. This follows the same trend that the modulus values show with respect to filler loading levels and further highlights a transition from particle-resin to particle-particle interactions.

The proximity of interfaces of neighboring particles should also affect modulus development. The contribution of the surface-bound methacrylate groups from the fillers on the total methacrylate group concentration for the model composite can be seen in Figure 3.8. The peak area representing methacrylate group concentration, which is obtained from the uncured material NIR spectra (fixed pathlength and cross-section) is plotted as a function of filler loading. As filler content increases, the reduction in the volume of the resin lowers the overall methacrylate group concentration. The total methacrylate peak area is represented by curve (a).

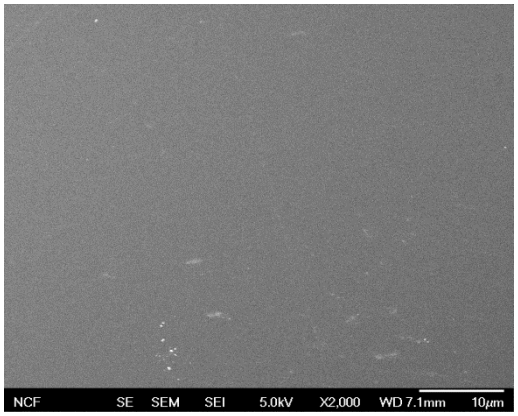

(a)

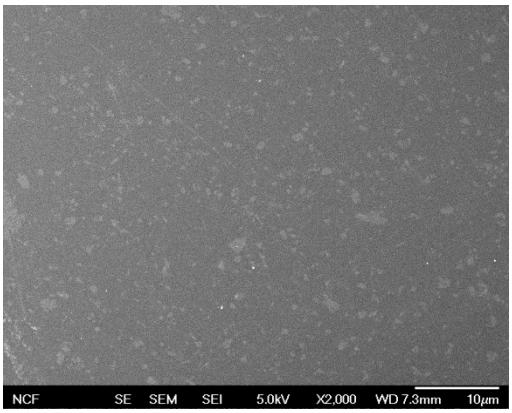

(b)

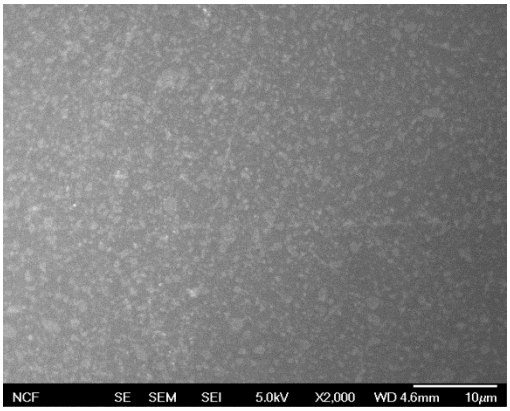

(c)

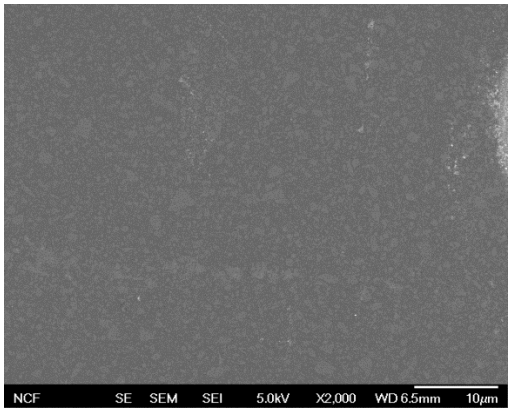

(d)

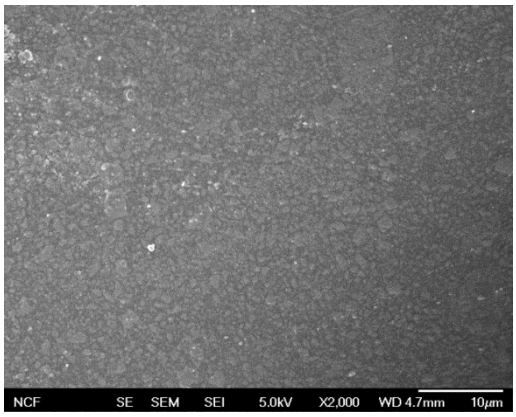

(e)

Figure 3.7. Scanning electron micrographs of polished surfaces of samples: (a) 0 wt%; (b) 20 wt%; (c) 40 wt%; (d) 60 wt%; (e) 70 wt%. All images are taken at 2000x magnification. The scale bar is 10 µm.

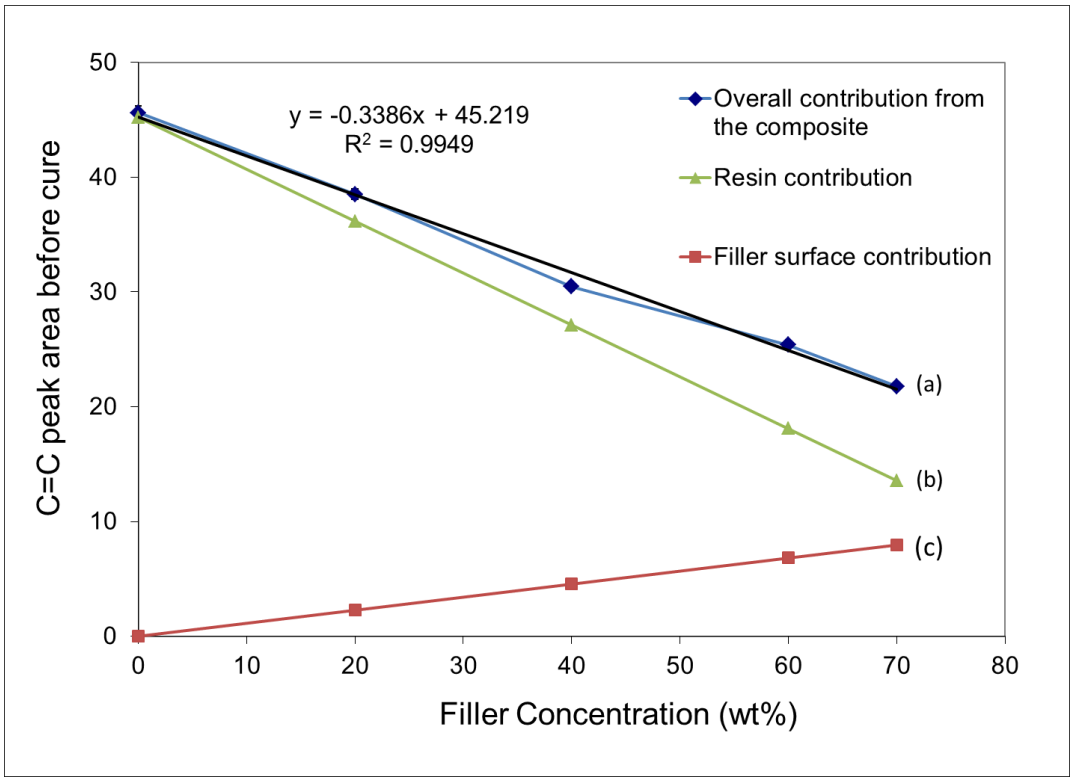

Figure 3.8. Contribution to methacrylate peak areas as a function of filler loading level from: (1) Composite (♦), (2) Resin (▲) and (3) Interface (■).

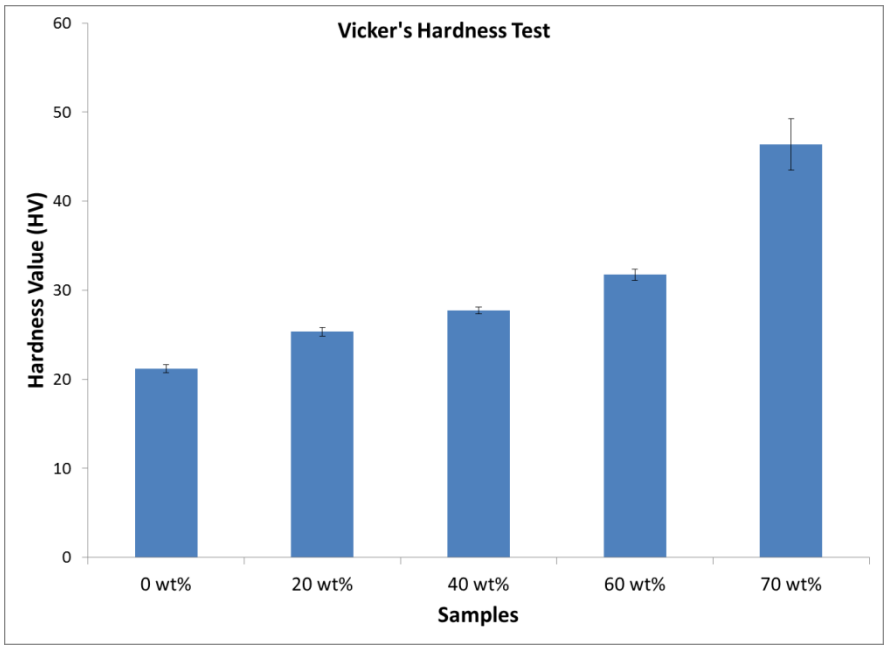

Figure 3.9. Vicker's hardness number (HV) as a function of filler loading.

This includes contributions from the bulk matrix as well as the surface-bound methacrylates. The contribution from just the resin can be calculated by using the volume fraction of the resin and the peak area for an unfilled resin sample (curve (b)). These values are lower than the overall methacrylate contribution, indicating that there is contribution from the filler surface. The difference between the two curves can be used to generate curve (c), which is an estimate of the contribution to the total methacrylate groups from those that are attached to the filler surface. As the filler content increases, the contributions from the resin and the filler approach each other and the filler contribution becomes increasingly significant. Given that the fillers used in this study are surface treated with a 5 wt% layer of silane and considering the available filler surface area, the thickness of the silane layer can be significant. At high loading levels, it is quite possible that the interfacial layers of silane on neighboring particles would impinge on each other. This interaction of neighboring interface regions also explains the accelerated increase in modulus at the highest filler loading level (70 wt%).

Vicker's Hardness Test

The abrupt rise of the modulus of the 70 wt% for all values of conversion is noteworthy and reinforces the concept of a threshold where particle-particle interactions become predominant. While modulus represents the bulk properties, the surface properties are also important for dental composites as it is the surface that has to withstand masticatory forces and display appropriate wear resistance. Indentation hardness tests give a relevant measure of the surface strength of materials. Figure 3.9 shows the variation in Vicker's hardness number (HV) with respect to filler loading. It can be seen that after a slow and steady rise in the hardness value, there is a more abrupt rise for the 70 wt% sample. This follows the same trend that the

modulus values show with respect to filler loading levels and further highlights a transition from particle-resin to particle-particle interactions.

3.4 Conclusion

The evolution of shrinkage, modulus and shrinkage stress was evaluated as a function of filler loading and metharylate group conversion. It was found that shrinkage varied linearly with conversion, while stress and modulus exhibited exponential behavior. The final value of stress in the filled systems appeared to be lower than what would be expected by the magnitude of the modulus and shrinkage. Taking the actual shrinkage of the polymer into consideration by subtracting the volume fraction of the filler solved this anomaly and the stress appeared to be proportional to the product of modulus and shrinkage for the entire range of conversion. The use of conversion as a basis for measurement for all the properties allowed legitimate comparison of all the measured properties. Further work can be done in a similar manner by incorporating fillers of different sizes, to represent current commercial dental composites that have mixed sizes of fillers.

3.5 Acknowledgements

The authors would like to thank the National Institutes of Health for support of this research through the grant NIH/NIDCR- R01DE014227. We also wish to thank Septodont-Confi-Dental and Evonik for their gracious donation of filler materials and Esstech, Inc. for donation of monomers.

3.6 References

[1] J. W. Stansbury, M. Trujillo-Lemon, H. Lu, X. Ding, Y. Lin, and J. Ge, "Conversion-dependent shrinkage stress and strain in dental resins and composites.," *Dental Materials*, vol. 21, no. 1, pp. 56–67, Jan. 2005.

[2] L. F. J. Schneider, L. M. Cavalcante, and N. Silikas, "Shrinkage Stresses Generated during Resin-Composite Applications: A Review," *Journal of Dental Biomechanics*, vol. 2010, pp. 1–15, 2010.

[3] S. J. Sadowsky, "An overview of treatment considerations for esthetic restorations: a review of the literature," *The Journal of Prosthetic Dentistry*, vol. 96, no. 6, pp. 433–42, Dec. 2006.

[4] J. L. Ferracane, "Placing Dental Composites—A Stressful Experience," *Operative Dentistry*, vol. 33, no. 3, pp. 247–257, May 2008.

[5] J. L. Ferracane, "Developing a more complete understanding of stresses produced in dental composites during polymerization.," *Dental Materials*, vol. 21, no. 1, pp. 36–42, Jan. 2005.

[6] J. W. Stansbury, M. Trujillo-Lemon, H. Lu, X. Ding, Y. Lin, and J. Ge, "Conversion-dependent shrinkage stress and strain in dental resins and composites.," *Dental materials*, vol. 21, no. 1, pp. 56–67, Jan. 2005.

[7] C. N. Bowman, N. B. Cramer, and J. W. Sansbury, "Recent Advances and Developments in Composite Dental Restorative Materials," *Journal of Dental Research*, vol. 90, no. 4, pp. 402–416, Oct. 2010.

[8] J. R. Condon and J. L. Ferracane, "Assessing the effect of composite formulation on polymerization stress," *Journal of the American Dental Association*, vol. 131, pp. 497–503, 2000.

[9] R. L. Bowen, "Use of Epoxy Resins in Restorative Materials," *Journal of Dental Research*, vol. 35, pp. 360–369, 1956.

[10] J. L. Ferracane, "Resin composite-state of the art.," *Dental Materials*, vol. 27, no. 1, pp. 29–38, Jan. 2011.

[11] S. Mitra, D. Wu, and B. Holmes, "An application of nanotechnology in advanced dental materials," *Journal of the American Dental Association*, vol. 134, pp. 1382–1390, 2003.

[12] J. L. Ferracane, "Current trends in dental composites.," *Critical Reviews in Oral Biology and Medicine*, vol. 6, no. 4, pp. 302–318, Jan. 1995.

[13] R. L. Sakaguchi and John M Powers, *Craig's Dental Restorative Mateirals*, 13th ed. Elsevier, 2012.

[14] N. Moszner, "New developments of polymeric dental composites," *Progress in Polymer Science*, vol. 26, no. 4, pp. 535–576, May 2001.

[15] Y. T. Miki Iga, Fumio Takeshige, Mitsuo Torii, “The Relationship between Polymerization Shrinkage Measured by a Modified Dilatometer and the Inorganic Filler Content of Light-Cured Composites,” *Dental Materials Journal*, vol. 10, no. 1, pp. 38–45, 1991.

[16] J. Cavalcanti, G. Queiroz, D. M. Monteiro, M. Antonio, and J. Resende, “Polymerization Shrinkage and Flexural Modulus of Flowable Dental Composites,” *Materials Research*, vol. 13, no. 3, pp. 381–384, 2010.

[17] F. C. Calheiros, R. R. Braga, Y. Kawano, and R. Y. Ballester, “Relationship between contraction stress and degree of conversion in restorative composites.,” *Dental Materials*, vol. 20, no. 10, pp. 939–46, Dec. 2004.

[18] G. Queiroz, D. M. Monteiro, M. Antonio, and J. Resende, “Evaluation of Linear Polymerization Shrinkage , Flexural Strength and Modulus of Elasticity of Dental Composites,” *Spectrum*, vol. 13, no. 1, pp. 51–55, 2010.

[19] B. Howard, N. D. Wilson, S. M. Newman, C. S. Pfeifer, and J. W. Stansbury, “Relationships between conversion, temperature and optical properties during composite photopolymerization.,” *Acta Biomaterialia*, vol. 6, no. 6, pp. 2053–9, Jun. 2010.

[20] A. Amirouche-Korichi, M. Mouzali, and D. C. Watts, “Effects of monomer ratios and highly radiopaque fillers on degree of conversion and shrinkage-strain of dental resin composites.,” *Dental Materials*, vol. 25, no. 11, pp. 1411–8, Nov. 2009.

[21] C. J. Kleverlaan and A. J. Feilzer, “Polymerization shrinkage and contraction stress of dental resin composites,” *Dental Materials*, vol. 21, no. 12, pp. 1150–7, Dec. 2005.

[22] M. Dewaele, D. Truffier-Boutry, J. Devaux, and G. Leloup, “Volume contraction in photocured dental resins: the shrinkage-conversion relationship revisited.,” *Dental Materials*, vol. 22, no. 4, pp. 359–65, Apr. 2006.

[23] M. Atai and D. C. Watts, “A new kinetic model for the photopolymerization shrinkage-strain of dental composites and resin-monomers.,” *Dental Materials*, vol. 22, no. 8, pp. 785–91, Aug. 2006.

[24] J. Lange, “Viscoelastic properties and transitions during thermal and UV cure of a methacrylate resin,” *Polymer Engineering*, vol. 5, no. 9, pp. 1651–1660, Sep. 1999.

[25] M. Braem, W. Finger, V. Vandoren, P. Lambrechts, and G. Vanherle, “Mechanical properties and filler fraction of dental composites,” *Dental Materials*, vol. 5, no. 5, pp. 346–349, Sep. 1989.

[26] N. Emami, M. Sjödahl, and K.-J. M. Söderholm, “How filler properties, filler fraction, sample thickness and light source affect light attenuation in particulate filled resin composites,” *Dental Materials*, vol. 21, no. 8, pp. 721–30, Aug. 2005.

[27] A. Arimoto, M. Nakajima, K. Hosaka, K. Nishimura, M. Ikeda, R. M. Foxton, and J. Tagami, “Translucency, opalescence and light transmission characteristics of light-cured resin composites.,” *Dental Materials*, vol. 26, no. 11, pp. 1090–7, Nov. 2010.

[28] H. Arikawa, T. Kanie, K. Fujii, H. Takahashi, and S. Ban, “Effect of filler properties in composite resins on light transmittance characteristics and color.,” *Dental Materials Journal*, vol. 26, no. 1, pp. 38–44, Jan. 2007.

[29] C. L. Davidson, A. J. De Gee, and A. Feilzer, “The competition between the composite-dentin bond strength and the polymerization contraction stress.,” *Journal of Dental Research*, vol. 63, no. 12, pp. 1396–1399, 1984.

[30] A. J. Feilzer, A. J. De Gee, and C. L. Davidson, “Quantitative determination of stress reduction by flow in composite restorations.,” *Dental Materials*, vol. 6, no. 3, pp. 167–171, 1990.

[31] R. H. Halvorson, R. L. Erickson, and C. L. Davidson, “The effect of filler and silane content on conversion of resin-based composite.,” *Dental Materials*, vol. 19, no. 4, pp. 327–33, Jun. 2003.

[32] F. Gonçalves, C. S. Pfeifer, J. L. Ferracane, and R. R. Braga, “Contraction stress determinants in dimethacrylate composites.,” *Journal of Dental Research*, vol. 87, no. 4, pp. 367–71, Apr. 2008.

[33] D. C. Watts, A. S. Marouf, and A. M. Al-Hindi, “Photo-polymerization shrinkage-stress kinetics in resin-composites: methods development.,” *Dental Materials*, vol. 19, no. 1, pp. 1–11, Jan. 2003.

[34] H. Lu, J. W. Stansbury, S. H. Dickens, F. C. Eichmiller, and C. N. Bowman, “Probing the origins and control of shrinkage stress in dental resin-composites: I. Shrinkage stress characterization technique.,” *Journal of Materials Science: Materials in Medicine*, vol. 15, no. 10, pp. 1097–103, Oct. 2004.

[35] F. C. Calheiros, R. R. Braga, Y. Kawano, and R. Y. Ballester, “Relationship between contraction stress and degree of conversion in restorative composites.,” *Dental Materials*, vol. 20, no. 10, pp. 939–46, Dec. 2004.

[36] J. R. Condon and J. L. Ferracane, “Reduction of composite contraction stress through non-bonded microfiller particles.,” *Dental Materials*, vol. 14, no. 4, pp. 256–60, Jul. 1998.

[37] P. Rittigstein and J. M. Torkelson, “Polymer – Nanoparticle Interfacial Interactions in Polymer Nanocomposites : Confinement Effects on Glass Transition Temperature and Suppression of Physical Aging,” *Polymer*, pp. 2935–2943, 2006.

[38] A. Bansal, H. Yang, C. Li, K. Cho, B. C. Benicewicz, S. K. Kumar, and L. S. Schadler, “Quantitative equivalence between polymer nanocomposites and thin polymer films.,” *Nature Materials*, vol. 4, no. 9, pp. 693–8, Sep. 2005.

CHAPTER 4

SHRINKAGE STRESS REDUCTION IN POLYMER-BASED DENTAL RESTORATIVES BY SURFACE MODIFICATION OF FILLERS

Abstract

Polymerization shrinkage stress is detrimental for the long term performance of dental composites. The role of the interface between the fillers and resin matrix in the development of shrinkage stress has not been explored. This gap in the knowledge provides a unique opportunity to explore the interface effect on stress development. A novel surface modification technique has been designed that explore its utility in reducing shrinkage stress. Commercial oligomers of varying molecular weights (1075, 4000, 6100) were attached to the surface of OX50 filler particles (40 nm diameter). The oligomers had a structure similar to BisGMA, one of the components of the resin system, to have compatibility with the resin. An industry standard, γ-MPS was used as the control filler. The oligomers had pendant hydroxyl groups, which were partially or fully reacted with isocyanatoethyl methacrylate, to have variation in reactivity on the oligomer backbone. It was found that shrinkage stress was reduced by using the experimental surface modification. The shrinkage stress for the γ-MPS-based composite was 2.60 ± 0.04 MPa and that for the best performing oligomer, 6100 molecular weight oligomer with 10 % methacrylate functionality, was 1.81 ± 0.11 MPa. A general trend was that shrinkage stress decreased as the length of the oligomer increased. Increasing the methacrylate functionality on the oligomer increased the shrinkage stress. The shrinkage and modulus of the experimental composites were similar to the γ-MPS-based composite control. The reason for the reduction in shrinkage stress was postulated to be the compliance of the interface.

4.1 Introduction

Polymer-based dental composite materials have been in use for more than 50 years [1][2] and now account for the majority of more than 100 million restorations that are placed each year in the US. These esthetic amalgam alternatives were introduced in the late 1950s for anterior restorations as an advancement over the existing silicate cements that do not bond to dentin and erode quite rapidly [3]. Despite their widespread use and steady improvements [4] there remain major issues with the use of polymeric dental restoratives regarding their contraction during polymerization, which in turn promotes considerable shrinkage stress [5][6]. The placement of a shrinking composite in a confined, adhesively bonded setting, as is the case when a restoration is placed in dental cavities, exacerbates the stress levels within the composite and can cause failure of the restoration or even damage the adjacent tooth structure. There has been a tremendous amount of research directed toward addressing the shrinkage, stress and mechanical properties of composite materials based on modification to the resin phase [7], but new studies focused on these concerns based on alteration of the filler component of the composites are lagging behind.

A commercial dental composite consists of three main components – 1) a polymeric resin matrix that forms a continuous phase throughout the composite, 2) a dispersed phase consisting of high modulus inorganic fillers that can be of a variety of shapes, sizes and composition and 3) an interface or interphase that bonds the two main phases that critically promotes stress transfer and helps to maintain mechanical integrity of the entire composite [8]. The interphase has a significant effect on the mechanical properties of composites under conditions of stress and strain. Good interfacial bonding between the filler and resin phases is extremely important to maintain excellent mechanical properties required for this challenging application of in-situ polymerized materials [9][10]. The absence of filler-resin interfacial adhesion can negatively

affect composite properties like wear resistance [11], fracture toughness [12] and bulk strength [13]. In the dental composites literature in particular, surprisingly little attention has been paid to the optimization of the interphase created by the presence of a coupling agent that binds the two phases together [14]. γ-Methacryloxypropyltrimethoxysilane (γ-MPS) has been the silane coupling agent of choice in the dental industry since the development of the modern composite since its hybrid functionality is capable of binding to both the filler surface and the organic resin via the respective presence of a surface condensable group and methacrylate functionality. It has been reported, however, that most of the methacrylate functionality due to the γ-MPS remains unreacted and buried in a disordered multi-layered interphase [15]. This can lead to inefficient covalent coupling between the filler and resin matrix phase, reducing the efficiency of stress transfer to the filler and leading to failure of the composite.

In the case of dental fillers, the application of γ-MPS is usually done at or near room temperature under relatively mild conditions as higher temperatures would degrade or consume the C=C bonds from the methacrylates [16]. The conditions of silane application are widely varied but usually involve aqueous conditions, which typically leads to a multi-layered interphase of the silane around the filler. The 3-carbon spacer of γ-MPS is relatively rigid and when combined with the multiple layers of the silane, it is essentially immobile near the surface of the filler and not very accessible to the resin monomers and propagating polymer chains adjacent to the filler during polymerization [17]. There have been a limited number of attempts to modify the interfacial region to improve composite properties. A mixture of functional and non-functional silanes on the filler surface was used in order to improve the hydrolytic stability of the composites [18][19]. Longer spacers than γ-MPS (up to C_{10}) have also been tried with the effect of creating a more hydrophobic interfaces and enhanced filler loading [20]. More recently,

dendrimers have been used to functionalize the filler surface to successfully reduce shrinkage stress [14].

With this background in mind, it is evident that the design of an efficient interface is essential for successful filler reinforcement of dental composites. It has been reported that the interface between a solid surface and a cross-linked polymer can be strengthened considerably by the addition of chains that are tethered at one end to the solid surface and extend into the polymer matrix [21]. The level of adhesion depends on the grafting density of these chains, which can be called "polymer brushes" that can be referred to as an assembly of polymer chains that are tethered to one end of a surface or an interface [22]. The use of a chemically grafted polymer brush with controlled spatial geometry and chemical functionality produces a significant increase in the strength and fracture energy of the interphase [23]. It has also been reported that a polymer brush layer exhibits greater wear resistance as compared to a conventional surface coating [24].

The benefits of polymer brushes encouraged us to explore its use in dental composites to design a novel surface treatment that involved tethering oligomeric chains on the surface of filler particles in order to enhance various properties in comparison to the traditional γ-MPS treatment. The primary targeted property studied here is polymerization shrinkage stress in the dental composites with the acknowledgement that properties such as conversion and mechanical strength must not be compromised. Another goal of the research was to study the effect of the interphase on material property development in dental composites and apply the knowledge gained to the design of improved materials.

4.2 Materials and Methods

4.2.1 Materials

Silica nanoparticles (Aerosil OX50, average diameter = 40 nm, surface area 50 m^2/g) were donated by Degussa (Germany). OX50 silanized with γ-MPS (γ-methacryloxypropyl-trimethoxysilane) was kindly donated by Septodont-Confi-Dental (Louisville, Colorado, USA). N-Methylaminopropyltrimethoxysilane (MAPTS) was purchased from Gelest. 2,2-Bis[4-(2-hydroxy-3-methacryloyloxypropyl-oxy)phenyl]propane (BisGMA) and triethylene glycol dimethacrylate (TEGDMA) monomers were donated by Esstech. A visible light initiating system consisting of 0.3 wt% camphorquinone (CQ) as initiator and 0.8 wt% ethyl 4-dimethylaminobenzoate (EDAB) (Sigma-Aldrich, Milwaukee, WI) as co-initiator was incorporated. Isocyanatoethylmethacrylate (IEM), poly(bisphenol A-co-epichlorohydrin), glycidyl end-capped, (referred to here as epoxy oligomer, with number average molecular weights of 1075, 4000, and 6100 Da), methylene chloride, anhydrous N,N-dimethyl formamide (DMF), anhydrous toluene, and dibutyltin dilaurate were obtained from Sigma-Aldrich (USA).

4.2.2 Modification of Epoxy Oligomers

The structure of the epoxy oligomers used is shown in Figure 4.1. This particular oligomer series was chosen as the structures are similar to that of BisGMA, which is one of the components of the resin system and is a dimethacrylate monomer developed for dental polymer applications with widespread use in current commercial dental composite materials. The structural similarity ensures enhanced compatibility of the treated fillers and the resin system. The epoxy oligomers were varied in chain length, with n in Figure 4.1 going from 2 to 20. Three oligomers were used with molecular weights 1075 (n=2), 4000 (n=12) and 6100 (n=20). This

allowed the study of the effect of length of the brush on the properties of the composite. The epoxy oligomers had pendant hydroxyl groups along their length that afforded a controllable and convenient way to introduce reactive methacrylate groups along the length of the oligomers. The reactive groups are necessary in order for covalent bonding to occur between the interface and the resin, thus completing the coupling between the filler and the matrix. A covalent attachment usually results in enhanced bulk mechanical properties in a composite, primarily in flexure or tension rather than compression. Hence it is viewed as necessary to maintain at least some degree of reactivity at the surface of the fillers.

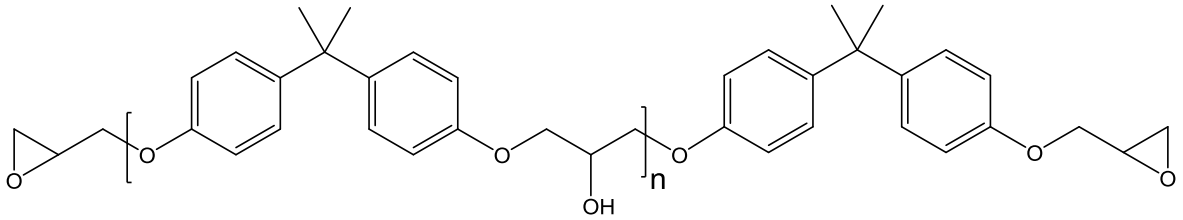

Figure 4.1 Structure of epoxy oligomer series used to modify the OX50 surface (n varies from 2 to 20)

The hydroxyl groups on the oligomers were reacted with IEM in order to introduce methacrylate functionality along their length. Two series of modified oligomers were created using this synthesis; one series utilized 10 % of all the possible hydroxyl groups in a urethane-forming reaction with IEM, while the other had all of the hydroxyls converted to the urethane methacrylate functionality. The 10 % group would have a reduced level of reactive group concentration minimizing the degree of covalent linkage with the resin while the 100 % group would have the maximum covalent engagement with the resin. By this modification, the effect of the length of the oligomer and the reactive group concentration on the properties of the experimental composites could be examined somewhat independently. The representation of the final oligomer structure is shown in Figure 4.2.

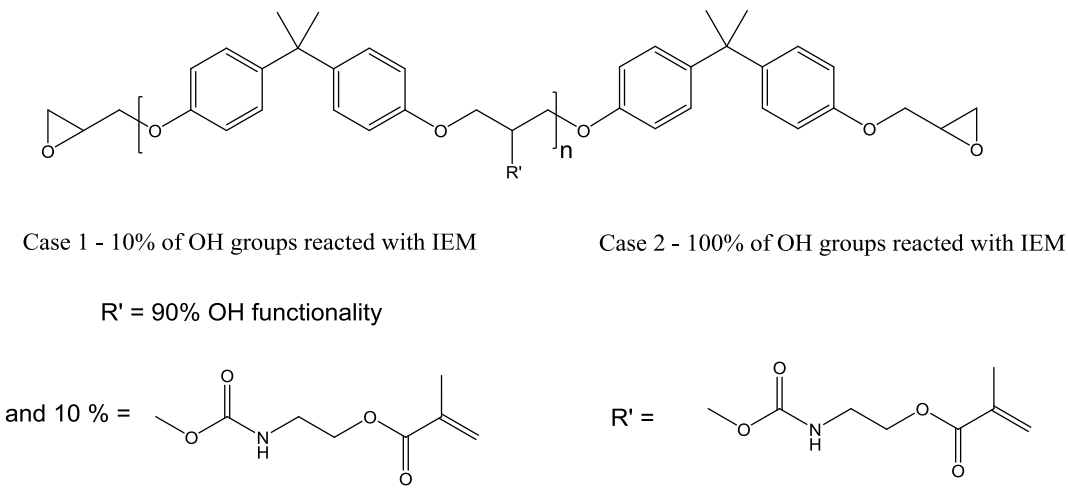

Figure 4.2. Final structure of the epoxy oligomers

4.2.3 Modification of the Filler Surface

The bare silica particles were first treated treated with MAPTS and then the epoxy-terminated, pre-formed oligomers were attached to the amine end groups of the silane. OX50 particles were first dried in a rotary dryer at about 165 ^{o}C under vacuum for 3 hours before further treatment. This was done to ensure removal of surface bound moisture that can potentially react with the silanes and promote the formation of multiple layers of the silane. Anhydrous toluene was used as a solvent for the silanization process. It was refluxed for twohours and then the particles were added and further refluxed for an hour to ensure good dispersion. The MAPTS was added to the solution so that the final concentration in the mixture was 1.5 % by weight. This reaction mixture was allowed to reflux for 6 hours after which the particles were separated from the solvent by centrifugation. The particles were washed three times with toluene and two times with methylene chloride to ensure that all traces of unreacted silane were removed. The silanized particles were then dried overnight under vacuum at 50 ^{o}C to remove all traces of solvent. The dried and silanized particles were then added to anhydrous DMF, which contained a five-fold excess of the modified epoxy oligomers to minimize potential

head and tail surface coupling. The reaction mixture was heated to 45 ^{o}C and the reaction was allowed to continue for 24 hours. The particles were separated and isolated by following the centrifugation procedure described above.

4.2.4 Composite Preparation

The resin matrix for the composites was a mixture of BisGMA and TEGDMA in the ratio 70:30 by mass. The resin included a free radical visible light initiating system comprised of 0.3 wt% camphorquinone and 0.8 wt% ethyl 4-N,N-dimethylaminobenzoate. The fillers were added to the resin and homogeneously dispersed with a centrifugal speedmixer (DAC 150 FVZ, Flakteck Inc.). All composite pastes had a final filler loading level of 30 wt%. Composites with γ-MPS-treated OX50 particles were similarly prepared and used as the control. The freshly prepared composites were allowed to sit under vacuum to ensure elimination of air bubbles prior to being used.

4.2.5 Characterization of Fillers

Thermogravimetric analysis (Pyris 7 TGA, Perkin Elmer) was used to determine the amount of surface functionalization on the OX50 particles after each stage of modification. Samples were placed in platinum pans in a nitrogen atmosphere and heated from 50 ^{o}C to 850 ^{o}C at 10 ^{o}C/min and the mass loss as a function of temperature was recorded.

4.2.6 Shrinkage Stress Measurements

Shrinkage stress was measured using a cantilever beam based instrument referred to as the tensometer (American Dental Association, Paffenberger Research Center, MD, USA). This

instrument measures the force generated by an actively polymerizing material that is partially constrained from a free shrinkage state. The material is bonded to the opposing ends of two diametrically placed quartz rods. The polished ends of the glass rods are freshly treated with γ-MPS, to promote bonding with the polymerizing material. The upper quartz rod is attached to the cantilever beam and is able to move along with the shrinking composite. The resistance of the calibrated cantilever beam to deflection is controlled by the position of the attached rod. The lower quartz rod is fixed to the tensometer base and is immobile. A dental curing light (IQ2, Caulk, Dentsply), with an output wavelength of 465 nm, was adapted to the bottom of the lower quartz rod, which serves as a light guide to transmit the curing light to the material. A detailed description of the stress measurement involving the tensometer has been published previously [25]. The testing protocol uses specimen discs of 1.5 mm thickness and 6 mm diameter. For the initial shrinkage stress measurements (Figure 4.5), the light intensity reaching the sample was measured at 350 mW/cm^2. The samples were irradiated for 40 s with the dynamic stress development profile continuously monitored for 20 min. Real-time double bond conversion measurements based on simultaneous near-IR spectroscopy were made during the stress measurements.

4.2.7 Shrinkage Measurements

Polymerization shrinkage was measured using a linomter (ACTA Foundation, Netherlands). In this method composite paste specimens were placed between an aluminum disc and a glass slide that were greased to allow the free shrinkage of the sample along the radial direction. Specimens were 1.5 mm in thickness and 6 mm in diameter. The sample was irradiated from the top of the glass slide (350 mW/cm^2 for 40 s). The displacement of the freely moving

aluminum disc was measured by linear variable differential transformer (LVDT) and converted to a dynamic volumetric shrinkage plot that extended to 10 minutes to capture the initial post-cure shrinkage behavior.

4.2.8 Flexural Modulus and Strength Measurements

Flexural modulus and strength were measured in a 3-point bending mode (858 Mini Bionix II, MTS Systems, Eden Prairie, MA). The composite pastes were injected into a cavity measuring 2x2x10 mm. The mold cavity was formed by Teflon spacers on the sides and clamped glass slides on the top and bottom. The composite samples were cured using the dental curing light at 550 mW/cm^2 for 3 minutes on both the sides to promote uniform conversion throughout the sample. The crosshead speed used was 1 mm/min.

4.2.9 Infrared Spectroscopic Characterization

Infrared spectroscopy was used to monitor the conversion of the resin and the surface modification of the fillers using an FTIR (Nexus 670, Nicolet Instruments, Madison, WI). Double bond conversion was monitored in transmission mode using near-infrared (NIR) spectroscopy. The area of the peak at 6165 cm^{-1} representing the methacrylate $=CH_2$ absorption was used to track conversion. For the simultaneous measurement of conversion with shrinkage stress and also during rheometry measurements, the NIR signal from the source was guided through the sample using an outbound optical fiber and the NIR signal transmitted through the sample was collected by the inbound optical fiber and conducted to the detector. Diffuse reflectance infrared Fourier transform spectroscopy (DRIFTS) was used to study the filler surfaces. For the DRIFTS experiments OX50 filler particles representing the various surface

treatments, including the unmodified filler, were mixed with KBr powder and spectra were taken at a resolution of 4 cm^{-1}, using KBr as a background.

4.3 Results and Discussion

The amount of surface coverage due to the epoxy oligomer attachment was determined by thermogravimetric analysis (TGA). Figure 4.3 represents the TGA curves for the various systems. The nomenclature of the brushes used here is as follows:- OX50 Mw-10% or OX50 Mw-100%, where Mw represents the molecular weight of the brush and 10% or 100% represents the percentage of hydroxyl groups on the oligomer that were pre-reacted with the IEM. It can be seen that there is an increase in the weight loss going from unmodified OX50 particles to silanized particles and then those modified with the epoxy brushes. There is an approximately 1 % mass loss difference between the unmodified and silanized particles. Technical data (Degussa, Inc.) reveals that the OX50 particles have a surface silanol group density of 2.2 per nm^2. If we assume each silanol group reacts with a MAPTS molecule then using the molecular weight of the silane, we can estimate that the weight loss should be about 3 %. Since the weight loss is about 1 %, this indicates that about 1/3rd of the silanol sites have reacted with the MAPTS. Using this data the relative coverage of the different epoxy brushes on the surface were estimated. Table 4.1 gives the net weight loss of each of the epoxy brushes and fraction of the silane sites that are covered.

From Table 4.1 it is apparent that the fraction of epoxy oligomers attached to the filler surface reduces as the length of the oligomer increases beyond that of the shortest oligomer used here. This is due to the fact that the longer the oligomer, the greater the steric hindrance encountered in the “grafting-to” approach employed here that reduces the amount of oligomers reaching the

surface of the filler. It can also be seen that the fillers with the epoxy oligomers exhibit a 2-stage decomposition process. The first decomposition step at around 200 ^{o}C when some of the less thermally stable components on the attached chains start decomposing. The second stage where much more mass loss is observed may be due to the breakage of Si-C bonds and subsequent decomposition and volatilization of the decomposition products.

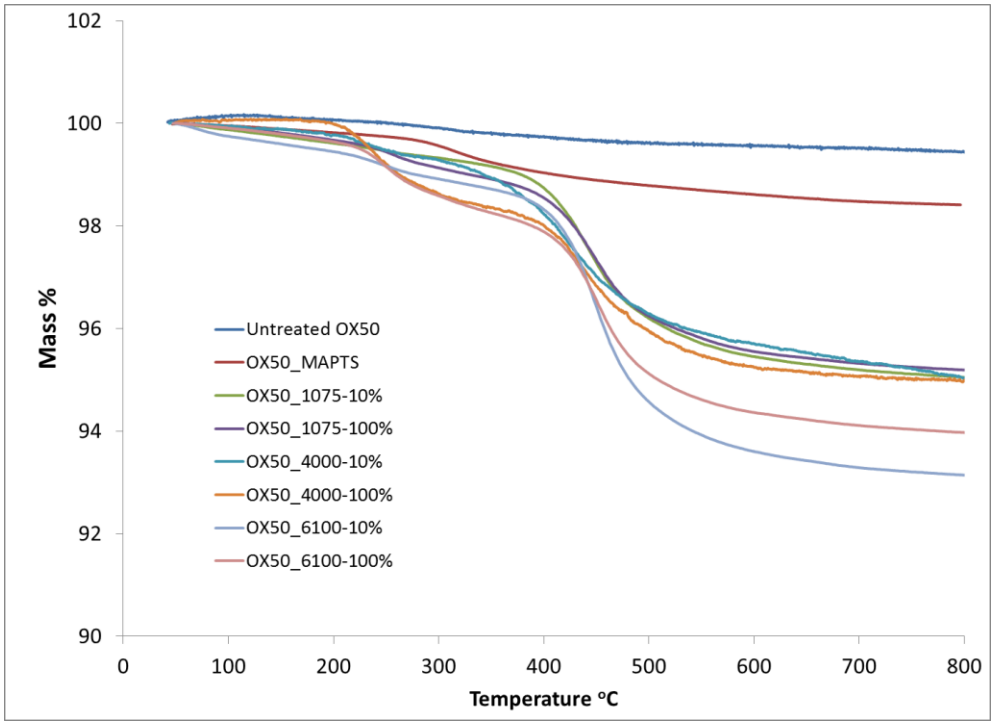

Figure 4.3. TGA curves for the OX50 particles with different surface modifications

Table 4.1. Weight loss contribution on the filler and fraction of the surface silanol sites covered by the modified epoxy oligomer series.

Sample	% mass loss	Fraction of surface silanol sites covered
OX50_1075-10%	3.4	0.17
OX50_1075-100%	3.4	0.16
OX50_4000-10%	4.5	0.06
OX50_4000-100%	4.6	0.05
OX50_6100-10%	4.6	0.04
OX50_6100-100%	5.4	0.03

4.3.1 FTIR Characterization

Mid-IR spectra of OX50 at various stages in the modification process are shown in Figure 4.4. Unmodified and dried OX50 particles showed a sharp peak at about 3747 cm^{-1} representing free silanol groups. Upon silanization with MAPTS, this peak disappears, indicating reaction of the surface silanols and also hydrogen bonding with the carbonyl of the methacrylate group on MAPTS. A broad peak representing the N-H stretching appears around 3346 cm^{-1}. The multiple peaks at 2871-2972 cm^{-1} correspond to the stretching mode of C-H in $–CH_2$, -CH- and $–CH_3$. When the epoxy oligomers are added on top of the MAPTS layer, a carbonyl peak appears at about 1720 cm^{-1} and the C=C peak appears at 1635 cm^{-1}. The two peaks are stronger in the filler with the 6100-100% oligomer, confirming the presence of a greater number of methacrylate groups than the 6100-10% oligomer.

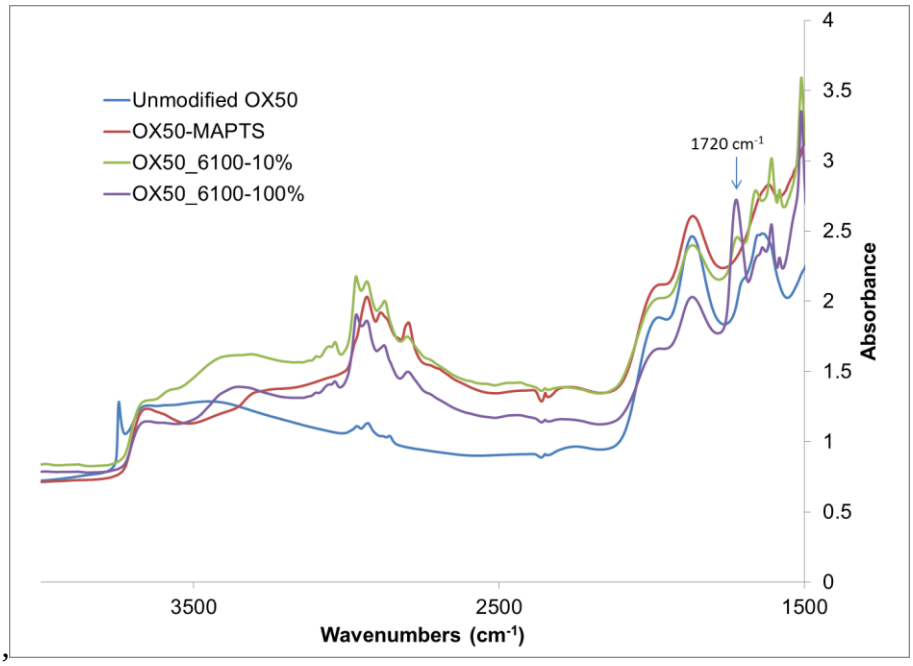

Figure 4.4. DRIFTS spectra of OX50 particles at various stages of surface modification - (a) Unmodified OX50, (b) OX50 with MAPTS, (c) OX50_6100-10%, and (d) OX50_6100-100%.

4.3.2 Shrinkage Stress Results

Figures 4.5 and 4.6 show the shrinkage stress of all the modified composites compared with a γ-MPS-based control. The epoxy oligomers that have only 10 % of their pendant hydroxyl groups modified are presented in Figure 4.5 whereas the ones with 100 % hydroxyl group conversion are shown in Figure 4.6. In both the cases, it can be seen that the experimental composites produce lower shrinkage stress as compared to the γ-MPS based control. In Figure 4.5, the γ-MPS control has the highest shrinkage stress at 2.59 ± 0.04 MPa. The modified composites show a reduction in the shrinkage stress that follows the increase in the molecular weight of the epoxy oligomers with the OX50_1075-10% at 2.20 ± 0.02 MPa, OX50_4000-10% at 2.08 ± 0.04 MPa and OX50_6100-10% at 1.81 ± 0.11 MPa. Figure 4.6 does not show the same linear progression of the shrinkage stress with respect to the molecular weight of the oligomers. The OX50_4000-100% shows the least reduction in stress with the final stress at 2.36 ± 0.04

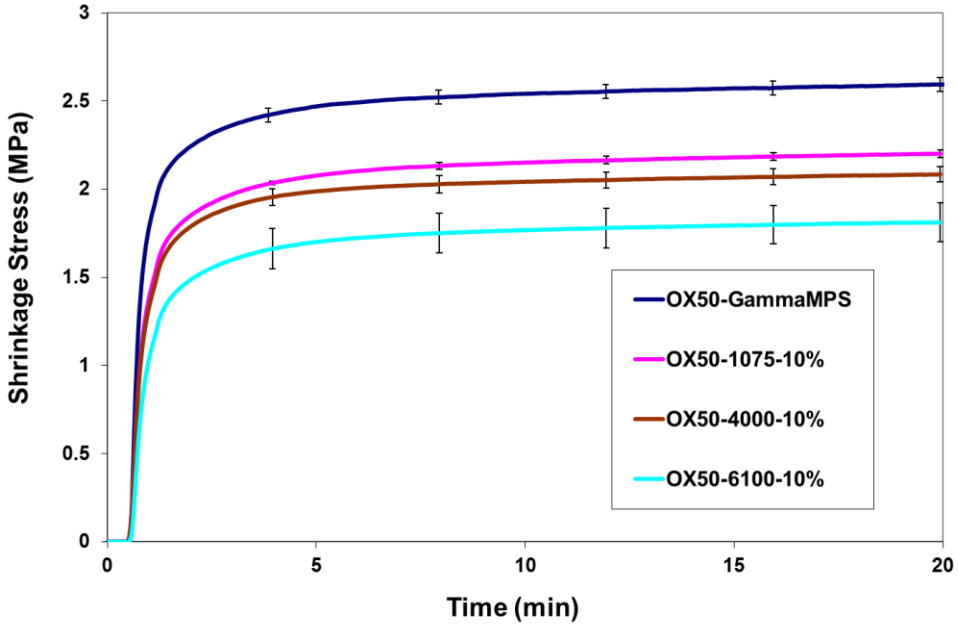

Figure 4.5. Shrinkage stress measurements of experimental composites with 10 % hydroxyl group modification of oligomers, compared with the γ-MPS control. Irradiation conditions – Visible light at 350 mW/cm^2 for 40s

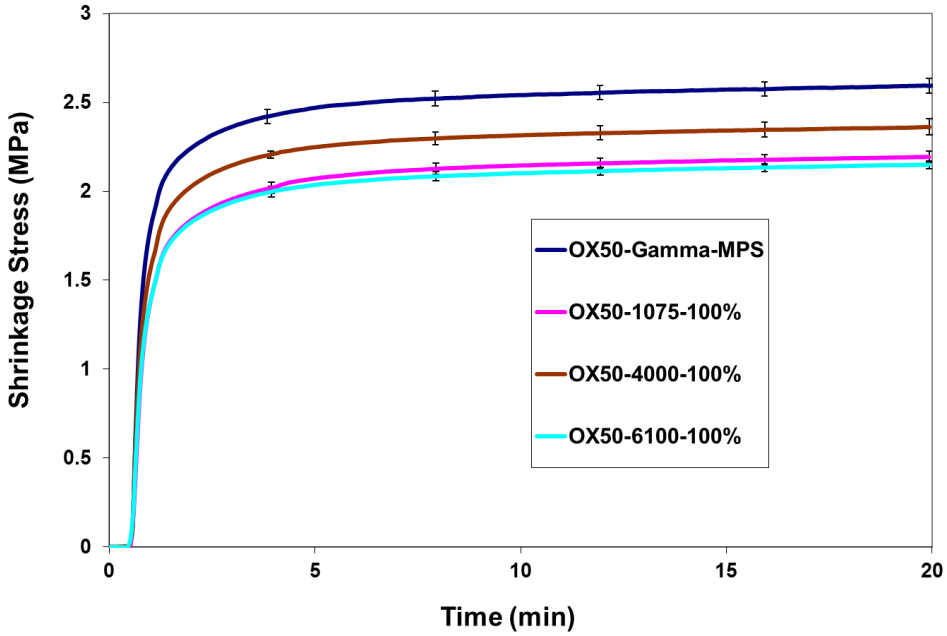

Figure 4.6. Shrinkage stress measurements of experimental composites with 100 % hydroxyl group modification of oligomers compared with the γ-MPS control. Irradiation conditions – Visible light at 350 mW/cm^2 for 40s.

MPa, followed by OX50_1075-100% at 2.19 ± 0.03 MPa and OX50-6000-100% at 2.15 ± 0.02 MPa. In comparisons between the two series it can be seen that the oligomers with 10 % hydroxyl group modification produced lower stress as compared with their 100 % hydroxyl group modified counterparts of equivalent molecular weight, except for the oligomer with 1075 molecular weight where there is no significant difference between the two functionalization levels. It must be noted that the matrix double bond conversion at the end of all the runs was at the same level at around 65 %, ascertaining that the reduction in shrinkage stress was not due to reduction in shrinkage caused by a decrease in the conversion of the experimental systems.

Figure 4.7 shows the development of double bond conversion of the resin in the composites. This provides confirmation of the fact that all the composites reach an equivalent limiting level of final conversion, regardless of the surface treatment and degree of functionalization. The rate of reaction is the same in all the cases as well. So it is apparent that the surface treatment does not directly affect the reaction kinetics of the composite systems or restrict conversion in the vicinity of the interface.

Shrinkage measurements revealed no significant difference between any of the composite materials (Figure 4.8). The composites contracted by the same amount, about 5%, under similar irradiation conditions. The rate of shrinkage development in the initial stages was found to be similar for all the composites. The conversion of all the composites at the end of the shrinkage run was also at similar levels.

The results of the flexural modulus and strength measurements are shown in Figure 4.9. Again there is no significant difference between the various composites. All of them showed equivalent strength and modulus values. This is encouraging, as it is confirmation of the fact that

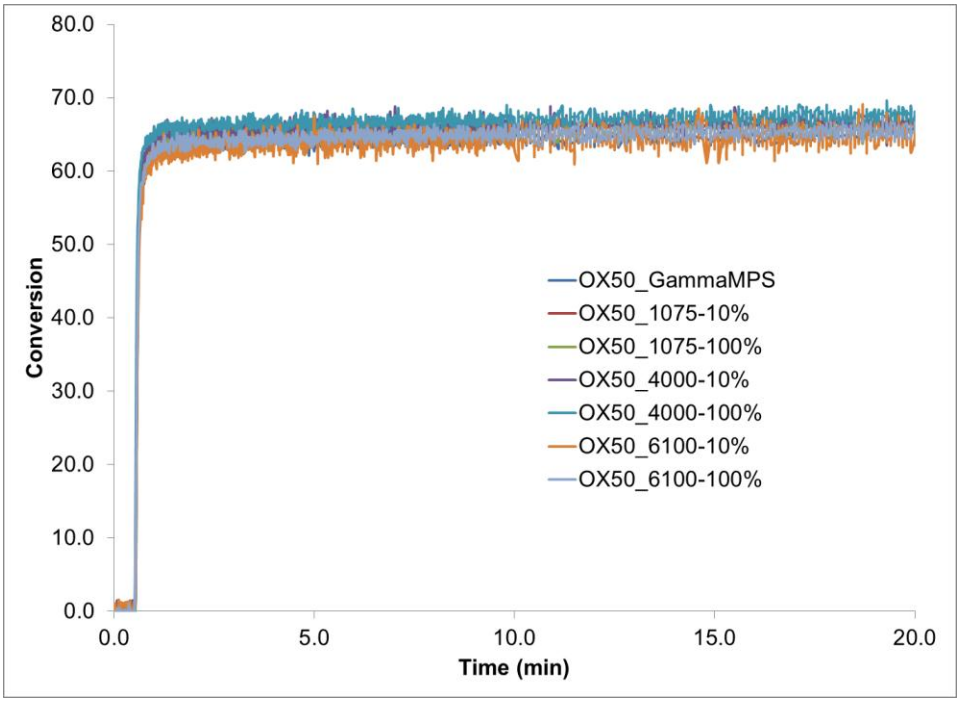

Figure 4.7. Comparison of double bond conversion of experimental composites with γ-MPS-based control. Irradiation conditions – Visible light at 350 mW/cm^2 for 40s.

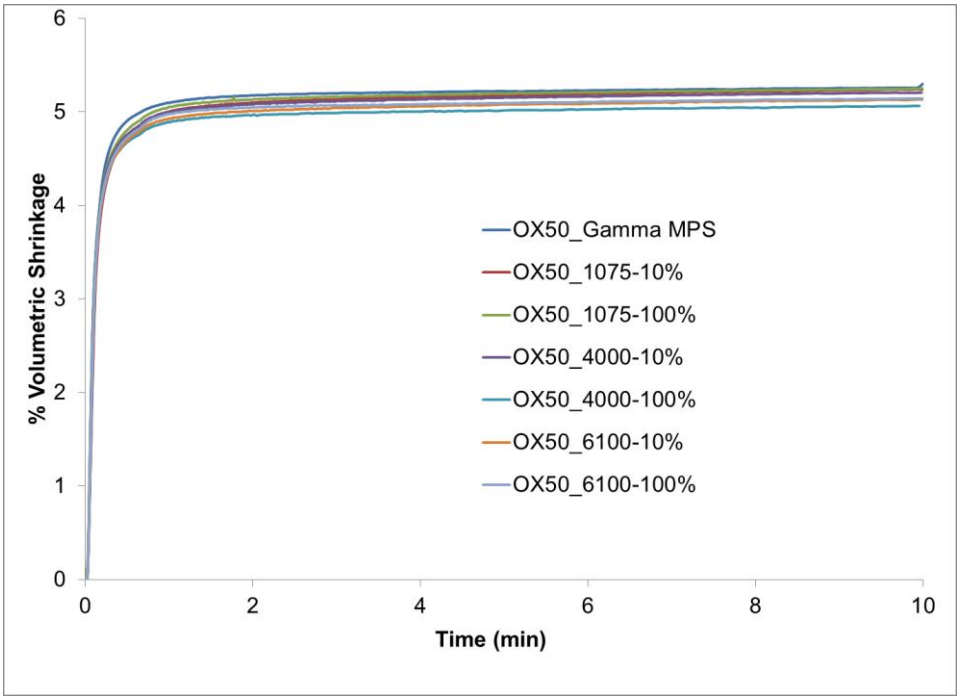

Figure 4.8. Comparison of shrinkage of experimental composites with γ-MPS-based control. Irradiation conditions – Visible light at 350 mW/cm^2 for 40s.

the novel surface treatment does not have a detrimental effect on the basic properties of the composites. Composites with untreated fillers show a reduction in mechanical strength due to lack of covalent attachment with the resin. In the experimental fillers, as seen from the TGA data, very few of the surface sites are covered with the oligomers. It is encouraging that the mechanical properties are sustained in spite of this relatively low coverage.

It was interesting to note the significant decreases in the shrinkage stress of the experimental composites in comparison with the γ-MPS-based control, while the degree of conversion, shrinkage and flexural modulus/strength were maintained. Shrinkage stress development in polymerizing composites is a complicated process, with dependence on factors such as shrinkage, resin matrix conversion, filler loading level, viscoelastic properties, modulus of the composite and kinetics. Unlike the comparisons drawn in the dental materials literature involving polymerization stress of different commercial composite formulations, here most of these factors were held constant with the focus on the filler/resin interface. Factors within each measurement technique such as sample geometry, irradiation conditions and filler loading level were also kept constant for all the samples. The only difference between the samples was the surface treatment of the fillers. By maintaining the other factors constant, we could better elucidate the effect of the surface treatment on the properties of the dental composites.

Most of the research involving reduction in the stress levels in polymerizing dental composites has dealt with the design of new resin compositions or the application of alternative curing strategies [7]. Very little work has focused on modifying or designing new filler systems to deal with stress development. Fillers are used for a variety of factors including the necessary esthetic tooth-like appearance but a primarily role of the filler is to reinforce the resin and improve the mechanical properties of the composite to a level that is beyond the reach of the

lower moduli resins being used. Coupling is necessary between the filler and the resin phase in order to reduce wear of the composite particularly in occlusal conditions and silane coupling agents like γ-MPS are used for this purpose. Efficient coupling between the filler and the resin matrix helps to transfer the applied stress to the filler, thereby minimizing the stress on the weaker matrix phase. The attachment of the resin monomers to the filler surface actually places a restriction on their movement while it is polymerizing and actually increases the localized internal stress in the composite.

The "polymer brush" approach used here helps to reduce the stress in the composites, while maintaining mechanical integrity, as can be seen from the results shown above. Figure 4.4 shows that as the length of the oligomer increases the final stress in the composite decreases. We hypothesize that the oligomer layer actually acts as a stress-relieving layer and helps in reducing the absolute stress levels in the composite. As the resin matrix monomers start to cure, copolymerization occurs with the pendant methacrylates along the length of the oligomers. The resin actually tries to shrink away from all the surfaces, including the walls of the cavity in which it is placed as well as the surfaces of the fillers. In doing so, the shrinking resin would pull at the surface of the fillers, potentially extending the oligomer layer. By virtue of their flexible nature and attachment to both the filler surface and the polymerizing matrix, the oligomeric chains act as springs, akin to springs in a viscoelastic model. These springs can help to relieve the developing stress due to their movement to adjust the shrinking of the resin. It has been hypothesized, that in the initial stages of cure when the cross-linking in the resin is in its nascent stages, the growing polymer chains can compensate for shrinkage and relieve stress by flow [26]. A comparison can be made between this theory and the mechanism by which the oligomer layer relieves stress. The oligomers are relatively free to move and in the initial stages of curing can

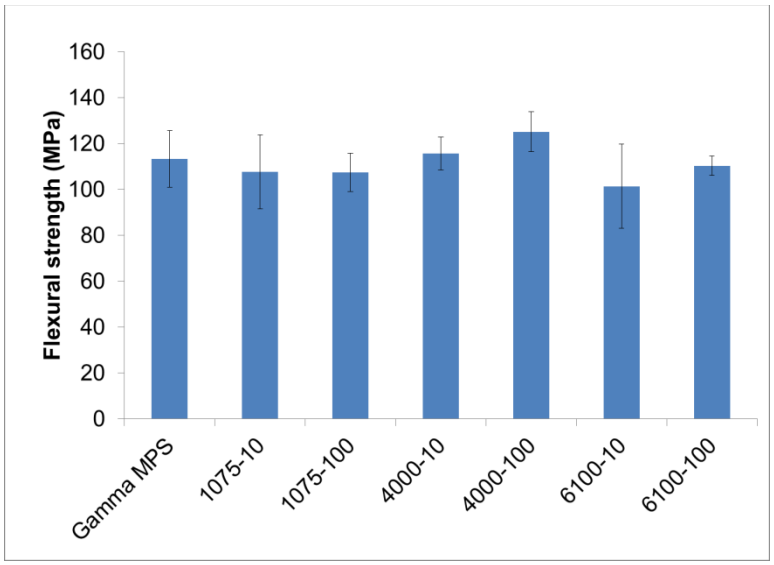

(a)

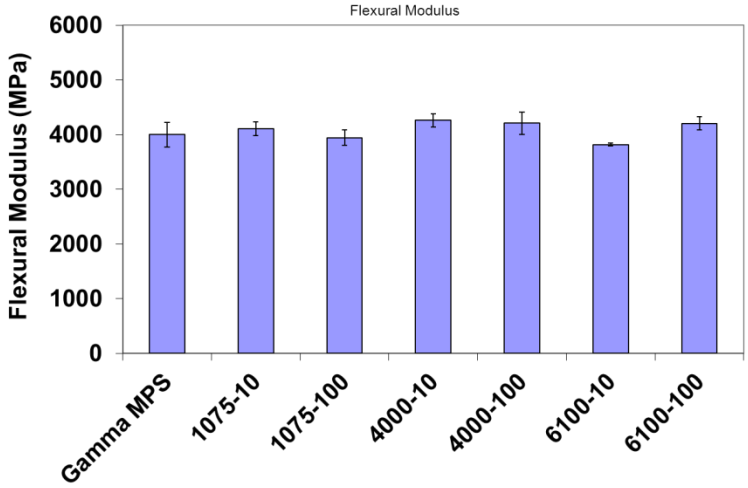

(b)

Figure 4.9. Flexural (a) strength and (b) modulus of experimental composites compared with γ-MPS-based control

help relieve the stress by “flowing”. The longer the oligomer length the more flexible it is and more is its ability to relieve stress, as proved by the results in Figure 4.4.

If the oligomer layer were very dense, however, then the chains would not have much freedom of movement and would not be able to relieve the stress to the same extent. Due to the grafting-to approach used here, as can be seen from the TGA results described before, the grafting density of the chains is quite low and we hypothesize this low surface density helps in giving the chains an additional degree of freedom in movement.

When the methacrylate functionality on the oligomers is increased by reacting all the hydroxyl groups on the chains with IEM, there are now more points along the oligomer length where the resin monomers can react and be pinned into the developing polymeric network structure. As the resin polymerizes and more of the pendant methacrylates react, this places more restrictions on the movement of the oligomeric chains. Consequently, there are restrictions placed on the movement of the resin due to the reaction too. Both these factors combine to partially negate the effect of the stress relieving capacity of the oligomers. Comparing Figures 4.5 and 4.6, we can see that for the oligomers with 6100 and 4000 molecular weight the stress increases as the methacrylate functionality on the chains increases. In the case of the oligomer with the 1075 molecular weight, the stresses in both the cases are the same. This may be due to the fact that this oligomer only has an average of 2 hydroxyl groups per chain, whereas the 4000 and 6100 series have 12 and 20 respectively. There is very little difference between the low and the high level of methacrylate functionality in the 1075 molecular weight case, as compared with the greater oligomeric lengths. The difference is not significant enough to have an impact and hence the stress levels are similar in both the cases.

The γ-MPS control has a higher magnitude of relatively rigid methacrylate functionality on the filler surface. There is rapid attachment of the resin monomers at these reactive sites and subsequent restriction on their mobility. This results in an increase in the stress build up at the interface and hence the overall internal stress. The rigid interphase created as a result of this reaction does not allow in the reduction of stress by flow. Hence the γ-MPS based composite displays a higher level of stress as compared to the experimental composites.

Stress reduction can also be a result of reduction in modulus due to reduction in conversion or other factors such as effective crosslink density of the polymer network. But it was verified that all the composites reached the same final level of shrinkage (Figure 4.8). There was no significant difference between the moduli of all the composites either. As stated before, the conversion was similar in all the cases (Figure 4.7), giving a good basis for comparing the other properties, as all the properties can change with changes in conversion. A plot of real time shrinkage stress versus conversion for the composites is shown in Figure 4.10. Only the composites with the 10 % hydroxyl group modification are compared with the γ-MPS control here. In all cases the shrinkage stress develops gradually with increase in conversion in the initial stages. As volumetric shrinkage progresses and the composite crosses its gel point, the stress starts increasing perceptibly. It is after this point that subtle differences between the control and the experimental composites can be seen. Stress development in the γ-MPS control increases at a faster rate than the experimental surface-treated composites. A precipitous increase in the stress values with respect to small changes in the conversion is observed in all the composites. This would be the region near the vitrification point of the systems. It can be seen that the vitrification point is reached at earlier stages of conversion for the control. The control also reaches a higher value of final stress. There is a delay in reaching vitrification for the experimental composites

and their ultimate stress values are also lower. A delay in the vitrification could be due to the enhanced mobility afforded by the flexible oligomer layer. A decrease in the vitrification time has been observed with an increase in filler loading (Chapter 3). Altmann *et al*. [27] hypothesize that the increase in viscosity is due to the increase in filler content and increase in the glass transition temperature. The increased filler-matrix interaction places restrictions on the mobility of the polymer chains near filler surfaces. By the reverse logic, the higher mobility of chains near the experimental filler surfaces should allow for a delay in reaching the vitrification point. This is precisely what we notice in our experimental composites. This is also validated by the observation that if the filler particles have non-reactive surfaces that do not have a strong interaction with the resin, there is no effect of increase filler loading on the T_g values [28].

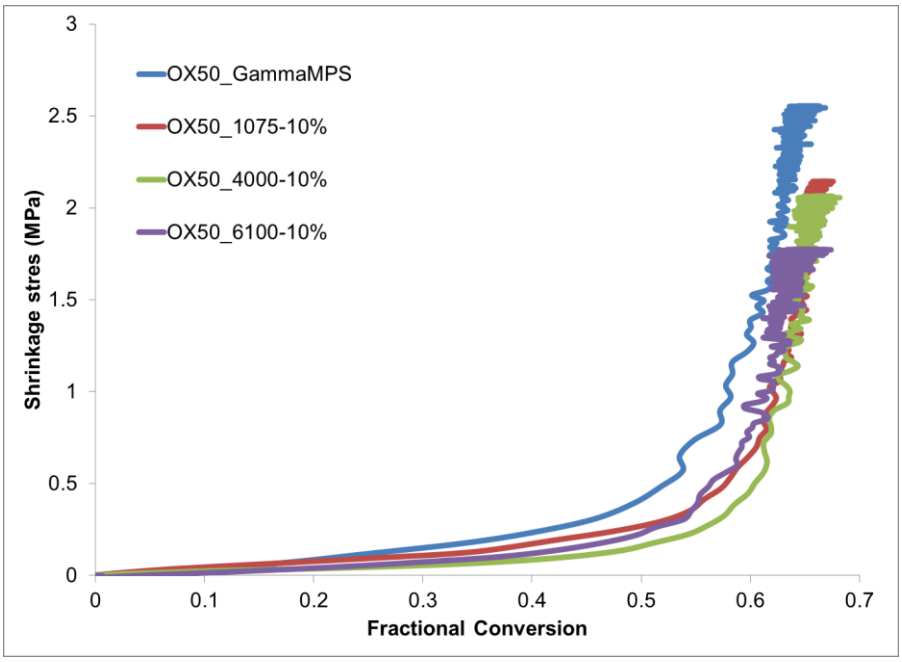

Figure 4.10. Real-time shrinkage stress with respect to conversion.

Viscosity of all the composite pastes was also measured to study the effect the particles have on the rheological properties. In Figure 4.11, it can be seen that the lowest viscosity is shown by the γ-MPS control. All the experimental composites exhibit higher viscosity levels, which might have implied that vitrification could be expected to occur at lower rather than the higher conversion levels observed here. This indicates that the strength of the interaction of the interfacial layer with the uncured resin is higher. Also, the layer could have a wider sphere of influence due to the flexible nature of the oligomers. Each of these factors would have an effect on the viscosity. Within each molecular weight, the 10 % composite series are higher in viscosity than their 100 % counterparts. This is due to the fact that 10 % composite series has more hydroxyl groups per chain and these have a higher degree of hydrogen bonding, thus increasing the viscosity. It has been theorized that a higher degree of viscosity does not allow for stress relaxation by flow in the pre-gel stage, leading to higher final stresses. Condon et al. [29] tested the effect of using non-functional but silanated fillers versus using unsilanized and functionally silanized particles in a composite on shrinkage stress. They found that composites with filler with a non-functional silanated surface showed the lowest viscosity and produced the lowest stress upon polymerization. The functional silanized filler bonded covalently to the resin and showed higher stress, while the unsilanized filler based composite showed the highest viscosity due to the stronger interactions between the surface silanol groups with the components of the resin phase and possibly due to filler particle aggregation effects. The unmodified filler yielded composites with stress equivalent to that of the functional filler based composite. However, the mechanical strength of composite materials with non-functional silane treated or untreated filler was significantly reduced compared with γ-MPS-treated filler based composites.

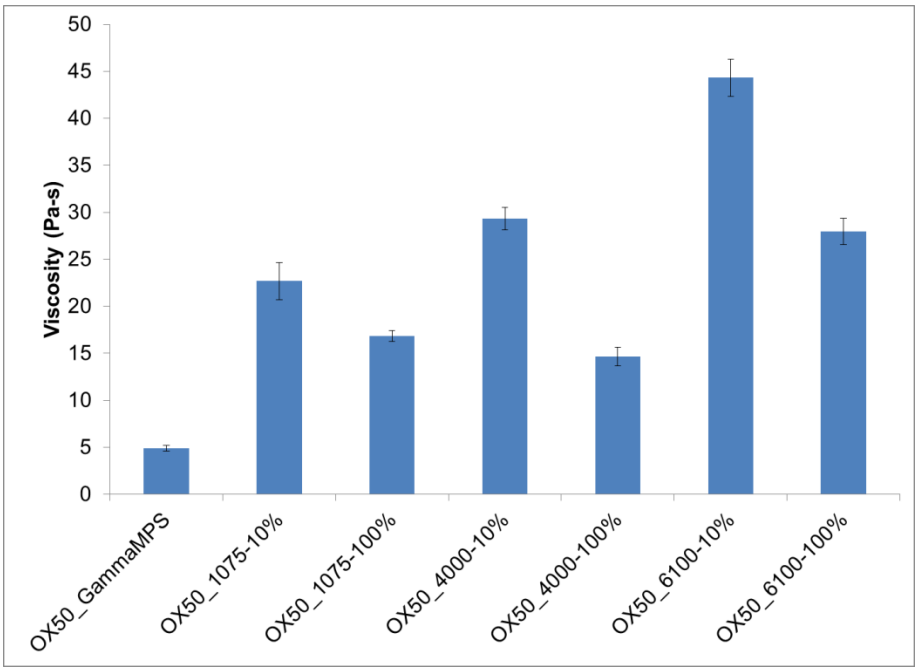

Figure 4.11. Viscosity of composite pastes

In our study, the experimental composite pastes have a higher viscosity than the γ-MPS control, but have similar modulus in their polymeric state. Intuitively, a higher initial paste viscosity would lead to early gelation and development of modulus. A consequence of this would be higher stress. However, we see the opposite effect where the stress develops later in the high viscosity system. The only way this can happen is due to the interfacial treatment with the brush structures likely delaying the effective transfer of stress between the matrix and filler. This further validates the effect the modified interface has in alleviating the final stress levels in the composite.

Dynamic mechanical analysis tests were conducted to determine the effect of the interfacial treatment on the thermomechanical properties of the composites. The storage modulus and loss tangent are plotted versus temperature in Figures 4.12 and 4.13 respectively. In Figure 4.12, it can be seen that in the glassy region, the storage modulus of the experimental composites increased as compared to the control. The results are summarized in Table 4.2.

Table 4.2. Storage modulus and Tg of composites

Sample	Storage modulus value at 25 ^{o}C (MPa)	T_g (^{o}C)
OX50-γ-MPS	2530 ± 300	164 ± 4
OX50_1075-10%	3880 ± 350	158 ± 3
OX50_1075-100%	3660 ± 450	158 ± 3
OX50_4000-10%	4070 ± 250	157 ± 2
OX50_4000-100%	3640 ± 200	158 ± 5
OX50_6100-10%	3810 ± 500	149 ± 4
OX50_6100-100%	4220 ± 400	156 ± 3

The increase in storage modulus in the glassy region for the experimental composites shows a reinforcing effect due to the modified interface. In the rubbery region however the storage modulus of the experimental composites is lower than that of the γ-MPS control, indicating a weakening of the interface in the rubbery regime. This result is consistent with the delayed vitrification noted in the polymerization stress evaluation of the brush-modified fillers. The T_g of the γ-MPS control was found to be slightly higher than that of all the other samples Table 4.2). This could be due to lesser adhesion at the interface or the flexibility of the interface region.

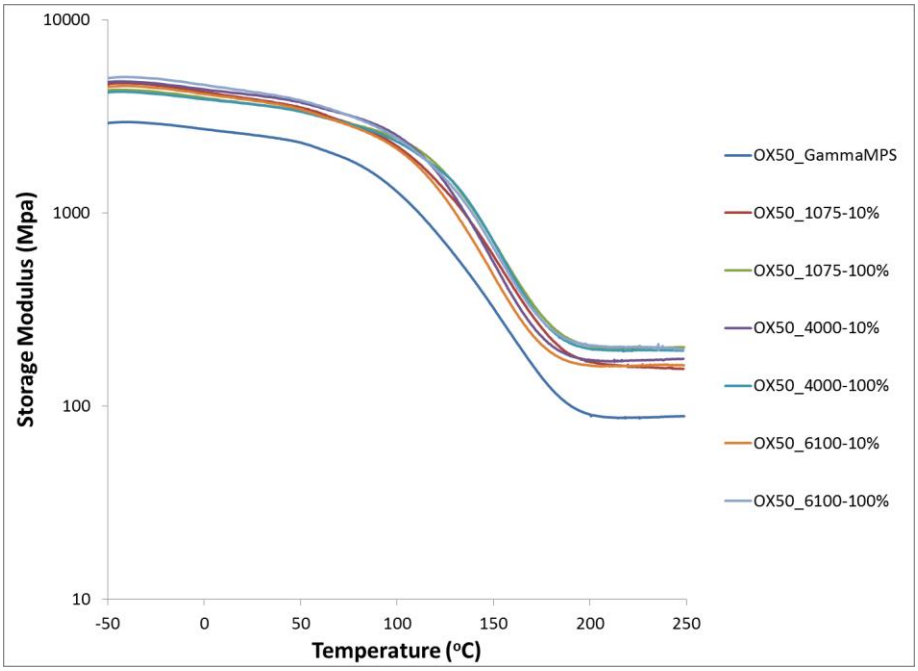

Figure 4.12. Storage modulus of experimental composites compared with γ-MPS control.

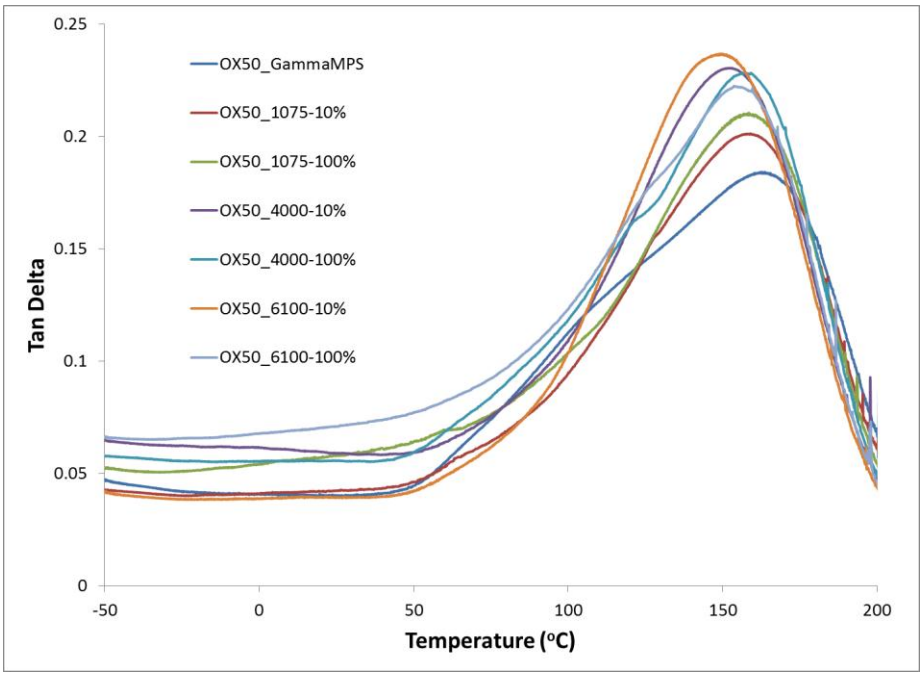

Figure 4.13. Loss tangent of experimental composites compared with γ-MPS control.

4.3.3 SEM Characterization

SEM images of cryogenically fractured composite bars were obtained to get information on the morphological effects due to the surface treatment. Figure 4.14 (a) shows the fractured surface of the γ-MPS based control and figure 4.14 (b) shows the surface of the 4000-100% based composite. It can be seen that the fracture surface of the experimental composite has a much rougher topography as compared with the control. This implies that in the experimental composites, the propagating crack has to travel a larger distance and dissipates more energy while doing so. This would potentially lead to an increase in the fracture toughness of the composites.

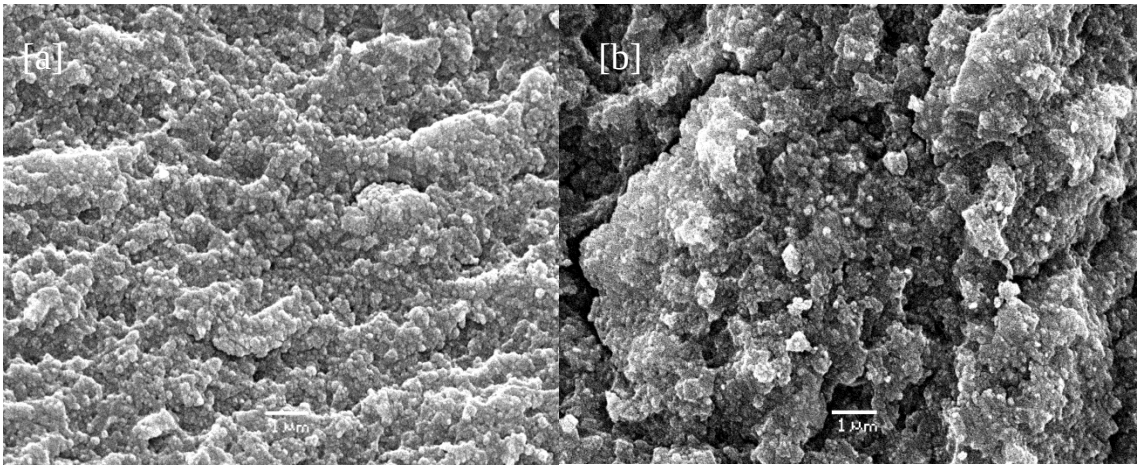

Figure 4.14. SEM fracture surface images of (a) OX50-γ-MPS based composite, (b) OX50_4000-100% based composite.

4.4 Conclusion

A novel surface modification technique was employed in order to improve polymerization shrinkage stress in dental composites. Oligomers with different chain lengths and different levels of surface reactivity were used to modify the surface of nanofillers. The results

show that the experimental composites have reduced shrinkage stress by as much as 30 % as compared with the traditionally used γ-MPS-based control while otherwise maintaining similar final conversion, shrinkage and modulus behavior. The surface modification procedure also has the potential to affect other properties such as dynamic modulus development and fracture toughness. It can be concluded that the surface modification technique used here has great potential to improve dental composites in terms of the critical property of polymerization stress development.

4.5 Acknowledgements

The authors would like to thank the National Institutes of Health for support of this research through the grant #R01DE014227. We also wish to thank Septodont-Confi-Dental and Evonik for their gracious donation of filler materials and Esstech, Inc. for donation of monomers.

4.6 References

[1] R. L. Bowen and W. A. Marjenhoff, "Dental Composites/Glass Ionomers: the Materials," *Advances in Dental Research*, vol. 6, pp. 44–49, 1992.

[2] L. G. Lovell, K. a. Berchtold, J. E. Elliott, H. Lu, and C. N. Bowman, "Understanding the kinetics and network formation of dimethacrylate dental resins," *Polymers for Advanced Technologies*, vol. 12, no. 6, pp. 335–345, Jun. 2001.

[3] K. J. Anusavice, *Phillips' Science of Dental Materials*, 11th ed. Elsevier, 2003.

[4] S. J. Sadowsky, "An overview of treatment considerations for esthetic restorations: a review of the literature," *The Journal of Prosthetic Dentistry*, vol. 96, no. 6, pp. 433–42, Dec. 2006.

[5] C. L. Davidson and A. J. Feilzer, "Polymerization shrinkage and shrinkage stress in polymer-based restoratives," *Journal of Dentistry*, vol. 25, no. 6, pp. 435–440, 1997.

[6] M. Rosin, A. D. Urban, C. Gärtner, O. Bernhardt, C. Splieth, and G. Meyer, "Polymerization shrinkage-strain and microleakage in dentin-bordered cavities of chemically and light-cured restorative materials.," *Dental Materials*, vol. 18, no. 7, pp. 521–8, Nov. 2002.

[7] C. N. Bowman, N. B. Cramer, and J. W. Sansbury, "Recent Advances and Developments in Composite Dental Restorative Materials," *Journal of Dental Research*, vol. 90, no. 4, pp. 402–416, Oct. 2010.

[8] J. M. Antonucci, S. H. Dickens, and B. O. Fowler, "Chemistry of Silanes : Interfaces in Dental Polymers and Composites," *Journal Of Research Of The National Institute Of Standards And Technology*, vol. 110, no. 5, pp. 541–558, 2005.

[9] Y. Bréchet, J.-Y. Cavaillé, E. Chabert, L. Chazeau, R. Dendievel, L. Flandin, and C. Gauthier, "Polymer Based Nanocomposites: Effect of Filler-Filler and Filler-Matrix Interactions," *Advanced Engineering Materials*, vol. 3, no. 8, p. 571, Aug. 2001.

[10] M. Harada, M. Morimoto, and M. Ochi, "Influence of network chain orientation on the mechanical property of epoxy resin filled with silica particles," *Journal of Applied Polymer Science*, vol. 87, no. 5, pp. 787–794, Jan. 2003.

[11] B. Lim, "Effect of filler fraction and filler surface treatment on wear of microfilled composites," *Dental Materials*, vol. 18, no. 1, pp. 1–11, Jan. 2002.

[12] S. Nakamura, E. Pavlovic, and E. Kramer, "Fracture Energy of Epoxy Interfaces with Layers of Different Silane Coupling Agents," *The Journal of Adhesion*, vol. 83, no. 4, pp. 351–365, 2007.

[13] P. K. Vallittu, “Curing of a silane coupling agent and its effect on the transverse strength of autopolymerizing polymethylmethacrylate-glass fibre composite.,” *Journal of Oral Rehabilitation*, vol. 24, no. 2, pp. 124–30, Feb. 1997.

[14] S. Ye, S. Azarnoush, I. R. Smith, N. B. Cramer, J. W. Stansbury, and C. N. Bowman, “Using hyperbranched oligomer functionalized glass fillers to reduce shrinkage stress.,” *Dental Materials*, vol. 28, no. 9, pp. 1004–11, Sep. 2012.

[15] R. H. Halvorson, R. L. Erickson, and C. L. Davidson, “The effect of filler and silane content on conversion of resin-based composite.,” *Dental Materials*, vol. 19, no. 4, pp. 327–33, Jun. 2003.

[16] Q. Liu, J. Ding, D. E. Chambers, S. Debnath, S. L. Wunder, and G. R. Baran, “Filler-coupling agent-matrix interactions in silica/polymethylmethacrylate composites.,” *Journal of Biomedical Materials Research*, vol. 57, no. 3, pp. 384–93, Dec. 2001.

[17] R. H. Halvorson, R. L. Erickson, and C. L. Davidson, “The effect of filler and silane content on conversion of resin-based composite.,” *Dental Materials*, vol. 19, no. 4, pp. 327–33, Jun. 2003.

[18] R. G. Craig and E. R. Dootz, “Effect of mixed silanes on the hydrolytic stability of composites.,” *Journal of Oral Rehabilitation*, vol. 23, no. 11, pp. 751–6, Nov. 1996.

[19] T. Nihei, S. Kurata, Y. Kondo, K. Umemoto, N. Yoshino, and T. Teranaka, “Enhanced Hydrolytic Stability of Dental Composites by Use of Fluoroalkyltrimethoxysilanes,” *Journal of Dental Research*, vol. 81, no. 7, pp. 482–486, Jul. 2002.

[20] K. S. Wilson, K. Zhang, and J. M. Antonucci, “Systematic variation of interfacial phase reactivity in dental nanocomposites.,” *Biomaterials*, vol. 26, no. 25, pp. 5095–103, Sep. 2005.

[21] F. Brochard-Wyart, P. G. De Gennes, L. Leger, Y. Marciano, and E. Raphael, “Adhesion promoters,” *Journal of Physical Chemistry*, vol. 98, no. 38, pp. 9405–9410, 1994.

[22] B. Zhao, “Polymer brushes: surface-immobilized macromolecules,” *Progress in Polymer Science*, vol. 25, no. 5, pp. 677–710, Jun. 2000.

[23] W. S. Gutowski, S. Li, C. Filippou, P. Hoobin, and S. Petinakis, “Interface/interphase engineering of polymers for adhesion enhancement: Part II. Theoretical and technological aspects of surface-engineered interphase-interface systems for adhesion enhancement,” *The Journal of Adhesion*, vol. 79, no. 5, pp. 483–519, May 2003.

[24] D. Julthongpiput, M. LeMieux, and V. . Tsukruk, “Micromechanical properties of glassy and rubbery polymer brush layers as probed by atomic force microscopy,” *Polymer*, vol. 44, no. 16, pp. 4557–4562, Jul. 2003.

[25] H. Lu, J. W. Stansbury, S. H. Dickens, F. C. Eichmiller, and C. N. Bowman, “Probing the origins and control of shrinkage stress in dental resin-composites: I. Shrinkage stress characterization technique.,” *Journal of Materials Science. Materials in Medicine*, vol. 15, no. 10, pp. 1097–103, Oct. 2004.

[26] C. L. Davidson and a J. de Gee, “Relaxation of polymerization contraction stresses by flow in dental composites,” *Journal of Dental Research*, vol. 63, no. 2, pp. 146–148, Feb. 1984.

[27] N. Altmann and P. J. Halley, “The effects of fillers on the chemorheology of highly filled epoxy resins : I . Effects on cure transitions and kinetics,” *Polymer International*, vol. 119, no. May 2002, pp. 113–119, 2003.

[28] S. Kang, “Preparation and characterization of epoxy composites filled with functionalized nanosilica particles obtained via sol–gel process,” *Polymer*, vol. 42, no. 3, pp. 879–887, Feb. 2001.

[29] J. R. Condon and J. L. Ferracane, “Reduction of composite contraction stress through non-bonded microfiller particles.,” *Dental Materials*, vol. 14, no. 4, pp. 256–60, Jul. 1998.

CHAPTER 5

INFLUENCE OF SURFACE MODIFICATION ON SHRINKAGE STRESS IN A MODEL DENTAL COMPOSITE: A MECHANISTIC STUDY

Abstract

Surface modification of fillers for optimizing material properties in dental composites has received very little attention. Current research mostly focuses on the development of low-shrinkage monomers for resin systems. We have designed a novel way to reduce shrinkage stress by treatment of filler surfaces with polymer brushes. We synthesized two series of oligomers – one with a rigid backbone and the other with a more flexible backbone. Each series of oligomers was made with three different molecular weights. Each such oligomer was then either used as it was or modified to contain methacrylate functional groups. In this manner, eighteen different oligomers were made, with sizes in the range of about 2000 to 20000 Da. These were attached to the OX50 filler surface and mixed with resin to test shrinkage stress reduction potential, with OX50 filler treated with γ-MPS as the control. The shrinkage stress for OX50- γ-MPS was 3.16 ± 0.14 MPa while that for the material with the lowest shrinkage stress was 2.17 ± 0.12 MPa. Shrinkage stress was found to vary greatly with methacrylate functionality on the oligomer. Increase in methacrylate functionality increased the stress. Increase in length only slightly reduced the shrinkage stress, while more flexibility of the oligomer structure appeared to increase the stress. Rheometry measurements showed a tendency toward a delayed network formation in the experimental composites. It was postulated that the delay in a system-wide network formation is due to the hindrance caused by the particle surfaces. Particles treated with γ-MPS formed a network faster due to the ease of accessibility to the surface methacrylate groups and hence showed an early rise in stress. The surface modification of filler particles with

oligomers was successful in reducing shrinkage stress in a model dental composite and the method has enormous potential to improve properties with more refinement.

5.1 Introduction

The trend in the last decade for the incorporation of nanosized fillers in polymeric dental composites [1], [2] has led to the exciting possibility of exploiting the high surface area to volume ratio of these inclusions to enhance the performance of these materials. In the dental industry, nanoparticles have been promoted to improve the wear properties and achieve superior polish compared to composites based on micron-sized particles[1], [3]. The high surface area maximizes the interaction of the reinforcing filler particle with the resin matrix. Filler surfaces are treated with functional organosilanes that can react covalently with the resin matrix phase, thus helping the fillers adhere to the resin [4]. The utility of the surface area of fillers has been limited to this link between the two phases to provide adequate stress transfer when the composite is stressed due to physical and thermal effects and also to improve filler dispersion. This leaves an enormous gap in the application of these nanoparticle-based composites that does not take full advantage of their potential.

Polymerization shrinkage stress due to shrinkage in constrained conditions has been a continuing problem in dental composite systems since their introduction [5]. Addition of high modulus fillers that are covalently linked to the polymer matrix results in additional constraints being placed on shrinkage of the resin. Studies conducted with untreated fillers and fillers treated with non-functional silanes that do not bond with the matrix phase show reduced stress development as compared with those that have covalent attachment with the resin [6]. The surfaces of such particles can serve as defect sites where localized free shrinkage can take place.

This reduces the overall volumetric shrinkage and consequently, stress development. This points to the significant role of the interface between the filler and matrix phases in controlling the stress development in the composite. Keeping these factors in mind, this research focuses on utilizing the high surface area of filler particles to aid in controlling shrinkage stress in polymeric dental composites.

Current research directed towards the reduction of shrinkage stress mainly focuses on the development of low shrinkage monomers and polymerization strategies. Novel resin formulations that include silorane materials (combination of siloxane and oxirane chemistries) that undergo a cationic ring-opening polymerization process [7], thiol-ene photopolymerizations that offer a hybrid chain/step-growth reaction mechanism [8], [9] and phase separation during polymerization to create internal interfaces within the resin phase. In a clinical situation, diagonal layering techniques are used wherein instead of filling the entire cavity with the restorative material, incremental portions of composite are sequentially placed and polymerized until the entire cavity is filled [10]. This technique relies on the fact that the more free surface a shrinking composite has as compared to its bonded surfaces, the lower is the stress that develops.

Since dental composite materials are typically characterized by very high filler contents and there is now a trend toward the incorporation of increasing amounts of nanosized fillers in these formulations, new strategies to improve material performance should include consideration of the resin-filler interface. Interfaces in dental composites have not received much attention. They serve as links between the resin phase and the fillers, but have no utility beyond that. This provides an excellent chance to use surface modification schemes to improve material properties. Polymer brushes have been used to modify surfaces and interfaces in a variety of applications. They find applications in adhesives, protein-resistant biosurfaces, surfactants and compatibilizers

[11–15]. They can be used in nanocomposites to be able to combine properties their properties like environmental responsiveness and that of fillers like mechanical and optical properties.

This work has used fillers grafted with polymer brushes to create either more rigid or more flexible interfaces of controlled dimension within particulate-filled polymeric materials as a means to test their effect on properties of model dental composites. The main property of interest was the shrinkage stress that develops during polymerization while also verifying that other critical properties such as modulus were not adversely affected. The goal of this investigation was to demonstrate and elucidate a mechanism the uses interfacial surface modification to control stress development. The specific factors that were studied were: brush flexibility, length and reactive group placement.

5.2 Materials and Methods

5.2.1 Materials

Silica nanoparticles (Aerosil OX50, average diameter = 40 nm, surface area 50 m^2/g) were donated by Evonik (Germany). OX50 silanized with γ-MPS (γ-methacryloxypropyl-trimethoxy silane) was kindly donated by Septodont Confi-Dental (Louisville, Colorado, USA). N-methylaminopropyltrimethoxysilane (MAPTS) was purchased from Gelest. 2,2-bis[4-(2-hydroxy-3-methacryloyloxypropyl-oxy)phenyl]propane (BisGMA) and triethylene glycol dimethacrylate (TEGDMA) monomers were donated by Esstech, Inc.. . A visible light initiating system consisting of 0.3 wt% camphorquinone (CQ) as initiator and 0.8 wt% ethyl 4-dimethylaminobenzoate (EDAB) (Sigma-Aldrich, Milwaukee, WI) as co-initiator was incorporated. Isocyanatoethylmethacrylate (IEM), methylene chloride, reagent alcohol, anhydrous toluene, and dibutyltin dilaurate, triethylamine were obtained from Sigma-Aldrich

(USA). Monomers used for making flexible oligomers – 1,6 - Hexanediylbis[oxy(2-hydroxy-3,1-propanediyl)] bisacrylate (HPDA) and 1,6-Hexanedithiol (HDT) and those used for rigid oligomer synthesis – Bisphenol A glycerolate (1 glycerol/phenol) diacrylate (BisGDA) and 1,2-Ethanedithiol (EDT), were also purchased from Sigma-Aldrich (USA) and used without further purification

5.2.2 Synthesis of Oligomers

Two related series of oigomers that were relatively either more flexible or more rigid were synthesized in various molecular weights (Table 5.2) using a Michael addition reaction between the diacrylate and dithiol monomers. The structures of the monomers used are shown in Figure 5.1. Scheme 1 shows the monomers, HPDA and HDT, used to synthesize the flexible oligomer series and Scheme 2 shows the monomers BisGDA and EDT used to synthesize the rigid oligomer series. For the synthesis, in general, monomers in each scheme were dissolved in chloroform in varied ratios. It was desired to have oligomers with acrylate functionalities at the ends and so acrylates were always kept in excess. A few drops of triethylamine as catalyst were added to the reaction mixture. The mixture was stirred constantly and progress of the reaction was monitored using FT-IR by following the reduction of the thiol peak at 2575 cm^{-1}. Upon completion of the reaction, the oligomer was separated from the unreacted mixture by dropwise addition in hexanes. The supernatant solution was discarded and the oligomers were isolated by removal of the residual solvent under reduced pressure.

The reasons for selecting HPDA and BisGDA were two-fold. HPDA has a flexible core structure while BisGDA has a more rigid core structure. The HDT molecule is also flexible and contributes to the overall flexibility of the final oligomer. The EDT molecule is flexible but

smaller and combining it with the BisGDA structure gives semi-rigid oligomers that can be compared with the more flexible structural analogs. The second reason was that both BisGDA and EDT introduce hydroxyl groups all along the oligomer backbone. These can be modified with a variety of functionalities to promote specific interactions with the resin. In this study, the oligomers were mainly modified with IEM, which has a methacrylate functionality that can react with the methacrylate-based resin system. For each of the oligomers synthesized, either all, i.e., 100%, 50% or none, i.e., 0% of the hydroxyl groups were reacted with IEM. Thus each oligomer was transformed into three different oligomers that had the same core structure but differed in the amount of pendant methacrylate groups along the chain. Figure 5.2 shows the general scheme of attaching IEM to any oligomer. Table 5.1 shows the general scheme of naming the oligomers.

Scheme 1 for flexible oligomers

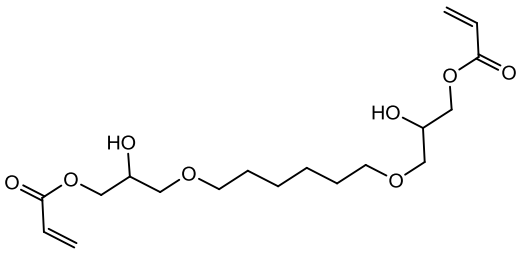

1,6-Hexanediylbis[oxy(2-hydroxy-3,1-propanediyl)] bisacrylate
(HPDA)

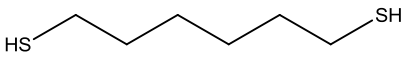

1,6-hexanedithiol
(HDT)

Scheme 2 for semi-rigid oligomers

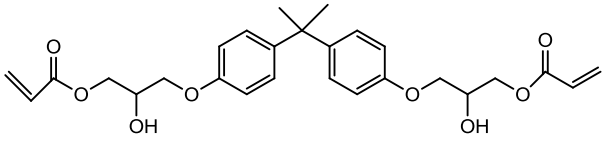

Bisphenol A glycerolate (1 glycerol/phenol) diacrylate
(BisGDA)

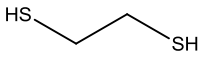

1,2-ethanedithiol
(EDT)

Figure 5.1. Monomers used in the synthesis of flexible and rigid oligomers.

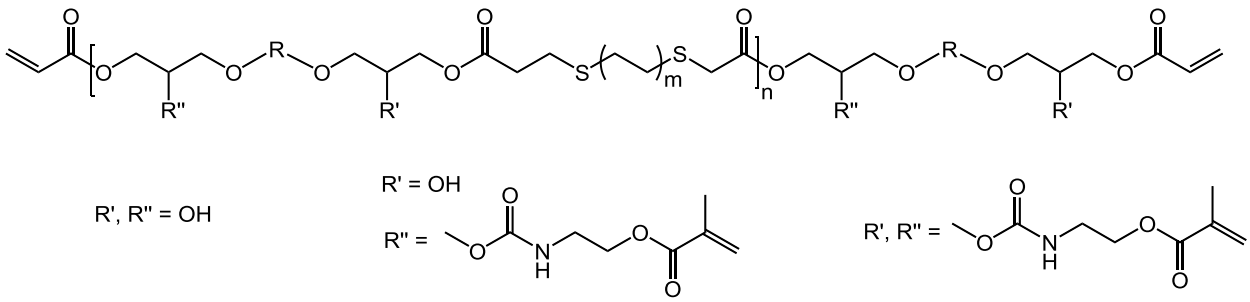

Figure 5.2. General scheme for attaching isocyanatoethyl methacrylate (IEM) to an oligomer. A generic structure representing the final oligomer is presented. R' and R" represent the different functionalities that can replace the existing –OH functionality. 3 cases are presented -1) R', R" = OH - 0 % methacrylate on oligomer; 2) R' = OH and R" = urethane functionality with methacrylate at free end – 50 % methacrylate on oligomer; 3) R',R" = urethane functionality with methacrylate at free end – 100 % methacrylate on oligomer.

5.2.3 GPC Characterization

A Viscotek triple detector gel permeation chromatography (GPC) system, equipped with Viscotek VE 3580 refractive index detector and Viscotek 270 dual light scattering/viscosity detector, was used for characterization of the size of the oligomers. The mobile phase was HPLC grade tetrahydrofuran at a flow rate of 1 mL/min. Samples were prepared in HPLC grade THF to a concentration of about 5g/L and 10 µL of sample was injected for analysis.

5.2.4 Differential Scanning Calorimetry

Calorimetric transitions of the materials were determined by DSC runs in a Netzsch Instruments 204 F1 DSC. About 5 mg samples were sealed in aluminum pans and run in the range -110 ^{o}C to 50 ^{o}C at 10 ^{o}C/min. Indium was used as the calibration standard. The glass transition temperatures were determined from the mid-point of the phase transitions in the DSC scans.

Table 5.1. Terminology that is used for the synthesized oligomers

	Rigid brush			Flexible brush		
Methacrylate functionality as % of hydroxyls on oligomer	0 %	50 %	100 %	0 %	50 %	100 %
Low molecular weight	RL0	RL50	RL100	FL0	FL50	FL100
Medium molecular weight	RM0	RM50	RM100	FM0	FM50	FM100
High molecular weight	RH0	RH50	RH100	FH0	FH50	FH100

5.2.5 Modification of the Filler

The bare silica particles were first treated treated with MAPTS and then the oligomers were attached to the amine end of the silane. OX50 particles were first dried in a rotary dryer at about 165 ^{o}C under vacuum for 3 hours before further treatment. This was done to ensure removal of surface bound moisture that can potentially react with the silanes and promote the formation of multiple layers of the silane. Anhydrous toluene was used as a solvent for the silanization process. It was refluxed for two hours and then the particles were added and further refluxed for an hour to ensure good dispersion. The MAPTS was added to the solution so that the final concentration in the mixture was 1.5 % by weight. This reaction mixture was allowed to reflux for six hours after which the particles were separated from the solvent by centrifugation. The particles were washed three times with toluene and two times with methylene chloride to ensure that all traces of unreacted silane were removed. The silanized particles were then dried overnight under vacuum at 50 ^{o}C to remove all traces of solvent. The dried and silanized

particles were then added to reagent alcohol in which 5X excess of oligomers were already mixed. The reaction mixture was heated to 45 ^{o}C and the reaction was allowed to continue for three days. The particles were then centrifuged to remove the solvent and washed five times with methylene chloride to remove excess solvent and dried in a vacuum oven at 45 ^{o}C. Figure 5.3 shows the general scheme of attaching the silane and then oligomers to the silica particles.

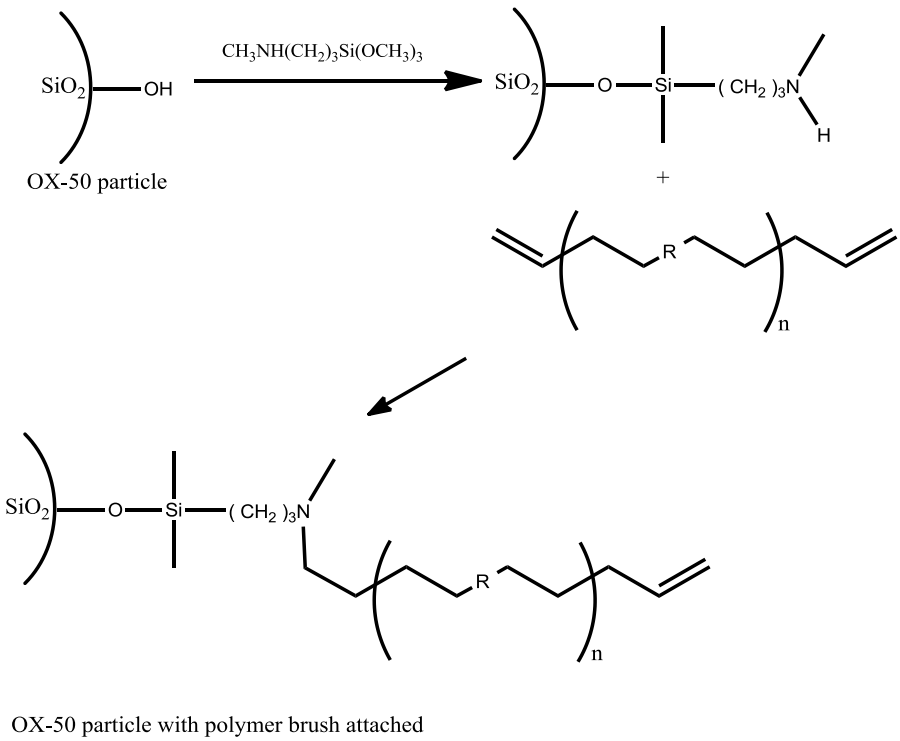

Figure 5.3. Scheme for attaching oligomer to silica particle.

5.2.6 Composite Preparation

The resin matrix for the composites was a mixture of BisGMA and TEGDMA in the ratio 70:30 by weight. The resin included a free radical visible light initiating system comprised of 0.3 wt% camphorquinone and 0.8 wt% ethyl 4-dimethylaminobenzoate. The fillers were added to the resin and mixed in a speedmixer (DAC 150 FVZ, Flakteck Inc.) and dispersed in the resin to make a composite paste that had a final filler loading of 30 wt%. Composites with γ-MPS-treated

OX50 particles were used as the control. The freshly prepared composites were evacuated to ensure elimination of air bubbles prior to being used.

5.2.7 Thermogravimetric Analysis

Thermogravimetric analysis (Pyris 7 TGA, Perkin Elmer) was used to determine the amount of surface functionalization on the OX50 particles after each stage of modification. Samples were placed in platinum pans in a nitrogen atmosphere and heated from 50 ^{o}C to 850 ^{o}C at 10 ^{o}C/min and the mass loss as a function of temperature was recorded.

5.2.8 Shrinkage Stress Measurements

Shrinkage stress was measured using a cantilever beam based instrument referred to as the tensometer (American Dental Association, Paffenberger Research Center, MD, USA). This instrument measures the force generated by an actively polymerizing material that is partially constrained from a free shrinking state. The material is bonded to the opposing ends of two diametrically placed quartz rods. The polished ends of the glass rods are freshly treated with γ-MPS, to promote bonding with the polymerizing material. The upper quartz rod is attached to the cantilever beam and is free to move along with the shrinking composite and the lower quartz rod is fixed to the base. A dental curing light (IQ2, Caulk, Dentsply), with an output wavelength of 465 nm, was adapted to the bottom of the lower quartz rod, which serves as a light guide to transmit the curing light to the material. A detailed description of the stress measurement involving the tensometer has been published previously [16]. The testing protocol uses specimen discs of 1.5 mm thickness and 6 mm diameter. The light intensity reaching the sample was measured at 350 mW/cm^2. The samples were irradiated for 40 s with the dynamic stress

development profile continuously monitored for 16 min. Real-time double bond conversion measurements based on simultaneous near-IR spectroscopy were made during the stress measurements.

5.2.9 Shrinkage Measurements

Polymerization shrinkage was measured using a linomter (ACTA Foundation, Netherlands). In this method composite paste specimens were placed between an aluminum disc and a glass slide that were greased to allow the free shrinkage of the sample along the radial direction. Specimens were 1.5 mm in thickness and 6 mm in diameter. The sample was irradiated from the top of the glass slide (350 mW/cm^2 for 40 s). The displacement of the freely moving aluminum disc was measured by linear variable differential transformer (LVDT) and converted to a dynamic volumetric shrinkage plot that extended to 10 minutes to capture the post-cure shrinkage behavior.

5.2.10 Flexural Modulus and Strength Measurements

Flexural modulus and strength were measured in a 3-point bending mode (858 Mini Bionix II, MTS Systems, Eden Prairie, MA). The composite pastes were injected into a cavity measuring 2x2x10 mm. The cavity was surrounded by Teflon spacers on the sides and clamped glass slides on the top and bottom. They were cured using visible light from both the sides to promote uniform conversion throughout the sample. The crosshead speed used was 1 mm/min.

5.2.11 Infrared Spectroscopic Characterization

Infrared spectroscopy was used to monitor the conversion of the resin and the surface modification of the fillers using an FTIR (Nexus 670, Nicolet Instruments, Madison, WI). Double bond conversion was monitored in transmission mode using near-infrared (NIR) spectroscopy. The area of the peak at 6165 cm^{-1} representing the methacrylate $=CH_2$ absorption was used to track conversion. For the simultaneous measurement of conversion with shrinkage stress and also during rheometry measurements, the NIR signal from the source was guided through the sample using an outbound optical fiber and the NIR signal transmitted through the sample was collected by the inbound optical fiber and conducted to the detector. Diffuse reflectance infra-red fourier transform spectroscopy (DRIFTS) was used to study the filler surfaces. For the DRIFTS experiments OX50 filler particles representing the various surface treatments, including the unmodified filler, were mixed with KBr powder and spectra were taken at a resolution of 4 cm-1, using KBr as a background.

5.2.12 Dynamic Mechanical Analysis

Elastic modulus and tan δ measurements were made on rectangular specimens (1x3.5x25 mm) in a DMA Q800 (TA Instruments) in the multifrequency strain mode. A sinusoidal force at 1 Hz frequency was applied. The measurements were done from -50 ^{o}C to 250 ^{o}C at 2 ^{o}C/min.

5.2.13 Rheometery

A rheometer (ARES 4400, TA instruments) was used for rheometer measurements. Two types of rheometer measurements were made. One was a frequency scan in the dynamic mode to measure complex moduli and viscosity, using a parallel plate mode. These measurements were

made on the uncured pastes of the samples. The second measurement was made to find the crossover point during cure. For this, the samples were placed between two quartz plates (22 mm diameter) in a parallel plate geometry with a sample spacing of 0.5 mm. A dynamic method was used to measure G' and G" with a frequency of 20 Hz and a starting strain of 40%. A torque-based automatic strain reduction was used to prevent overloading of the instrument as the modulus increased during cure. The frequency and strain were chosen such that the sample was always in the linear viscoelastic region, before and during cure. A light source (Acticure, EFOS, Mississiaugua, Ontario, Canada) with a 400-500 nm filter was used to cure the samples. Crossover point was taken as the point at which the value of G' surpassed G".

5.3 Results and Discussion

The interface between filler particles and polymer matrix in model dental composites was modified with oligomers/polymers that had differences in flexibility, length and reactive group concentrations. This was done using a grafting-to approach by preparing the oligomers in advance and then attaching them to the filler surface via an organofunctional silane (MAPTS). In general, it was found that all three parameters – flexibility, length and reactive group concentration had a significant effect on the polymerization shrinkage stress.

5.3.1 GPC and DSC Characterization of Oligomers

The molecular weight of the synthesized oligomers was measured using GPC. Glass transition measurements were done using DSC. The aim of the synthesis was to get a broad range of molecular weights and glass transition temperatures so that interfaces with a variety of physical properties could be created. Table 5.2 shows the molecular weight and glass transition

temperatures of the starting oligomers. The range of T_g was from -9.3 ^oC to about -65.4 ^oC. To put things in perspective, the T_g of a BisGMA/TEGDMA (70/30 wt/wt) mixture in its uncured state is about -22 ^oC. So oligomers that had T_gs on either side of the resin T_g were made.

Table 5.2. GPC and DSC characterization of oligomers.

Oligomer Type	**Size**	**Mol. Wt.**	**T_g (^oC)**
Rigid	High	21000	-9.3
Rigid	Medium	8000	-14.1
Rigid	Low	3000	-32.1
Flexible	High	16000	-52.2
Flexible	Medium	5500	-59.8
Flexible	Low	2000	-65.4

A word must be said about the nomenclature of oligomers used in this chapter. There are two main series – “rigid” and “flexible”. The rigid series represents the oligomers made by reacting BisGDA and EDT, while the flexible series represents the oligomers made by reacting HPDA and HDT. In each series, oligomers with three different sizes were made – low, medium and high (Table 5.2). Each of these oligomers then had 0%, 50% or 100% of its hydroxyl groups reacted with IEM. So if a rigid, high molecular weight oligomer had 100% of its hydroxyl groups replaced by methacrylate groups, it would be referred to as – “Rigid High 100% or RH100”. This scheme, in addition to the naming scheme given in Table 5.1, is followed throughout the entire chapter to refer to the oligomers.

5.3.2 Shrinkage Stress Measurements

Figure 5.4 shows the comparison of shrinkage stress measurement for the γ-MPS control and the long rigid brush series. The γ-MPS control shows the highest shrinkage stress among all the samples at 3.16 ± 0.14 MPa. As the amount of methacrylate groups on the brush increase, there is a corresponding increase in the shrinkage stress from 2.18 ± 0.12 for the RH0 to 2.48 ± 0.04 MPa for the RH50 and 2.66 ± 0.05 for the RH100 sample. It can be seen that the shrinkage stress increase rates also follow the same trend. The rate is smallest for the RH0 and follows the increase in the methacrylate group concentration on the brush.

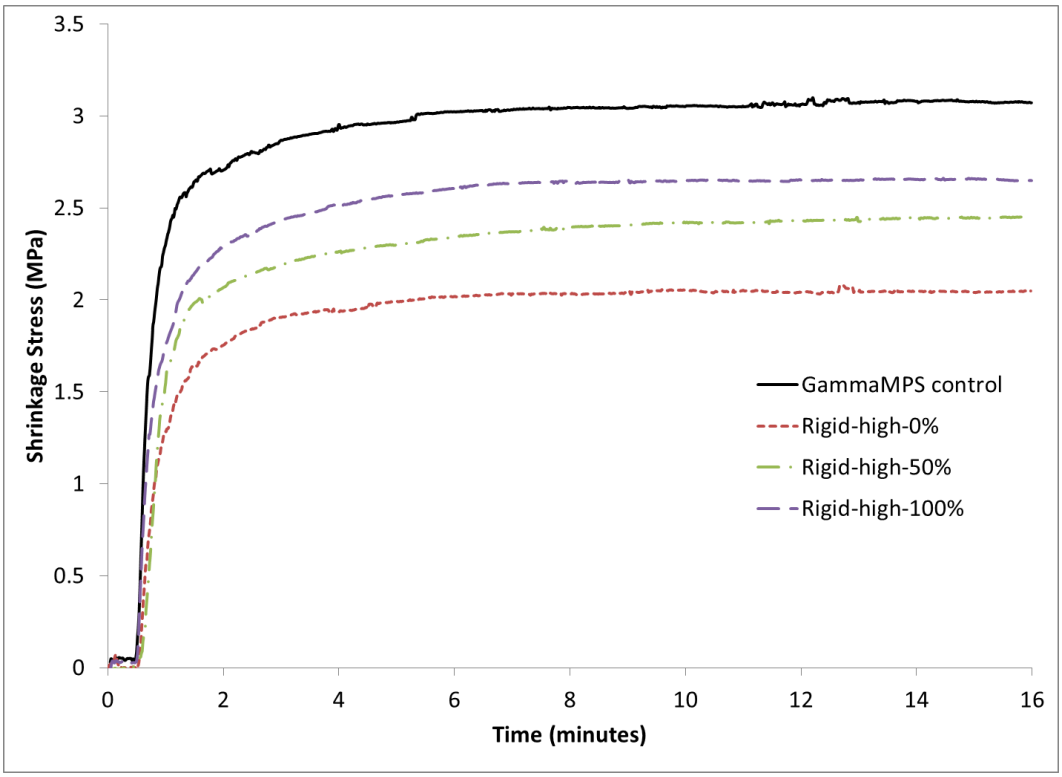

Figure 5.4. Comparison of shrinkage stress of the rigid high molecular weight series with the γ-MPS control. Visible light irradiation at t = 30s, for 40 s.

A summary of all the shrinkage stress, shrinkage, flexural modulus, glass transition and storage modulus results for the entire series of oligomers and also the γ-MPS control is shown in Table 5.3. Figures 5.5 and 5.6 show the final values of stress, for the rigid and flexible series, respectively. In both the series, there is a rise in shrinkage stress as the amount of reactive methacrylate groups increases from 0 % to 100 %. For the rigid oligomer series, there is no significant difference in stress as the length of the attached oligomer increases. For the flexible oligomer series, the lowest molecular weight brush shows a higher shrinkage stress as compared with the two higher molecular weight brushes. Except for the flexible low molecular weight brush, all the other brush systems exhibited lower shrinkage stress as compared to the control γ-MPS system.

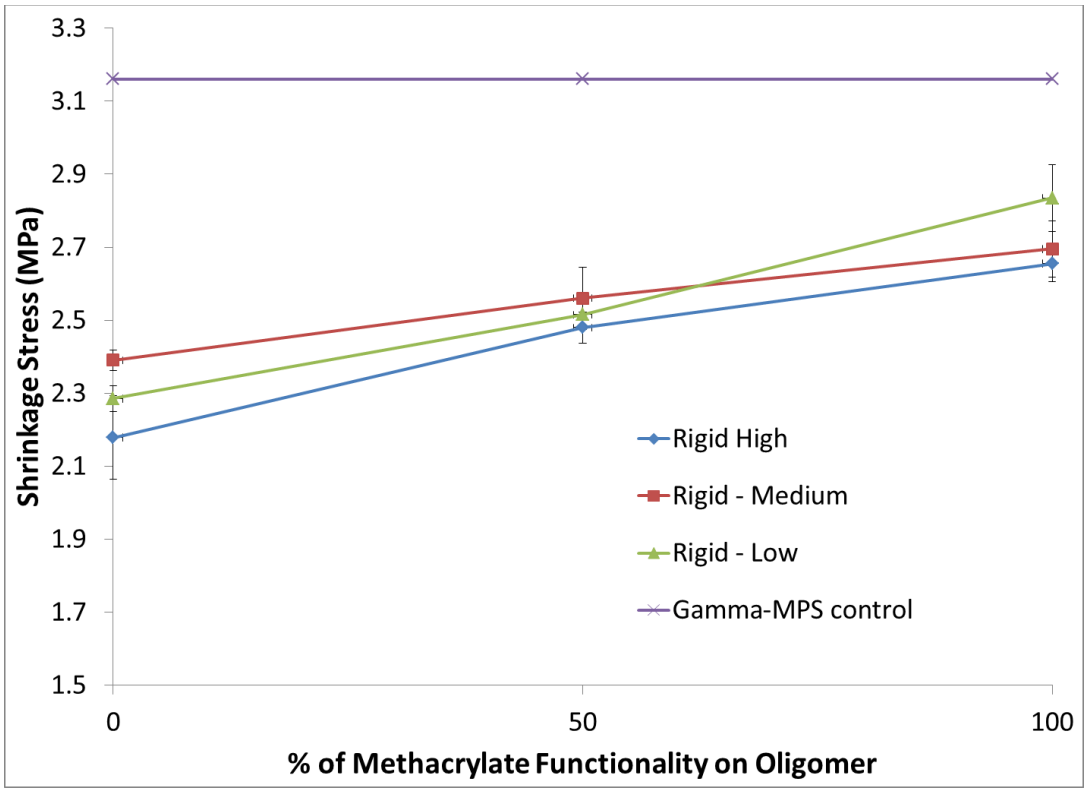

Figure 5.5. Shrinkage stress values for the rigid oligomer series at varied reactive group concentration. Visible light irradiation at t = 30s, for 40 s. Shrinkage stress values were taken at the end of the run at t = 16 min.

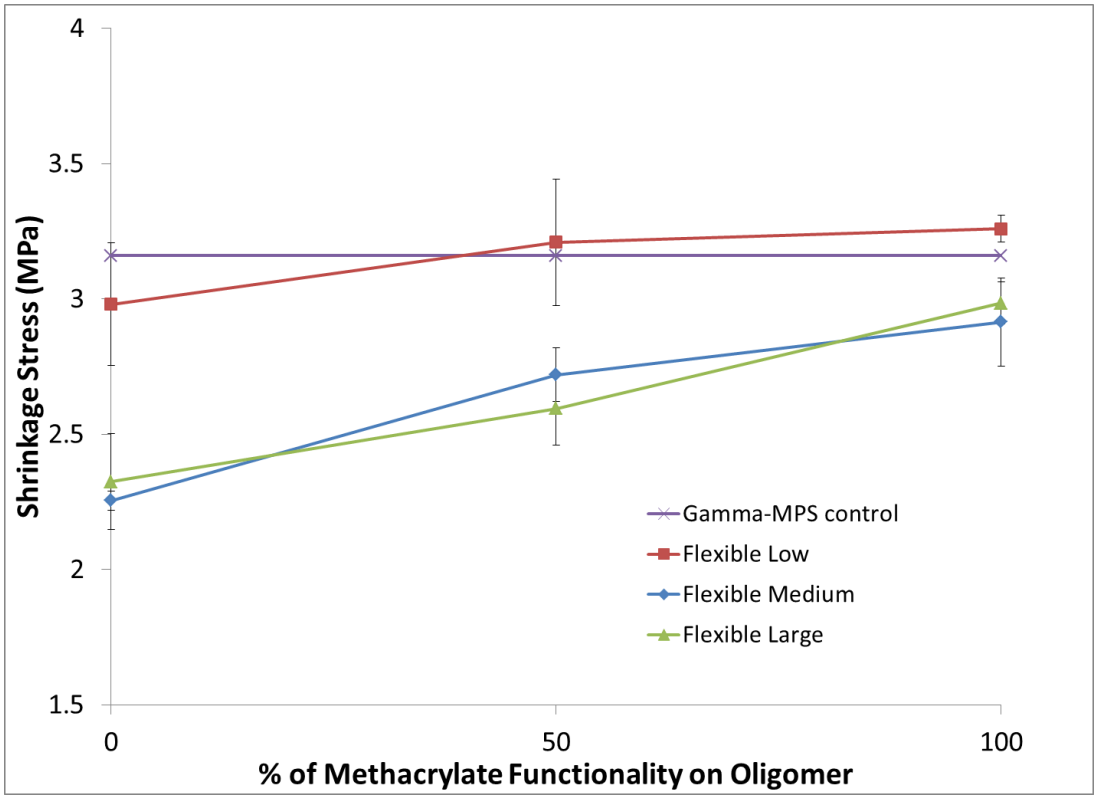

Figure 5.6. Final shrinkage stress values for the flexible brush series at varied reactive group concentration. Visible light irradiation at t = 30s, for 40 s. Shrinkage stress values were taken at the end of the run at t = 16 min.

Due to the simultaneous measurement of shrinkage stress and monomer conversion with respect to time, it is possible to plot stress as a function of conversion by use of the common time index. Two representative plots are presented here. Figure 5.7 shows the results for the rigid high molecular weight series when compared with the γ-MPS control. It can be seen that the onset of stress development in the control sample occurs at a very early stage in conversion and increases at a uniform rate until there is a rapid, late-stage rise in stress that is linked to the vitrification process. The stress development profile in the rigid high molecular weight system with 0 % methacrylate is the last to take off. This happens after about 20 % conversion and is followed by an initially very low rate of stress increase that progressively accelerates until the steep rise that coincides with vitrification. The stress in the 100 % methacrylated (RH100) sample starts to rise

after about 10 % conversion and rises at a similar rate but at lower values compared with the γ-MPS control. The RH100 surface treatment yields the highest final stress among the different brushes. The RH50 brush system lies in between the two extremes, in terms of rate of stress increase and final stress.

Table 5.3. Shrinkage stress, Shrinkage, Flexural Modulus, Glass Transition and Storage Modulus for the entire range of samples.

Surface treatment	Shrinkage Stress (MPa)	Shrinkage (%)	Flexure modulus (MPa)	T_g (^oC)	Storage Modulus (at 25 ^oC)(MPa)
GAMMA MPS	3.16 ± 0.14	5.50 ± 0.06	4410 ± 320	140.1 ± 0.1	2700 ± 300
RL0	2.29 ± 0.04	5.41 ± 0.10	4400 ± 490	144.0 ± 0.6	3900 ± 300
RL50	2.52 ± 2.01	5.35 ± 0.07	4600 ± 180	144.8 ± 2.0	3000 ± 500
RL100	2.84 ± 0.09	5.40 ± 0.15	4380 ± 240	146.9 ± 3.7	2800 ± 500
RM0	2.39 ± 0.03	5.37 ± 0.16	4240 ± 300	147.0 ± 3.8	3000 ± 600
RM50	2.56 ± 0.08	5.24 ± 0.14	4570 ± 180	142.8 ± 4.0	3000 ± 100
RM100	2.70 ± 0.08	5.31 ± 0.07	4500 ± 250	146.3 ± 1.7	2900 ± 400
RH0	2.17 ± 0.12	5.35 ± 0.05	4640 ± 300	148.9 ± 1.0	3700 ± 400
RH50	2.48 ± 0.04	5.27 ± 0.06	4550 ± 120	143.4 ± 4.8	2700 ± 300
RH100	2.66 ± 0.05	5.37 ± 0.21	4490 ± 200	147.6 ± 1.7	3400 ± 100
FL0	2.98 ± 0.23	5.49 ± 0.10	4890 ± 260	150.5 ± 5.4	2600 ± 600
FL50	3.21 ± 0.23	5.35 ± 0.06	4900 ± 160	141.5 ± 3.1	3400 ± 500
FL100	3.26 ± 0.05	5.42 ± 0.06	4730 ± 200	150.1 ± 2.3	3500 ± 300
FM0	2.26 ± 0.04	5.20 ± 0.10	4100 ± 470	148.3 ± 1.3	2700 ± 300
FM50	2.72 ± 0.10	5.57 ± 0.14	4790 ± 160	145.6 ± 2.1	2700 ± 200
FM100	2.92 ± 0.16	5.28 ± 0.15	4730 ± 290	147.3 ± 0.1	2800 ± 100
FH0	2.33 ± 0.18	5.49 ± 0.10	4440 ± 220	146.5 ± 1.8	2900 ± 600
FH50	2.60 ± 0.13	5.55 ± 0.06	4230 ± 780	144.9 ± 2.2	3400 ± 200
FH100	3.04 ± 0.05	5.42 ± 0.06	4610 ± 200	146.3 ± 1.3	3300 ± 500

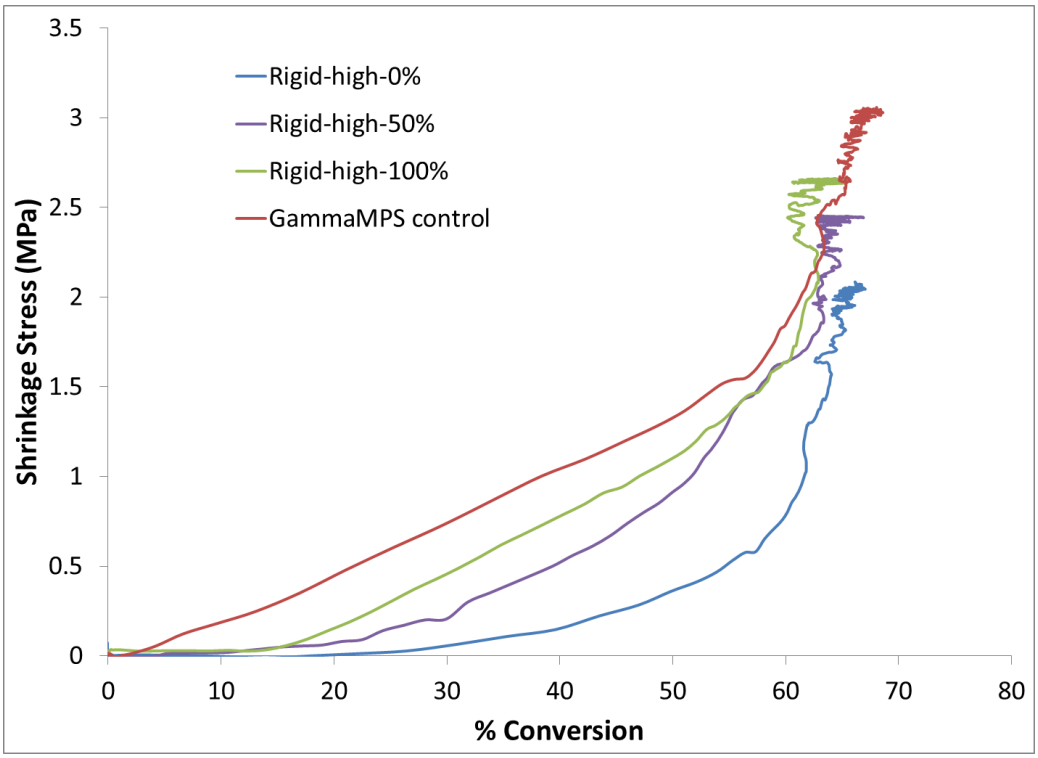

Figure 5.7. Variation of shrinkage stress with respect to conversion of the rigid high molecular weight series with the γ-MPS control. Visible light irradiation at t = 30 s, for 40 s. Shrinkage stress values were taken at the end of the run at t = 16 min.

Figure 5.8 compares the development of stress with respect to conversion for both the high molecular weight rigid and flexible brushes, each with no methacrylate reactive groups appended on the oligomeric chains. Both the systems show a similar onset for the stress development. The rigid brush system reaches a lower final stress compared with the flexible system. It is interesting to note that during the vitrification stage, which is where the stress rises very steeply, both the systems follow almost the same path in approaching their respective final stress points.

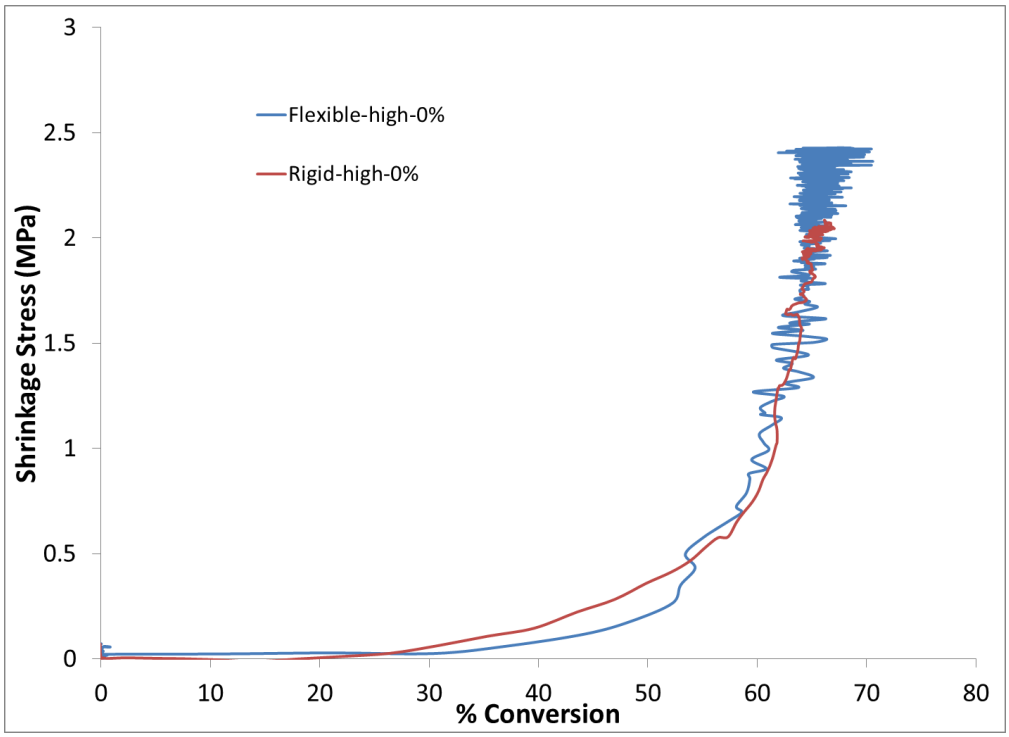

Figure 5.8. Variation of shrinkage stress of the rigid and low high molecular weight systems that have 0 % methacrylate groups. Visible light irradiation at t = 30s, for 40 s. Shrinkage stress values were taken at the end of the run at t = 16 min.

Figures 5.7 and 5.8 point to toward the formation of a load bearing network strong enough to register a positive force on the tensometer that varies considerably depending on the surface treatment of the filler particles. Gelation is the formation of an infinite network and it is assumed that at this point the network becomes strong enough to be able to bear and exert loads. In our study, the "gelation" we are looking at is the formation of an infinite network that includes particles as crosslinkers and not at the gelation of just the monomer. This is the point where the shrinkage stress starts rising. In order to confirm whether the "gel-point" conversion was indeed changing with addition of fillers with different surface treatments, a rheometric analysis was used that coupled a photo-rheometer with FT-IR spectroscopy to measure the point in conversion where the storage modulus (G') crosses the loss modulus (G"). This crossover point represents

the initial transformation of liquid to solid character and it is widely accepted as an indication of macrogelation [17].

5.3.3 Crossover Point Measurements

A typical plot showing crossover of G' with respect to G" is shown in Figure 5.9. Before cure, the material is in a liquid state and G' is lower than G". As the material cures, the storage modulus rises faster than the loss modulus and this gives rise to a crossover point. This measurement, when done in conjunction with real-time FT-near-IR measurements, can give the conversion where gelation occurs. Figures 5.10 and 5.11 give the gel-point conversion values for the rigid and flexible brush systems, respectively.

There is a reasonable similarity between Figures 5.10 and 5.11 and their counterparts, Figures 5.5 and 5.6, respectively. The progression of shrinkage stress with respect to the oligomeric brush flexibility, length and methacrylate functionality in Figures 5.5 and 5.6 follows the progression of the crossover point with respect to the same parameters. The curing conditions are different in both the measurements but the similarity of the trends in the properties shows that indeed there is a change in the gel point of the experimental systems due to the filler surface modification. As mentioned before, for gelation to occur, an infinite network has to form in the polymer due to chemical or physical cross-linking. The particles being introduced into the composite paste can either act as multifunctional rigid bridges between the growing polymer chains or they can suppress bulk matrix network formation. The interaction of the particles with the resin during polymerization depend on the surface treatment of the filler particles. Assuming that the particles are well dispersed in the resin monomer, upon curing, if they can quickly form covalent linkages that contribute rigidity similar to or greater than that of the bulk matrix, then a

continuous network can be formed quickly with a gel point conversion similar to that of the unfilled resin. If however, the surface treatment is such that the covalent linkage between the two phases is delayed or absent, then a delay in the gelation of the system with respect to conversion would be anticipated since the minimum network percolation path length is increased.

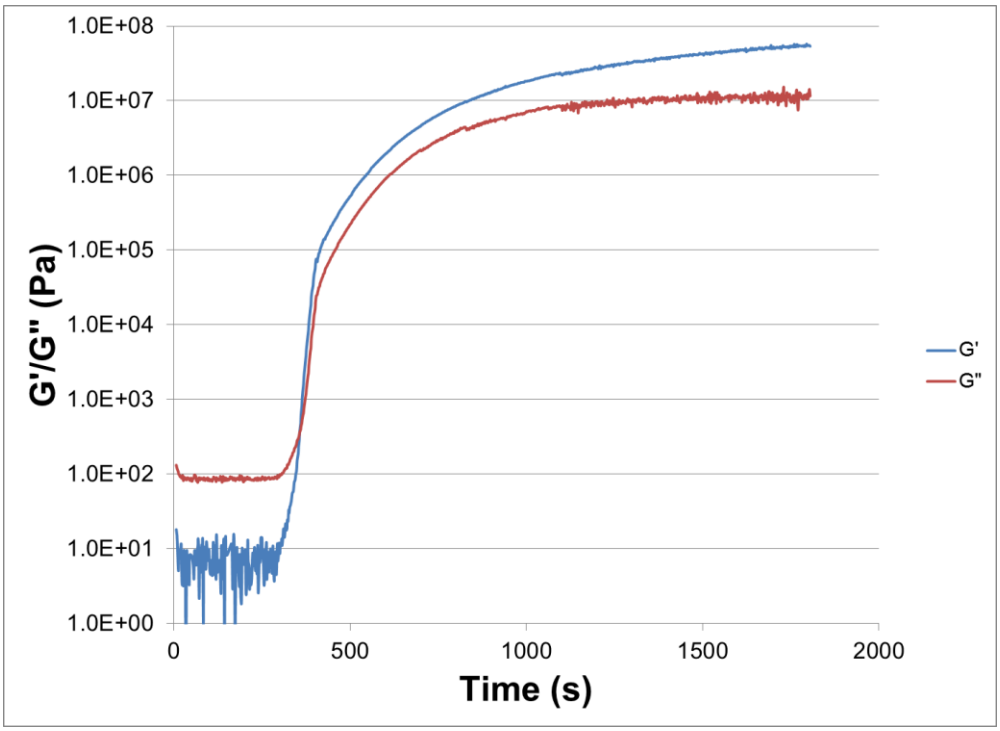

Figure 5.9. Typical plot of crossover of storage modulus (G') over loss modulus (G)" during cure during real time cure in a photorheometer.

For the brush systems with no appended methacrylates, there is at most only one acrylate functionality at the end of each tethered brush. If the oligomeric brush layer around the particle is reasonably thick, there is a significant probability of the acrylate functionality being buried in the interface and relatively inaccessible to the growing polymer chains around the particle. If the particles are present at a high volume fraction, they, along with the interfacial layer around them can form a percolating network [18]. This confines the resin between particles and limits its

ability to form a continuous network. If however, the brushes had reactive groups that could copolymerize with the resin and which were accessible to the resin, it would increase the chances of promoting covalent linkages between the two phases. In Figures 5.10 and 5.11, there is an initial steep decline in the crossover conversion, going from 0 % methacrylate to 50 % methacrylate but it levels off in leading to the 100 % methacrylate brush. This indicates that, for a given length of the brush, once a certain effective reactive group threshold concentration has been reached, there is no further effect of increasing it further.

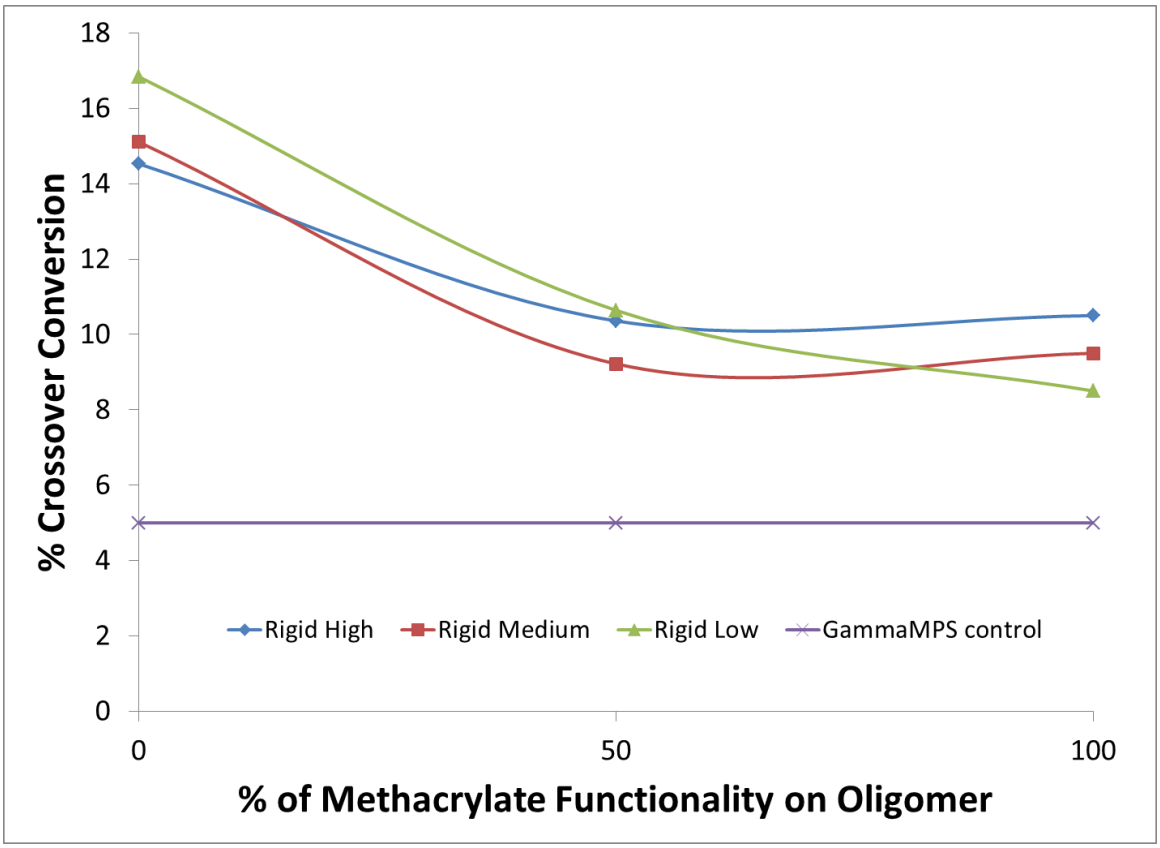

Figure 5.10. Effective gel point of photocured composite samples based on rigid ologomers. Irradiation intensity = 1 mW/cm^2 for the duration of the experiment.

The flexibility of the chains also has an effect on the crossover point. There are certain subtle differences between Figures 5.10 and 5.11. In Figure 5.10, all the curves are packed closely together with no significant differences at each methacrylate concentration level, which

is an indication that the length of the oligomer has very little effect on the crossover point. In case of the flexible oligomers, however, there is a significant difference between the lowest molecular weight oligomer and the two higher molecular weight brush structures.

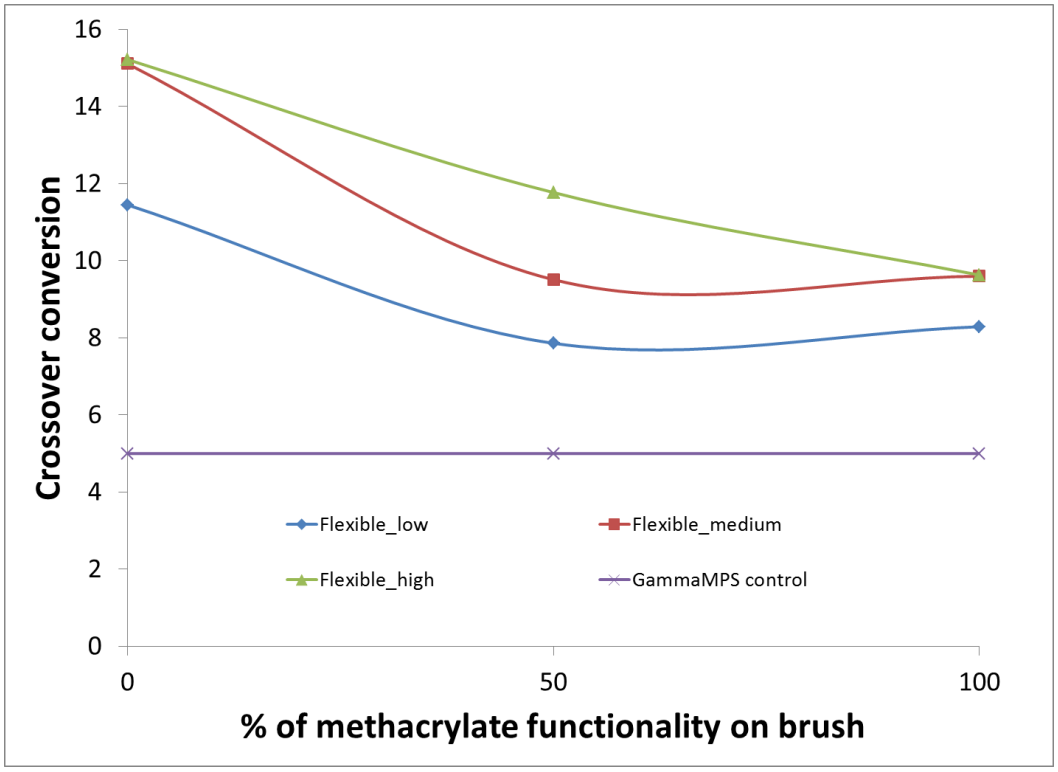

Figure 5.11. Effective gel point of photocured composite samples based on flexible oligomers. Irradiation intensity = 1 mW/cm^2 for the duration of the experiment.

At moderate to high filler loading involving micro- or nano-fillers, interparticle distances begin to approach the dimensions that can be accessed by modified interfacial surface layers. For matrix gelation to occur, a continuous network has to start forming in the entire sample. If particles are dispersed in the resin, they would have to form essential parts of the network, unless the network can bypass them and form around them. At higher filler loadings this becomes increasingly difficult as the growing microgels would have to connect through at least somewhat constrained spaces in between the particles. If however the particles have reactive groups on

them, the resin can react with these and form a covalent connection at any stage of the polymerization reaction. Filler particles can act as bridges or extended rigid crosslinks, helping the network to form. If there is an interface around the particles with reduced reactivity towards the resin, either due to low concentration of monomers in the interphase or due to a low concentration of polymerizable groups on the oligomeric chains, the network connections between the resin and filler would take a longer time, or a later stage of network development, to form. Gelation is clearly occurring in the resin that surrounds the particles. So the filler particles are not interfering with the microscale gelation. The particles only affect the overall gelation of the material, considered as a whole. This is the effect that is observed in the rheometer studies. There is very scarce literature studying the effect of chemical cross-linking due to fillers on the gelation of the network. In one of the few studies that have been done [19], the authors studied fumed silica with two different surface treatments – an octyl silane and a methyl silane. It was found that using both the fillers increased the gel times of the reaction, although no reasons were given as to why this occurred. Gaines and co-workers [20], while looking at effect of nanoparticles on network formation in disordered block copolymers found that at high concentrations, the effect of the nanoparticles was to impart a solid-like behavior to the polymer melt, suggesting an existence of a colloidal network comprised of the nanoparticles. This suggests the synergistic effect a network of nanoparticles can have on the polymer around them.

5.3.4 Rheology of Composite Pastes

Linear oscillatory measurements on a rheometer were performed to explore the effect of the surface treatment on the viscoelastic behavior of the composite pastes. Changes in viscosity and also storage and loss moduli with respect to frequency were monitored. Measurements were

conducted on samples with fillers treated with oligomers that had either a low or high level (0 % and 100 %) of methacrylate functionality along the backbone. These represent the two extremes in terms of methacrylate functionality and it was assumed that the mid-level functionalized methacrylate oligomers (50 %) would fall in between the two extremes.

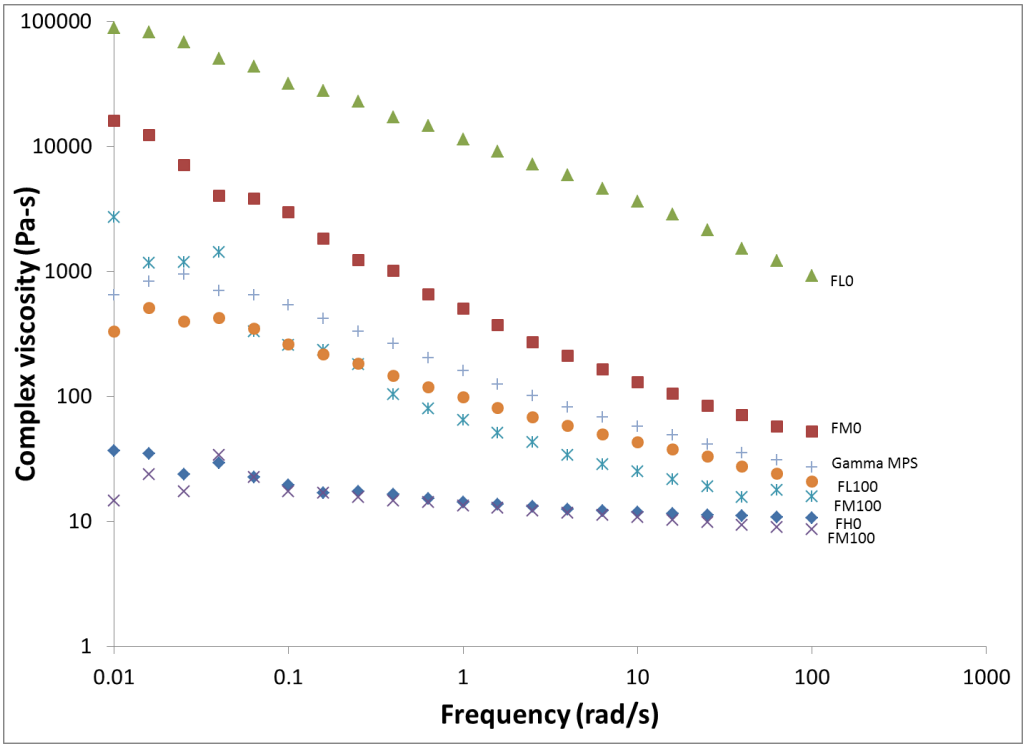

Figure 5.12. Complex viscosity as a function of frequency for composites based on particles treated with flexible oligomers. (The terms short, medium and long refer to high, medium and low molecular weight oligomers, respectively).

Figure 5.12 shows the comparison of viscosity the OX50-GammaMPS control samples with the composites based on the flexible oligomer series. A general observation that can be

made is that composite pastes that had particles with brushes treated with the methacrylate functionality had a lower viscosity as compared with those without the appended methacrylate groups. The analogous oligomer structure with no methacrylates has hydroxyl groups that can hydrogen bond with the BisGMA monomers, thereby increasing the particle-matrix interactions and the overall viscosity. When the hydroxyl groups are reacted with IEM, the resulting urethane methacrylates contribute weaker hydrogen bonding and the composite pastes exhibit lower viscosity. Further reduction in the composite viscosity would be anticipated if the hydroxyl groups were replaced with simple methacrylate esters via reaction with methacrylic acid or methacryloyl chloride. The highest molecular weight oligomer-based composite shows the lowest viscosity. Polymer brushes have been known to stabilize particles in colloidal systems by improving the dispersion character of the particles in the matrix. Reduction of aggregation and better dispersion reduces the viscosity of colloidal systems and this effect is observed in these composite systems. As both the methacrylated and unmethacrylated version of the high molecular weight oligomer-based composite show a lower viscosity, it can be inferred that the brush structure aids in the filler dispersion. It can be surmised that the longer the oligomers (within limits), the better the stabilization of the particles and the accompanying reduction in viscosity. The low molecular weight oligomer-based composite with no methacrylate groups (0 %) produced the highest viscosity. This again may be partially due to less stabilization of the filler dispersion and also due to the presence of interactions involving the hydroxyl groups. Both these factors would work in favor of increasing the attractive interaction with the resin and lead to an increased viscosity. The OX50-GammaMPS control and the medium-sized flexible oligomer-based composite had viscosities in between the two extremes.

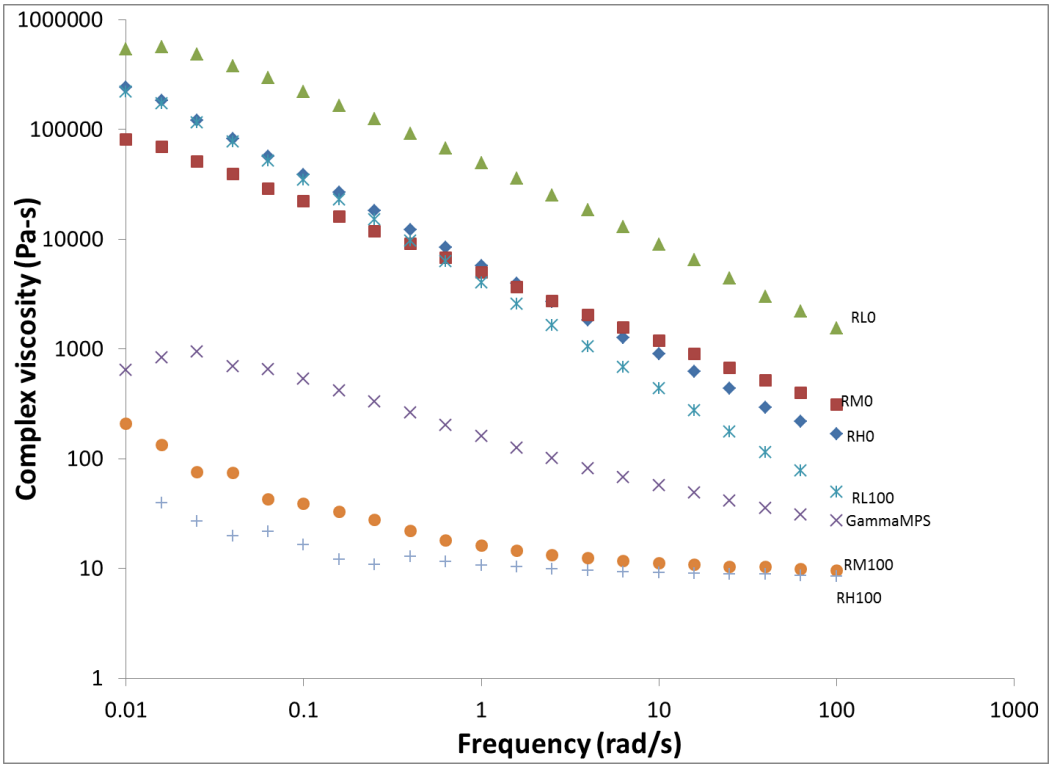

Figure 5.13. Complex viscosity as a function of frequency for composites based on particles treated with rigid oligomers . (The terms short, medium and long refer to high, medium and low molecular weight oligomers, respectively).

The trend in viscosities for the rigid oligomer-based composite systems shows some significant differences from that of the composite paste materials based on the flexible oligomer-based ones. With the rigid oligomer-based composites, once again the zero-methacrylate systems (0 %) provide a higher paste viscosity than the corresponding high-methacrylate (100 %) systems. However, the major difference is that the high molecular weight rigid oligomer-based composite does not have the lowest viscosity but has higher viscosity than the composites based on the short and medium molecular weight oligomers at 100 % methacrylate coverage. The rigid oligomers are made of an aromatic backbone and the resin system has BisGMA that also has an aromatic backbone. There are attractive interactions due to pi-pi stacking of the aromatic rings between all the oligomers and the resin. This leads to an increase in the viscosity of the systems. The long oligomers, due to their increased size have more potential for the attractive,

predominantly intermolecular interactions and the viscosity of composites with fillers treated with these oligomers is higher. The composites with particles with medium and low molecular weight oligomers with low methacrylate coverage however have higher viscosities than those based on the high molecular weight oligomers. This may be due to the fact that in addition to the pi-pi stacking interactions, the hydrogen bonding interactions are also present. The length effect of the long rigid oligomer may not be as strong as the hydrogen bonding effect and this can explain the higher viscosity of the shorter chains.

A common observation for the viscosity measurements for both the rigid and flexible oligomer-based materials is that the viscosity decreases with increasing frequency, showing psuedoplastic behavior. The higher shear forces at higher frequencies can more effectively disrupt the attractive interactions that exist between particles as well as between the particles and the resin matrix, which favors alignment of particles. This offers less resistance to flow and results in a lowering of the viscosity. It must be noted that that absolute value of viscosity is higher for the rigid brush system and this is due to the stronger attractive force between the oligomers and the resin.

The storage and loss moduli for all the flexible oligomer-based composite pastes with 0 % methacrylate and the γ-MPS control are shown in Figure 5.14. The composite pastes mostly show liquid-like behavior over the entire frequency range. The trend in modulus values is very similar to the corresponding viscosity plots (Figure 5.12). The long flexible oligomer-based composite paste shows a predominantly liquid-like behavior, while the medium-sized oligomer system shows a cross-over from solid-like to liquid-like behavior and for the short oligomer-based composite paste, the G’ and G” curves lie on top of each other, indicating that this is near an effective gel point of the system. The OX50-γ-MPS control system is liquid-like and shows

higher moduli than the high molecular weight oligomer-based system but lower than that of the medium and low molecular weight oligomer-based composites.

Figure 5.15 shows the moduli for the composites with flexible oligomers with 100 % methacrylate on the backbone. The moduli of these oligomer-based systems are lower than those of the γ-MPS control systems with the longest oligomer system having the lowest moduli. This trend is also the same as seen in the viscosity plot for this system (Figure 5.12).

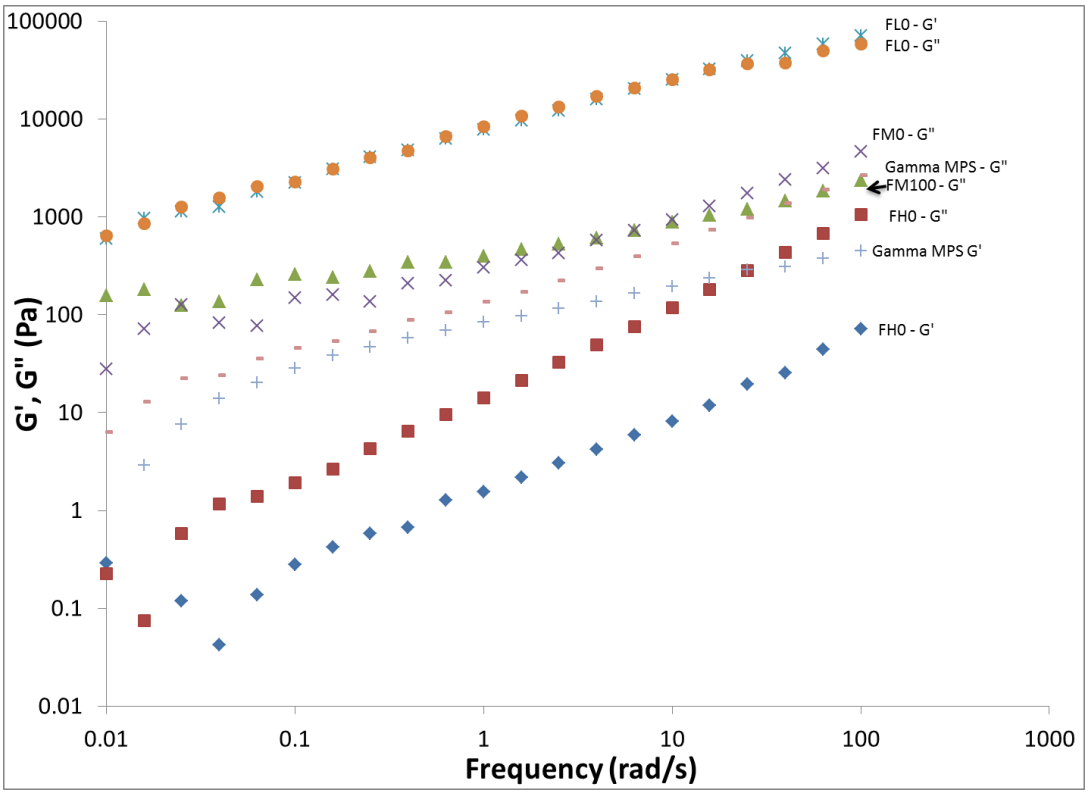

Figure 5.14. Storage and loss moduli of composites based on particles treated with flexible oligomers with no methacrylate coverage compared with the γ-MPS control system. (The terms short, medium and long refer to high, medium and low molecular weight oligomers, respectively).

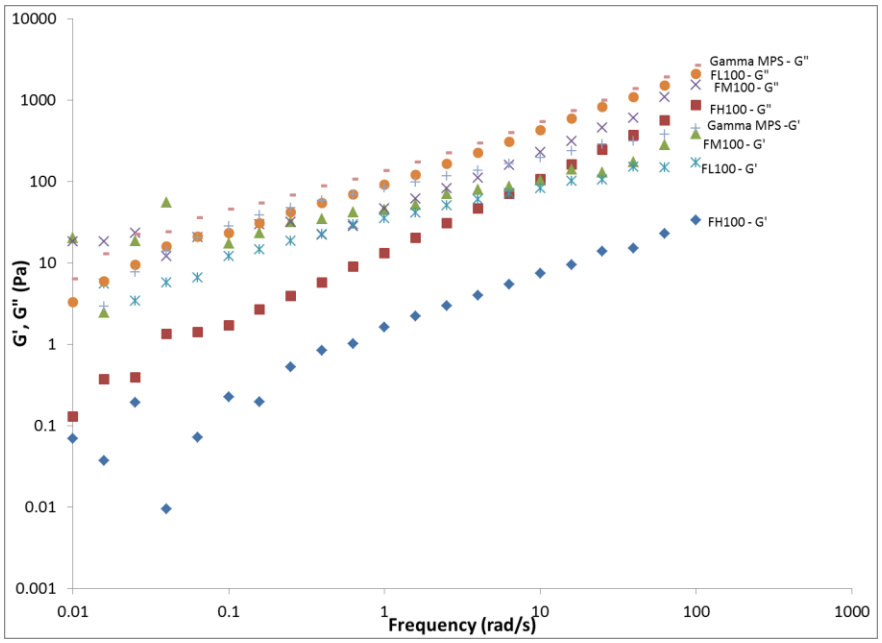

Figure 5.15. Storage and loss moduli of composites based on particles treated with flexible oligomers with 100 % methacrylate coverage compared with the γ-MPS control system. (The terms short, medium and long refer to high, medium and low molecular weight oligomers, respectively)

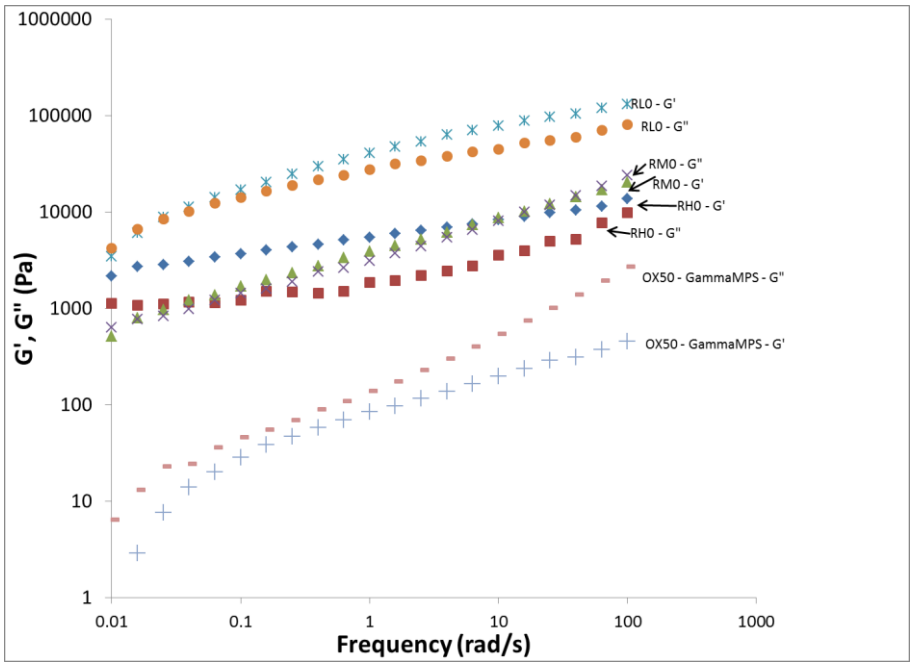

Figure 5.16. Store and loss moduli of composites based on particles treated with rigid oligomers with no methacrylate coverage compared with the γ-MPS control system. (The terms short, medium and long refer to high, medium and low molecular weight oligomers, respectively)

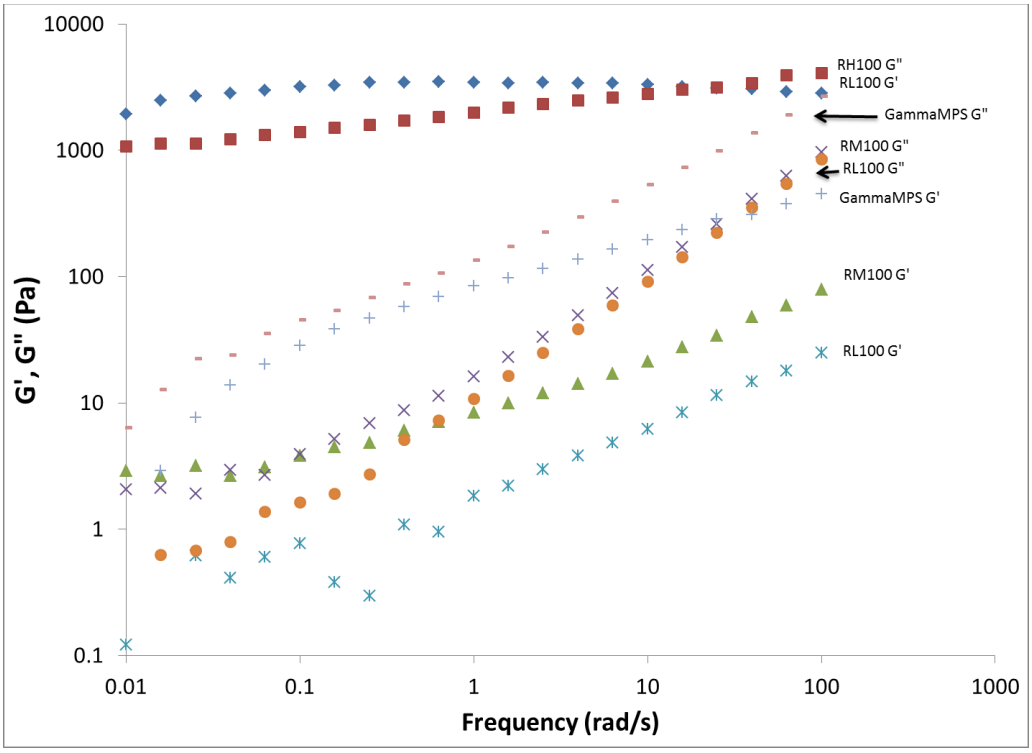

Figure 5.17. Store and loss moduli of composites based on particles treated with rigid oligomers with 100 % methacrylate coverage compared with the γ-MPS control system. (The terms short, medium and long refer to high, medium and low molecular weight oligomers, respectively)

Figure 5.16 shows the complex moduli of the rigid oligomer-based system with no methacrylates on the chains. All the experimental systems have higher moduli as compared to the OX50-γ-MPS control. The slopes of the frequency-dependent moduli are reduced compared to the flexible oligomer-based systems, indicating a tendency toward a more solid-like behavior. In fact, for the high molecular weight oligomer-based sample, G' is higher than G" over the entire frequency range. For the medium-molecular weight oligomer-based sample, G' and G" overlap each other and for the small-sized brush, G' is slightly higher than G".

Figure 5.17 shows the complex moduli of rigid oligomer-based composites with high level of methacrylate (100 %). The high molecular weight oligomer-based sample shows solid-like behavior. The G' has a plateau region, which is indicative of the solid behavior. The medium-molecular weight sample initially shows solid-like behavior and then G' and G" cross over to exhibit liquid-like behavior. The low molecular weight sample is liquid like throughout the frequency range.

5.3.5 Interface Characterization by Staining with RuO_4

In order to study the interaction of the interfacial structure with the resin matrix upon polymerization, it was crucial to be able to look directly at the interface. This was done using TEM of sections of composites. The organic layer on the particles was stained with ruthenium tetroxide. In TEM measurements without staining, there was insufficient contrast between the interfacial layer and the polymer matrix and the staining created a contrast that helped to differentiate between the two phases. Imaging was done on the isolated free particles and also polymerized composite samples to detect changes in the interface before and after curing.

Figure 5.18 (a) shows the TEM image for an OX50 particle that has been functionalized with the high molecular weight rigid 0 % methacrylated oligomer. These particles were lightly scattered on a TEM grid and the image taken. A faint interfacial layer can be seen around the particle. From the observations, the thickness of the interface appeared to be between 1 nm and 4 nm. It must be mentioned that these thicknesses are representative of a large number of particles that were scanned. When these stained particles are mixed in the resin and polymerized, a dramatic change takes place in the interfacial layer. A representative image is shown (Figure 5.18 (b)). Here, it can be seen that the interface layer is now more clearly visible and extends

away from the filler surface to a greater extent than in free particle. The thickness of the interface here is between 8 to 9 nm. Similar measurements were carried out with the particles that were untreated, representing a negative control, γ-MPS, which is the positive control and the rigid high molecular weight oligomer with 100% methacrylates, to compare the effect of methacrylate functionality. Figures 5.19 (a) and (b) show the free γ-MPS control particles and those embedded in the polymer matrix, respectively. The free γ-MPS particles show a smaller interfacial layer of about 2 nm and this layer does not show an appreciable increase in thickness in the composite after polymerization. This is to be expected, since the γ-MPS is a short molecule so there can be no extension of the layer away from the surface. In the case of the untreated OX50 particles (Figures 5.20 (a) and (b)), we see no presence of any interface in the free particles or the composite specimen. This is expected again as there is no functionality on the surface of the untreated fillers that can be stained by the ruthenium tetroxide. Figures 5.21 (a) and (b) show the fillers treated with the high molecular weight rigid oligomer with 100 % methacrylate functionality. The bare particles (Figure 5.21 (a)) clearly show the presence of the oligomer attached to the surface. Figure 5.21 (b) shows the fillers embedded in the polymer matrix. The figure is not very clear and there was no sign of an expanded interface on the particles. There was a faint trace of an interface region that had similar thicknesses as the bare particles, but it was not conclusive. This particular oligomer, since the methacrylate functionality is high, it was expected from the gel-point rheology measurements that the since the gel-point was reached faster than in the corresponding 0 % methacrylate sample, the oligomer layer would have less time to extend away from the surface along with the resin that is shrinking away from the surface. Once the network is in an advanced stage of development, it is frozen in place and the oligomers cannot be stretched further.

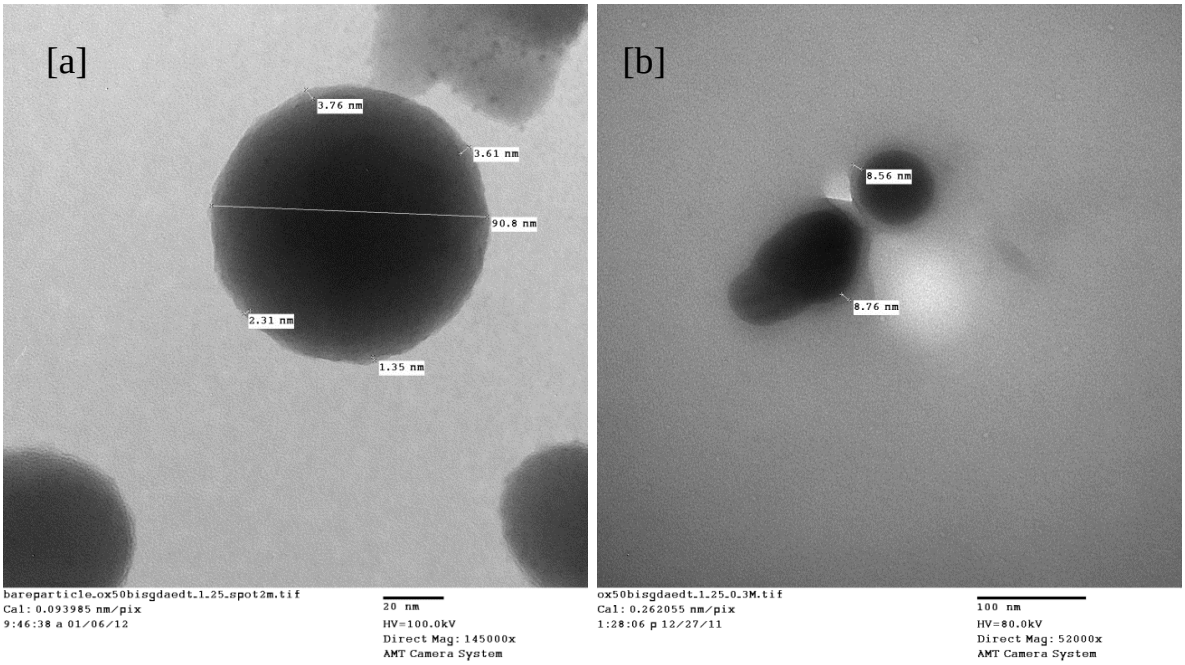

Figure 5.18. TEM images of OX50 particles treated with RH0 oligomer (rigid, high molecular weight, 0% methacrylate functionality. (a) Particles sprinkled on TEM grid (b) Section of composite with particles embedded in the resin

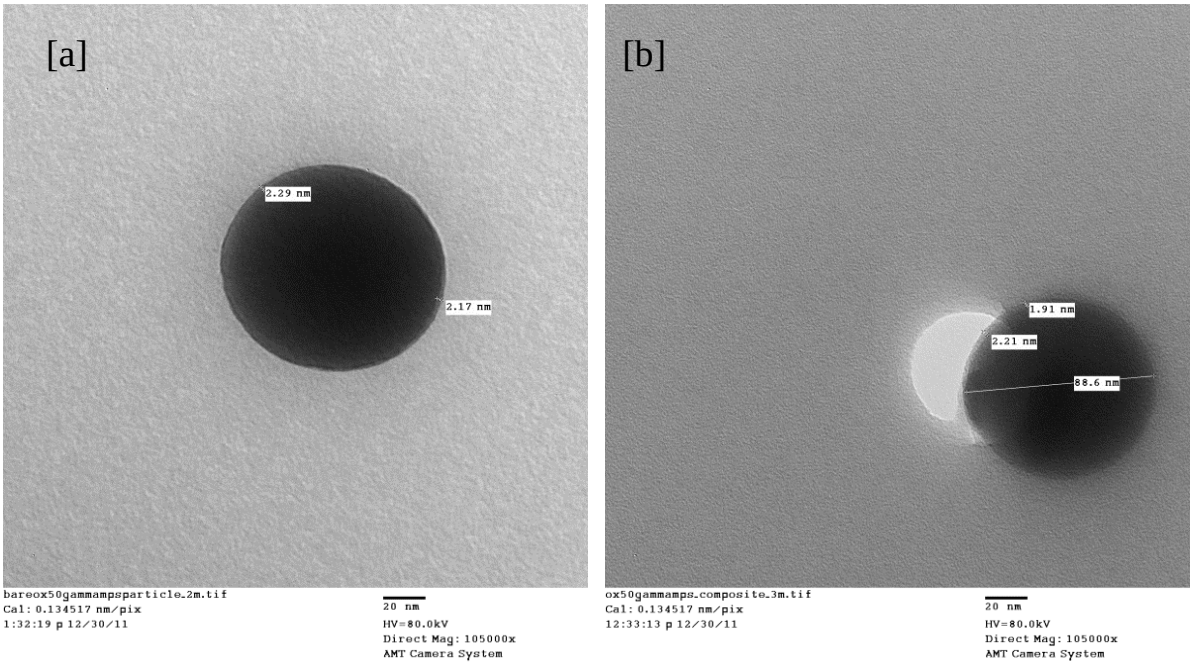

Figure 5.19. TEM images of OX50 particles treated with γ-MPS (a) Particles sprinkled on TEM grid (b) Section of composite with particles embedded in the resin

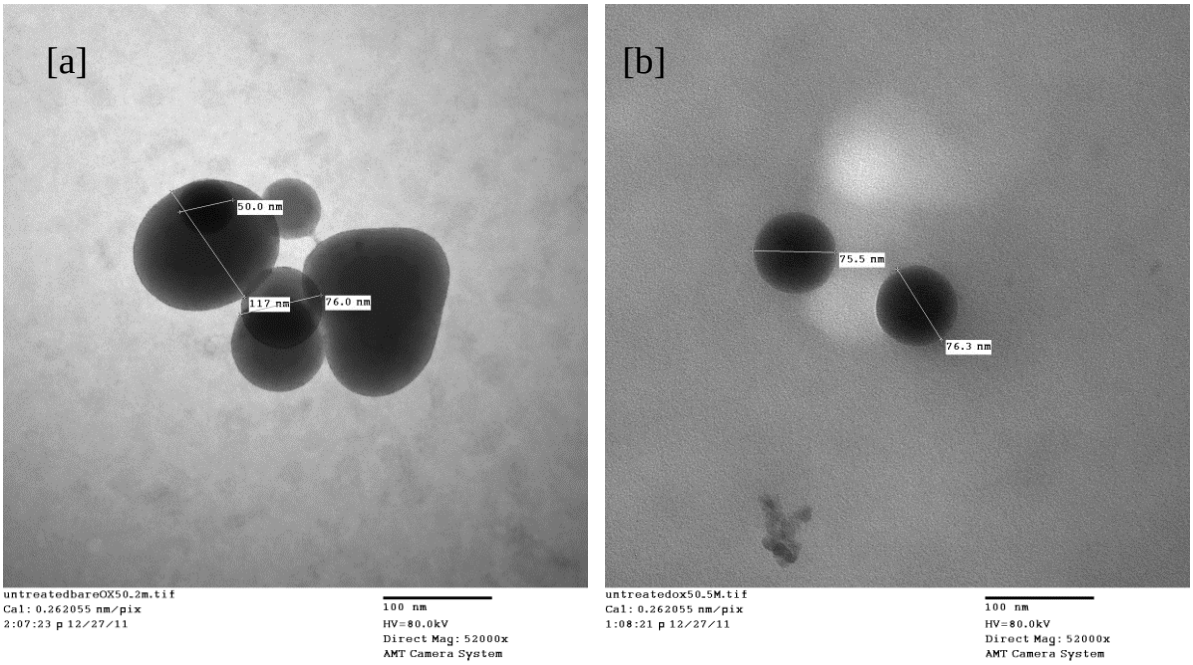

Figure 5.20. TEM images of untreated OX50 (a) Particles sprinkled on TEM grid (b) Section of composite with particles embedded in the resin.

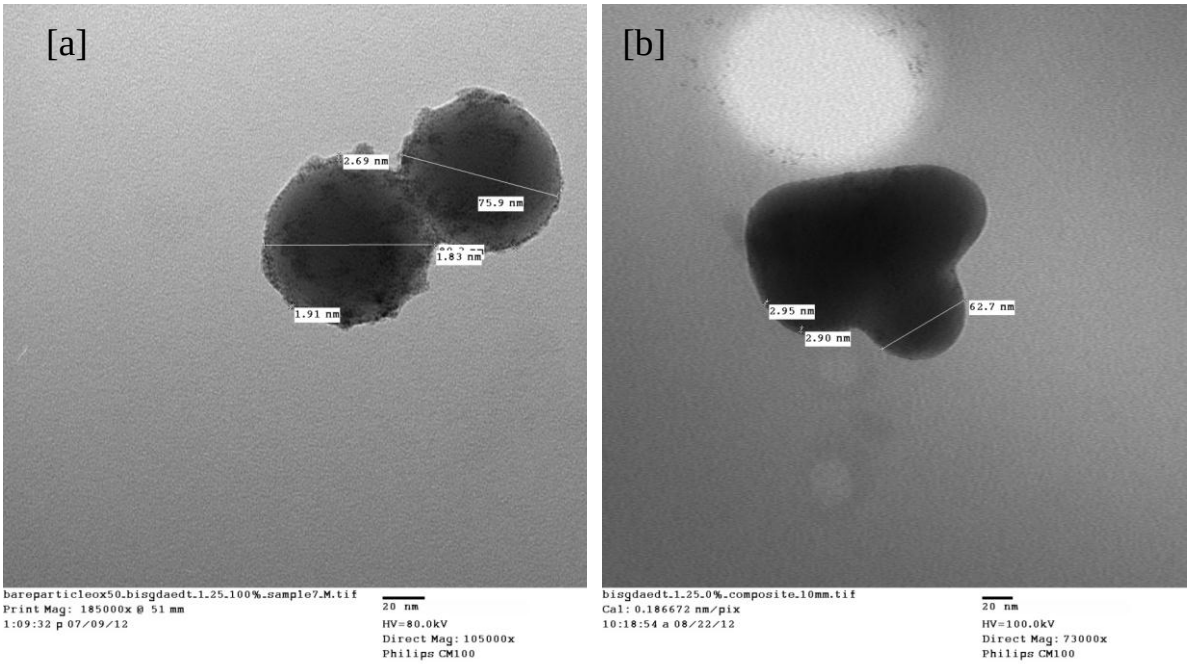

Figure 5.21. TEM images of particles treated with RH100 oligomer (rigid, high molecular weight, 100% methacrylate functionality. (a) Particles sprinkled on TEM grid (b) Section of composite with particles embedded in the resin.

From all the measurements, it is apparent that the filler and filler modification play a very important role in the stress development of composites. From the way the stress measurements are conducted in the tensometer, it is necessary for a continuous load-bearing network to form in the material in order for the tensometer to register a force capable of deflection of the cantilever beam. Similarly, in the crossover point experiments conducted with the rheometer, a significant network has to form to register an increase in the modulus. When fillers are at a high volume fraction, a continuous network can only efficiently form when the particles are integrated into the network rather than forcing network development to bypass the filler particles. It can be visualized that the interface between the particles and the resin matrix would play a significant role in connections between the developing polymer with the particles. The oligomer length, flexibility and reactive methacrylate groups concentration on the polymer are varied here to allow focus on each of these parameters in a more isolated fashion.

As the length of the oligomer increases, in our grafting-to approach, there are fewer chains per unit area on the particles, due to steric hindrance while depositing them on the surface. Depending on the interaction between the resin monomer and the brush and entropic considerations, the brush structure may be extended or collapsed on the surface. The length and surface density of the brushes will determine the thickness of the brush layer. In our studies we have detected an approximately 2 - 5 nm layer of the brush. As the polymerization begins, the polymerizing resin has a tendency to shrink away from the surface of the filler. At the same time, the resin is engaged with interactions with the brush layer, either through copolymerization with the methacrylate reactive sites along the brush or through non-covalent interactions or a combination of both. With these attractive interactions and the potential retraction of the matrix from the filler particle, the surface-bound oligomeric chains start getting pulled away from the

surface. The extent to which they move is anticipated to depend on the strength of the interactions and physical nature of the brush**.** This movement of the brush layer that is partially attached to the moving polymerization front can be seen as a compliance effect. It is well understood that shrinkage stress is reduced when fillers with non-functional or with no surface treatment at all are introduced in a dental resin [21]. On a macroscale, the application of a low modulus liner to the interface between a tooth and the dental restorative has been shown to relieve some of the shrinkage stress [22]. The situation encountered with the brush layer is similar but over a much smaller length scale. In the γ-MPS control case, the polymerizing resin front in contact with the interface/surface is not allowed to move away from the surface, creating restrictions and leading to the stress being built up. In the brush modified filler, the polymerizing resin has additional freedom to shrink, due to the compliance of the interfacial layer. This delays the stress build up, a fact that we have seen in the shrinkage stress development results. It can be inferred that as the length of the tethered brush structures is increased, the brushes can extend to a greater degree. This effectively delays the time (and conversion) at which significant stress build up starts to occur as demonstrated here.

Restriction on polymer mobility around filler particles has been studied extensively [23–26]. Attractive interactions between the surface of the fillers and the polymer around them can cause slowing down of the relaxation of the polymers. The existence of a bound polymer layer around filler particles that has also been hypothesized [25], [27], [28]. This bound layer can vary in thickness depending on the strength of the interactions between the two phases. As observed in the rheology work, the surface modifications indeed have a very wide range of viscosities and complex moduli, showing liquid-like to solid-like behavior. It can be expected that the mobilities

of the different oligomers used in this study will also vary and affect the relaxation behavior and dynamics around the particles, ultimately affecting the curing behavior of the monomer.

The reactive methacrylate group concentration on the brushes also has a significant effect on the development of polymerization stress. As the concentration of methacrylate groups increases, the shrinkage stress was found to increase. As mentioned previously, free shrinking resin produces lower stress than it would have had it had an anchor points to restrict the shrinkage. Reactive groups can act as anchors. If there are very few reactive groups on the oligomers, the polymerizing resin has nothing to hold on to and can shrink away from the surface, essentially shrinking freely. With greater concentrations and absolute numbers of reactive groups on the brush structures, the resin matrix phase can copolymerize with these groups and form sufficient links with the interfacial layer to impose restrictions on the free shrinkage. If the reaction with the brushes happens quickly and crosslinked network can be formed at the interface, then the restriction on mobility occurs earlier and the shrinkage stress rises faster. If the number of reactive groups on the brush is low but not zero or if the available reactive sites are not very accessible, effectively slowing down the reaction between the brush and the resin, the stress does develop but more slowly. All these factors work in conjunction to decide the ultimate stress in a polymerizing composite.

5.4 Conclusion

A variety of oligomers were synthesized having a wide range of properties. Composites made with particles treated with these oligomers showed superior performance by having low shrinkage stress as compared with composites that had fillers treated with a conventional silane. Shrinkage stress was reduced by as much as 30 % in the experimental composites. The

mechanism of stress reduction was hypothesized to be a delayed network buildup due to a slow reaction at the interface. Rheology experiments confirmed the delayed buildup of a load-bearing network. Concentration of reactive groups on the surface of the filler particles were found to be an important factor in determining the stress reduction potential. Fine tuning this surface modification technique can be used to even further improve its stress reduction capacity.

5.5 Acknowledgements

The authors would like to thank the National Institutes of Health for support of this research through the grant NIH/NIDCR- R01DE014227. We also wish to thank Septodont-Confi-Dental and Evonik for their gracious donation of filler materials and Esstech, Inc. for donation of monomers.

5.6 References

[1] J. L. Ferracane, "Resin composite-state of the art.," *Dental Materials*, vol. 27, no. 1, pp. 29–38, Jan. 2011.

[2] S. Mitra, D. Wu, and B. Holmes, "An application of nanotechnology in advanced dental materials," *Journal of the American Dental Association*, vol. 134, pp. 1382–1390, 2003.

[3] K. J. Anusavice, *Phillips' Science of Dental Materials*, 11th ed. Elsevier, 2003.

[4] J. M. Antonucci, S. H. Dickens, and B. O. Fowler, "Chemistry of Silanes : Interfaces in Dental Polymers and Composites," *Journal Of Research Of The National Institute Of Standards And Technology*, vol. 110, no. 5, pp. 541–558, 2005.

[5] J. W. Stansbury, M. Trujillo-lemon, H. Lu, X. Ding, Y. Lin, and J. Ge, "Conversion-dependent shrinkage stress and strain in dental resins and composites," *Dental Materials*, vol. 21, pp. 56–67, 2005.

[6] J. R. Condon and J. L. Ferracane, "Reduced polymerization stress through non-bonded nanofiller particles.," *Biomaterials*, vol. 23, no. 18, pp. 3807–15, Sep. 2002.

[7] W. Weinmann, C. Thalacker, and R. Guggenberger, "Siloranes in dental composites," *Dental Materials*, vol. 21, no. 1, pp. 68–74, Jan. 2005.

[8] N. B. Cramer, C. L. Couch, K. M. Schreck, J. a Carioscia, J. E. Boulden, J. W. Stansbury, and C. N. Bowman, "Investigation of thiol-ene and thiol-ene-methacrylate based resins as dental restorative materials.," *Dental Materials*, vol. 26, no. 1, pp. 21–8, Jan. 2010.

[9] J. A. Carioscia, H. Lu, J. W. Stanbury, and C. N. Bowman, "Thiol-ene oligomers as dental restorative materials," *Dental Materials*, vol. 21, no. 12, pp. 1137–43, Dec. 2005.

[10] J. L. Ferracane, "Placing Dental Composites—A Stressful Experience," *Operative Dentistry*, vol. 33, no. 3, pp. 247–257, May 2008.

[11] B. Zhao, "Polymer brushes: surface-immobilized macromolecules," *Progress in Polymer Science*, vol. 25, no. 5, pp. 677–710, Jun. 2000.

[12] S. Minko, "Responsive Polymer Brushes," *Polymer Reviews*, vol. 46, no. 4, pp. 397–420, Dec. 2006.

[13] E. P. Giannelis, R. Krishnamoorti, and E. Manias, "Polymer-Silicate Nanocomposites : Model Systems for Confined Polymers and Polymer Brushes," *Polymer*, vol. 138, 1999.

[14] L. Andruzzi, A. Hexemer, X. Li, C. K. Ober, E. J. Kramer, G. Galli, E. Chiellini, and D. A. Fischer, "Control of surface properties using fluorinated polymer brushes produced by

surface-initiated controlled radical polymerization," *Langmuir*, vol. 20, no. 24, pp. 10498–506, Nov. 2004.

[15] S. Peng and B. Bhushan, "Smart polymer brushes and their emerging applications," *RSC Advances*, vol. 2, no. 23, p. 8557, 2012.

[16] H. Lu, J. W. Stansbury, S. H. Dickens, F. C. Eichmiller, and C. N. Bowman, "Probing the origins and control of shrinkage stress in dental resin-composites: I. Shrinkage stress characterization technique.," *Journal of Materials Science. Materials in Medicine*, vol. 15, no. 10, pp. 1097–103, Oct. 2004.

[17] F. Chambon and H. H. Winter, "Linear viscoelasticity at the gel point of a crosslinking PDMS with imbalanced stoichiometry," *Journal of Rheology*, vol. 31, no. 8, pp. 683–697, 1987.

[18] R. Qiao and L. Catherine Brinson, "Simulation of interphase percolation and gradients in polymer nanocomposites," *Composites Science and Technology*, vol. 69, no. 3–4, pp. 491–499, Mar. 2009.

[19] B.-S. Chiou, S. R. Raghavan, and S. a. Khan, "Effect of Colloidal Fillers on the Cross-Linking of a UV-Curable Polymer: Gel Point Rheology and the Winter−Chambon Criterion," *Macromolecules*, vol. 34, no. 13, pp. 4526–4533, Jun. 2001.

[20] M. K. Gaines, S. D. Smith, J. Samseth, S. A. Khan, and R. J. Spontak, "Nanoparticle Network Formation in Nanostructured and Disordered Block Copolymer Matrices," *Nanoscale Research Letters*, vol. 5, no. 10, pp. 1712–1718, Jan. 2010.

[21] J. R. Condon and J. L. Ferracane, "Reduction of composite contraction stress through non-bonded microfiller particles.," *Dental Materials*, vol. 14, no. 4, pp. 256–60, Jul. 1998.

[22] L. C. A. Oliveira, S. Duarte, C. A. Araujo, and A. Abrahão, "Effect of low-elastic modulus liner and base as stress-absorbing layer in composite resin restorations.," *Dental Materials*, vol. 26, no. 3, pp. e159–69, Mar. 2010.

[23] P. Akcora, S. K. Kumar, V. García Sakai, Y. Li, B. C. Benicewicz, and L. S. Schadler, "Segmental Dynamics in PMMA-Grafted Nanoparticle Composites," *Macromolecules*, vol. 43, pp. 8275–8281, Sep. 2010.

[24] A. Bansal, H. Yang, C. Li, B. C. Benicewicz, S. K. Kumar, and L. S. Schadler, "Controlling the Thermomechanical Properties of Polymer Nanocomposites by Tailoring the Polymer – Particle Interface," *Polymer*, pp. 2944–2950, 2006.

[25] L. Chen, K. Zheng, X. Tian, K. Hu, R. Wang, C. Liu, Y. Li, and P. Cui, "Double Glass Transitions and Interfacial Immobilized Layer in in-Situ-Synthesized Poly(vinyl alcohol)/Silica Nanocomposites," *Macromolecules*, vol. 43, no. 2, pp. 1076–1082, Jan. 2010.

[26] H. Lu and S. Nutt, “Restricted Relaxation in Polymer Nanocomposites near the Glass Transition,” *Macromolecules*, vol. 36, no. 11, pp. 4010–4016, Jun. 2003.

[27] M. Qu, F. Deng, S. M. Kalkhoran, A. Gouldstone, A. Robisson, and K. J. Van Vliet, “Nanoscale visualization and multiscale mechanical implications of bound rubber interphases in rubber–carbon black nanocomposites,” *Soft Matter*, vol. 7, no. 3, p. 1066, 2011.

[28] R. Ruggerone, V. Geiser, S. Dalle Vacche, Y. Leterrier, and J.-A. E. Månson, “Immobilized Polymer Fraction in Hyperbranched Polymer/Silica Nanocomposite Suspensions,” *Macromolecules*, vol. 43, no. 24, pp. 10490–10497, Dec. 2010.

CHAPTER 6

STRESS RELAXATION BEHAVIOR OF A MODEL DENTAL RESIN FILLED WITH CONVENTIONAL AND EXPERIMENTAL FILLERS

Abstract

Stress relaxation is an intrinsic part of stress evolution that occurs during the polymerization process. Real-time measurement of stress during polymerization cannot capture the stress relaxation aspect. Slight variations in the formulation of dental composites can lead to dramatic differences in final stress values upon polymerization. This is likely due to differential stress relaxation processes occurring during cure. The stress relaxation potential of the material changes as the network develops upon polymerization. This work evaluates the potential for stress relaxation in different systems, using a classic stress relaxation test. Unfilled resin and a filled composite with Ba glass fillers were evaluated initially. It was found that the degree of stress relaxation decreased for both the systems with increasing conversion. This was attributed to the stiffening of the network with increasing cross-link density, leading to reduced cooperative moments, thus hindering stress relaxation. Incorporation of fillers placed additional restrictions on polymer network development, thus reducing stress relaxation potential. The effect of composite filler surface modification on stress relaxation was tested by incorporating fillers that were altered with two different oligomers. An oligomer with a rigid backbone structure was synthesized was and then further modified to yield two different oligomers – RH0, which had no methacrylate groups on its backbone and RH100, which had a high concentration of methacrylate groups that could copolymerize with the resin matrix. γ-MPS-treated fillers were used as the control. Stress relaxation was modeled using a Maxwell-model with two elements, giving two characteristic times for stress relaxation. All composites showed equivalent stress

relaxation for moderate values of conversion. However, at the highest value of conversion tested (ca. 60 %) the RH0-based composite showed greater stress relaxation compared to the γ-MPS control and the RH100-based composites. Characteristic relaxation times showed that the RH0-based composite exhibited faster relaxation at short time scales. The slower relaxation in the RH100 and γ-MPS-based composites was attributed to the creation of a network with higher crosslink density in the vicinity of the filler particles, inducing less mobility in this interfacial region. At longer time scales, the γ-MPS-based composite had slower relaxation compared to either composite with the oligomer-based surface treatment with both RH0- and RH-100-based composites showing similar relaxation times. This implies that the longer relaxation times were more dominated by the general structure of the interface and its long-range effects. This study showed that the interface can be modified to alter stress relaxation characteristics of composites and can lead to beneficial properties for clinical applications.

6.1 Introduction

The use of polymeric dental restoratives in a clinical situation involves the placement of a highly filled liquid monomeric paste into the confined volume of an adhesive-pretreated cavity preparation followed by photopolymerization under ambient conditions in either single or multiple increments [1], [2]. This polymerization is accompanied by volumetric shrinkage and progressive free volume reduction as the liquid monomeric matrix phase is transformed into a glassy, high modulus polymer network [3], [4]. When this thermodynamically derived polymerization-based volumetric shrinkage is limited as a consequence of the constraint imposed by the bonded interfaces, stresses are generated within the composite restorative that are further transferred to the adhesively bonded interface as well as to the surrounding tooth structure. The heterogeneous stress thus generated can lead to failure of the restorative itself or disruption of the

bond with the tooth if the force exceeds the bond strength at any point within this interface. It has been suggested that viscoelastic materials like dental restoratives can relieve stress by flow before the gel-point is attained [5], [6]; however, gelation is known to occur at very low conversion in the bulk dimethacrylate polymerizations typical in dental composite materials. As the restorative polymerization progresses through the post-gel rubbery regime and into the glassy state, stress continues to build up in the system. Any potential stress relaxation in such a constrained system depends on the continuously changing elastic properties and elastic limits associated with the dynamic polymeric network formation within the composite. Stress relief as polymer network evolution occurs as well as the stress relaxation potential of fully cured composite materials is of interest to better understand the practical application of dental restorative materials [7]. The rate at which these stresses relax is also important as the faster the relaxation process at certain phases of the polymerization, the better the practical outcome may be in terms of the final residual stress level.

The rate and amount of relaxation in such a situation can be measured using classical mechanical stress relaxation experiments. These experiments provide information about the time-dependent viscoelastic nature of polymeric materials. In a typical stress relaxation experiment, a sample is “instantaneously” deformed to a certain strain and held at that strain. This deformation stresses the sample and the stress gradually decays. The stress can decay due to a number of factors like molecular rearrangement near the Tg, viscous flow, bond interchange and chain scission [8]. Stress relaxation would depend on a number of factors including the modulus and viscosity of the material, double bond conversion, strain rate of deformation and deformation amount.

This technique can be applied to the study of dental polymers and composite stress relaxation. There is scant literature focused on the effect of double bond conversion on stress relaxation. Fillers impart very significant effects on modulus and polymerization shrinkage so the presence of fillers and more specifically, the type of interfacial coupling between the resin matrix and the reinforcing filler used in a dental composite, may be expected to have a significant effect on not only stress development, but also stress relaxation behavior. The composite materials used here contain fillers modified with either a conventional γ-methacryloxypropyltrimethoxysilane (γ-MPS)-based reactive coupling agent or a series of experimental interfacial brush systems. It is of interest to compare stress relaxation between unfilled polymers as well as filled systems that contain either control or experimental fillers. This study when done as a function of methacrylate conversion can yield useful information about stress relaxation potential during polymerization including guidance on the design of filler resin interfaces to mitigate stress development in polymeric composite materials.

6.2 Materials and methods

6.2.1 Materials

Barium glass (mean particle size 0.7 μm) with a coating of 5 wt % γ-methacryloxypropyltrimethoxysilane (γ-MPS), was used as the inorganic filler (Esstech, Inc., Essington, PA). Silica nanoparticles (Aerosil OX50, average diameter = 40 nm, surface area 50 m^2/g) were donated by Evonik (Germany). OX50 silanized with γ-MPS (γ-methacryloxypropyl-trimethoxysilane) was donated by Septodont-Confi-Dental (Louisville, Colorado, USA). N-methylaminopropyltrimethoxysilane (MAPTS) was purchased from Gelest. 2,2-bis[4-(2-hydroxy-3-methacryloyloxypropyl-oxy)phenyl]propane (BisGMA) and triethylene glycol

dimethacrylate (TEGDMA) monomers were donated by Esstech. A visible light initiating system consisting of 0.3 wt% camphorquinone (CQ) as initiator and 0.8 wt% ethyl 4-dimethylaminobenzoate (EDAB) (Sigma-Aldrich, Milwaukee, WI) as co-initiator was incorporated. p-xylene bis-(N,N-diethyldithiocarbamate) (XDT) was made according to the synthesis described by Otsu, *et al*. [9]. Isocyanatoethylmethacrylate (IEM), bisphenol A glycerolate (1 glycerol/phenol) diacrylate (BisGDA) and 1,2-ethanedithiol (EDT) were purchased from Sigma-Aldrich (USA) and used without further purification.

6.2.2 Oligomer Synthesis

The structures of the monomers used for the synthesis are shown in Figure 6.1. For the synthesis, monomers were dissolved in chloroform in the ratio – BisGDA/EDT = 1.25/1.00. It was desired to have oligomers with acrylate functionalities at the ends and so BisGDA was kept in excess. A few drops of triethylamine as catalyst were added to the reaction mixture. The mixture was stirred constantly and progress of the reaction was monitored using FT-IR by following the reduction of the thiol peak at 2575 cm^{-1}. Upon completion of the reaction, the oligomer was separated from the unreacted mixture by dropwise addition in hexanes. The supernatant solution was discarded and the oligomers redissolved in chloroform. This solution was dried in a roto-vap and then under a high-vac to remove the solvent. The oligomer had pendant hydroxyl groups on its chain and these were reacted with IEM to give an oligomer with 100% hydroxyl functionality replaced with methacrylates. The final structures of the oligomer are shown in Figure 6.2. This particular oligomer scheme was chosen as it had been proven in Chapter 5 to give good results for reduction of shrinkage stress.

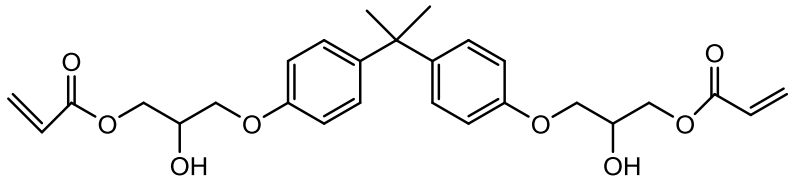

Bisphenol A glycerolate (1 glycerol/phenol) diacrylate
(BisGDA)

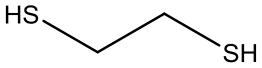

1,2-ethanedithiol
(EDT)

Figure 6.1. Structures of monomers used for the oligomer synthesis

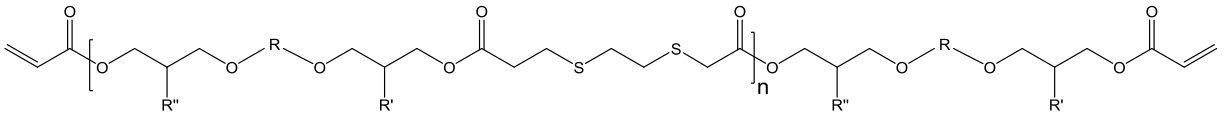

R', R'' = OH

R =

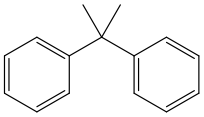

R', R'' =

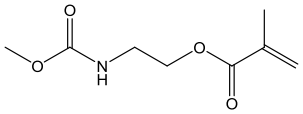

Case 1 - 0% methacrylate. All pendant OH groups are intact

Case 2 - 100% methacrylate. All pendant OH groups are replaced with a urethane methacrylate

Figure 6.2. Structures of oligomers used to treat fillers

6.2.3 GPC Characterization

A Viscotek triple detector gel permeation chromatography (GPC) system, equipped with Viscotek VE 3580 refractive index detector and Viscotek 270 dual light scattering/viscosity detector, was used for characterization of the size of the oligomer. The mobile phase was HPLC grade tetrahydrofuran at a flow rate of 1 mL/min. Samples were prepared in HPLC grade THF to a concentration of about 5g/L and 10 µL of sample was injected for analysis.

6.2.4 Modification of the OX50 filler

The bare OX50 silica particles were first treated treated with n-methylaminopropyltrimethoxysilane and then the oligomers were attached to the amine end of the silane. For this, the OX50 particles were first dried in a rotary dryer at about 165 ^{o}C under vacuum for three hours before further treatment. This was done to ensure removal of surface bound moisture that can potentially react with the silanes and promote the formation of multiple layers of the silane. Anhydrous toluene was used as a solvent for the silanization process. It was refluxed for two hours and then the particles were added and further refluxed for an hour to ensure good dispersion. The MAPTS was added to the solution so that the final concentration in the mixture was 1.5 % by weight. This reaction mixture was allowed to reflux for 6 hours after which the particles were separated from the solvent by centrifugation. The particles were washed three times with toluene and two times with methylene chloride to ensure that all traces of unreacted silane were removed. The silanized particles were then dried overnight under vacuum at 50 ^{o}C to remove all traces of solvent. The dried and silanized particles were then added to reagent alcohol in which 5X excess of oligomers were already mixed. The reaction mixture was heated to 45 ^{o}C and the reaction was allowed to continue for three days. The particles were then centrifuged to remove the solvent and washed 5 times with methylene chloride to remove excess solvent and dried in a vacuum oven at 45 ^{o}C.

6.2.5 Composite Preparation

The resin matrix for the composites was a mixture of BisGMA and TEGDMA in the ratio 70:30 by weight. Two different initiating systems were used. For the study on unfilled resin and composite with 0.7 µm filler, 0.1 wt% of p-xylene bis-(N,N-diethyldithiocarbamate) (XDT) as a

photoiniferter (initiator-chain transfer agent-terminator). XDT was used as it was desired to have a wide range of stable monomer conversions. [10]. XDT can initiate living radical polymerization when a formulated sample is irradiated. When the irradiation stops, the propagating radical is capped by the less active iniferter radical. This capping is thermally stable. The liquid samples were put in a 1x3x25 mm Teflon mold and sandwiched with glass slides. A curing light (Acticure 4000) with a 365 nm filter, was used to cure the samples. Samples were placed about 8 cm away from a collimating lens attached to the light source and irradiated on both sides with a light intensity of about 10 mW/cm^2 for different times to get a wide range of conversions.

For the OX50 filler-based composites, the resin included a free radical visible light initiating system comprised of 0.3 wt% camphorquinone and 0.8 wt% ethyl 4-dimethylaminobenzoate. The fillers were added to the resin and mixed in a speedmixer (DAC 150 FVZ, Flakteck Inc.) and dispersed in the resin to make a composite paste that had a final filler loading of 30 wt%. Composites with γ-MPS-treated OX50 particles were used as the control. The freshly prepared composites were evacuated under vacuum to ensure elimination of air bubbles prior to being used. Samples were put in a Teflon mold (dimension 1x3x25 mm) and sandwiched between glass slides. They were cured with the Acticure 4000 light equipped with a 400-500 nm filter. Light intensity was again kept at 10 mW/cm^2 for a range of times to get a wide range of conversion.

6.2.6 Stress Relaxation Test

The stress relaxation tests were carried out on an MTS machine (858 Mini Bionix II, Eden Prairie, MN USA). Samples were placed between two grips in the MTS machine. They

were then quickly extended to a constant strain of 0.5 % and held at that position for 10 min and the stress decay monitored.

6.3 Results and Discussion

Stress relaxation measurements are used to understand the viscoelastic behavior of polymers and polymer-based materials. Double bond conversion and fillers can affect the viscoelastic properties of the composite. In a polymerizing composite, the developing stress consists of two components – stress development and stress relaxation. Stress measurements give us an idea of the overall stress in the composite, without looking at the contribution of the individual components. The stress relaxation work in this chapter is done with a view to evaluating the stress relaxation potential of the unfilled polymer and filled composites – with fillers treated with the γ-MPS control and also with an interfacial brush structure.

Stress relaxation experiments were carried out on unfilled BisGMA/TEGDMA resin and composites made with this resin and 1) 60 wt% 0.7 μm barium glass filler silanized with γ-MPS, 2) 30 wt% OX50 silanized with γ-MPS, 3) 30 wt% OX50 with high molecular weight rigid brush surface-treated with 0 % (sample name RH0) and 100 % (sample name RH100) methacrylate functionality.

6.3.1 Stress Relaxation of Unfilled Resin and Composite with 0.7 μm Barium Glass Filler

Table 6.1 summarizes the values of peak stress, normalized stress relaxation amount compared to the peak stress in each case and the maximum stress relaxation rate, normalized to the peak stress. It can be seen that the peak stress for each system increases as the methacrylate conversion increases. This would be expected since the modulus is known to increase with

conversion and a basic definition of stress is that it is proportional to modulus/strain. For the unfilled resin, the peak stress increases from 0.04 ± 0.01 MPa at 29.0 ± 1.5 % conversion to 10.35 ± 0.05 MPa at 89.9 ± 1.0 % conversion. For the filled system with 0.7 µm fillers, the peak stress increases from 1.18 ± 0.21 MPa at 26.1 ± 1.3 % conversion to 16.63 ± 0.98 MPa at 85.0 ± 2.0 % conversion. The peak stresses for the intermediate conversions lie in between the two extremes with the peak stress levels rising rapidly in the latter stages of conversion as a result of the exponential increase in modulus as a function of conversion. For calculations of stress recovery and stress relaxation rates, the stress data for each sample was normalized with respect to the peak stress for that particular sample. The higher peak stress for the filled systems as compared to the unfilled system, at similar levels of conversion, is related to the reinforcing effect of the high modulus fillers [11]. As the materials are strained to the same extent, the high modulus fillers (barium glass has an elastic modulus of approximately 75 GPa) contributes to a higher overall modulus and stress in the composite. It should be noted, however, that efficient coupling between the filler particles and the resin matrix is essential for the elastic modulus to increase. Efficient transfer of the applied load between the two phases is necessary for the filler phases to absorb the strain energy, otherwise decoupling of the two phases can occur, leading to lower modulus materials and also to bulk mechanical failure of the composite.

Figure 6.3 shows typical stress relaxation curves obtained for these two systems. The monomer conversion of the unfilled system is at 57.3 ± 1.8 % and that for the filled system is at 56.6 ± 1.5 %, so the two systems have similar conversions and can be legitimately compared. The data has been normalized with respect to the highest initial stress value at the same strain for each system. It can be seen that the amount of stress recovery in the unfilled system is more than

that of the filled system. Also the stress relaxation rate of the unfilled system is faster than that of the filled system.

A look at what happens during a stress relaxation test can explain these observations. When the unfilled resin sample is suddenly extended and held at a constant strain, the polymer chains try to relax to restore the isotropy. Polymers can relax via chemical or physical mechanisms. In the present case, we do not expect any chemical changes under the test conditions, which are well within the elastic limit of all these materials. Physical mechanisms for relaxation include viscous flow before gelation [12], relaxation of trapped entanglements and molecular relaxation below or near the glass transition temperature [8]. For the case in Figure 6.3, the conversion of the samples puts them well over the gel-point conversion [7] and into the glassy, vitrified state. The most likely mechanism for relaxation would be relaxation of entanglements and molecular motion. With the addition of fillers that are covalently bound to the polymer matrix, additional restrictions are placed on the polymer chain movement due to the restricted movement near the surface of the filler particles [13], [14]. The reduced resin volume fraction means that for a given level of strain, the resin phase of the filled materials experiences a greater effective strain than in the unfilled polymer. These restricted movements have "long range" effects as the entire network is crosslinked. Upon being strained, as the polymer chains relax, the restrictions on mobility hinder the process, leading to a slowing down of the relaxation. This explains the slower rate of relaxation seen in the filled system. A lower stress recovery can also be explained by the fact that the viscous component of the composite is increased by the addition of fillers. The elastic recovery is reduced with the addition of fillers and the viscous loss is increased.

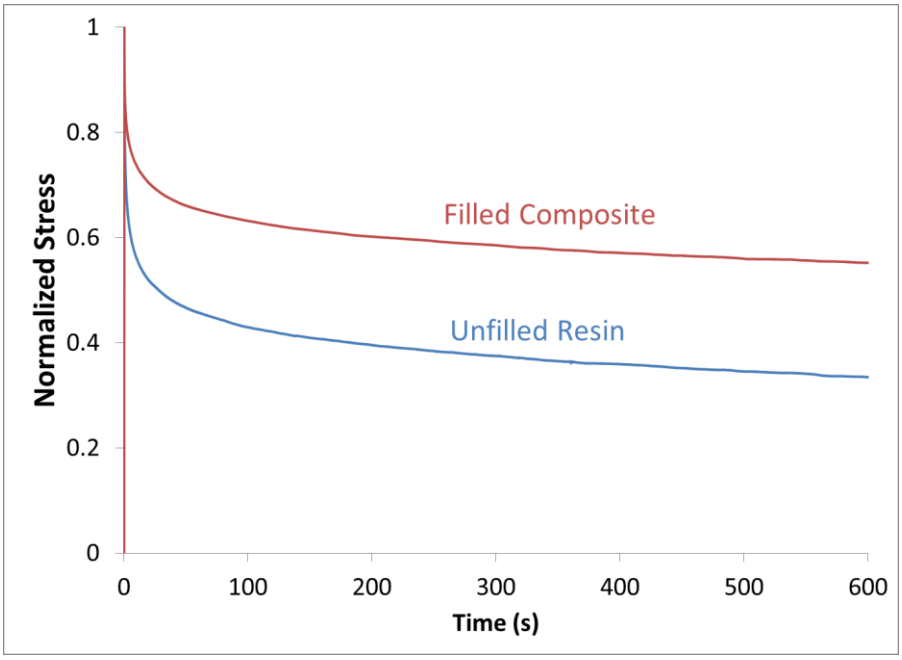

Figure 6.3. Comparison of normalized stress relaxation curves for (a) Unfilled BisGMA/TEGDMA resin at approximately 60 % conversion and (b) BisGMA/TEGDMA resin filled with 0.7 µm barium glass particles at 60 wt%. Stress values have been normalized by the peak stress for the respective measurement.

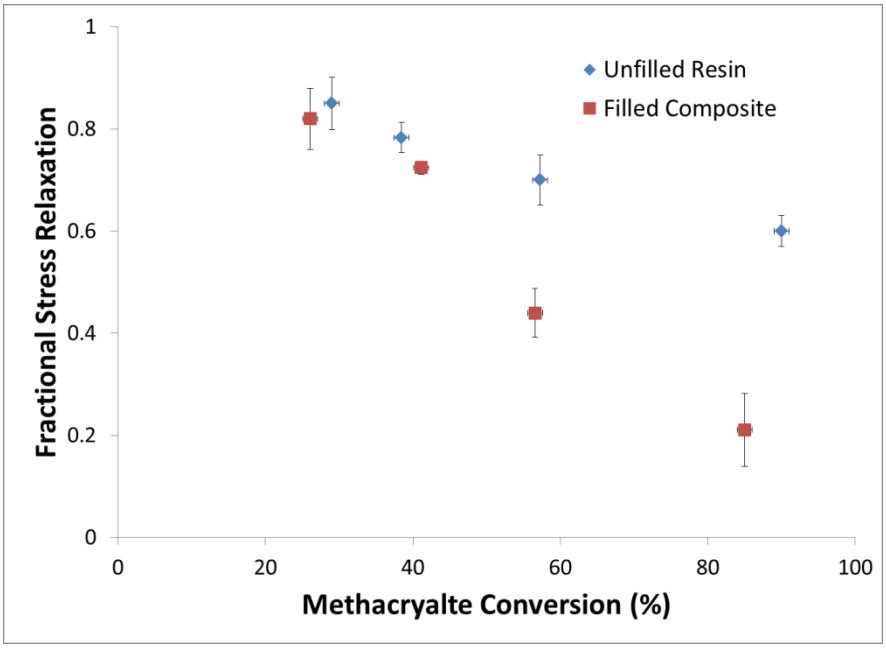

Figure 6.4. Comparison of fractional residual stress for (♦) Unfilled resin at 60% conversion and (■) resin filled with 0.7 µm particles at 60 wt%. All stress values have been normalized with respect to the peak stress for the respective measurement.

Table 6.1. Summary of results for unfilled resin and filled composite (0.7 µm filler at ca. 60 wt%)

	Methacrylate Conversion (%)	Peak Stress (MPa)	Fractional stress relaxation amount (normalized to peak stress)	Stress relaxation rate (normalized to peak stress) s^{-1}
Unfilled resin	29.0 ± 1.5	0.04 ± 0.01	0.85 ± 0.05	5.93 ± 1.15
	38.5 ± 0.06	1.05 ± 0.12	0.78 ± 0.03	5.59 ± 0.35
	57.3 ± 1.8	7.25 ± 0.9	0.70 ± 0.05	3.56 ± 0.20
	89.9 ± 1.0	10.35 ± 0.5	0.60 ± 0.03	2.50 ± 0.10
Filled composite	26.1 ± 1.3	1.18 ± 0.21	0.82 ± 0.06	5.75 ± 1.10
	41.1 ± 1.3	3.51 ± 0.43	0.72 ± 0.01	4.17 ± 0.81
	56.6 ± 1.5	11.55 ± 1.22	0.44 ± 0.05	1.61 ± 0.28
	85.0 ± 2.0	16.63 ± 0.98	0.21 ± 0.07	1.16 ± 0.36

Error! Reference source not found.4 shows the normalized stress relaxation or recovery amount over a wide range of conversion. It can be seen that the stress recovery decreases as the methacrylate conversion increases, for both the systems. For the unfilled system, the stress recovery ranges from 85 ± 5 % at 29.0 ± 1.5 % conversion to 60 ± 3 % at 90.0 ± 1.0 % conversion. For the filled system, the stress recovery is in the range of 82 ± 6 % at 26.1 ± 1.3 % conversion to 21 ± 7 % at 85.0 ± 2.0 % conversion. So it is evident that there is more stress recovery in the unfilled resin system than the filled system, except at the lower range of

conversion. At the low end of conversion, the material has a lower viscosity and is capable of enhanced stress relaxation by plastic deformation. As conversion increases, the material becomes more viscous and stiffer, it loses this capability and this results in a lower stress recovery. In case of the filled system, at the lower end of conversion, the covalent linkage between the filler surface and the polymerizing monomers around it is not fully developed. Hence there are fewer restrictions placed on the early polymer network with respect to relaxation and the limiting extent of relaxation does not depend on the presence of the filler. It is also essential that the fillers do not present a hindrance in terms of a percolation network, so that the resin phase is continuous and can relax without being affected by the fillers. As the monomer conversion and the crosslinking degree increase, the system becomes more viscous and the network loses mobility as its glass transition temperature and stiffness increase. The free volume in the polymer also reduces, reducing the freedom for relaxation of polymer chains by segmental motion. This can explain the progressive reduction in stress recovery as the conversion increases in both the systems. The rate of stress relaxation is affected by the same factors as the stress recovery and follows the same trend as that of stress recovery (Figure 6.5). The network loses mobility with increasing crosslink density as the monomer conversion increases and relaxation at the molecular level becomes slower. The addition of fillers enhances the effect of lower mobility, more so with increasing conversion, and the rates of relaxation here are even slower. In literature, researchers have noticed faster relaxation rates with the addition of fillers [11], [15]. They attribute these to debonding of the polymer from the filler surface and also breaking down of aggregates, particularly at high strain values. With the strong covalent binding between the fillers and the polymer in our system and the low strains being used, these debonding and “de-aggregation” processes are not expected to occur. Also with the 0.7 μm filler particles, aggregation is unlikely

to occur due to their large size. Hence the reduced rate of relaxation with addition of well-bonded fillers is not considered to be an anomaly.

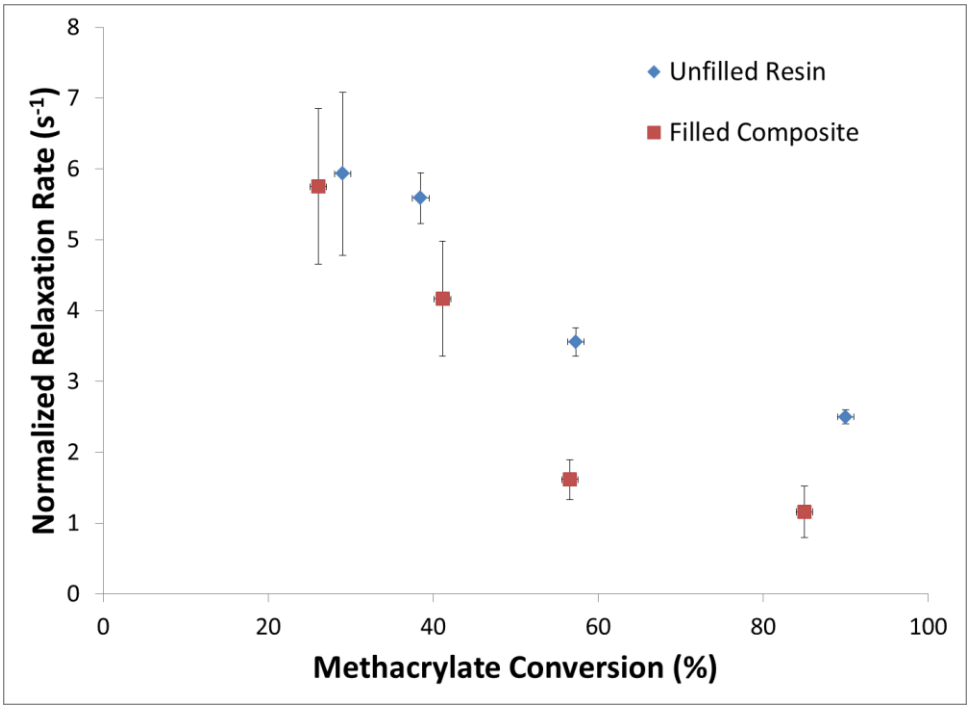

Figure 6.5Comparison of stress relaxation rates for (♦) unfilled resin and (■) resin filled with 0.7 micron filler at 60 wt %, as a function of conversion. All stress values have been normalized with respect to the peak stress for the respective measurement.

6.3.2 Effect of Surface Modification on Stress Relaxation

The high surface area of particulate fillers increases their potential for interaction with the resin. Different filler surface treatments would be expected to respond differently in terms of stress relaxation. Modification of the filler surface could introduce a gradient in filler properties, starting from the filler surface and going towards the bulk polymer until the properties match those of the polymer. This can lead to gradients in the glass transition temperature and elastic modulus. If the volume fraction of the particles is high and they have a smaller size, the effective percolation limit, which refers to the point at which the hybrid interfacial zones begin to overlap,

can be reached fairly quickly and the particles can start interacting with each other or the polymer brush chains can start bridging the particles together. All these factors would affect the viscoelastic properties of the composite and consequently, stress relaxation.

The high surface area OX50 fillers with three different surface modifications were used for studying the effect of the interface on stress relaxation. γ-MPS was used as the control while the high molecular weight rigid brushes (Chapter 5) with either 0 % or 100 % methacrylate functionality were used as the experimental materials (Table 6.2). As described in the Materials and Methods section, collimated light was used to cure the sample uniformly to different conversion values, depending on the time of irradiation. The stress relaxation test was carried out as soon as conversion became effectively constant, which was about five minutes after starting the polymerization.

Table 6.2. Listing and terminology for OX50 filler-based samples used in the stress relaxation study.

Sample	Terminology used
OX50-GammaMPS	OX50-GammaMPS
OX50 with high Mw rigid oligomer that has no methacrylates on the chain	OX50 – RH0
OX50 with high Mw rigid oligomer that has complete coverage of methacrylate groups on the chain	OX50 – RH100

Figure 6.6 shows the final normalized stress recovery data for all the samples at the end of the tests. The data were taken at three separate points of conversion, as listed in Table 6.3 and an attempt was made to have overlapping conversion at the point of measurement for all the samples, to facilitate comparison between the different samples. It can be seen that in the low to

moderate range of double bond conversion, the stress relaxation amounts seem to be similar for all the samples. Over the whole range, however, the stress relaxation amount for sample OX50-RH0 is constant and it does not vary with the conversion. The stress relaxation amount for OX50-γMPS and OX50-RH100 samples is also constant in the low to moderate range of conversion. However, at the higher end of conversion, when the samples reach a vitrification-limited maximum conversion value under the ambient photopolymerization conditions, there is a reduction in the degree of stress relaxation. From the results of the previous section on relaxation of unfilled resin and filled system with 0.7 μm-size filler, the degree of stress recovery was reduced as the double bond conversion increased. This was attributed to the increased crosslinking and stiffness of the material, which reduced the mobility of the polymer chains. The drop in the extent of stress relaxation observed at the high end of conversion for the OX50-filler-based systems can also be attributed to the increasing cross-linking between the fillers and the developing matrix, which subsequently contributes to the reduced mobility of the polymer chains. However, this is only for the OX50-γMPS and OX50-RH100, which have many polymerizable methacrylate groups on the surface and hence the ability to covalently react with the polymer. The OX50-RH0 sample, however, does not have methacrylate groups along the oligomer brush chains. It only has one terminal acrylate group at the chain end that can potentially co-polymerize with the methacrylate-based resin. Given the low density of the brushes on the surface of the filler, this offers relatively few sites for covalent attachment between the filler and the matrix. As hypothesized in Chapter 5, the brush layer around the filler particle is compliant and upon co-polymerizing with the resin monomer, it can be extended away from the surface of the filler. If this indeed happens, this provides an avenue for the developing stress to relax due to the flexibility in the layer. While continued polymerization within the resin

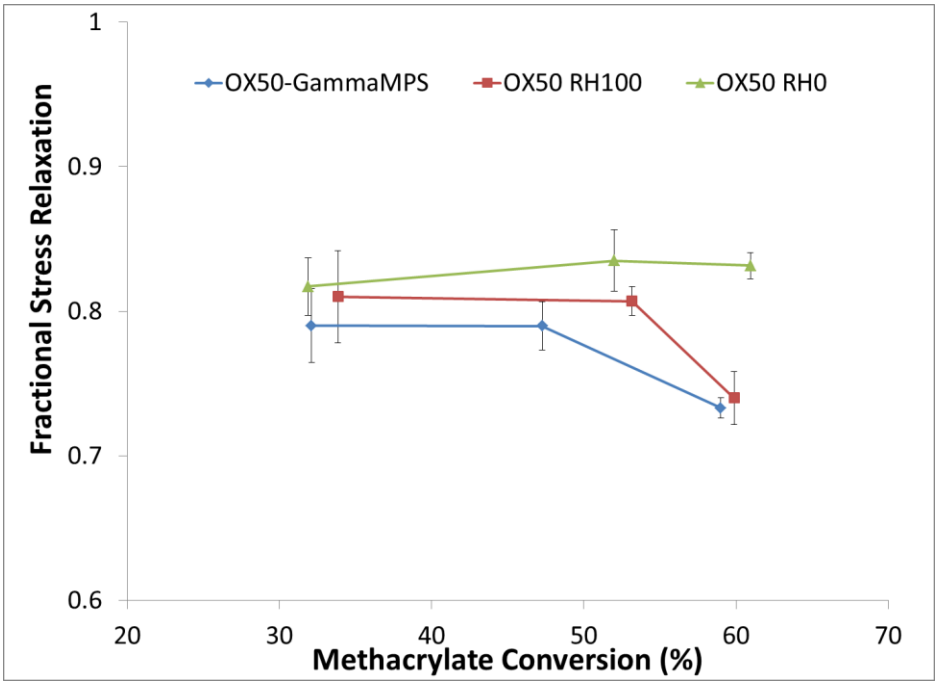

Figure 6.6. Comparison of stress relaxation of 30 wt% OX50 in BisGMA/TEGDMA with three different surface modifications – 1) (●) – γ-MPS; 2) (■) – High Mw rigid brush – 100% methacrylate; 3) (▲) High Mw rigid brush – 0% methacrylate.

phase would lead to more entanglements with the surface-bound brush structure, these physical interactions can re-equilibrate significantly when micro- or macro-scopic strain is applied. The OX50-γMPS particles have the short chain γ-MPS molecules on the surface and they do not have the same kind of flexibility to be able to relax the stress. The OX50-RH100 fillers have the same rigid brush backbone as the OX50-RH0 fillers, with the difference being the presence of significant numbers of methacrylate groups all along the oligomer backbone. So the structure of the backbone should allow the brush to assist in relaxing the stress, but due to the more extensive co-polymerization with the resin monomer, the brushes have a greater potential to become fixed in the network. As the network becomes more rigid at higher levels of conversions, the brush structure lacks the potential mobility available to the 0 % methacrylate analog. Chances of copolymerizing with the resin also increase as the resin infiltrates the brush layer and the

conversion increases, leading to increasing rigidity around the filler particle. This could explain the lower stress relaxation amount seen at the high end of conversion.

Table 6.3. Summary of stress relaxation results for composites based on OX50 filler particles with different surface treatments. Loading level of OX50 is 30 wt %.

Surface treatment	Conversion	Peak Stress (MPa)	Normalized stress relaxation amount	Normalized stress relaxation rate
GammaMPS	32.1 (0.1) 47.3 (4.2) 59.0 (0.3)	0.57 (0.02) 2.66 (0.55) 3.31 (0.09)	0.79 (0.03) 0.78 (0.02) 0.73 (0.01)	4.56 (0.01) 8.32 (5.56) 6.84 (0.28)
High M_w brush - 0%	31.9 (4.4)) 52.0 (3.0) 60.4 (0.8)	0.14 (0.10) 3.06 (0.25) 3.51 (0.28)	0.83 (0.02) 0.84 (0.02) 0.83 (0.01)	6.09 (0.23) 7.01 (0.67) 7.96 (0.06)
High M_w brush - 100%	33.9 (0.8) 53.2 (0.8) 60.4 (0.8)	0.36 (0.10) 3.01 (0.33) 3.84 (0.26)	0.81 (0.03) 0.81(0.01) 0.74 (0.02)	5.48 (0.25) 6.00 (1.85) 6.23 (0.39)

6.3.3 Stress Relaxation Modeling

Stress relaxation modeling can help in understanding the mechanisms that underlie the observed behavior of various materials due to changes in their structure. This understanding can help with better designs for application specific problems. A simplistic way of representing viscoelastic behavior of polymeric materials is via springs and dashpots to denote purely elastic and purely viscous behavior, respectively [8], [16]. A combination of these two elements in series is called a Maxwell element (Figure 6.7) and can generally be used to describe stress relaxation. The spring component responds immediately to applied stresses and the dashpot responds gradually, representing elasticity and viscous flow.

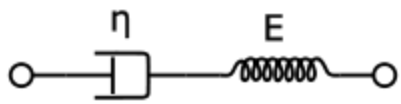

Figure 6.7. Maxwell element, representing series array of springs and dashpots.

The solution of the Maxwell model for a single time constant and finite, non-zero final stress gives rise to the following expression:

$$\sigma_t = \sigma_\infty + \sigma_o e^{-\left(\frac{t}{\tau}\right)} \qquad [6.1]$$

Where, σ_t = stress at time t, σ_∞ = stress at infinite time or final equilibrium stress, σ_o = initial stress at t = 0, and τ = relaxation time constant.

The one element Maxwell model is usually too simple and inadequate to describe stress relaxation in polymers. Crosslinked polymers can be very heterogeneous systems with a distribution of relaxation times. For explaining such systems a generalized Maxwell model may be more appropriate. This consists of Maxwell elements connected in parallel, as shown in Figure 6.8. This model represents a distribution of relaxation times that a heterogeneous system consisting of materials with different properties might have. The solution for stress as a function of time for this particular model is expressed as:

$$\sigma_t = \sigma_\infty + \sum_{i=1}^{z} \sigma_i e^{-\left(\frac{t}{\tau_i}\right)} \qquad [6.2]$$

Where, τ_i = relaxation time constant for the ith element, σ_i = stress in the ith element at time t, and Z = number of elements.

This element, as opposed to the single Maxwell element, is very complicated and difficult to interpret. An alternate approach is the intermediate path that makes use of the two elements in parallel. The reason for doing this is that the filler phase in composite can be considered to be surrounded by two phases – an interphase due to the surface modification and a non-homogeneous bulk polymer. Different relaxation times can be associated with the structural character of the various regions of the polymeric composite materials.

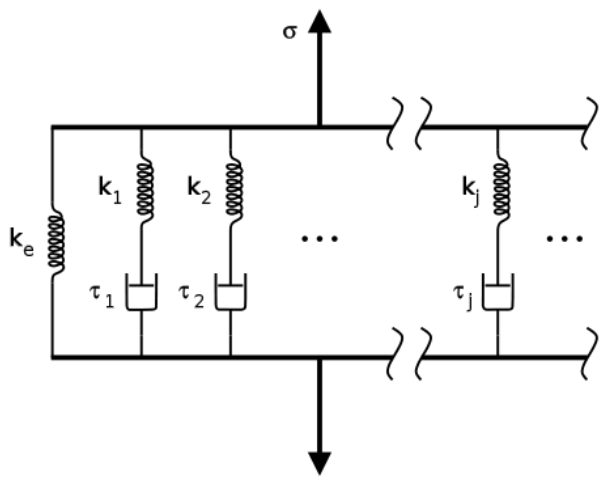

Figure 6.8. Generalized Maxwell model, consisting of Maxwell elements connected in parallel.

The final model that was used to model the stress relaxation results was:

$$\sigma_t = \sigma_\infty + \sigma_1 e^{-\left(\frac{t}{\tau_1}\right)} + \sigma_2 e^{-\left(\frac{t}{\tau_2}\right)} \qquad [6.3]$$

The data for each sample was normalized with respect to the peak stress for that particular sample and fitted to the model using Matlab's curve-fitting toolbox. Table 6.4 summarizes the results of the simulation. We focus on the two time constants, τ_1 and τ_2.

Table 6.4. Results of fitting stress relaxation data to a two time constant Maxwell model

Surface treatment	Conversion	τ_1, 1st time constant (s)	τ_2, 2nd time constant (s)
	33.9 (0.8)	1.14 (0.07)	42.4 (0.9)
	53.2 (0.8)	1.90 (0.20)	71.3 (3.1)
γ-MPS	60.4 (0.8)	2.60 (0.09)	84.6 (2.5)
	32.1 (0.1)	0.78 (0.01)	33.6 (0.7)
	47.3 (4.2)	0.99 (0.20)	60.1 (3.0)
High M_w brush – 0%	59.0 (0.3)	1.21 (0.18)	72.5 (3.5)
	31.9 (4.4))	0.85 (0.03)	32.2 (4.7)
	52.0 (3.0)	1.97 (0.00)	63.5 (3.4)
High M_w brush – 100%	60.4 (0.8)	2.18 (0.08)	73.7 (0.6)

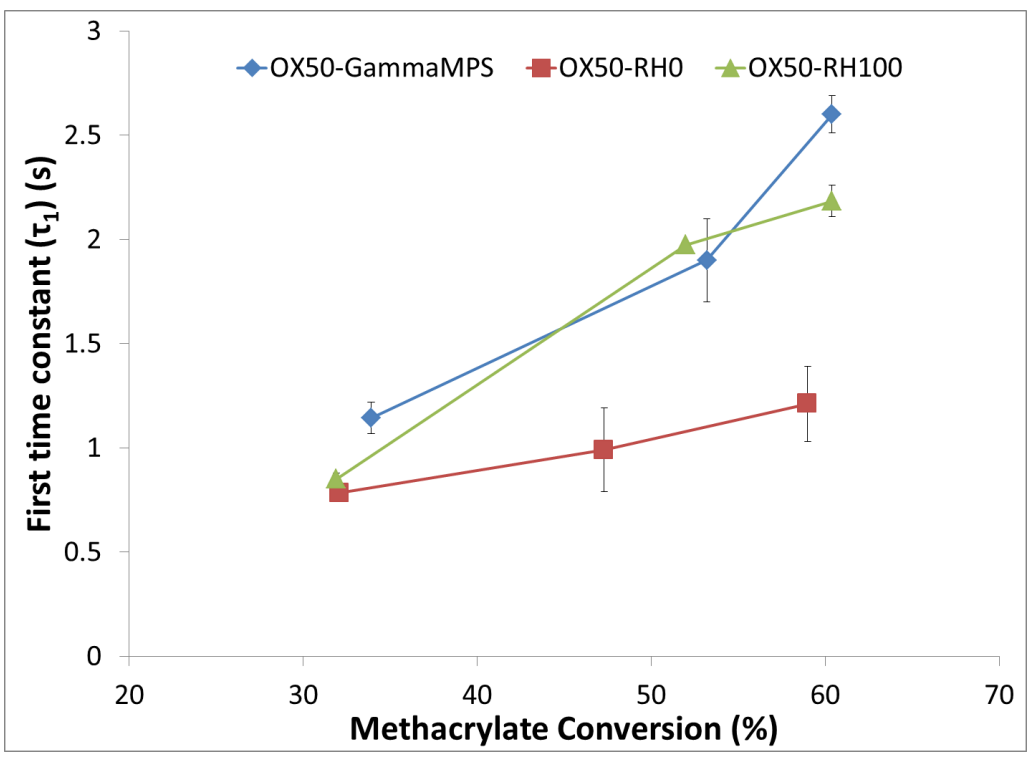

Figure 6.9. First time constant, τ_1, plotted a function of conversion for composite samples based on OX50 filler - – 1) (●) γ-MPS; 2) (■) High M_w rigid oligomer – 0% methacrylate; 3) (▲) High M_w rigid oligomer – 100% methacrylate.

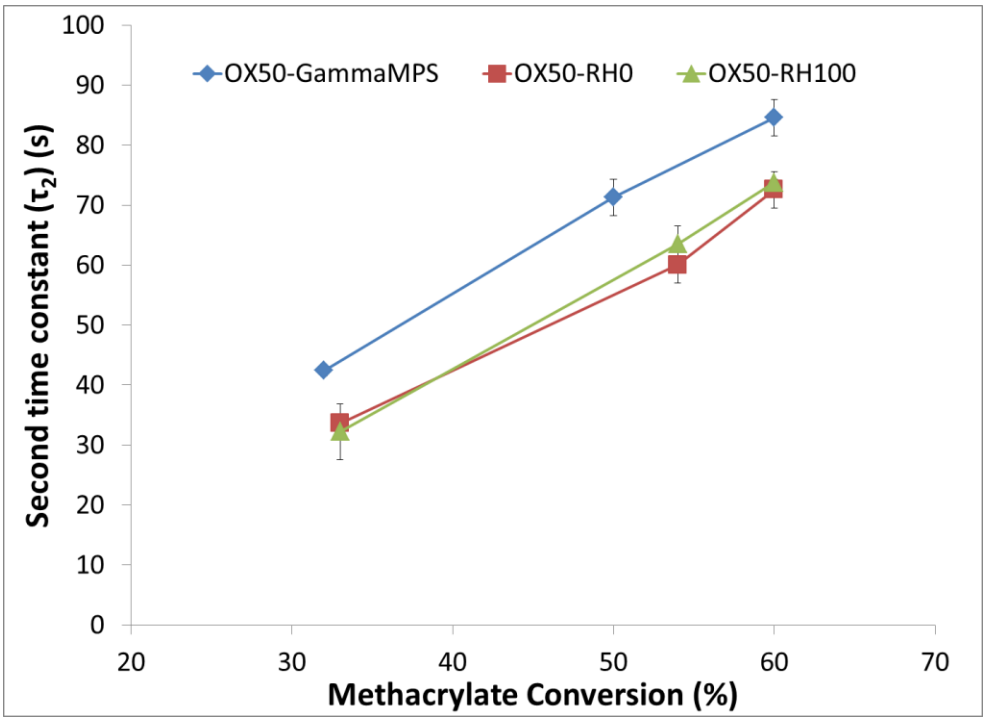

Figure 6.10. Second time constant, τ_2, plotted a function of conversion for composite samples based on OX50 filler – 1) (●) γ-MPS; 2) (■) High M_w rigid brush – 0% methacrylate; 3) (▲) High M_w rigid brush – 100% methacrylate.

The two time constants, τ_1 and τ_2, are plotted as a function of conversion in Figures 6.9 and 6.10, respectively. A noteworthy trend in each case is that the OX50-RH0 composite sample displays the lowest relaxation times in terms of both τ_1, which represents the short time scales and τ_2 that corresponds to the extended time scale of the relaxation times. For the slow relaxation regime, at low conversion, the OX50-RH0 and OX50-RH100 composites have a similar relaxation time but as the conversion proceeds, the relaxation time of the OX50-RH0 composite increases slowly, while the increase for the OX50-RH100 material is more rapid. The OX50-GammaMPS composite has a higher relaxation time at the low conversion region and then the curve accelerates and at the high end of conversion, the composite has the highest relaxation time amongst all the samples. For the longer relaxation time scales in Figure 6.10, the OX50-RH0 and

OX50-RH100 overlap completely over the entire conversion range. OX50-GammaMPS shows higher relaxation times for any given conversion range. It is of interest that the curves are parallel to each other, which means that even at low conversion, differences in the interfacial structure are responsible for differences in stress relaxation behavior.

According to Viovy et al. [17], a polymer chain subjected to a step strain can relax in the following manner - immediately in response to the strain, “there is local equilibration [18], [19] followed by the retraction of inside its “tube” (the tube here is the sort of a casing in which the polymer can be assumed to be confined in a relaxed state), followed by “reptation” by which the chain recovers an isotropic configuration”. Although these theoretical studies have been made in less constrained systems, where there is no cross-linking, we can still apply the same fundamentals in explaining the relaxation processes here. The fast relaxation process is due to local equilibration and is the immediate consequence of the imposed step strain. Due to the crosslinked nature of the composite as a whole, cooperative movements would determine the speed of this process. The OX50-GammaMPS and OX50-RH-100 composites have interfaces between the fillers and the growing polymer that have a high number of methacrylate groups that can covalently react with the polymer. This can impose restrictions on mobility of the polymer around the filler, leading to a slower response time. The restrictions would be increased as the connection points or the mobility of the connecting segments between the surface-attached molecules and the polymer increase. This can explain the faster relaxation times for these two composites. The fact that the relaxation time for the OX50-GammaMPS composite at the higher range of conversion increases more than the OX50-RH100 can be explained by the fact that the filler surface in the OX50-GammaMPS sample is covered entirely by methacrylate functionalities that are fully exposed to the monomer/polymer around the filler, increasing the

chances of reacting quickly with the surrounding polymer, thereby slowing down the relaxation faster than that for the OX50-RH100 composite. In case of the OX50-RH0 composite, the surface-tethered oligomer has only one terminal acrylate group that can co-polymerize with the methacrylate-based monomers. This effectively reduces the chances of a quick reaction, or at least an immediate increase in the mobility restriction between the two phases, allowing the polymer phase to relax faster than in the case of the other two composites.

In the case of the slow relaxation regime, the polymers relax by reptation or slower short range movements, once the polymer has recoiled in its "tube". There is a significant difference in the relaxation times between the OX50-GammaMPS composite and the two experimental composites, OX50-RH0 and OX50-RH100, which have the same relaxation times. Due to the similar relaxation times of the experimental composites, in spite of their different influence on the short relaxation time regime, it appears that the slower relaxation may be more influenced by the bulk polymer than by the interface effects. The influence of the interface can extend deep into the bulk polymer, depending on the way the interface is modified. If the bulk polymer influences the slower relaxation more and the OX50-GammaMPS composite shows higher relaxation times, then it can be speculated that the γ-MPS treated fillers have longer range influence on the mobility restrictions of the bulk polymer than any of the experimental materials.

Interactions between nanoparticles and polymers have been studied quite extensively over the last few years. A study on effects of silica and alumina nanosphere addition to polystyrene, PMMA and poly (2-vinylpyridine) found the glass transition to either increase, decrease or stay the same, depending on the strength of the interactions between the fillers and the polymers [20]. In another study, a slower relaxation of PDMS polymer chains near the polymer-filler interface was attributed to the mobility restriction imposed by physical

interactions [21]. Regions of reduced or enhanced mobility near the filler surface that interact with their neighbors have been postulated [14]. As the filler particle size is reduced and a percolation threshold is approached, the regions around the filler particles start to interact with each other Depending on the type of interactions, the glass transition could be either lowered or increased and this would accordingly alter the overall stress relaxation characteristics of the material.

6.4 Conclusion

Stress relaxation measurements were carried out on unfilled resin and composites with large filler (0.7 μm) treated with a conventional silane (γ-MPS) and nano filler (fumed silica, 40 nm diameter), that were surface treated with a conventional silane (γ-MPS) and with experimental oligomers. It was found that surface interactions influence the stress relaxation characteristics of the materials to a great extent. The addition of micron-sized filler slowed down the relaxation process when compared to the unfilled resin matrix, for the same levels of methacrylate conversion. The stress recovery was also reduced due to the fillers. In case of the nano fillers, it was found that the stress recovery in the experimental systems was fast when fewer reactive groups were present at the filler interface. The higher stress recovery is attributed to the reduced mobility restrictions due to the interfacial interactions with the bulk polymer. This has very important implications in the design of future dental materials and also for the nanocomposites field in general. The increased stress recovery implies that there is potential for enhanced stress reduction in dental composites by merely changing the interface between otherwise conventional fillers and polymer matrices.

6.5 Acknowledgements

The authors would like to thank the National Institutes of Health for support of this research through the grant NIH/NIDCR- R01DE014227. We also wish to thank Septodont-Confi-Dental and Evonik for their gracious donation of filler materials and Esstech, Inc. for donation of monomers.

6.6 References

[1] J. L. Ferracane, "Placing Dental Composites—A Stressful Experience," *Operative Dentistry*, vol. 33, no. 3, pp. 247–257, May 2008.

[2] J. L. Ferracane, "Resin composite—State of the art," *Dental Materials*, pp. 1–10, Nov. 2010.

[3] J. W. Stansbury, M. Trujillo-lemon, H. Lu, X. Ding, Y. Lin, and J. Ge, "Conversion-dependent shrinkage stress and strain in dental resins and composites," *Dental Materials*, vol. 21, pp. 56–67, 2005.

[4] H. Lu, J. W. Stansbury, S. H. Dickens, F. C. Eichmiller, and C. N. Bowman, "Probing the origins and control of shrinkage stress in dental resin composites. II. Novel method of simultaneous measurement of polymerization shrinkage stress and conversion.," *Journal of biomedical materials research. Part B, Applied biomaterials*, vol. 71, no. 1, pp. 206–13, Oct. 2004.

[5] C. L. Davidson and a J. de Gee, "Relaxation of polymerization contraction stresses by flow in dental composites.," *Journal of Dental Research*, vol. 63, no. 2, pp. 146–8, Feb. 1984.

[6] a J. Feilzer, a J. De Gee, and C. L. Davidson, "Quantitative determination of stress reduction by flow in composite restorations.," *Dental Materials*, vol. 6, no. 3, pp. 167–71, Jul. 1990.

[7] H. Lu, J. W. Stansbury, and C. N. Bowman, "Towards the elucidation of shrinkage stress development and relaxation in dental composites.," *Dental Materials*, vol. 20, no. 10, pp. 979–86, Dec. 2004.

[8] L. H. Sperling, *Introduction to Physical Polymer Science*. John Wiley and Sons, 2006.

[9] T. Otsu and A. Kuriyama, "Living Mono- and Biradical Polymerizations in Homogeneous System Synthesis of AB and ABA Type Block Copolymers," *Polymer B*, vol. 142, pp. 135–142, 1984.

[10] T. Otsu, "Iniferter concept and living radical polymerization," *Journal of Polymer Science Part A: Polymer Chemistry*, vol. 38, no. 12, pp. 2121–2136, Jun. 2000.

[11] J. M. Nedeljkovic and V. Djokovic, "Stress relaxation in hematite nanoparticles-polystyrene composites," *Macromolecular Rapid Communications*, vol. 21, no. 14, pp. 994–997, 2000.

[12] C. L. Davidson and a J. de Gee, "Relaxation of polymerization contraction stresses by flow in dental composites," *Journal of Dental Research*, vol. 63, no. 2, pp. 146–148, Feb. 1984.

[13] R. Ruggerone, V. Geiser, S. Dalle Vacche, Y. Leterrier, and J.-A. E. Månson, "Immobilized Polymer Fraction in Hyperbranched Polymer/Silica Nanocomposite Suspensions," *Macromolecules*, vol. 43, no. 24, pp. 10490–10497, Dec. 2010.

[14] A. Bansal, H. Yang, C. Li, K. Cho, B. C. Benicewicz, S. K. Kumar, and L. S. Schadler, "Quantitative equivalence between polymer nanocomposites and thin polymer films.," *Nature Materials*, vol. 4, no. 9, pp. 693–8, Sep. 2005.

[15] A. P. Meera, S. Said, Y. Grohens, A. S. Luyt, and S. Thomas, "Tensile Stress Relaxation Studies of TiO 2 and Nanosilica Filled Natural Rubber Composites," *Industrial & Engineering Chemistry Research*, vol. 48, no. 7, pp. 3410–3416, Apr. 2009.

[16] M. T. Shaw and W. J. Macknight, *Introduction to Polymer Viscoelasticity*, 3rd ed. 2005.

[17] J. L. Viovy, L. Monnerie, and J. F. Tassin, "Tube Relaxation : A Necessary Concept in the Dynamics of Strained Polymers," *Journal of Polymer Science: Polymer Physics Edition*, vol. 21, pp. 2427–2444, 1983.

[18] S. F. Edwards and M. Doi, "Dynamics of Rod-like Macromolecules in Concentrated Solution. Part 1," *Journal of the Chemical Society, Faraday Transactions 2: Molecular and Chemical Physics*, vol. 74, pp. 560–570, 1978.

[19] F. S. Edwards and M. Doi, "Dynamics of Rod-like Macromolecules in Concentrated Solution. Part 2," *Journal of the Chemical Society, Faraday Transactions 2: Molecular and Chemical Physics*, vol. 74, pp. 918–932, 1978.

[20] P. Rittigstein and J. M. Torkelson, "Polymer – Nanoparticle Interfacial Interactions in Polymer Nanocomposites : Confinement Effects on Glass Transition Temperature and Suppression of Physical Aging," *Polymer*, pp. 2935–2943, 2006.

[21] D. Fragiadakis, P. Pissis, and L. Bokobza, "Glass transition and molecular dynamics in poly(dimethylsiloxane)/silica nanocomposites," *Polymer*, vol. 46, no. 16, pp. 6001–6008, Jul. 2005.

CHAPTER 7

INFLUENCE OF NANOFILLER AND MICROFILLER FRACTIONS ON SHRINKAGE STRESS AND LIGHT TRANSMISSION IN DENTAL COMPOSITES

Abstract

Objectives: Shrinkage stress due to polymerization is a major problem that complicates the placement and decreases the service life of commercial dental composites. In addition, light transmission in dental composites, which are reliant on visible light photopolymerization their formation, is affected due to the presence of a high volume of filler particles. This chapter explores the effects of an experimental filler surface modification approach as a way of addressing both these problems.

Methods: An oligomer made from bisphenol A glycerolate (1 glycerol/phenol) diacrylate (BisGDA) and 1,2-ethanedithiol (EDT) was synthesized and attached to the surface of Aerosil OX50 particles (average diameter - 40 nm) and barium glass particles (0.7 µm). A conventional silane treatment (γ-methacryloxypropyltrimethoxysilane) was used as the control. The shrinkage stress and light transmission of composites having varying proportions of the OX50 and Barium glass particles, with a total filler mass fraction of 50 %, were measured. Refractive index measurements were used to elucidate the light transmission behavior of the composites.

Results: The experimental surface-modified composites outperformed the conventional silane-treated control composite in both shrinkage stress reduction and light transmission. Addition of OX50 particles treated with the experimental oligomer had a significant effect on shrinkage stress and light transmission, while the type of surface treatment on the larger barium glass filler had no significant effect. At constant overall filler content, increasing the ratio of

OX50 particles treated with γ-MPS with respect to the barium glass fillers treated with the same silane resulted in an increase in shrinkage stress. Steady increase the ratio of the OX50 fillers treated with the experimental oligomer resulted in a significant lowering of the polymerization shrinkage stress. Optical clarity upon cure also increased with the addition of the experimental fillers as compared to the same ratios of γ-MPS treated fillers.

Significance: Reduction of shrinkage stress and increase in light transmission due to a single surface treatment has important implications in the field of dental composites and also nanocomposites in general. Shrinkage stress reduction can potentially increase the durability of the composites while the improved light transmission will increase the depth of cure, which leads to higher conversion and consequently, better overall mechanical properties.

7.1 Introduction

Polymer-based dental restoratives, by tradition, are a mixture of several major components: 1) a monomeric phase usually consisting of dimethacrylate-based resin monomers, 2) a reinforcing phase consisting of particulate inorganic fillers and 3) an organosilane coupling agent to serve as a link between the two phases. Minor components include initiating systems, stabilizers and coloring agents [1], [2]. The resin system generally consists of 2,2-bis[p-(2'-hydroxy-3'methacryloxypropoxy)phenyl]-propane, popularly known as BisGMA, or related dimethacrylates combined with other liquid organic monomers that serve as diluents to give the resin mixture a workable consistency [3]. The filler phase is very crucial in giving the restorative mechanical integrity, having a significant effect on mechanical strength, toughness, polymerization shrinkage, viscoelastic properties, wear resistance and appearance [4]. With the basic formulation of the resin phase remaining fairly consistent over time, it is the fillers that

have undergone substantial changes over the last few decades in efforts to optimize the formulations to suit various clinical applications [5].

The sizes of filler particles in current dental restoratives range from approximately 10-40 nm up to about 0.2-2 μm and the filler volume fraction in these composite materials can range from about 20 % to 70 % [1], [2], [6]. Current dental composites have either a mixture of micron and nano-sized particles or purely nanosized ones [7]. The implications of introducing nano-sized fillers in composites are tremendous. The very high surface area to volume ratio of nanoparticles gives them unique properties that are different from their micrometer-sized counterparts. The enhanced interactions can result in improved toughness, strength, moduli and optical properties [8–10]. At the same time it can also have a negative effect on the filler loading limits and the glass transition temperature [11]. The negative or the positive effects of these properties depends on the strength of the interfacial interactions.

In practice, nanofillers form only a small fraction of the total filler loading in modern dental composites. Most often the nanofillers are added as “space fillers”, to increase the loading of fillers by way of the nanoparticles getting into the interstitial spaces in between the micro particles. The increased interactions with the nanoparticle surfaces lead to large increases in viscosity of the material, limiting their use. Nanofillers also help in reducing the wear and improving polishing characteristics in composites. Due to their small size, nanoparticles pose less and in some cases no effect on visible light transmission [8]. This allows improved restoration esthetics where the significant translucency of tooth enamel can be better matched. Additionally, since dental composites are photocured with visible light (typically 400-500 nm), curing efficiency and depth of cure are potential advantages for composite material with excellent light transmission characteristics.

Despite all the advances in materials science technology in dental materials, they still suffer from the problem of shrinkage and the associated shrinkage stress. Stresses in these composites are a result of the restricted shrinkage during polymerization. As stress is proportional to both shrinkage and modulus, the addition of high modulus fillers affects it in two ways. As fillers are added to the resin, the fractional volume of the resin is reduced and there is lower volumetric shrinkage as compared to the case of an unfilled resin. This leads to a reduction in the stress. At the same time, the fillers can also contribute to increasing stress due to their higher modulus. Fillers become covalently attached to the resin, usually via an organosilane such as γ-methacryloxypropyltrimethoxy silane (γ-MPS). This link helps transfer the stresses that the composite experiences in a cavity onto the filler. These attachments can also serve as sites that restrict the shrinkage of the resin, leading to stress development. Confirmation of this observation can be seen in reports that show that composites that have untreated fillers or those treated with non-functional silanes can lead to lower stresses compared to composites that have functional fillers [12].

It can be inferred that for a given mass fraction of filler, the higher the surface area of the fillers in a composite, the larger the number of sites where the shrinking resin can be attached. Nanoparticles, due to their high surface area, would amplify this effect. Prior work (Chapters 4 and 5) has shown that interfaces can be modified in order to mitigate the shrinkage stresses that arise in dental composites. The specific interactions between the interfacial layer and the resin phase can lead to substantial reductions in the final shrinkage stress without compromise in the interrelated properties of polymerization shrinkage and final modulus development. The previous studies were carried out mainly on OX50 nanofiller particles, which have an average diameter of 40 nm. The high interfacial area helps in reinforcing the positive effect of the interfacial layer.

However, as mentioned before, modern dental composites have fillers that are generally a mixture of both microparticles and a small amount of nanoparticles. Although the nanoparticles have a high surface area, if their amount is small, then the effect of the large area may not be significant. Using micro particles is also essential to achieve higher filler loading, which is essential for enhanced wear behavior and low coefficients of thermal expansion in the composite materials. Nanoparticles, due to their high surface energy, increase the viscosity of the system, which can make handling and placement of the restorative difficult. Micron-sized particles are needed to overcome this and increase filler loading. Hence it is practically important to use both micro- and nano-particles to get the best overall properties from dental composite materials.

This work provides an examination of an experimental polymer brush-based interfacial treatment applied to both micron and nano-sized fillers with an emphasis on gaining a better understanding of how the interface affects shrinkage stress in dental composites composed of bimodal fillers. As a control, γ-MPS functionalized micro- and nano-particles are used. Ratios of both the particles are varied in a continuous manner to examine how the shrinkage stress varies with respect to each type of filler.

7.2 Materials and Methods

7.2.1 Materials

Silica nanoparticles (Aerosil OX50, average diameter = 40 nm, surface area 50 m^2/g) were donated by Evonik (Germany). 0.7 micron Barium glass particles, both unmodified and treated with γ-MPS (γ-methacryloxypropyl-trimethoxy silane) and OX50 particles silanized with γ-MPS were kindly donated by Septodont Confi-Dental (Louisville, Colorado, USA). N-methylaminopropyltrimethoxysilane (MAPTS) was purchased from Gelest. 2,2-bis[4-(2-

hydroxy-3-methacryloyloxypropyl-oxy)phenyl]propane (BisGMA) and triethylene glycol dimethacrylate (TEGDMA) monomers were donated by Esstech, Inc.. A visible light initiating system consisting of 0.3 wt% camphorquinone (CQ) as initiator and 0.8 wt% ethyl 4-dimethylaminobenzoate (EDAB) (Sigma-Aldrich, Milwaukee, WI) as co-initiator was incorporated. Isocyanatoethylmethacrylate (IEM), methylene chloride, reagent alcohol, anhydrous toluene, and dibutyltin dilaurate, triethylamine were obtained from Sigma-Aldrich (USA). Monomers used for making for the oligomer synthesis – Bisphenol A glycerolate (1 glycerol/phenol) diacrylate (BisGDA) and 1,2-Ethanedithiol (EDT), were also purchased from Sigma-Aldrich (USA) and used without further purification.

7.2.2 Synthesis of Oligomer

The structures of the monomers used for the synthesis are shown in Figure 7.1. For the synthesis, monomers were dissolved in chloroform in the ratio – BisGDA/EDT = 1.25/1.00. It was desired to have oligomers with acrylate functionalities at the ends and so BisGDA was kept in excess. A few drops of triethylamine as catalyst were added to the reaction mixture. The mixture was stirred constantly and progress of the reaction was monitored using FT-IR by following the reduction of the thiol peak at 2575 cm^{-1}. Upon completion of the reaction, the oligomer was separated from the unreacted mixture by dropwise addition in hexanes. The supernatant solution was discarded and the oligomers redissolved in chloroform. This solution was dried in a roto-vap and then under a high-vac to remove the solvent. The final structure of the oligomer is shown in Figure 7.2. This particular oligomer scheme was chosen as it had been proven in Chapter 5 to give good results for reduction of shrinkage stress.

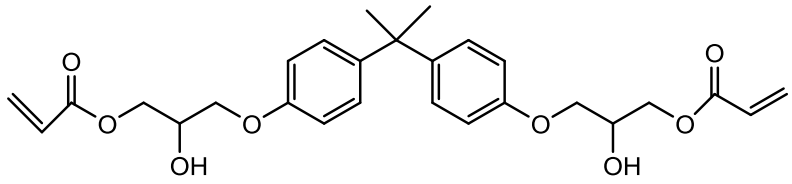

Bisphenol A glycerolate (1 glycerol/phenol) diacrylate
(BisGDA)

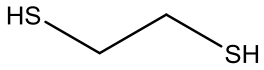

1,2-ethanedithiol
(EDT)

Figure 7.1. Structures of monomers used for synthesis of the oligomer

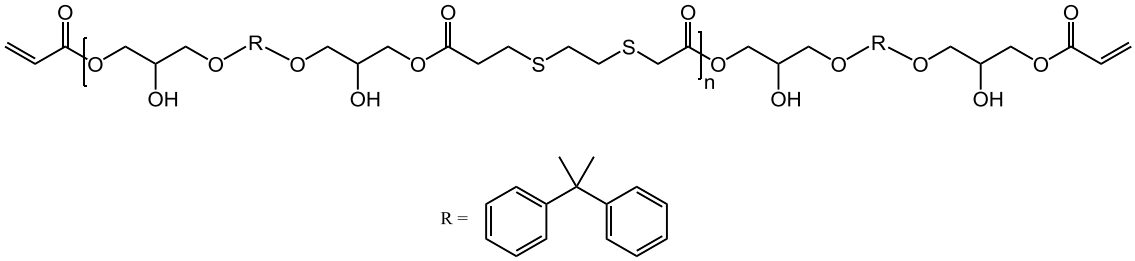

Figure 7.2. Structure of final oligomer.

7.2.3 GPC Characterization

A Viscotek triple detector gel permeation chromatography (GPC) system, equipped with Viscotek VE 3580 refractive index detector and Viscotek 270 dual detector, was used for characterization of the size of the oligomer. The mobile phase was HPLC grade tetrahydrofuran at a flow rate of 1 mL/min. Samples were prepared in HPLC grade THF to a concentration of about 5g/L and 10 µL of sample was injected for analysis.

7.2.4 Modification of the Filler

The bare silica particles were first treated treated with MAPTS (N-methylaminopropyltrimethoxysilane) and then the oligomers were attached to the amine end of the silane. OX50 particles were first dried in a rotary dryer at about 165 ^{o}C under vacuum for three hours before further treatment. This was done to ensure removal of surface bound moisture that can potentially react with the silanes and promote the formation of multiple layers of the silane. Anhydrous toluene was used as a solvent for the silanization process. It was refluxed for two hours and then the particles were added and further refluxed for an hour to ensure good dispersion. The MAPTS was added to the solution so that the final concentration in the mixture was 1.5 % by weight. This reaction mixture was allowed to reflux for six hours after which the particles were separated from the solvent by centrifugation. The particles were washed three times with toluene and two times with methylene chloride to ensure that all traces of unreacted silane were removed. The silanized particles were then dried overnight under vacuum at 50 ^{o}C to remove all traces of solvent. The dried and silanized particles were then added to reagent alcohol in which 5X excess of oligomer was already mixed. The reaction mixture was heated to 45 ^{o}C and the reaction was allowed to continue for three days. The particles were then centrifuged to remove the solvent and washed 5 times with methylene chloride to remove excess solvent and dried in a vacuum oven at 45 ^{o}C.

7.2.5 Composite Preparation

The resin matrix for the composites was a mixture of BisGMA and TEGDMA in the ratio 70:30 by weight. The resin included a free radical visible light initiating system comprised of 0.3 wt. % camphorquinone and 0.8 wt. % ethyl-4-dimethylaminobenzoate. The fillers were added to

the resin and mixed in a speedmixer (DAC 150 FVZ, Flakteck Inc.) and dispersed in the resin to make a composite paste. Composites with γ-MPS-treated particles were used as the control. The ratios of the different fillers used to make the composite are shown in Table 7.1. The total weight of the fillers was 50 % of the composite. The freshly prepared composites were allowed to sit under vacuum to ensure elimination of air bubbles prior to being used.

Table 7.1. Filler combinations used in the mixed filler composites

Ratio of OX50 to 0.7 µm filler	Gamma MPS series	Brush series
5/45	C1	L1
10/40	C2	L2
15/35	C3	L3
20/30	C4	L4
25/25	C5	L5

7.2.6 Shrinkage Stress Measurements

Shrinkage stress was measured using a cantilever beam based instrument referred to as the tensometer (American Dental Association, Paffenberger Research Center, MD, USA). This instrument measures the force generated by an actively polymerizing material that is partially constrained from a free shrinking state. The material is bonded to the opposing ends of two diametrically placed quartz rods. The polished ends of the glass rods are freshly treated with γ-MPS, to promote bonding with the polymerizing material. The upper quartz rod is attached to the cantilever beam and is free to move along with the shrinking composite and the lower quartz rod is fixed to the base. A dental curing light (IQ2, Caulk, Dentsply), with an output wavelength of 465 nm, was adapted to the bottom of the lower quartz rod, which serves as a light guide to

transmit the curing light to the material. A detailed description of the stress measurement involving the tensometer has been published previously [13]. The testing protocol uses specimen discs of 1.5 mm thickness and 6 mm diameter. The light intensity reaching the sample was measured at 350 mW/cm^2. The samples were irradiated for 40 s with the dynamic stress development profile continuously monitored for 10 min. Real-time double bond conversion measurements based on simultaneous near-IR spectroscopy were made during the stress measurements.

7.2.7 Flexural Modulus Measurements

Flexural modulus and strength were measured in a 3-point bending mode (858 Mini Bionix II, MTS Systems, Eden Prairie, MA). The composite pastes were injected into a cavity measuring 2x2x10 mm. The cavity was surrounded by Teflon spacers on the sides and clamped glass slides on the top and bottom. They were cured using the dental curing light from both the sides to promote uniform conversion throughout the sample. The crosshead speed used was 1 mm/min.

7.2.8 Infrared Spectroscopic Characterization

Infrared spectroscopy was used to monitor the conversion of the resin and the surface modification of the fillers using an FTIR (Nexus 670, Nicolet Instruments, Madison, WI). Double bond conversion was monitored in transmission mode using near-infrared (NIR) spectroscopy. The area of the peak at 6165 cm^{-1} representing the methacrylate $=CH_2$ absorption was used to track conversion.

7.2.9 Light Transmission

Light transmission measurements were made using an Ocean Optics UV-vis detector (189.8 - 890.6 nm). Infrared light was passed through the specimen and light intensity was recorded during photopolymerization (Acticure 4000, 320-500 nm, 25 mW/cm^2, 10 min cure time, 3 cm from sample). Specimen material was placed in a Teflon mold (1 mm thickness, 10 mm diameter) sandwiched between glass slides, and mounted on an optical bench. The fiber from the IR light source was fixed to a collimating lens placed approximately 5 cm from the sample. The UV-vis fiber (SMA connection) was placed approximately 3 cm from the sample. Spectra Suite software was used to monitor and record the light transmission at 760 nm wavelength for 10 min, with an integration time of 50 ms and 20 scans to average.

7.2.10 Refractive Index Measurements

Refractive index measurements were made using an ATAGO refractometer. . For polymer and composite disc samples, 1-3 drops of a high refractive index liquid (bromonaphthalene) was placed on the measurement surface. The top cover was closed and secured and the light was turned on. The refractive index was measured using the viewing window by focusing and aligning the horizontal light-to-dark transition with the crosshairs and recording the numerical refractive index value.

7.3 Results and Discussion

Current research focused on the study of variations in shrinkage stress and light transmission in dental composites made by combining fillers of two different sizes and with two different surface treatments. The fillers used were 1) Barium glass – average size 0.7 µm and 2)

Fumed silica – Aerosil OX50 (diameter – 40 nm). The surface treatment used as the control was γ-MPS and the experimental surface treatment being compared was based on the high molecular weight rigid oligomeric brush structure. The particular oligomer was used here as it had the best performance for shrinkage stress reduction (Chapter 5).

7.3.1 Shrinkage Stress Study

Initial shrinkage stress measurements were carried out on composites made from a single filler type and particle size, in order to determine how each filler individually affected the shrinkage stress. Figure 7.3 shows the shrinkage stress variation as a function of filler loading for the 0.7 µm barium glass particles, for both the surface treatments. The stress values taken are the final stress values at the end of the 10 min evaluation interval. Over the range of filler loading evaluated here, the shrinkage stress decreased as a function of filler loading for both the systems. This is a trend that was seen during investigation of the effect of filler loading on mechanical properties of composites in Chapter 3. As the filler loading increases, the volume fraction of the resin phase decreases, which is known to contribute a proportional reduction in shrinkage for a given level of conversion. In general, the lower shrinkage translates to a lower stress. There is a small difference between the two systems, with the long rigid oligomer system showing a slightly lower stress as compared to the γ-MPS control for all the loading levels, except for the 5 wt% filled material where any differences would be expected to be minimal. The generally lower stress can be attributed to the effect of the oligomer to alter the stress transfer between the filler and the evolving matrix (Chapter 5).

Following this, the effect of OX50 particles on shrinkage stress was evaluated (Figure 7.4). It can be seen that the γ-MPS system shows no change in shrinkage stress as the OX50 loading level

increases. The greater interfacial surface area and lower volume fraction of the OX50 filler compared with equivalent loading contents of the micron-sized barium glass filler particles explains why the effect of reduced shrinkage and increasing modulus are balanced in terms of polymerization stress production as the OX50 filler loading is increased. However, the composites with fillers treated with the oligomer show a decrease in stress as the OX50 loading is increased. The 10 wt% sample has similar shrinkage stress as its γ-MPS counterpart and then there is a significant decrease in stress as the oligomer modified OX50 loading level reaches 20 wt%. There is a continued but not statistically significant reduction in stress between the 20 wt% and 30 wt% composites with the oligomer system. The reduction of stress in the experimental system can again be attributed to the interface modification that delays the effective stress transfer between filler and matrix when compared to γ-MPS-based interface.

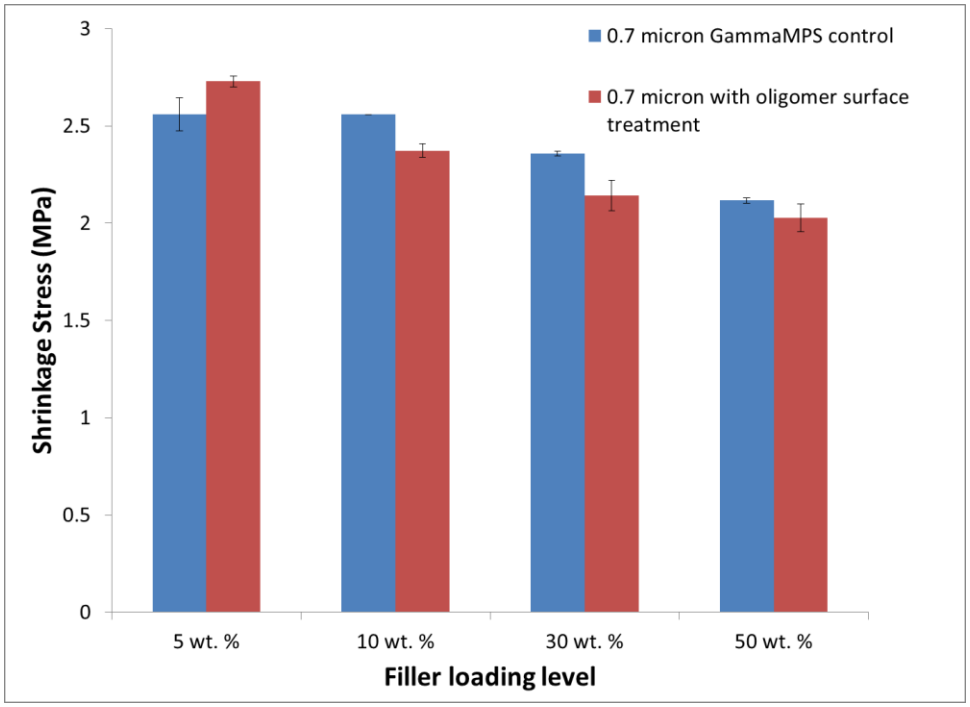

Figure 7.3. Comparison of shrinkage stress between 0.7 µm fillers treated with γ-MPS control and experimental oligomer at various loading levels of the filler

These results were encouraging as the addition of increasing amounts of experimental OX50 filler led to significant reductions in the stress state developed during photopolymerization of the composites. It also makes a case for being able to increase the amount of nanofiller used in composites with important beneficial effects achieved by merely modifying the interface. The two filler types were then mixed with each other in order to test the effect of varying amounts of each particle type on shrinkages stress. The total loading of the two fillers was arbitrarily kept at

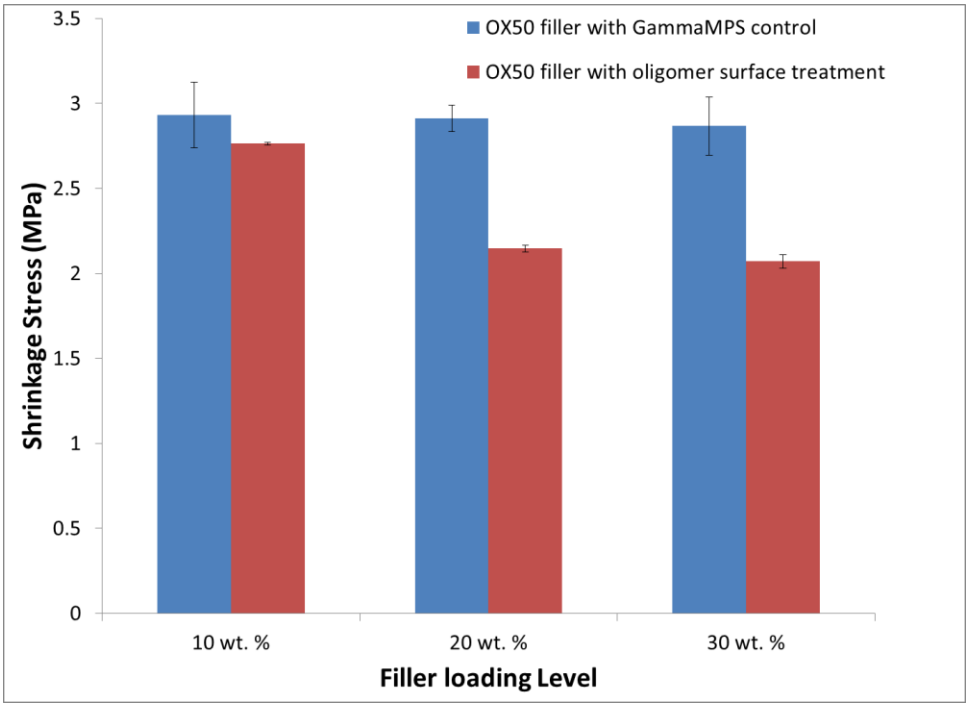

Figure 7.4. Comparison of shrinkage stress between OX50 fillers treated with γ-MPS control and oligomer

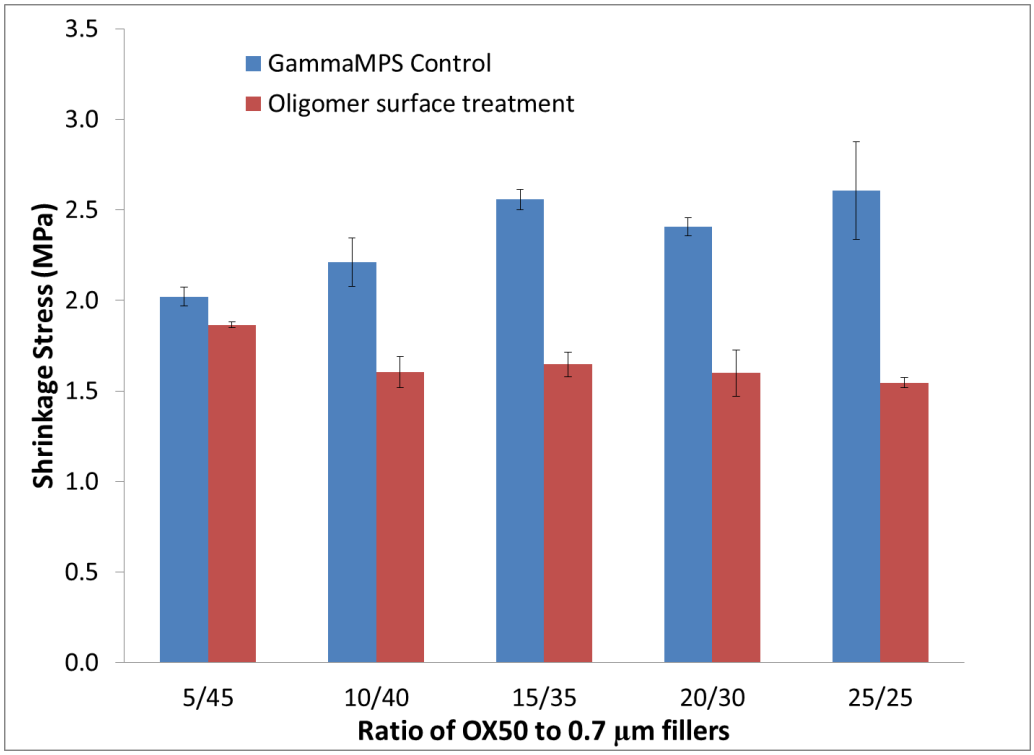

Figure 7.5. Comparison of shrinkage stress for composites with varying ratios of OX50/0.7 µm barium glass fillers. The total mass fraction of fillers is 50 wt%.

the 50 wt% level. For the γ-MPS-based composite system, there was a steady increase in the shrinkage stress as the fraction of OX50 was increased. For the composite system based on fillers treated with the oligomer, the shrinkage stress decreases from the L1 system to the L2 system. There is no significant difference between the L2 system and the others with increasing fractions of OX50 (Figure 7.5).

Table 7.2. Shrinkage stress values for composite systems with a mixture of OX50 and 0.7 µm fillers. Standard deviation values are in parentheses.

		Ratio of OX50/0.7 µm filler	5/45	10/40	15/35	20/30	25/25
		Shrinkage Stress (MPa)	2.02 (0.05)	2.21 (0.13)	2.56 (0.06)	2.41 (0.05)	2.61 (0.27)

Surface treatment	γ-MPS	Methacrylate Conversion	61.78 (0.25)	62.17 (0.40)	62.90 (0.35)	63.07 (0.51)	62.35 (0.62)
	Oligomer	Shrinkage Stress (MPa)	1.87 (0.01)	1.61 (0.08)	1.65 (0.07)	1.60 (0.13)	1.55 (0.03)
		Methacrylate Conversion	64.37 (0.46)	64.48 (0.01)	64.36 (0.85)	64.39 (1.74)	61.17 (0.54)

From Table 7.2 it is clear that the addition of OX50 fillers has a significant impact on the shrinkage stress of the composites. At 50 wt%, the systems with only 0.7 µm barium glass fillers have shrinkage stress of 2.11 ± 0.01 MPa for the γ-MPS control and 2.03 ± 0.07 MPa for the oligomer-based one, indicating no significant difference between them. The shrinkage stresses diverge from this point and at the highest OX50 loading for the γ-MPS system, the stress value is 2.61 ± 0.27 MPa while that for the highest loading of the long rigid oligomer is 1.55 ± 0.03 MPa. So while γ-MPS surface treatment has the effect of increasing the stress, the oligomer treatment has the opposite effect. This is positive confirmation of the effect of the interface on influencing shrinkage stress and the role of nano-sized fillers in controlling it.

For a given level of filler loading, the 0.7 µm fillers have a much lower surface area as compared to the OX50 particles. The surface area of the untreated 0.7 µm fillers was found to be about 10 m^2/g from BET surface area measurements and that of OX50 particles is 50 ± 15 m^2/g (source: Evonik). So 50 wt% of 0.7 µm particles would have roughly the same surface area as 10 wt% of OX50. Small increases in amounts of OX50 would increase the surface area significantly. As seen in Chapters 4 and 5, the application of oligomers on the surface of fillers can have the beneficial effect of reducing shrinkage stress. A higher surface area would only

enhance this effect since it is then able to directly interact with a greater fraction of the resin matrix.

At 50 wt% filler loading, the interparticle spacing is relatively small. As the resin starts polymerizing, it starts to interact with the methacrylate groups on the surface of the γ-MPS based fillers. The γ-MPS molecules present a short tether between the surface connection of the filler and the reactive methacrylate group that potentially engages with the resin-based monomer molecules in matrix network formation. In the case of the oligomer, the molecules form a thicker layer around the surface, as evidenced from the TEM images in Chapter 5. The only polymerizable groups that this oligomer has are the acrylate groups at the end of the chains. The oligomer seems to lie in a collapsed state on the surface of the filler. The oligomer has hydroxyl groups along its length and the MAPTS silanes that have not reacted with the oligomer and the free silanols on the silica surface, can have attractive hydrogen bonding with them [14]. These forces would make it more probable for the oligomer to be in a collapsed state. The acrylate groups at the ends of the filler would most likely be buried in this layer and the resin molecules would have to diffuse through this to be able to polymerize with them.

For shrinkage stress to start developing, it is essential to form a continuous network in the sample for the LVDT to detect the deflection of the cantilever beam of the tensometer to register a positive stress reading. To form this network, the filler particles act as multifunctional bridges between different parts of the resin that are polymerizing. From the lower shrinkage stress rates of the long rigid oligomer based composites as compared to the γ-MPS control and similar polymerization rates, it can be concluded that the interface in the experimental composite is delaying the formation of a continuous network structure. This is likely due to the delay in forming covalent links between the resin monomers and the interfacial layer or possibly that

there is a delay in the effective network reinforcement by the filler based on when these covalent connections can become network reinforcing structures.

As the fraction of OX50 increases, the surface area in contact with the resin and the interparticle spacing are inversely related. In case of the γ-MPS control, this would mean many more points of restrictive attachment with the resin phase. This is reflected as increasing shrinkage stress with increasing OX50 fraction since this effect appears to supersede the volumetric shrinkage reduction associated with the higher filler content. In case of the oligomer, the interaction is different and the delay in reaction is more enhanced. There is a drop in the shrinkage stress going from the L1 sample to the L2 sample but further increases in OX50 do not lead to any significant reduction in shrinkage stress. This implies that there is a limit to the effectiveness of the interfacial area increase on the reduction in shrinkage stress. This indicates that perhaps a certain critical interparticle distance is necessary for the interfacial layer to be effective. Reducing the interparticle distance beyond this limit does not aid the mechanism by which the stress is reduced.

7.3.2 Modulus Measurements

A reduction in shrinkage stress can be the result of a reduced modulus as stress is a function of modulus. To ascertain whether there was any lowering of modulus with the corresponding reduction in shrinkage stress, flexural modulus measurements were made on all the mixed filler samples (Figure 7.6). It was found that there was no significant difference in modulus within both the systems across all the ratios of OX50 fumed silica to 0.7 μm barium glass fillers and also between composites with the same ratio from the two different surface

treated systems. This ensured that any reduction in stress was not due to an undesirable corresponding reduction in modulus.

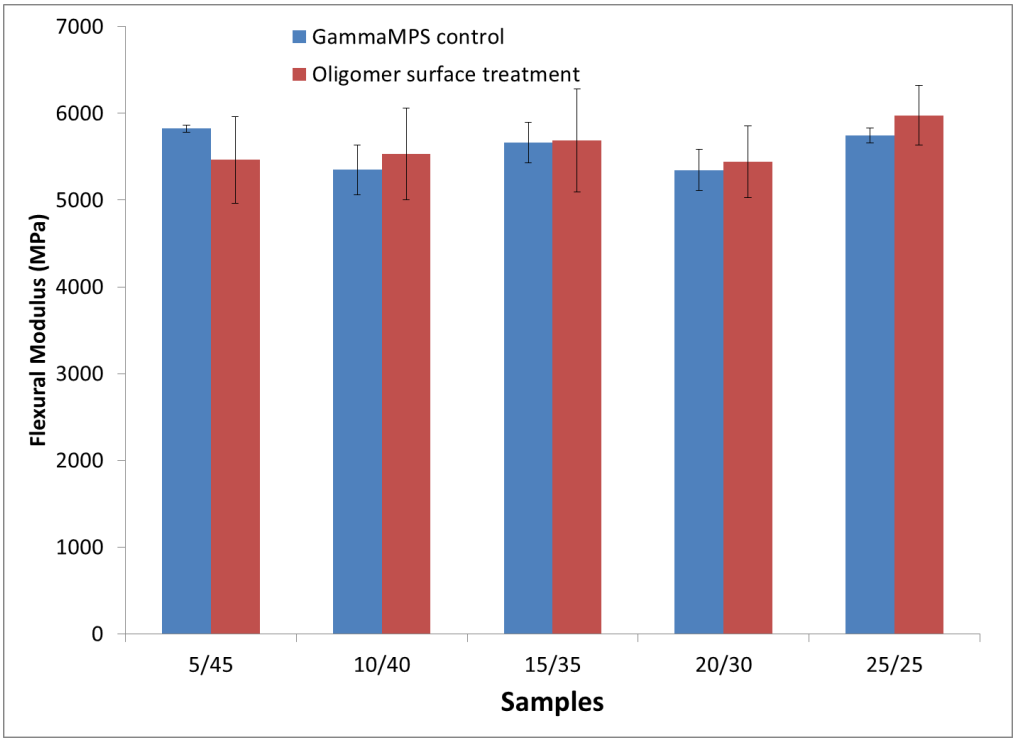

Figure 7.6. Flexural modulus of composites with different ratios of OX50 to 0.7 µm glass filler.

7.3.3 Light Transmission

Figure 7.7 shows the discs made of the mixed filler samples for the γ-MPS control and the experimental brush system samples, placed on series of numbers printed on a paper. Each number represents a specific ratio of OX50 to 0.7 µm fillers. It is apparent that overall, the experimental interfacial brush system provides composites with lower optical density or greater translucency as compared to analogous composites based on the γ-MPS filler surface treatment.

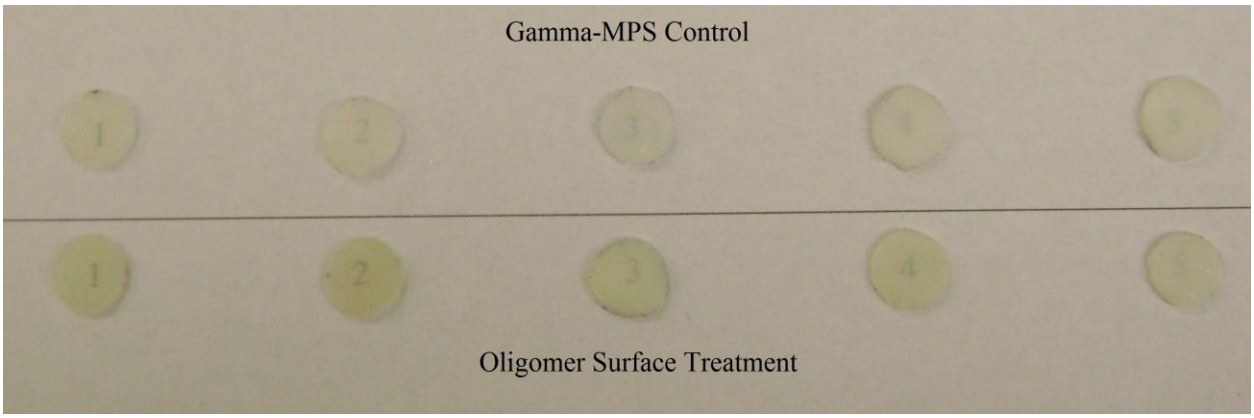

Figure 7.7. Comparison of optical translucency of composites made with fillers treated with 1) γ-MPS and 2) Experimental oligomer. The proportion of OX50 is increasing from left to right.

To quantify the optical clarity of the different composite samples, light transmission was measured for these systems (Figure 7.8), in their uncured and cured states. The light transmission intensity here has been normalized with respect to the intensity of light passing through an uncured BisGMA/TEGDMA resin mixture that does not contain any initiator (assuring a photo-inert state). It can be seen that there is no difference in transmitted light intensity through the uncured pastes in either of the systems. Upon polymerization, the transmitted light intensity increases for all the samples at all the filler fractions. The increase is highest for the 5/45 OX50/0.7 µm filler fraction and lowest for the 25/25 OX50/0.7 µm filler fraction, in both the systems. Increase in the light transmission efficiency during polymerization in composite materials has been observed before [15]. There is a large refractive index mismatch between the uncured resin and the glass fillers. The uncured resin has a refractive index of 1.5216 ± 0.003 and the barium glass filler has a refractive index of 1.5449 ± 0.0027 [15]. The refractive index of the OX50, which in the unmodified state is pure silicon dioxide, which has a much lower refractive index of 1.4603 at 486 nm. As the resin polymerizes, the refractive index increases due to densification of the matrix and moves towards that of the glass filler. This results in an increase in the light transmission due to the narrowing of the difference in the refractive indices.

Due to the lower refractive index of OX50 particles, increasing their amount would increase the difference in refractive index with the polymerized resin and this trend is reflected in the reduced light intensity.

The experimental brush-modified composites show a higher degree of light transmission than the γ-MPS control for each of the filler fractions. The difference increases for moderate amounts of OX50 (10/40 and 15/35 fractions) and again reduces as the amount of OX50 increases. There are two possible reasons for the improved light transmission. One reason is that the brush surface treatment improves the dispersion of the filler particles in the resin matrix. This can lead to better light transmission by reducing the scattering of light due to particle aggregation [16]. The other reason is that the filler surface modification locally changes the refractive index within the composites. Light transmission is reduced when there is a mismatch between the refractive indices of the different phases that make up the composite. If refractive index is the reason for the improved light transmission, the resin matrix refractive index has to be closer to the filler refractive index.

Filler dispersion was tested by taking SEM images of the samples (Figure 7.9). Although not very clear, the images do not seem to indicate any difference in dispersion of the 0.7 μm

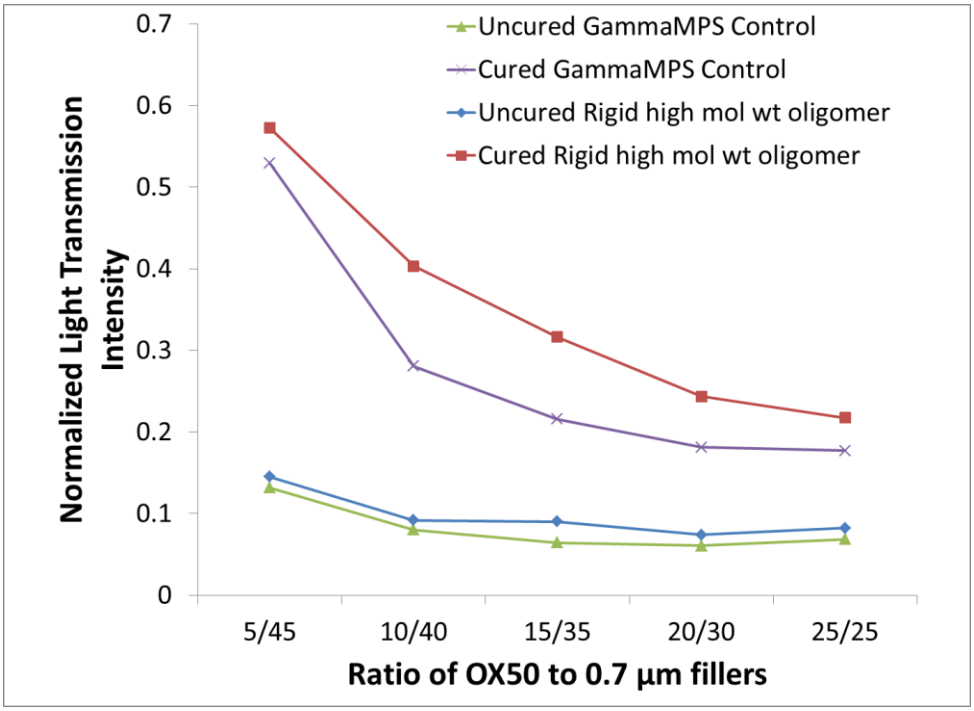

Figure 7.8. Comparison of light transmission through samples with different filler ratios and surface treatments. The light source was an infrared beam from the FT-IR with a wavelength of 760 nm.

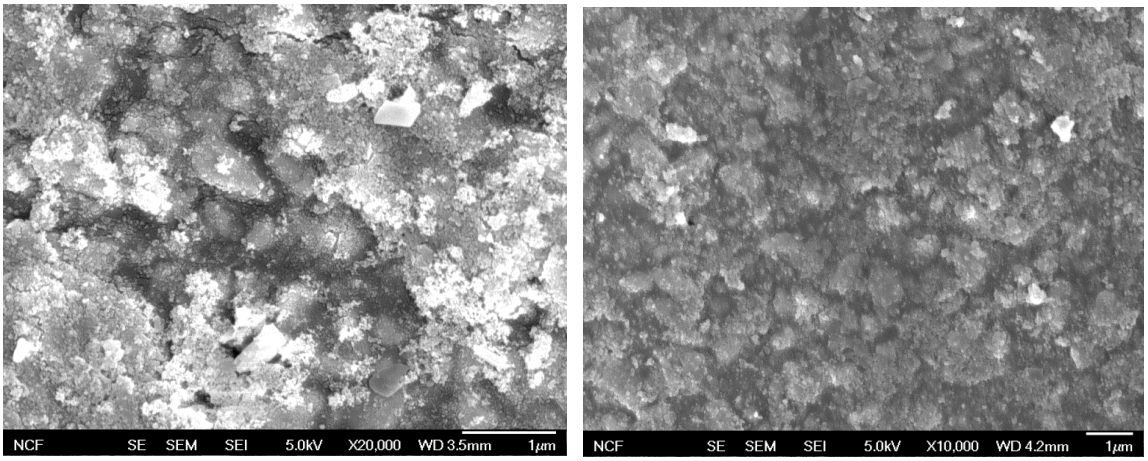

(a) (b)

Figure 7.9. SEM images of polished surfaces of composites with 10/40 ratio of OX50/0.7 µm fillers surface treated with (a) γ-MPS and (b) Experimental oligomer.

fillers. The OX50 particles cannot be seen clearly so no comment can be made about their dispersion in the matrix.

Figure 7.10 shows the variation of the refractive index of cured composite samples with varying amounts of OX50 and Figure 7.11 shows the variation of refractive index for the cured composites with 0.7 μm barium glass filler, for both types of filler surface treatment. It can be seen that for the OX50 system, in case of the γ-MPS treated particles, there is a steady decrease in the refractive index going from 10 wt% to 30 wt%. In case of the oligomer system, the refractive index at 10 wt% and 20 wt% is equivalent to that of its γ-MPS counterpart. At 30 wt%, however, there is no further decrease and the refractive index is at the same level as 20 wt%. For the 0.7 μm particles, the refractive index stays fairly constant with loading and there is no significant difference in its value between the different loading levels. It should be pointed out that the refractive index of the cured unfilled resin is 1.5495 at a conversion of 65 % [15].

Figure 7.12 shows the variation of refractive index for cured composite samples that had mixed fillers. As the relative amount of OX50 increased, the refractive index of all the samples decreased steadily. The decrease for the γ-MPS-based system was more rapid than the brush-treated system. The reduction in transmission due to an increase in the relative amount of OX50 particles follows from the observations in Figures 7.10 and 7.11, where intensity again decreased as OX50 particle concentration in the composite increased.

Transmission loss due to light scattering by small particles can be depicted by the Rayleigh approximation –

$$T = \frac{I}{I_o} = exp\left\{-\frac{32\pi^4\varphi_p x r^3 n_m^4}{\lambda^4}\left[\frac{(n_p/n_m)^2 - 1}{(n_p/n_m)^2 + 2}\right]^2\right\} \quad [7.1]$$

Where, T = transmission loss, I and I_o are the intensities of transmitted and incident light respectively, φ_p is the particle volume fraction, x is the optical path length, r is the radius of the particles, n_p and n_m are the refractive indices of the particles and polymer matrix respectively and λ is the incident wavelength. From this equation it is clear that to minimize transmission losses, for a given incident wavelength, there are a few parameters that can be experimentally adjusted. Particle size and volume fraction, path length and refractive indices of the particle and matrix are the parameters that can be changed. In our system, the path length is the same for all the samples. Particle size for OX50 is the same in both the systems, for a given ratio. Hence for the same volume fraction of particles and geometry, the main parameters that can be controlled are the refractive indices of particles and the polymer matrix. A smaller the refractive index difference between the particles and polymer matrix results in less of a transmission loss. The refractive index of the particle is an intrinsic constant and cannot be changed. Hence it is the refractive index of the polymer matrix that has to be controlled. Howard *et al*. [15] have shown that the refractive index of the resin system that has been used in this study increases as the conversion increases and reaches close to the refractive index of the 0.7 μm barium glass filler particles. It follows that in order for the experimental brush-modified filler system to exhibit higher transmission, the refractive index of the polymer matrix and consequently, the monomer conversion must be higher than that of the γ-MPS-based system. The bulk conversion was monitored in these systems and there is no significant difference in its value in between the different systems.

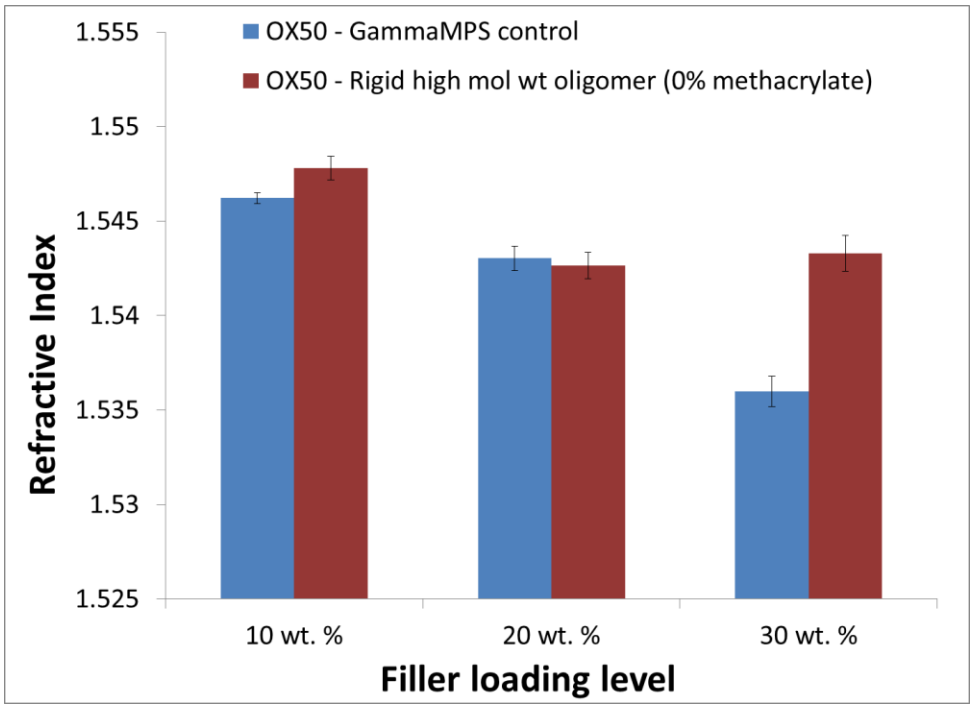

Figure 7.10. Refractive indices of cured samples with varying OX50 particle loading and filler surface treatment.

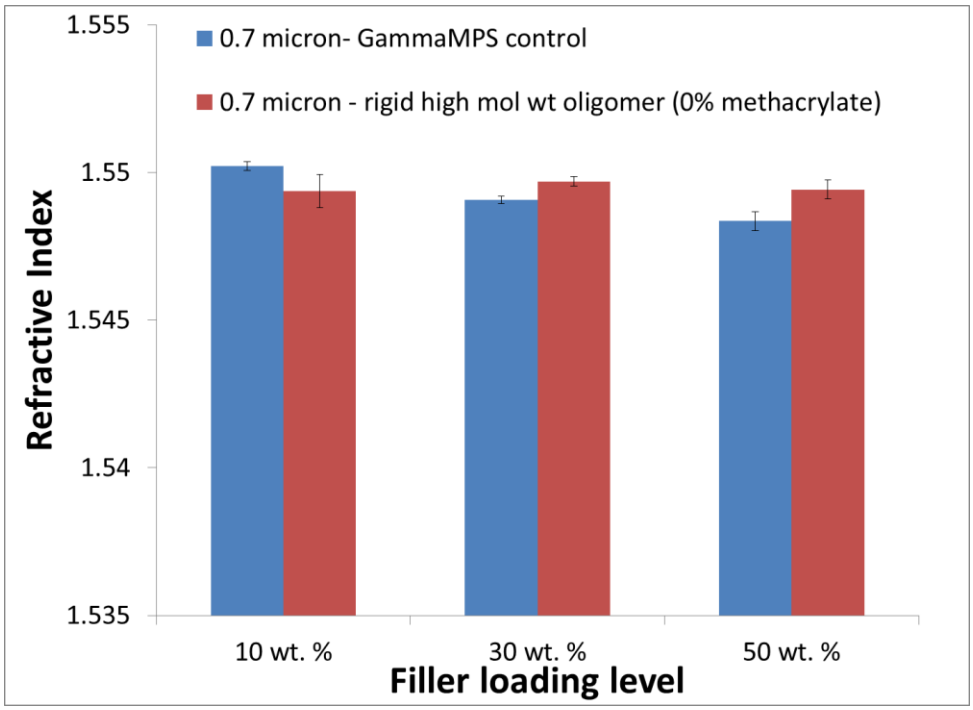

Figure 7.11. Refractive indices of cured samples with varying 0.7 µm particle loading and filler surface treatment.

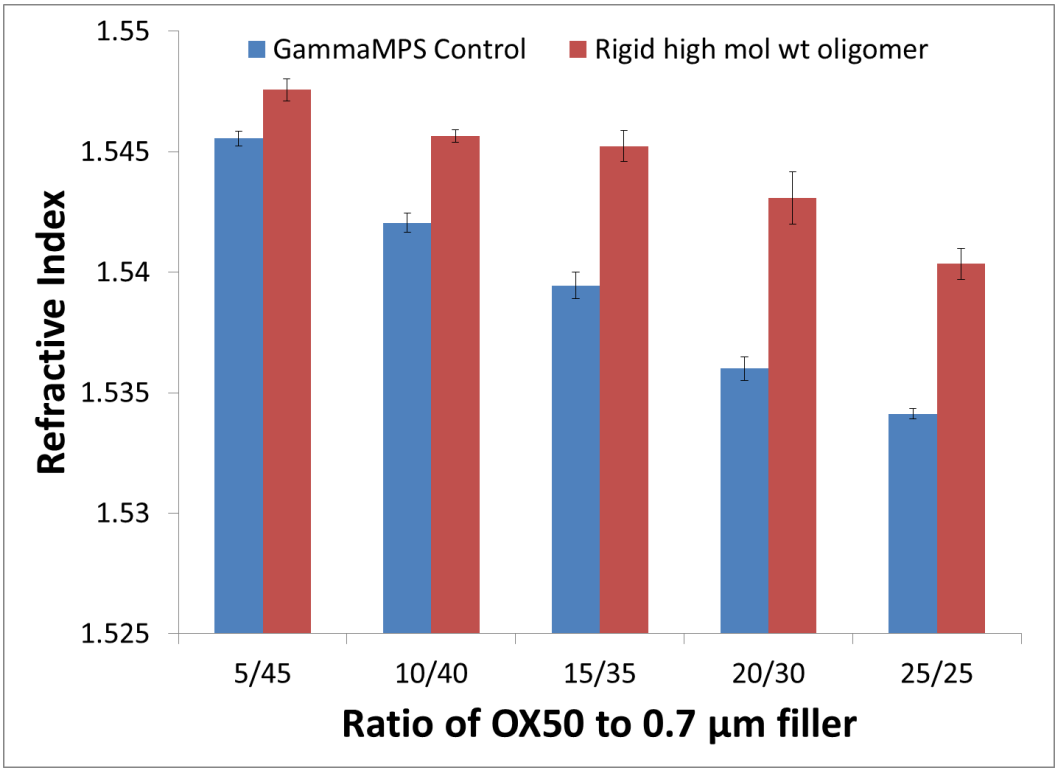

Figure 7.12. Refractive index variation in cured composites with different filler ratios and filler surface treatments

There are two possible explanations of this dichotomy that lies at the interface between the filler particles and the polymer matrix. The oligomer is made up of aromatic groups that can give high refractive index to the bulk material [17]. It was shown in Chapter 5 in TEM images that there is a distinct interphase around the filler particles modified with the oligomer. This interphase, made with the aromatic oligomer, could possibly have a high refractive index. The resin, with BisGMA as one of its components, also has a high refractive index. The surface of the fillers has a low density of the oligomer. This should allow the high refractive resin to infiltrate into the oligomer layer. This may lead to a gradual gradient of refractive index around the filler. One the other hand, the interface due to the γ-MPS molecules can create a sharp gradient due to the mismatch in refractive index with the resin matrix. It has been reported that the γ-MPS layer around particles actually consists of multiple layers of γ-MPS molecules [18] and this may lead

to an even more abrupt gradient in refractive index. This maximizes the scattering potential, which should be less in the composites with the oligomer-treated fillers. The enhanced scattering could result in the loss of light transmission that is observed in the γ-MPS-based composites.

A second explanation is as follows. It was discussed in Chapter 5 that the interface created due to the brush treatment on the fillers places less restriction on the polymerizing monomer around it than that around the γ-MPS-treated fillers. It is known that double bond conversion is hampered if restrictions are placed on its mobility during cure [19]. The enhanced mobility of the monomers due to the reduced restrictions can potentially cause an effective delay in gelation and may also result in a higher limiting conversion. However, since the overall bulk conversion of the sample is not significantly different across the samples, it can be inferred that any difference is small and is due to the conversion difference at the interface. There is suggestive evidence that there is a gradient of properties in the interphase region around particles in nanocomposites due to confinement effects that affect the mobility of the polymer around filler particles [20–22]. The length and slope of the gradient would depend on the interaction between the interface and the polymer. If, as in the case of the γ-MPS-treated fillers, there is an unfavorable interaction between the particles and the polymer in terms of restricting the mobility of the growing polymer, the gradient can be large. If, however, there is less restriction on the developing polymer and the polymers near the particle surface are allowed to reach the same conversion as the bulk polymer, the gradient would be shortened. This would be the case of the brush-treated filler-based composite systems. If the gradient is shortened, there would be more total polymer at a higher conversion in the experimental composites as compared to the γ-MPS-based ones. This would narrow down the gap between the refractive index of the polymer and

the 0.7 μm filler particles. This explains the improved light transmission in the experimental composites.

It is noteworthy that the interphase effect due to the brush-modified nanoparticles helps in pushing up the refractive index of the polymer closer to that of the 0.7 μm particles. This is a very interesting relationship at play in these clinically relevant bimodal composites. If the filler nanoparticles are present without the near micron-sized particles, the refractive index mismatch would increase due to the low refractive index of the nanoparticles. This leads to reduced light transmission. If the micro particles alone were present as the filler, this leads to good transmission with little effect of the surface treatment, as seen in Figure 7.11. But the formulation of current dental composites demands the inclusion of nanoparticle to have better wear properties, higher filler loading and improved aesthetics [7]. Hence to have the best composites, both sizes of particles are necessary but the optical properties are enhanced quite substantially by the introduction of the oligomeric surface modification of the nano-sized filler.

7.4 Conclusion

Modern dental composites are multicomponent mixtures consisting of filler particles with a distributed range of sizes. Low shrinkage stress is necessary for long term durability whereas optical clarity is necessary for increased depth of cure and also for the ability to manipulate color characteristics. The mixed mode filler particles that have large differences in sizes and refractive indices make it difficult to achieve optimal properties. Tailoring of the interface is one way of improving these properties. The modification of the interface done in this chapter gave composites with not only reduced shrinkage stress but also better optical clarity. This has

significant implications as one single surface treatment led to the improvement of multiple properties of the composite.

7.5 Acknowledgements

The authors would like to thank the National Institutes of Health for support of this research through the grant NIH/NIDCR- R01DE014227. We also wish to thank Septodont-Confi-Dental and Evonik for their gracious donation of filler materials and Esstech, Inc. for donation of monomers.

7.6 References

[1] R. L. Sakaguchi and John M Powers, *Craig's Dental Restorative Mateirals*, 13th ed. Elsevier, 2012.

[2] K. J. Anusavice, *Phillips' Science of Dental Materials*, 11th ed. Elsevier, 2003.

[3] R. L. Bowen and W. A. Marjenhoff, "Dental Composites/Glass Ionomers: the Materials," *Advances in Dental Research*, vol. 6, pp. 44–49, 1992.

[4] N. Moszner and U. Salz, "Recent Developments of New Components for Dental Adhesives and Composites," *Macromolecular Materials and Engineering*, vol. 292, no. 3, pp. 245–271, Mar. 2007.

[5] J. L. Ferracane, "Resin composite-state of the art.," *Dental Materials*, vol. 27, no. 1, pp. 29–38, Jan. 2011.

[6] S. Klapdohr and N. Moszner, "New Inorganic Components for Dental Filling Composites," *Monatshefte fur Chemie*, vol. 136, no. 1, pp. 21–45, Dec. 2005.

[7] S. Mitra, D. Wu, and B. Holmes, "An application of nanotechnology in advanced dental materials," *Journal of the American Dental Association*, vol. 134, pp. 1382–1390, 2003.

[8] N. Emami, M. Sjödahl, and K.-J. M. Söderholm, "How filler properties, filler fraction, sample thickness and light source affect light attenuation in particulate filled resin composites," *Dental Materials*, vol. 21, no. 8, pp. 721–30, Aug. 2005.

[9] E. Bugnicourt, J. Galy, J.-F. Gérard, and H. Barthel, "Effect of sub-micron silica fillers on the mechanical performances of epoxy-based composites," *Polymer*, vol. 48, no. 6, pp. 1596–1605, Mar. 2007.

[10] S. Garoushi, L. V. J. Lassila, and P. K. Vallittu, "Influence of nanometer scale particulate fillers on some properties of microfilled composite resin.," *Journal of Materials Science. Materials in Medicine*, vol. 22, no. 7, pp. 1645–1651, Jul. 2011.

[11] P. Rittigstein and J. M. Torkelson, "Polymer – Nanoparticle Interfacial Interactions in Polymer Nanocomposites : Confinement Effects on Glass Transition Temperature and Suppression of Physical Aging," *Polymer*, pp. 2935–2943, 2006.

[12] J. R. Condon and J. L. Ferracane, "Reduction of composite contraction stress through non-bonded microfiller particles.," *Dental Materials*, vol. 14, no. 4, pp. 256–60, Jul. 1998.

[13] H. Lu, J. W. Stansbury, S. H. Dickens, F. C. Eichmiller, and C. N. Bowman, "Probing the origins and control of shrinkage stress in dental resin-composites: I. Shrinkage stress characterization technique.," *Journal of Materials Science. Materials in Medicine*, vol. 15, no. 10, pp. 1097–103, Oct. 2004.

[14] L. White and C. Tripp, “Reaction of (3-Aminopropyl)dimethylethoxysilane with Amine Catalysts on Silica Surfaces,” *Journal of Colloid and Interface Science*, vol. 232, no. 2, pp. 400–407, Dec. 2000.

[15] B. Howard, N. D. Wilson, S. M. Newman, C. S. Pfeifer, and J. W. Stansbury, “Relationships between conversion, temperature and optical properties during composite photopolymerization.,” *Acta Biomaterialia*, vol. 6, no. 6, pp. 2053–9, Jun. 2010.

[16] S. Zhou, L. Wu, M. Xiong, Q. He, and G. Chen, “Dispersion and UV-VIS Properties of Nanoparticles in Coatings,” *Journal of Dispersion Science and Technology*, vol. 25, no. 4, pp. 417–433, Jan. 2005.

[17] R. Seto, T. Kojima, K. Hosokawa, Y. Koyama, G. Kohnishi, and T. Takata, “Synthesis and property of 9,9′-spirobifluorene-containing aromatic polyesters as optical polymers with high refractive index and low birefringence,” *Polymer*, vol. 51, pp. 4744–4749, 2010.

[18] R. H. Halvorson, R. L. Erickson, and C. L. Davidson, “The effect of filler and silane content on conversion of resin-based composite.,” *Dental Materials*, vol. 19, no. 4, pp. 327–33, Jun. 2003.

[19] C. S. Pfeifer, N. D. Wilson, Z. R. Shelton, and J. W. Stansbury, “Delayed gelation through chain-transfer reactions: Mechanism for stress reduction In methacrylate networks,” *Polymer*, vol. 52, no. 15, pp. 3295–3303, Jul. 2011.

[20] A. Bansal, H. Yang, C. Li, K. Cho, B. C. Benicewicz, S. K. Kumar, and L. S. Schadler, “Quantitative equivalence between polymer nanocomposites and thin polymer films.,” *Nature Materials*, vol. 4, no. 9, pp. 693–8, Sep. 2005.

[21] P. Rittigstein, R. D. Priestley, L. J. Broadbelt, and J. M. Torkelson, “Model polymer nanocomposites provide an understanding of confinement effects in real nanocomposites.,” *Nature materials*, vol. 6, no. 4, pp. 278–82, Apr. 2007.

[22] R. Qiao and L. Catherine Brinson, “Simulation of interphase percolation and gradients in polymer nanocomposites,” *Composites Science and Technology*, vol. 69, no. 3–4, pp. 491–499, Mar. 2009.

CHAPTER 8

CONCLUSION AND RECOMMENDATIONS

Dental composite materials are now widely accepted and used due to their aesthetic qualities, ease of use, less cavity preparation than the erstwhile amalgam-based restoratives and also less environmental risks than the amalgams. With almost half a century of use, these materials have come a long way in terms of improvement of mechanical properties and clinical performance. However, there are still concerns regarding the long-term durability of these composites, mainly due to the problems of volumetric shrinkage and the associated shrinkage stress. Shrinkage is inevitable with the polymeric nature of the composites and a majority of the current research focuses on developing new monomer systems with lower shrinkage. Less focus is given to utilizing the other two components of the composites – the fillers and the interface between the resin and the fillers – as a tool to reduce shrinkage stress. There are reports in literature, however, showing that low shrinkage does not necessarily lead to lower stress. This necessitates a detailed examination of the factors that determine shrinkage stress development in photocured composite materials. This thesis explores this question by focusing on the filler phase of model dental composites.

Firstly, we have explored the relationship of shrinkage stress with shrinkage and modulus by varying filler content and double bond conversion. Studies looking at variation of shrinkage stress mostly focus on one or two of the above parameters. Double bond conversion is also rarely reported for such studies. As a monomer system is transformed into a highly crosslinked, vitrified polymer, there is a drastic change in material properties. The material is different at each point in its conversion profile, hence it is important to always report the conversion, to have a

legitimate basis of comparison of different materials. We have sought to bring the different parameters that affect shrinkage stress to create a clearer picture of the factors affecting its development. We found that shrinkage, modulus and stress all increase with respect to conversion. The amount and type of filler determines the magnitudes of the properties and alters the conversion dependence of the polymer property evolution in composites. While shrinkage increases almost linearly through most of the range of conversion, modulus and stress increased only gradually in the initial stages, followed by a precipitous rise as the limiting conversion value was approached. For higher filler loadings, when the volume fraction of the resin is less, the stress apparently did not increase in proportion to the modulus. At this stage, the shrinkage, although increasing slowly, seemed to be affecting the stress more than the modulus. The issue of whether shrinkage or modulus affect the stress more was resolved by considering the actual increased strain on the polymer that is present at a reduced volume fraction, rather than the strain on the entire composite. Taking this "real" strain into account reveals that the stress is indeed proportional to both modulus and shrinkage.

With this picture in mind, a novel way to alleviate the shrinkage stress was devised. This involved functionalizing the surface of the fillers with polymer brushes. The idea was that by tailoring the polymers or oligomers that were attached to the surface, a compliant interface could be designed. The compliance of the interface would locally help relieve the strain on the polymer phase, thereby reducing the stress. To test this hypothesis, commercial oligomers with three different molecular weights were taken and modified to have two different levels of methacrylate groups on their chains. It was found that, in general, the longer the length of the oligomer, the lower was the shrinkage stress, compared to the conventional silane (γ-MPS)-treated control. Also a higher number of methacrylate groups resulted in higher stress, for the same molecular

weight of the oligomer. This was encouraging and we went ahead with designing oligomers that could be varied in structure even more than the commercial oligomers. This would help in determining more parameters that affect stress development.

With this aim, two series of oligomers were synthesized. One series was made from monomers that had a more rigid backbone, while the other had a more flexible backbone. Each series had oligomers with three different molecular weights, to cover a wide range of oligomer lengths. Furthermore, each oligomer was modified to contain either no methacrylate groups or a high number of methacrylate groups on its backbone. In this manner, eighteen different oligomers were made, creating a wide range of properties. Composites made with fillers functionalized with these oligomers were tested for shrinkage stress development. It was observed that, similar to the commercial oligomers study, the addition of reactive groups to the oligomers resulted in an increase in shrinkage stress. An increase in the length of the oligomer also affected the shrinkage stress, but to a lesser extent. There was a tendency for the shrinkage stress to reduce with increase in oligomer length. There was no significant trend in the effect of the flexibility of the oligomer on shrinkage stress. A possible reason for this is that the “rigid” oligomers that were made not rigid enough to show a perceptible difference in properties.

This study showed the importance of the interface in affecting stress development. It was postulated that the filler surface played a significant role in the development of a network in the composite. The oligomer treatment hampered the formation of the network, slowing the speed at which the network was formed. Increase in reactive groups on the surface hastened the network development. An important lesson from this was the need to optimize surface reactive group concentration in composites. In commercial composites, fillers are overwhelmingly treated with reactive groups, with the idea that this will provide a strong link between the filler and polymer

phases. From our work, it can be inferred that this is not the best solution if stress is a major problem in the application.

In addition, an interesting aspect of interface dynamics was observed. By staining the interface with ruthenium tetroxide, it was possible to view it on the filler surface, before and after polymerization. It was observed that in the composite that had the least shrinkage stress, the interface seemed to expand. This was in accordance with the hypothesis that interface compliance might play a role in the development of stress.

The interface modification played an important role in changing optical properties of the composites. When fillers of different sizes were mixed together, it was found that fillers treated with the experimental oligomer had better light transmission than those with the conventional γ-MPS treatment. Nanometer-sized fillers were found to affect the light transmission to a large extent, most likely due to their large surface area which affected the dynamics of the polymer layer around them. This has important implications for depth of cure in composites. Enhanced light transmission would allow light to penetrate deeper into the composite, increasing the degree of cure at larger depths.

Stress relaxation forms an important component of stress development. But it is difficult to quantify during real-time cure. Standard stress relaxation experiments were carried out in partially cured samples, to estimate the potential for stress relaxation over the conversion range representing uncured monomer to the fully cured composite. Data from experiments was fitted to a two component Maxwell model. Here it was found that the experimental oligomers had a faster relaxation time and more stress recovery as compared to the γ-MPS-based composites, over the

range of conversion tested. This was attributed to the compliance of the interfacial layer created by the oligomers.

Overall, the surface modification technique using oligomers helped alleviate stress and also improve optical properties in dental composites. This has implications for the general area of composite materials, and should not be limited to the dental field. Shrinkage and shrinkage stress are a problem in other areas of polymer application as well, like coatings, adhesives and optical storage devices. Our method can be used in all these fields to alleviate the problem of stress.

This thesis also brings up new avenues for further research. From the effects of the interphase, it is obvious that the properties of the interface region have a significant effect on material properties. It would be interesting to probe the properties of this interface. The interface or interphase region is estimated to be of the order of nanometers, making it challenging to measure its properties. However, using mechanical and thermal nanoindentation with AFM, nanoscale properties can be measured accurately. Using thermal AFM tips, the glass transition region around the particles can be probed. High stiffness AFM tips can be used to probe the modulus around the particles. Combining these, we can get a very good picture of the properties of the interphase. This is, however, very challenging and that is what makes it more interesting to study.

Another interesting area to study would be how a substrate affects the bulk glass transition temperature in thin films. It has been seen that the glass transition temperature very near the substrate in thin films can be different than the bulk glass transition temperature. It can be inferred that the surface treatment of the substrate would also affect this phenomenon. An

interesting study would be to see how far from the substrate do surfaces treated with polymer brushes affect the glass transition. Varying the properties of the brush should vary the distance from the substrate where the properties of the thin film match those of the bulk.

The brush treatment in this thesis was done using a “grafting-to” approach. This results in a low density of brushes on the surface, which may in part account for the excellent success of the approach demonstrated here. To better control the surface grafting density without altering the range of the brush molecular weight, a “grafting-from” approach can be used, where brushes can be made by surface initiation from sites on the particles. This alternative would likely also need to include a strategy to control the concentration of the surface initiation sites. This would lead to more control of the brush density and length. It would be interesting to study the use of fillers made with this method on shrinkage stress development and possibly in combination with resin compositions designed as low shrinkage/low stress alternatives to the traditional dimethacrylate resins used here.

BIBILIOGRAPHY

Akcora, P., Kumar, S. K., García Sakai, V., Li, Y., Benicewicz, B. C., & Schadler, L. S. (2010). Segmental Dynamics in PMMA-Grafted Nanoparticle Composites. *Macromolecules*, *43*, 8275–8281. doi:10.1021/ma101240j

Altmann, N., & Halley, P. J. (2003). The effects of fillers on the chemorheology of highly filled epoxy resins : I . Effects on cure transitions and kinetics. *Polymer International*, *119*(May 2002), 113–119. doi:10.1002/pi.1058

Amirouche-Korichi, A., Mouzali, M., & Watts, D. C. (2009). Effects of monomer ratios and highly radiopaque fillers on degree of conversion and shrinkage-strain of dental resin composites. *Dental Materials*, *25*(11), 1411–8. doi:10.1016/j.dental.2009.06.009

Andruzzi, L., Hexemer, A., Li, X., Ober, C. K., Kramer, E. J., Galli, G., Chiellini, E., et al. (2004). Control of surface properties using fluorinated polymer brushes produced by surface-initiated controlled radical polymerization. *Langmuir*, *20*(24), 10498–506. doi:10.1021/la049264f

Antonucci, J. M., Dickens, S. H., & Fowler, B. O. (2005). Chemistry of Silanes : Interfaces in Dental Polymers and Composites. *Journal Of Research Of The National Institute Of Standards And Technology*, *110*(5), 541–558.

Anusavice, K. J. (2003). *Phillips' Science of Dental Materials* (11th ed.). Elsevier.

Arikawa, H., Kanie, T., Fujii, K., Takahashi, H., & Ban, S. (2007). Effect of filler properties in composite resins on light transmittance characteristics and color. *Dental Materials Journal*, *26*(1), 38–44. Retrieved from http://www.ncbi.nlm.nih.gov/pubmed/17410891

Arimoto, A., Nakajima, M., Hosaka, K., Nishimura, K., Ikeda, M., Foxton, R. M., & Tagami, J. (2010). Translucency, opalescence and light transmission characteristics of light-cured resin composites. *Dental Materials*, *26*(11), 1090–7. doi:10.1016/j.dental.2010.07.009

Atai, M., & Watts, D. C. (2006). A new kinetic model for the photopolymerization shrinkage-strain of dental composites and resin-monomers. *Dental Materials*, *22*(8), 785–91. doi:10.1016/j.dental.2006.02.009

Ausiello, P., Apicella, A., & Davidson, C. L. (2002). Effect of adhesive layer properties on stress distribution in composite restorations - a 3D finite element analysis. *Dental Materials*, *18*, 295–303.

Bansal, A., Yang, H., Li, C., Benicewicz, B. C., Kumar, S. K., & Schadler, L. S. (2006). Controlling the Thermomechanical Properties of Polymer Nanocomposites by Tailoring the Polymer – Particle Interface. *Polymer*, 2944–2950. doi:10.1002/polb

Bansal, A., Yang, H., Li, C., Cho, K., Benicewicz, B. C., Kumar, S. K., & Schadler, L. S. (2005). Quantitative equivalence between polymer nanocomposites and thin polymer films. *Nature Materials*, *4*(9), 693–8. doi:10.1038/nmat1447

Baroudi, K., Saleh, A. M., Silikas, N., & Watts, D. C. (2007). Shrinkage behaviour of flowable resin-composites related to conversion and filler-fraction. *Journal of Dentistry*, *35*(8), 651–5. doi:10.1016/j.jdent.2007.05.001

Beatty, M. W., Swartz, M. L., Moore, B. K., Phillips, R. W., & Roberts, T. a. (1998). Effect of microfiller fraction and silane treatment on resin composite properties. *Journal of biomedical materials research*, *40*(1), 12–23. Retrieved from http://www.ncbi.nlm.nih.gov/pubmed/9511094

Boaro, L. C. C., Gonçalves, F., Guimarães, T. C., Ferracane, J. L., Versluis, A., & Braga, R. R. (2010). Polymerization stress, shrinkage and elastic modulus of current low-shrinkage restorative composites. *Dental Materials*, *26*(12), 1144–50. doi:10.1016/j.dental.2010.08.003

Bonilla, E. D., Yashar, M., & Caputo, A. A. (2003). Fracture toughness of nine flowable resin composites. *The Journal of Prosthetic Dentistry*, *89*(3), 261–7. doi:10.1067/mpr.2003.33

Bowen, R L. (1956). Use of Epoxy Resins in Restorative Materials. *Journal of Dental Research*, *35*, 360–369. doi:10.1177/00220345560350030501

Bowen, R. (1965). Method of preparing a monomer having phenoxy and methacrylate groups linked by hydroxy glyceryl groups. *US Patent 3,179,623*. Retrieved from http://www.google.com/patents?hl=en&lr=&vid=USPAT3179623&id=3ploAAAAEBAJ&oi=fnd&dq=Method+of+preparing+a+monomer+having+phenoxy+and+methacrylate+groups+linked+by+hydroxy+glyceral+groups&printsec=abstract

Bowen, Rafael L, & Marjenhoff, W. A. (1992). Dental Composites/Glass Ionomers: the Materials. *Advances in Dental Research*, *6*, 44–49. doi:10.1177/08959374920060011601

Bowman, C. N., Cramer, N. B., & Sansbury, J. W. (2010). Recent Advances and Developments in Composite Dental Restorative Materials. *Journal of Dental Research*, *90*(4), 402–416. doi:10.1177/0022034510381263

Braem, M., Doren, V. E., Lambrechts, P., & Vanherle, G. (1987). Determination of Young's modulus of dental composites: A phenomenological model. *Journal of Materials Science*, *22*(6), 2037–2042. doi:10.1007/BF01132936

Braem, M., Finger, W., Vandoren, V., Lambrechts, P., & Vanherle, G. (1989). Mechanical properties and filler fraction of dental composites. *Dental Materials*, *5*(5), 346–349. doi:10.1016/0109-5641(89)90128-0

Brochard-Wyart, F., De Gennes, P. G., Leger, L., Marciano, Y., & Raphael, E. (1994). Adhesion promoters. *Journal of Physical Chemistry*, *98*(38), 9405–9410. doi:10.1021/j100089a009

Bréchet, Y., Cavaillé, J.-Y., Chabert, E., Chazeau, L., Dendievel, R., Flandin, L., & Gauthier, C. (2001). Polymer Based Nanocomposites: Effect of Filler-Filler and Filler-Matrix Interactions. *Advanced Engineering Materials*, *3*(8), 571. doi:10.1002/1527-2648(200108)3:8<571::AID-ADEM571>3.0.CO;2-M

Bugnicourt, E., Galy, J., Gérard, J.-F., & Barthel, H. (2007). Effect of sub-micron silica fillers on the mechanical performances of epoxy-based composites. *Polymer*, *48*(6), 1596–1605. doi:10.1016/j.polymer.2007.01.053

Cadenaro M, Codan B, Navarra CO, Marchesi G, Turco G, Di Lenarda R, B. L. (2011). Contraction stress, elastic modulus, and degree of conversion of three flowable composites. *European journal of Oral Sciences*, *119*, 241–245. doi:10.1111/j.1600-0722.2011.00820.x

Calheiros, F. C., Braga, R. R., Kawano, Y., & Ballester, R. Y. (2004a). Relationship between contraction stress and degree of conversion in restorative composites. *Dental Materials*, *20*(10), 939–46. doi:10.1016/j.dental.2004.03.003

Calheiros, F. C., Braga, R. R., Kawano, Y., & Ballester, R. Y. (2004b). Relationship between contraction stress and degree of conversion in restorative composites. *Dental Materials*, *20*(10), 939–46. doi:10.1016/j.dental.2004.03.003

Carioscia, J. A., Lu, H., Stanbury, J. W., & Bowman, C. N. (2005). Thiol-ene oligomers as dental restorative materials. *Dental Materials*, *21*(12), 1137–43. doi:10.1016/j.dental.2005.04.002

Cavalcanti, J., Queiroz, G., Monteiro, D. M., Antonio, M., & Resende, J. (2010). Polymerization Shrinkage and Flexural Modulus of Flowable Dental Composites. *Materials Research*, *13*(3), 381–384.

Chaijareenont, P., Takahashi, H., Nishiyama, N., & Arksornnukit, M. (2012). Effect of different amounts of 3-methacryloxypropyltrimethoxysilane on the flexural properties and wear resistance of alumina reinforced PMMA. *Dental Materials Journal*, *31*(4), 623–628. doi:10.4012/dmj.2012-056

Chambon, F., & Winter, H. H. (1987). Linear viscoelasticity at the gel point of a crosslinking PDMS with imbalanced stoichiometry. *Journal of Rheology*, *31*(8), 683–697. Retrieved from http://rheology.tripod.com/z04.08.pdf

Chen, L., Zheng, K., Tian, X., Hu, K., Wang, R., Liu, C., Li, Y., et al. (2010). Double Glass Transitions and Interfacial Immobilized Layer in in-Situ-Synthesized Poly(vinyl alcohol)/Silica Nanocomposites. *Macromolecules*, *43*(2), 1076–1082. doi:10.1021/ma901267s

Chen, Q., Chasiotis, I., Chen, C., & Roy, a. (2008). Nanoscale and effective mechanical behavior and fracture of silica nanocomposites. *Composites Science and Technology*, *68*(15-16), 3137–3144. doi:10.1016/j.compscitech.2008.07.013

Chiou, B.-S., Raghavan, S. R., & Khan, S. a. (2001). Effect of Colloidal Fillers on the Cross-Linking of a UV-Curable Polymer: Gel Point Rheology and the Winter−Chambon Criterion. *Macromolecules*, *34*(13), 4526–4533. doi:10.1021/ma010281a

Choi, K. M., & Stansbury, J. W. (1996). New Families of Photocurable Oligomeric Fluoromonomers for Use in Dental Composites. *Chemistry of Materials*, *4756*(20), 2704–2707.

Chung, C. M., Kim, M. S., Kim, J. G., & Jang, D. O. (2002). Synthesis and photopolymerization of trifunctional methacrylates and their application as dental monomers. *Journal of Biomedical Materials Research*, *62*(4), 622–7. doi:10.1002/jbm.10359

Condon, J R, & Ferracane, J. L. (1998). Reduction of composite contraction stress through non-bonded microfiller particles. *Dental Materials*, *14*(4), 256–60. Retrieved from http://www.ncbi.nlm.nih.gov/pubmed/10379253

Condon, John R, & Ferracane, J. L. (2000). Assessing the effect of composite formulation on polymerization stress. *Journal of the American Dental Association*, *131*, 497–503. Retrieved from http://www.jada-plus.com/content/131/4/497.short

Condon, John R, & Ferracane, J. L. (2002a). Reduced polymerization stress through non-bonded nanofiller particles. *Biomaterials*, *23*(18), 3807–15. Retrieved from http://www.ncbi.nlm.nih.gov/pubmed/12164184

Condon, John R, & Ferracane, J. L. (2002b). Reduced polymerization stress through non-bonded nanofiller particles. *Biomaterials*, *23*(18), 3807–15. Retrieved from http://www.ncbi.nlm.nih.gov/pubmed/12164184

Craig, R. G., & Dootz, E. R. (1996). Effect of mixed silanes on the hydrolytic stability of composites. *Journal of Oral Rehabilitation*, *23*(11), 751–6. Retrieved from http://www.ncbi.nlm.nih.gov/pubmed/8953479

Cramer, N. B., Couch, C. L., Schreck, K. M., Carioscia, J. a, Boulden, J. E., Stansbury, J. W., & Bowman, C. N. (2010). Investigation of thiol-ene and thiol-ene-methacrylate based resins as dental restorative materials. *Dental Materials*, *26*(1), 21–8. doi:10.1016/j.dental.2009.08.004

Davidson, C. L., & De Gee, a J. (1984a). Relaxation of polymerization contraction stresses by flow in dental composites. *Journal of Dental Research*, *63*(2), 146–148. Retrieved from http://www.ncbi.nlm.nih.gov/pubmed/6229557

Davidson, C. L., & De Gee, a J. (1984b). Relaxation of polymerization contraction stresses by flow in dental composites. *Journal of Dental Research*, *63*(2), 146–8. Retrieved from http://www.ncbi.nlm.nih.gov/pubmed/6229557

Davidson, C. L., De Gee, A. J., & Feilzer, A. (1984). The competition between the composite-dentin bond strength and the polymerization contraction stress. *Journal of Dental Research*, *63*(12), 1396–1399. Retrieved from http://www.ncbi.nlm.nih.gov/pubmed/6239886

Davidson, C. L., & Feilzer, A. J. (1997). Polymerization shrinkage and shrinkage stress in polymer-based restoratives. *Journal of Dentistry*, *25*(6), 435–440.

Debnath, S. (2003). Silane treatment effects on glass/resin interfacial shear strengths. *Dental Materials*, *19*(5), 441–448. doi:10.1016/S0109-5641(02)00089-1

Debnath, S., Ranade, R., Wunder, S. L., McCool, J., Boberick, K., & Baran, G. (2004). Interface effects on mechanical properties of particle-reinforced composites. *Dental Materials*, *20*(7), 677–86. doi:10.1016/j.dental.2003.12.001

Degussa. (n.d.). *Technical Bulletin Fine Particles*.

Demmjen, Z., & Pukanszky, B. (1997). Effect of Surface Coverage of Silane Treated CaCO3, on the Tensile Properties of Polypropylene Composites. *Polymer Chemistry*, *18*(6), 741–747.

Dewaele, M., Truffier-Boutry, D., Devaux, J., & Leloup, G. (2006). Volume contraction in photocured dental resins: the shrinkage-conversion relationship revisited. *Dental Materials*, *22*(4), 359–65. doi:10.1016/j.dental.2005.03.014

Dickens, S. H., Stansbury, J. W., Choi, K. M., & Floyd, C. J. E. (2003). Photopolymerization Kinetics of Methacrylate Dental Resins. *Macromolecules*, *36*(16), 6043–6053. doi:10.1021/ma021675k

Druffel, T., Buazza, O., Lattis, M., Farmer, S., Spencer, M., Mandzy, N., & Grulke, E. a. (2008). The role of nanoparticles in visible transparent composites. In Z. Gaburro, S. Cabrini, & D. Talapin (Eds.), *Nanotechnology Applications in Coatings* (p. 70300F–70309). San Diego, CA. doi:10.1117/12.795273

Edwards, F. S., & Doi, M. (1978). Dynamics of Rod-like Macromolecules in Concentrated Solution. Part 2. *Journal of the Chemical Society, Faraday Transactions 2: Molecular and Chemical Physics*, *74*, 918–932.

Edwards, S. F., & Doi, M. (1978). Dynamics of Rod-like Macromolecules in Concentrated Solution. Part 1. *Journal of the Chemical Society, Faraday Transactions 2: Molecular and Chemical Physics*, *74*, 560–570.

Elliott, J. E., Lovell, L. G., & Bowman, C. N. (2001). Primary cyclization in the polymerization of bis-GMA and TEGDMA: a modeling approach to understanding the cure of dental

resins. *Dental Materials*, *17*(3), 221–229. Retrieved from http://www.ncbi.nlm.nih.gov/pubmed/11257295

Emami, N., Sjödahl, M., & Söderholm, K.-J. M. (2005). How filler properties, filler fraction, sample thickness and light source affect light attenuation in particulate filled resin composites. *Dental Materials*, *21*(8), 721–30. doi:10.1016/j.dental.2005.01.002

Feilzer, a J., De Gee, a J., & Davidson, C. L. (1990). Quantitative determination of stress reduction by flow in composite restorations. *Dental Materials*, *6*(3), 167–71. Retrieved from http://www.ncbi.nlm.nih.gov/pubmed/2086289

Feilzer, A. J., De Gee, A. J., & Davidson, C. L. (1990). Quantitative determination of stress reduction by flow in composite restorations. *Dental Materials*, *6*(3), 167–171.

Feresenbet, E., Raghavan, D., & Holmes, G. a. (2003). The influence of silane coupling agent composition on the surface characterization of fiber and on fiber-matrix interfacial shear strength. *The Journal of Adhesion*, *79*(7), 643–665. doi:10.1080/00218460309580

Ferracane, J L. (1995). Current trends in dental composites. *Critical Reviews in Oral Biology and Medicine*, *6*(4), 302–318. Retrieved from http://www.ncbi.nlm.nih.gov/pubmed/8664421

Ferracane, J L. (2008). Placing Dental Composites—A Stressful Experience. *Operative Dentistry*, *33*(3), 247–257. doi:10.2341/07-BL2

Ferracane, Jack L. (2005). Developing a more complete understanding of stresses produced in dental composites during polymerization. *Dental Materials*, *21*(1), 36–42. doi:10.1016/j.dental.2004.10.004

Ferracane, Jack L. (2011). Resin composite-state of the art. *Dental Materials*, *27*(1), 29–38. doi:10.1016/j.dental.2010.10.020

Ferracane, Jack L. (2010). Resin composite—State of the art. *Dental Materials*, 1–10. doi:10.1016/j.dental.2010.10.020

Floyd, C. J. E., & Dickens, S. H. (2006). Network structure of Bis-GMA- and UDMA-based resin systems. *Dental Materials*, *22*(12), 1143–9. doi:10.1016/j.dental.2005.10.009

Fragiadakis, D., Pissis, P., & Bokobza, L. (2005). Glass transition and molecular dynamics in poly(dimethylsiloxane)/silica nanocomposites. *Polymer*, *46*(16), 6001–6008. doi:10.1016/j.polymer.2005.05.080

Gaines, M. K., Smith, S. D., Samseth, J., Khan, S. A., & Spontak, R. J. (2010). Nanoparticle Network Formation in Nanostructured and Disordered Block Copolymer Matrices. *Nanoscale Research Letters*, *5*(10), 1712–1718. doi:10.1007/s11671-010-9775-y

Garoushi, S., Lassila, L. V. J., & Vallittu, P. K. (2011). Influence of nanometer scale particulate fillers on some properties of microfilled composite resin. *Journal of Materials Science. Materials in Medicine*, *22*(7), 1645–1651. doi:10.1007/s10856-011-4352-1

Garoushi, S., Vallittu, P. K., Watts, D. C., & Lassila, L. V. J. (2007). Effect of nanofiller fractions and temperature on polymerization shrinkage on glass fiber reinforced filling material. *Dental Materials*, *4*, 606–610. doi:10.1016/j.dental.2007.06.020

Ge, J., Trujillo, M., & Stansbury, J. (2005). Synthesis and photopolymerization of low shrinkage methacrylate monomers containing bulky substituent groups. *Dental Materials*, *21*(12), 1163–9. doi:10.1016/j.dental.2005.02.002

Giachetti, L., Scaminaci Russo, D., Bambi, C., & Grandini, R. (2006). A review of polymerization shrinkage stress: current techniques for posterior direct resin restorations. *The Journal of Contemporary Dental Practice*, *7*(4), 79–88. Retrieved from http://www.ncbi.nlm.nih.gov/pubmed/16957794

Giannelis, E. P., Krishnamoorti, R., & Manias, E. (1999). Polymer-Silicate Nanocomposites : Model Systems for Confined Polymers and Polymer Brushes. *Polymer*, *138*.

Gonçalves, F., Pfeifer, C. S., Ferracane, J. L., & Braga, R. R. (2008). Contraction stress determinants in dimethacrylate composites. *Journal of Dental Research*, *87*(4), 367–71. Retrieved from http://www.ncbi.nlm.nih.gov/pubmed/18362321

Guggenberger, R., & Weinmann, W. (2000). Exploring beyond methacrylates. *American Journal of Dentistry*, *13*, 82 – 85.

Gutowski, W. S., Li, S., Filippou, C., Hoobin, P., & Petinakis, S. (2003). Interface/interphase engineering of polymers for adhesion enhancement: Part II. Theoretical and technological aspects of surface-engineered interphase-interface systems for adhesion enhancement. *The Journal of Adhesion*, *79*(5), 483–519. doi:10.1080/00218460309562

Halvorson, R. H., Erickson, R. L., & Davidson, C. L. (2003a). The effect of filler and silane content on conversion of resin-based composite. *Dental Materials*, *19*(4), 327–33. Retrieved from http://www.ncbi.nlm.nih.gov/pubmed/12686298

Halvorson, R. H., Erickson, R. L., & Davidson, C. L. (2003b). The effect of filler and silane content on conversion of resin-based composite. *Dental Materials*, *19*(4), 327–33. Retrieved from http://www.ncbi.nlm.nih.gov/pubmed/12686298

Harada, M., Morimoto, M., & Ochi, M. (2003). Influence of network chain orientation on the mechanical property of epoxy resin filled with silica particles. *Journal of Applied Polymer Science*, *87*(5), 787–794. doi:10.1002/app.11454

Howard, B., Wilson, N. D., Newman, S. M., Pfeifer, C. S., & Stansbury, J. W. (2010). Relationships between conversion, temperature and optical properties during composite photopolymerization. *Acta Biomaterialia*, *6*(6), 2053–9. doi:10.1016/j.actbio.2009.11.006

Ishida, H., & Koenig, J. L. (1978). The Reinforcement Mechanism of Fiber-Glass Reinforced Plastics Under Wet Conditions: A Review. *Polymer Engineering & Science*, *18*(2).

Jandt, K. D., & Sigusch, B. W. (2009). Future perspectives of resin-based dental materials. *Dental Materials*, *25*(8), 1001–6. doi:10.1016/j.dental.2009.02.009

Julthongpiput, D., LeMieux, M., & Tsukruk, V. . (2003). Micromechanical properties of glassy and rubbery polymer brush layers as probed by atomic force microscopy. *Polymer*, *44*(16), 4557–4562. doi:10.1016/S0032-3861(03)00404-X

Kang, S. (2001). Preparation and characterization of epoxy composites filled with functionalized nanosilica particles obtained via sol–gel process. *Polymer*, *42*(3), 879–887. doi:10.1016/S0032-3861(00)00392-X

Klapdohr, S., & Moszner, N. (2005). New Inorganic Components for Dental Filling Composites. *Monatshefte fur Chemie*, *136*(1), 21–45. doi:10.1007/s00706-004-0254-y

Klee, J. E., Neidhart, F., & Mu, R. (1999). Monomers for low shrinking composites , 2 Synthesis of branched methacrylates and their application in dental composites. *Macromolecular Chemistry and Physics*, *523*(3), 517–523.

Kleverlaan, C. J., & Feilzer, A. J. (2005). Polymerization shrinkage and contraction stress of dental resin composites. *Dental Materials*, *21*(12), 1150–7. doi:10.1016/j.dental.2005.02.004

Kloxin, C. J., Scott, T. F., & Bowman, C. N. (2009, April 14). Stress relaxation via addition-fragmentation chain transfer in a thiol-ene photopolymerization. *Macromolecules*. doi:10.1021/ma802771b

Lange, J. (1999). Viscoelastic properties and transitions during thermal and UV cure of a methacrylate resin. *Polymer Engineering*, *5*(9), 1651–1660. doi:10.1002/pen.11559

Lim, B. (2002). Effect of filler fraction and filler surface treatment on wear of microfilled composites. *Dental Materials*, *18*(1), 1–11. doi:10.1016/S0109-5641(00)00103-2

Lin-Gibson, S., Sung, L., Forster, A. M., Hu, H., Cheng, Y., & Lin, N. J. (2009). Effects of filler type and content on mechanical properties of photopolymerizable composites measured across two-dimensional combinatorial arrays. *Acta Biomaterialia*, *5*(6), 2084–94. doi:10.1016/j.actbio.2009.01.043

Lingois, P., & Berglund, L. (2002). Modeling elastic properties and volume change. *Journal of Materials Science*, *37*, 4573 – 4579.

Liu, Q., Ding, J., Chambers, D. E., Debnath, S., Wunder, S. L., & Baran, G. R. (2001). Filler-coupling agent-matrix interactions in silica/polymethylmethacrylate composites. *Journal of Biomedical Materials Research*, *57*(3), 384–93. Retrieved from http://www.ncbi.nlm.nih.gov/pubmed/11523033

Lovell, L. G., Berchtold, K. a., Elliott, J. E., Lu, H., & Bowman, C. N. (2001). Understanding the kinetics and network formation of dimethacrylate dental resins. *Polymers for Advanced Technologies*, *12*(6), 335–345. doi:10.1002/pat.115

Lu, H, Stansbury, J. W., Dickens, S. H., Eichmiller, F. C., & Bowman, C. N. (2004a). Probing the origins and control of shrinkage stress in dental resin-composites: I. Shrinkage stress characterization technique. *Journal of Materials Science: Materials in Medicine*, *15*(10), 1097–103. doi:10.1023/B:JMSM.0000046391.07274.e6

Lu, H, Stansbury, J. W., Dickens, S. H., Eichmiller, F. C., & Bowman, C. N. (2004b). Probing the origins and control of shrinkage stress in dental resin-composites: I. Shrinkage stress characterization technique. *Journal of Materials Science. Materials in Medicine*, *15*(10), 1097–103. doi:10.1023/B:JMSM.0000046391.07274.e6

Lu, Hongbin, & Nutt, S. (2003). Restricted Relaxation in Polymer Nanocomposites near the Glass Transition. *Macromolecules*, *36*(11), 4010–4016. doi:10.1021/ma034049b

Lu, Hui, Stansbury, J. W., & Bowman, C. N. (2004). Towards the elucidation of shrinkage stress development and relaxation in dental composites. *Dental Materials*, *20*(10), 979–86. doi:10.1016/j.dental.2004.05.002

Lu, Hui, Stansbury, J. W., Dickens, S. H., Eichmiller, F. C., & Bowman, C. N. (2004c). Probing the origins and control of shrinkage stress in dental resin composites. II. Novel method of simultaneous measurement of polymerization shrinkage stress and conversion. *Journal of biomedical materials research. Part B, Applied biomaterials*, *71*(1), 206–13. doi:10.1002/jbm.b.30088

Lu, Hui, Stansbury, J. W., Dickens, S. H., Eichmiller, F. C., & Bowman, C. N. (2004d). Probing the origins and control of shrinkage stress in dental resin composites. II. Novel method of simultaneous measurement of polymerization shrinkage stress and conversion. *Journal of biomedical materials research. Part B, Applied biomaterials*, *71*(1), 206–13. doi:10.1002/jbm.b.30088

Luo, J., Seghi, R., & Lannutti, J. (1997). Effect of silane coupling agents on the wear resistance of polymer-nanoporous silica gel dental composites. *Materials Science and Engineering: C*, *5*(1), 15–22. doi:10.1016/S0928-4931(96)00155-5

Masouras, K., Silikas, N., & Watts, D. C. (2008). Correlation of filler content and elastic properties of resin-composites. *Dental Materials*, *24*(7), 932–9. doi:10.1016/j.dental.2007.11.007

Matinlinna, J P, Lassila, L. V. J., & Vallittu, P. K. (2006). Evaluation of five dental silanes on bonding a luting cement onto silica-coated titanium. *Journal of Dentistry*, *34*(9), 721–6. doi:10.1016/j.jdent.2006.01.005

Matinlinna, Jukka P, Lassila, L. V. J., Ozcan, M., Yli-Urpo, A., & Vallittu, P. K. (2004). An introduction to silanes and their clinical applications in dentistry. *The International Journal of Prosthodontics*, *17*(2), 155–64. Retrieved from http://www.ncbi.nlm.nih.gov/pubmed/20037942

Matinlinna, Jukka P, Ozcan, M., Lassila, L. V. J., & Vallittu, P. K. (2004). The effect of a 3-methacryloxypropyltrimethoxysilane and vinyltriisopropoxysilane blend and tris(3-trimethoxysilylpropyl)isocyanurate on the shear bond strength of composite resin to titanium metal. *Dental Materials*, *20*(9), 804–13. doi:10.1016/j.dental.2003.10.009

Meera, A. P., Said, S., Grohens, Y., Luyt, A. S., & Thomas, S. (2009). Tensile Stress Relaxation Studies of TiO 2 and Nanosilica Filled Natural Rubber Composites. *Industrial & Engineering Chemistry Research*, *48*(7), 3410–3416. doi:10.1021/ie801494s

Miki Iga, Fumio Takeshige, Mitsuo Torii, Y. T. (1991). The Relationship between Polymerization Shrinkage Measured by a Modified Dilatometer and the Inorganic Filler Content of Light-Cured Composites. *Dental Materials Journal*, *10*(1), 38–45.

Minko, S. (2006). Responsive Polymer Brushes. *Polymer Reviews*, *46*(4), 397–420. doi:10.1080/15583720600945402

Mitra, S., Wu, D., & Holmes, B. (2003). An application of nanotechnology in advanced dental materials. *Journal of the American Dental Association*, *134*, 1382–1390.

Moszner, N. (2001). New developments of polymeric dental composites. *Progress in Polymer Science*, *26*(4), 535–576. doi:10.1016/S0079-6700(01)00005-3

Moszner, Norbert, & Salz, U. (2007). Recent Developments of New Components for Dental Adhesives and Composites. *Macromolecular Materials and Engineering*, *292*(3), 245–271. doi:10.1002/mame.200600414

Munksgaard, E. C., Peutzfeldt, A., & Asmussen, E. (2000). Elution of TEGDMA and BisGMA from a resin and a resin composite cured with halogen or plasma light. *European Journal of Oral Sciences*, *108*(4), 341–5. Retrieved from http://www.ncbi.nlm.nih.gov/pubmed/10946770

Nakamura, S., Pavlovic, E., & Kramer, E. (2007). Fracture Energy of Epoxy Interfaces with Layers of Different Silane Coupling Agents. *The Journal of Adhesion*, *83*(4), 351–365. doi:10.1080/00218460701282372

Nedeljkovic, J. M., & Djokovic, V. (2000). Stress relaxation in hematite nanoparticles-polystyrene composites. *Macromolecular Rapid Communications*, *21*(14), 994–997.

Retrieved from http://www.scopus.com/inward/record.url?eid=2-s2.0-23044522596&partnerID=40&md5=e1f45a6493dfd27f21c637e89de2a3d6

Nihei, T., Kurata, S., Kondo, Y., Umemoto, K., Yoshino, N., & Teranaka, T. (2002). Enhanced Hydrolytic Stability of Dental Composites by Use of Fluoroalkyltrimethoxysilanes. *Journal of Dental Research*, *81*(7), 482–486. doi:10.1177/154405910208100710

Nishiyama, N., Ishizaki, T., Horie, K., Tomari, M., & Someya, M. (1991). Novel polyfunctional silanes for improved hydrolytic stability at the polymer-silica interface. *Journal of Biomedical Materials Research*, *25*, 213–221.

Oliveira, L. C. A., Duarte, S., Araujo, C. A., & Abrahão, A. (2010). Effect of low-elastic modulus liner and base as stress-absorbing layer in composite resin restorations. *Dental Materials*, *26*(3), e159–69. doi:10.1016/j.dental.2009.11.076

Otsu, T. (2000). Iniferter concept and living radical polymerization. *Journal of Polymer Science Part A: Polymer Chemistry*, *38*(12), 2121–2136. doi:10.1002/(SICI)1099-0518(20000615)38:12<2121::AID-POLA10>3.0.CO;2-X

Otsu, T., & Kuriyama, A. (1984). Living Mono- and Biradical Polymerizations in Homogeneous System Synthesis of AB and ABA Type Block Copolymers. *Polymer B*, *142*, 135–142.

Park, H. Y., Kloxin, C. J., Scott, T. F., & Christopher, N. (2011). Stress Relaxation by Addition-Fragmentation Chain Transfer in Highly Crosslinked Thiol-Yne Networks. *Macromolecular Theory and Simulations*, *43*(24), 10188–10190. doi:10.1021/ma1020209.Stress

Payne, J. A., Francis, L. F., & McCormick, A. V. (1997). The effects of processing variables on stress development in ultraviolet-cured coatings. *Journal of Applied Polymer Science*, *66*(7), 1267–1277. doi:10.1002/(SICI)1097-4628(19971114)66:7<1267::AID-APP6>3.0.CO;2-E

Peng, S., & Bhushan, B. (2012). Smart polymer brushes and their emerging applications. *RSC Advances*, *2*(23), 8557. doi:10.1039/c2ra20451g

Peutzfeldt, A. (1997). Resin composites in dentistry: the monomer systems. *European Journal of Oral Sciences*, *105*(2), 97–116. Retrieved from http://www.ncbi.nlm.nih.gov/pubmed/9151062

Pfeifer, C. S., Wilson, N. D., Shelton, Z. R., & Stansbury, J. W. (2011). Delayed gelation through chain-transfer reactions: Mechanism for stress reduction In methacrylate networks. *Polymer*, *52*(15), 3295–3303. doi:10.1016/j.polymer.2011.05.034

Plueddemann, E. P. (1983). Silane adhesion promoters in coatings. *Progress in Organic Coatings*, *11*(3), 297–308. doi:10.1016/0033-0655(83)80012-0

Plueddemann, P. G. P. and E. P. (1991). Methods for improving the performance of silane coupling agents. *Journal of Adhesion Science and Technology*, *5*(10), 831–842.

Pukanszky, B. (2005). Interfaces and interphases in multicomponent materials: past, present, future. *European Polymer Journal*, *41*(4), 645–662. doi:10.1016/j.eurpolymj.2004.10.035

Qiao, R., & Catherine Brinson, L. (2009). Simulation of interphase percolation and gradients in polymer nanocomposites. *Composites Science and Technology*, *69*(3-4), 491–499. doi:10.1016/j.compscitech.2008.11.022

Qu, M., Deng, F., Kalkhoran, S. M., Gouldstone, A., Robisson, A., & Van Vliet, K. J. (2011). Nanoscale visualization and multiscale mechanical implications of bound rubber interphases in rubber–carbon black nanocomposites. *Soft Matter*, *7*(3), 1066. doi:10.1039/c0sm00645a

Queiroz, G., Monteiro, D. M., Antonio, M., & Resende, J. (2010). Evaluation of Linear Polymerization Shrinkage , Flexural Strength and Modulus of Elasticity of Dental Composites. *Spectrum*, *13*(1), 51–55.

Rittigstein, P., Priestley, R. D., Broadbelt, L. J., & Torkelson, J. M. (2007). Model polymer nanocomposites provide an understanding of confinement effects in real nanocomposites. *Nature materials*, *6*(4), 278–82. doi:10.1038/nmat1870

Rittigstein, P., & Torkelson, J. M. (2006). Polymer – Nanoparticle Interfacial Interactions in Polymer Nanocomposites : Confinement Effects on Glass Transition Temperature and Suppression of Physical Aging. *Polymer*, 2935–2943. doi:10.1002/polb

Rosin, M., Urban, A. D., Gärtner, C., Bernhardt, O., Splieth, C., & Meyer, G. (2002). Polymerization shrinkage-strain and microleakage in dentin-bordered cavities of chemically and light-cured restorative materials. *Dental Materials*, *18*(7), 521–8. Retrieved from http://www.ncbi.nlm.nih.gov/pubmed/12191665

Ruggerone, R., Geiser, V., Dalle Vacche, S., Leterrier, Y., & Månson, J.-A. E. (2010). Immobilized Polymer Fraction in Hyperbranched Polymer/Silica Nanocomposite Suspensions. *Macromolecules*, *43*(24), 10490–10497. doi:10.1021/ma102074x

Sadowsky, S. J. (2006). An overview of treatment considerations for esthetic restorations: a review of the literature. *The Journal of Prosthetic Dentistry*, *96*(6), 433–42. doi:10.1016/j.prosdent.2006.09.018

Sakaguchi, R. L., & John M Powers. (2012). *Craig's Dental Restorative Mateirals*. (Ronald L Sakaguchi & J. M. Powers, Eds.) (13th ed.). Elsevier.

Schneider, L. F. J., Cavalcante, L. M., & Silikas, N. (2010a). Shrinkage Stresses Generated during Resin-Composite Applications: A Review. *Journal of Dental Biomechanics*, *2010*, 1–15. doi:10.4061/2010/131630

Schneider, L. F. J., Cavalcante, L. M., & Silikas, N. (2010b). Shrinkage Stresses Generated during Resin-Composite Applications: A Review. *Journal of Dental Biomechanics*, *2010*, 1–40. doi:10.4061/2010/131630

Seto, R., Kojima, T., Hosokawa, K., Koyama, Y., Kohnishi, G., & Takata, T. (2010). Synthesis and property of 9,9′-spirobifluorene-containing aromatic polyesters as optical polymers with high refractive index and low birefringence. *Polymer*, *51*, 4744–4749.

Shaw, M. T., & Macknight, W. J. (2005). *Introduction to Polymer Viscoelasticity* (3rd ed.).

Sideridou, I. D., & Karabela, M. M. (2009a). Effect of the amount of 3-methacyloxypropyltrimethoxysilane coupling agent on physical properties of dental resin nanocomposites. *Dental materials : official publication of the Academy of Dental Materials*, *25*(11), 1315–24. doi:10.1016/j.dental.2009.03.016

Sideridou, I. D., & Karabela, M. M. (2009b). Effect of the amount of 3-methacyloxypropyltrimethoxysilane coupling agent on physical properties of dental resin nanocomposites. *Dental Materials*, *25*(11), 1315–24. doi:10.1016/j.dental.2009.03.016

Soderholm, K.-J. (2010). Review of the fracture toughness approach. *Dental Materials*, *26*(2), e63–77. doi:10.1016/j.dental.2009.11.151

Sperling, L. H. (2006). *Introduction to Physical Polymer Science*. John Wiley and Sons.

Stansbury, J. W., Trujillo-Lemon, M., Lu, H., Ding, X., Lin, Y., & Ge, J. (2005a). Conversion-dependent shrinkage stress and strain in dental resins and composites. *Dental materials*, *21*(1), 56–67. doi:10.1016/j.dental.2004.10.006

Stansbury, J. W., Trujillo-Lemon, M., Lu, H., Ding, X., Lin, Y., & Ge, J. (2005b). Conversion-dependent shrinkage stress and strain in dental resins and composites. *Dental Materials*, *21*(1), 56–67. doi:10.1016/j.dental.2004.10.006

Stansbury, J. W., Trujillo-lemon, M., Lu, H., Ding, X., Lin, Y., & Ge, J. (2005). Conversion-dependent shrinkage stress and strain in dental resins and composites. *Dental Materials*, *21*, 56–67. doi:10.1016/j.dental.2004.10.006

Tantbirojn, D., Pfeifer, C. S., Braga, R. R., & Versluis, A. (2011). Do low-shrink composites reduce polymerization shrinkage effects? *Journal of Dental Research*, *90*(5), 596–601. doi:10.1177/0022034510396217

Tegou, E., Bellas, V., Gogolides, E., Argitis, P., Eon, D., Cartry, G., & Cardinaud, C. (2004). Polyhedral Oligomeric Silsesquioxane (POSS) Based Resists: Material Design Challenges and Lithographic Evaluation at 157 nm. *Chemistry of Materials*, *16*(13), 2567–2577. doi:10.1021/cm035089x

Tham, W. L., Chow, W. S., & Ishak, Z. a. M. (2011). Effects of titanate coupling agent on the mechanical, thermal and morphological properties of poly(methyl methacrylate)/hydroxyapatite denture base composites. *Journal of Composite Materials*. doi:10.1177/0021998311401085

Vallittu, P. K. (1997). Curing of a silane coupling agent and its effect on the transverse strength of autopolymerizing polymethylmethacrylate-glass fibre composite. *Journal of Oral Rehabilitation*, *24*(2), 124–30. Retrieved from http://www.ncbi.nlm.nih.gov/pubmed/9061621

Versluis, A., Tantbirojn, D., Pintado, M. R., DeLong, R., & Douglas, W. H. (2004). Residual shrinkage stress distributions in molars after composite restoration. *Dental Materials*, *20*(6), 554–64. doi:10.1016/j.dental.2003.05.007

Viovy, J. L., Monnerie, L., & Tassin, J. F. (1983). Tube Relaxation : A Necessary Concept in the Dynamics of Strained Polymers. *Journal of Polymer Science: Polymer Physics Edition*, *21*, 2427–2444.

Wagner, H., & Vaia, R. (2004). Nanocomposites: issues at the interface. *Materials Today*, *7*(11), 38–42. doi:10.1016/S1369-7021(04)00507-3

Watts, D. C., Marouf, A. S., & Al-Hindi, A. M. (2003). Photo-polymerization shrinkage-stress kinetics in resin-composites: methods development. *Dental Materials*, *19*(1), 1–11. Retrieved from http://www.ncbi.nlm.nih.gov/pubmed/12498890

Weinmann, W., Thalacker, C., & Guggenberger, R. (2005a). Siloranes in dental composites. *Dental Materials*, *21*(1), 68–74. doi:10.1016/j.dental.2004.10.007

Weinmann, W., Thalacker, C., & Guggenberger, R. (2005b). Siloranes in dental composites. *Dental Materials*, *21*(1), 68–74. doi:10.1016/j.dental.2004.10.007

Wetzel, B., Rosso, P., Haupert, F., & Friedrich, K. (2006). Epoxy nanocomposites – fracture and toughening mechanisms. *Engineering Fracture Mechanics*, *73*(16), 2375–2398. doi:10.1016/j.engfracmech.2006.05.018

White, L., & Tripp, C. (2000). Reaction of (3-Aminopropyl)dimethylethoxysilane with Amine Catalysts on Silica Surfaces. *Journal of Colloid and Interface Science*, *232*(2), 400–407. doi:10.1006/jcis.2000.7224

Wilson, K. S., Allen, A. J., Washburn, N. R., & Antonucci, J. M. (2006). Interphase effects in dental nanocomposites investigated by small-angle neutron scattering. *Journal of Biomedical Materials Research Part A*. doi:10.1002/jbm.a

Wilson, K. S., & Antonucci, J. M. (2006). Interphase structure-property relationships in thermoset dimethacrylate nanocomposites. *Dental materials : official publication of the Academy of Dental Materials*, *22*(11), 995–1001. doi:10.1016/j.dental.2005.11.022

Wilson, K. S., Zhang, K., & Antonucci, J. M. (2005). Systematic variation of interfacial phase reactivity in dental nanocomposites. *Biomaterials*, *26*(25), 5095–103. doi:10.1016/j.biomaterials.2005.01.008

Ye, S., Azarnoush, S., Smith, I. R., Cramer, N. B., Stansbury, J. W., & Bowman, C. N. (2012). Using hyperbranched oligomer functionalized glass fillers to reduce shrinkage stress. *Dental Materials*, *28*(9), 1004–11. doi:10.1016/j.dental.2012.05.003

Zhao, B. (2000). Polymer brushes: surface-immobilized macromolecules. *Progress in Polymer Science*, *25*(5), 677–710. doi:10.1016/S0079-6700(00)00012-5

Zhou, S., Wu, L., Xiong, M., He, Q., & Chen, G. (2005). Dispersion and UV-VIS Properties of Nanoparticles in Coatings. *Journal of Dispersion Science and Technology*, *25*(4), 417–433. doi:10.1081/DIS-200025688